DENTINE EXTRACELLULAR MATRIX COMPONENTS LIBERATED BY CALCIUM SILICATE CEMENTS AND THEIR EFFECTS ON DENTAL PULP CELLS

by

PHILLIP LEO TOMSON

A thesis submitted to the University of Birmingham for the degree of
DOCTOR OF PHILOSOPHY

UNIVERSITY OF
BIRMINGHAM

Department of Oral Biology
The School of Dentistry
College of Medical and Dental Sciences
University of Birmingham
May 2013

ABSTRACT

Although the regenerative capacity of the dentine-pulp complex, induced by pulp capping agents, is well established, the molecular processes by which this occurs, are poorly understood. Calcium silicate cements are powerful stimulators of wound healing in the pulp. This project aimed to investigate the potential of calcium silicate cements to liberate dentine extracellular matrix (dECM) components, characterise growth factors present and determine if these dECM components, or any specific growth factor characterised, had bioactive effects on pulp wound healing. dECM was solubilised from human dentine using solutions of EDTA, calcium hydroxide, white MTA, grey MTA and Biodentine®. Proteomic analysis using cytokine arrays and multiplex ELISA demonstrated the presence of a broad range of growth factors, which were differentially released, suggesting that each agent had differing capacities to liberate such molecules. *In vitro* analysis of pulp cells exposed to dECM components released by calcium silicate cements, demonstrated increased capacity for cell proliferation and chemotaxis. A previously unidentified growth factor in dECM, hepatocyte growth factor, was shown to induce pulp cell proliferation, migration, differentiation and mineralisation *in vitro*. Growth factors liberated from dentine by the soluble components of pulp capping agents may regulate reparative events leading to pulp wound healing *in vivo*.

ACKNOWLEDGEMENTS

I am extremely grateful to all those who have supported, encouraged and inspired me over the years. Firstly, I would like to express my sincere thanks and appreciation to my supervisors, Professors Paul Cooper, Tony Smith and Phil Lumley, for their guidance, advice and support throughout this work.

I would also like to thank the staff of the Oral Biology laboratory - Gay Smith, Sue Finney, Michelle Holder and Jane Millard, all of whom have generously given of their time to assist me. I am grateful to my fellow PhD students, Jianyan Yan (University of Manchester) and, in particular, Lee Graham (University of Birmingham), for their help and guidance. Other research collaborators who have helped to make this work possible include Professor Alastair Sloan (Tissue Engineering and Reparative Dentistry, Cardiff University), Dr Yvonne Alexander (Institute of Cardiovascular Sciences, University of Manchester), Dr Liam Grover (School of Chemical Engineering, University of Birmingham) and Dr Stéphane Simon (University of Paris 7).

I would like to express particular thanks to my family for their continued support; I am indebted to my parents for all that they have done for me. Finally, special thanks go to my wife, Mary, who has shown unwavering support and patience throughout – she has been a true inspiration.

This work was supported by the following grants and organisations:

Royal College of Surgeons of England Faculty of Dental Surgery (Research Fellowship)

Royal College of Surgeons of Edinburgh (Pump Priming Grant)

The MRC/EPSRC Institutional Discipline Bridging Award (IDBA) to the University of Birmingham (BIBEMS)

TABLE OF CONTENTS

LIST OF FIGURES

CHAPTER 1 INTRODUCTION

CHAPTER 2 MATERIALS AND METHODS

CHAPTER 3 RESULTS

CHAPTER 4 RESULTS

CHAPTER 5 RESULTS

LIST OF TABLES

LIST OF ABBREVIATIONS

α -MEM	Alpha modified minimum essential medium
AA	Ascorbic acid
AAS	Atomic absorption spectroscopy
ADJ	Amelodentinal junction
ADM	Adrenomedullin
ALP	Alkaline phosphatase
ANOVA	Analysis of variance
AR	Amphiregulin
BCA	Bicinchoninic acid assay
BDNF	Brain-derived neurotrophic factor
BGP	Beta-glycerophosphate
BMP	Bone morphogenetic protein
BP	Binding protein
BSA	Bovine serum albumin
BSP	Bone sialoprotein
cDNA	Copy deoxyribonucleic acid
CEJ	Cementoenamel junction
Col-Iα	Collagen type I alpha
CSF	Colony-stimulating factor
dECM	Dentine extracellular matrix
Dex	Dexamethasone
DMEM	Dulbecco's modified minimum essential media
DMMB	Dimethylmethylene blue
DMP-1	Dentine matrix protein-1
DNA	Deoxyribonucleic acid
DPP	Dentine phosphoprotein
DPSC	Dental pulp stem cell
DSP	Dentine sialoprotein
DSPP	Dentine sialophosphoprotein
ECM	Extracellular matrix

EDTA	Ethylenediaminetetraacetic acid
EDXA	Energy dispersive X-ray analysis
EGF	Epidermal growth factor
ELISA	Enzyme-linked immunosorbent assays
FBS	Foetal bovine serum
FGF	Fibroblast growth factor
GAG	Glycosaminoglycan
GAPDH	Glyceraldehyde 3-phosphate dehydrogenase
G-CSF	Granulocyte colony stimulating factor
GDNF	Glial cell-derived neurotrophic factor
GM-CSF	Granulocyte macrophage colony stimulating factor
HGF	Hepatocyte growth factor
IGF	Insulin-like growth factor
Il	Interleukin
LPS	Lipopolysaccharide
LTA	Lipoteichoic acid
M-CSF	Macrophage colony stimulating factor
MDPC-23	Murine odontoblast-like cells
MEPE	Matrix extracellular phosphoglycoprotein
MMP	Matrix metalloproteinase
MSC	Mesenchymal stem cells
MTA	Mineral trioxide aggregate
NCP	Non-collagenous protein
NPY	Neuropeptide Y
NGF	Nerve growth factor
NK4	Four-kringle antagonist of hepatocyte growth factor
NT	Neurotrophin
OC	Osteocalcin
OD-21	Murine dental pulp cells
OPC	Ordinary Portland cement
OPN	Osteopontin
PBS	Phosphate buffered saline
PCR	Polymerase chain reaction

PDGF	Platelet-derived growth factor
pECM	Pulp extracellular matrix
PlGF	Placental growth factor
RDPC	Rat dental pulp cell
RDT	Remaining dentine thickness
RNA	Ribonucleic acid
RT	Reverse transcription
SCAP	Stem cells from apical papilla
SCF	Stem cell factor
SHED	Stem cells from human exfoliated deciduous teeth
SIBLINGs	Small integrin-binding ligand N-linked glycoprotein
SLRPs	Small leucine-rich proteoglycans
TGF-β	Transforming growth factor-beta
TLR	Toll-like family receptor
TNF-α	Tumor necrosis factor -alpha
VEGF	Vascular endothelial growth factor
WST	Water soluble tetrazolium salt
XPS	X-ray photoelectron spectroscopy
XRD	X-ray diffraction
1D SDS PAGE	One dimensional sodium dodecyl sulphate polyacrylamide gel electrophoresis

1.0 INTRODUCTION

1.1 Dentine-pulp complex

The dentine-pulp complex (Figure 1.1) is a unique mineralised connective tissue that is composed of two integrated constituents: the pulp - an underlying gelatinous soft connective tissue which has a rich vasculature and is well innervated, and the dentine - an outer casing of mineralised tissue. Although these tissues have chemical compositions and structures which differ (Linde and Goldberg, 1993), it is not possible to consider them as separate entities since their physiological processes during development, homeostasis, pathology and repair are intertwined and reliant upon one another. The major component of any connective tissue is extracellular matrix; this consists mainly of fibrillar proteins, which are predominantly collagen in the case of dentine, and this provides its structural integrity. Ground substance in the dentine extracellular matrix (dECM) provides viscoelasticity, amongst many other functions, and is principally comprised of proteoglycans, glycosaminoglycans (GAGs) and (glyco-)proteins.

Dentine is a permeable structure that is perforated by tubules, which traverse from the amelodentinal junction (ADJ) or cementoenamel junction (CEJ) to the pulp chamber. The pulp and dentine thus form a complex or continuum via the communication provided by the dentinal tubule and the odontoblast process, which projects into the tubule. In health, odontoblasts line the entirety of the pulp chamber. The extent to which the odontoblast process occupies the tubule has been debated within the literature; some authors suggest that it occupies the entire length of the tubule (Maniatopoulos and Smith, 1983, Sigal et al., 1985, Sigal et al., 1984), whilst others claim that it is confined to the pulpal third

(Garberoglio and Brannstrom, 1976, Thomas and Carella, 1983, Thomas and Carella, 1984). This controversy results from the relatively aggressive chemical treatments required for tissue preparation, which can result in process contraction. Enamel, the covering to coronal dentine, appears macroscopically to be impervious, but it actually behaves like a semi-permeable membrane (Bergman, 1963). This structural arrangement results in the dentinal tubules being fluid filled throughout their entire length as they are in communication with the extracellular fluids of the pulp, periradicular tissues and the whole of the oral cavity. Amongst a number of functions, dentinal fluid act as a conduit for communication. For example, external thermal stimulation of the tooth results in hydrodynamic activation of nerve fibres within the dentine-pulp complex; this arises from expansion or contraction of the dentinal fluid, brought about by temperature changes (Anderson et al., 1970). For the purpose of description only, dentine and the pulp will now be considered separately.

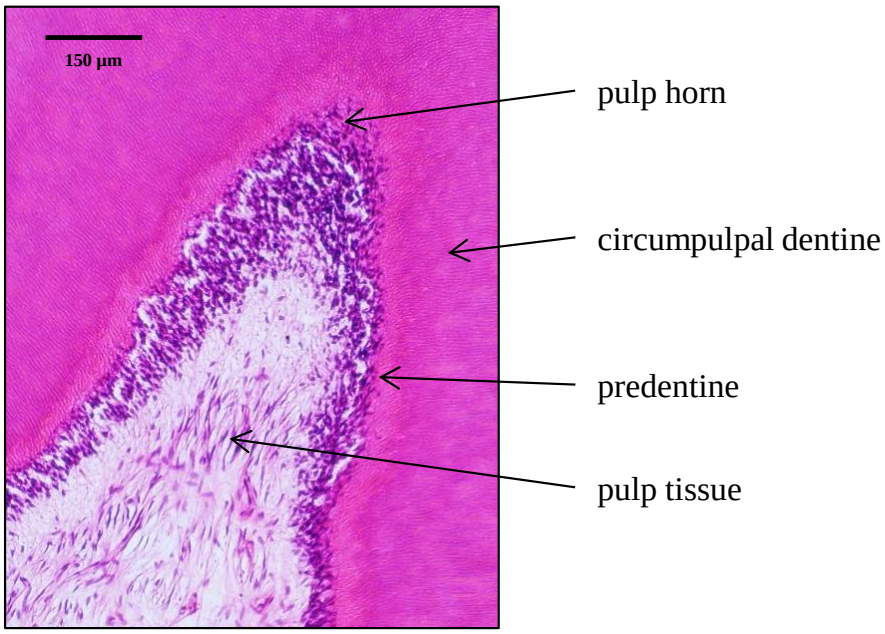

Figure 1.1 Histological section showing the structure of the dentine-pulp complex in a human third molar with haematoxylin and eosin staining (H&E). (Histological processing was performed by Sue Finney and image captured by the author at x10 magnification)

1.2 Dentine and its bioactive niches

Dentine is a porous biological composite comprised of hydroxyapatite crystal filler particles in a collagenous matrix (Pashley and Tay, 2012). By weight, it consists of 70% mineral phase, 20% organic matrix and 10% water; its mineral content is therefore less than enamel (96%), but more than bone and cementum (65%) (Goldberg et al., 2011). The mineral phase of dentine comprises of calcium-deficient and carbonate-rich hydroxyapatite plate-like crystals, which are considerably smaller than those found in enamel. The organic matrix is predominantly made up of type I collagen (90%) with the remainder including non-collagenous proteins (NCPs), GAGs and proteoglycans (Veis, 1993, Butler, 1998, Santos et al., 2009). This unique combination of constituents enables dentine to function as a bulk supportive structure for the tooth and to play an important active biological role during homeostasis and repair.

The dECM is secreted by the odontoblast, a specialised post-mitotic cell. Due to the varying secretory behaviour of this cell during its life, it will deposit different types of dentine, which are categorised into primary, secondary and tertiary dentine (Kuttler, 1959) (Figure 1.2). The dentine that is formed prior to eruption, up until the point at which the root end is complete, is termed primary dentine. The initial layer of primary dentine, deposited by newly differentiated odontoblasts adjacent to enamel, is referred to as mantle dentine; it is approximately 150 μm wide, contains loosely packed collagen fibrils and is less well mineralised. The remaining primary dentine is considerably more ordered with consistent tubular structure and is laid down at a rate of approximately 4 μm per day until crown and root formation is complete (Schour and Hoffman, 1939). Once the tooth is formed, odontoblast secretory activity significantly decreases and secondary dentine,

sometimes known as physiological dentine, begins to form at a much slower rate of around 0.4 μm per day. During the life of an unaffected tooth, the volume of the coronal pulp chamber decreases at a more rapid rate than that of the radicular pulp chamber indicating that secondary dentine is not deposited at an even rate throughout the entire pulp chamber. The boundary between primary and secondary dentine is demarcated by a subtle calciotraumatic line but the tubules traversing this maintain continuity. The only morphological difference between primary and secondary dentine is that the 'S-shaped' curvature of the dentinal tubules is more accentuated in secondary dentine, perhaps reflecting crowding of the odontoblasts as they move inwards towards the pulp core. Tertiary dentine refers to the dentine formed focally in response to noxious stimuli such as tooth wear, caries, trauma or iatrogenic intervention (Smith, 2012). Two types of tertiary dentine are formed and are termed reactionary and reparative dentine; both of these types of dentine are described below in more detail (section 1.5).

Circumpulpal dentine is deposited after the mantle dentine has been formed and makes up the remainder of the dentine structure. It exists in two forms; the majority of circumpulpal dentine is intertubular dentine whilst the minor component in humans is peritubular dentine. Peritubular dentine is secreted from the odontoblast process; it is more highly mineralised, rich in NCPs, but contains relatively few collagen fibrils compared with intertubular dentine. Intertubular dentine is secreted from the terminal web of the odontoblast and is predominantly composed of densely packed type I collagen fibrils (20-75 nm in diameter) that are interlaced with plate-like crystallites. These structures run parallel to the fibril long axis and are approximately 2-5 nm in thickness and are 60 nm in length (Goldberg et al., 2011). Collagen fibrils are coated with NCPs and overlap with each

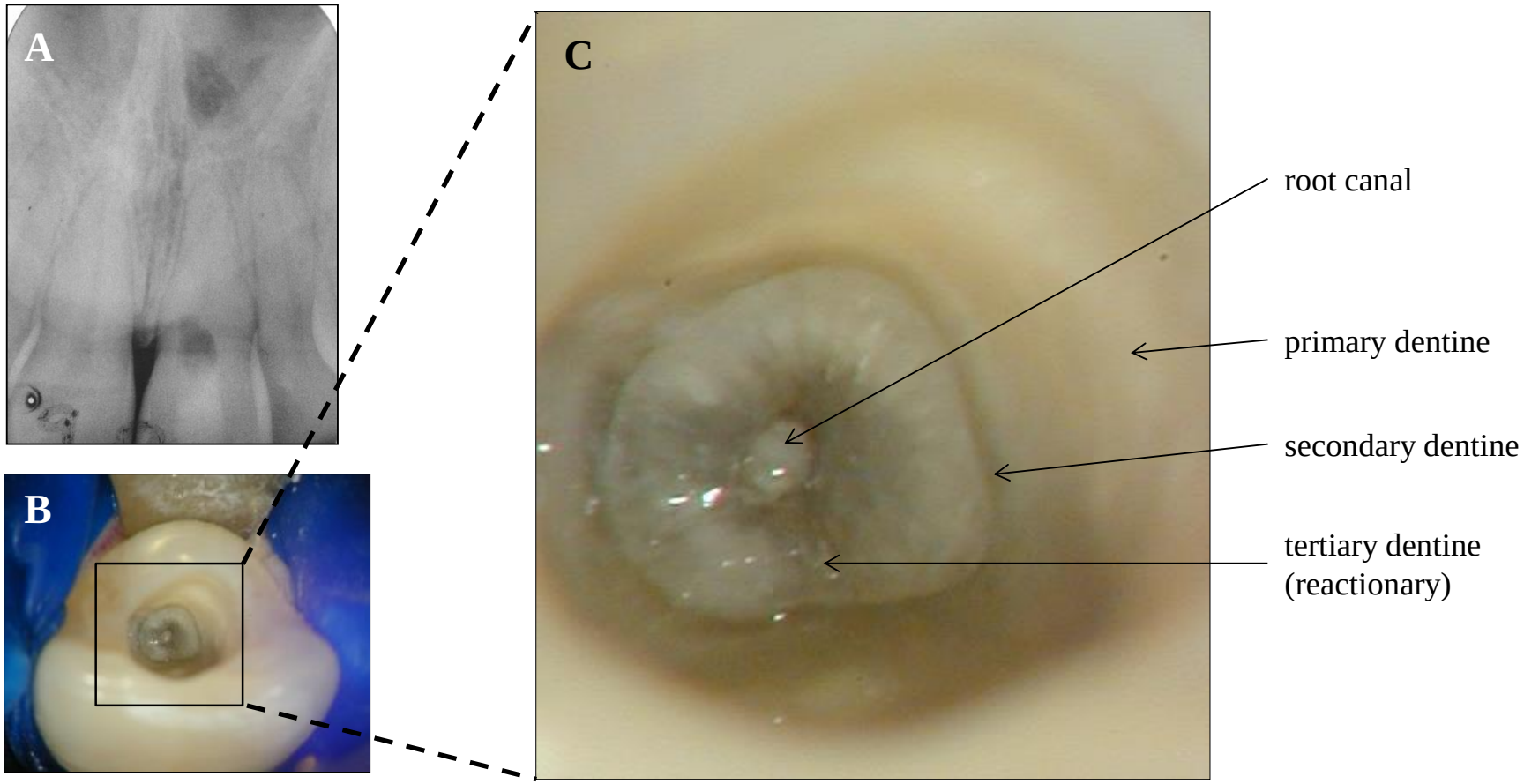

Figure 1.2 A case of a 24 year old female patient who had suffered trauma to her maxillary incisor 7 years earlier. **A**) Pre-operative periapical radiograph of maxillary central incisors following GDP's attempt to find the root canal. **B**) Access cavity in left maxillary incisor and **C**) higher resolution image of (**B**). This shows primary dentine to be a "creamy" colour. Secondary dentine is a darker colour compared with the primary dentine. Tertiary dentine is clearly demarcated by peripheral secondary dentine and has an "icy" mottled appearance interspersed with a more grey coloured dentine. The canal can be seen located in the centre of the tertiary dentine suggesting that the tertiary dentine was deposited at an equal rate by the odontoblasts lining the pulp chamber (clinical case by author).

other, creating gaps between them where GAGs are localised; the interaction of these with other bioactive molecules is considered in section 1.2.2.

1.2.1 Dentine extracellular matrix

As previously discussed, the majority of the dECM is comprised of collagenous proteins. Numerous other molecules, largely NCPs, make up the remainder of the dECM and these molecules may be considered the most bioactive in terms of being regulators of homeostasis and repair within the dentine-pulp complex. The broad range of NCPs are summarised in Table 1.1. The well characterised **s**mall **i**ntegrin-**b**inding **li**gand **N**-linked **g**lycoproteins (SIBLINGs) present within dECM are known to act as nucleation factors as they regulate hydroxyapatite crystal formation (Hunter and Goldberg, 1993, Goldberg et al., 1996, Fisher et al., 2001, He et al., 2003). Although most of these molecules have been detected in both bone as well as dentine, some are considered more characteristic of dentine. Indeed, dentine sialophosphoprotein (DSPP) is highly expressed by odontoblasts (Sreenath et al., 2003) whilst its cleaved products, dentine sialoprotein (DSP) and dentine phosphoprotein (DPP), are more abundant in the dECM compared with the bone matrix. The SIBLING, dentine matrix protein-1 (DMP-1), is also expressed by differentiating odontoblasts (Toyosawa et al., 2004) and is thought to be essential for maturation of predentine (Feng et al., 2003, Ye et al., 2004), however, despite its name, it is also implicated in mineralisation of bone and cementum (MacDougall et al., 1998). Depending on its degree of phosphorylation, DMP-1 has been shown to be a signalling molecule for promoting mineralisation but under certain conditions it can also act as an inhibitor (Tartaix et al., 2004). Bone sialoprotein (BSP), which is present in tertiary dentine, has been shown to play important roles in both initiating and inhibiting hydroxyapatite crystal growth

during mineralisation (Qin et al., 2004, Boskey et al., 2008). Osteopontin (OPN) and matrix extracellular phosphorylated protein (MEPE) are both present in dECM and are expressed by odontoblasts. Both of these molecules have also been reported to play a regulatory role during hydroxyapatite crystal growth and mineralisation (Boskey et al., 1993, Boskey et al., 2002, Gowen et al., 2003). The SIBLING molecules play a crucial role in the regulation of dECM secretion and mineralisation, particularly during initial dentine formation, homeostasis and repair, by acting not only as promoters but also as inhibitors of hydroxyapatite crystal formation. Other non-phosphorylated matrix proteins, such as osteocalcin, are expressed by odontoblasts and are thought to aid maturation of enamel early in primary dentinogenesis (Papagerakis et al., 2002), however, their role in dentine maturation is unclear. The small leucine-rich proteoglycans (SLRPs), decorin and biglycan, are thought to facilitate mineralisation in predentine through their ability to bind to calcium (Embery et al., 2001, Goldberg et al., 2003a).

Table 1.1 Summary of non-collagenous proteins present in dECM. Adapted from Goldberg and Smith 2004. Key to abbreviations is provided on page xii.

Phosphorylated matrix proteins (SIBLINGs)	Non-phosphorylated matrix proteins	Proteoglycans (SLRPs)	Matrix metalloproteinases (MMPs)
DSPP, DSP, DPP, DMP-1, BSP, OPN, MEPE	Matrix GLA protein, osteocalcin, osteonectin	Decorin, biglycan, lumican, fibromodulin, osteoadherin	Collagenase (MMP-1), gelatinases (MMP-2 and -9), stromelysin-1 (MMP-3), enamelysin (MMP-20)

Growth factors and cytokines	Serum derived proteins	Others
TGF-β1 IGF-I, IGF-II PDGF-AB, VEGF, PlGF, FGF-2, EGF BMP IL-1α, IL-1β, IL-4, IL-6, IL-8, IL-12	Albumin, lipoproteins, αHS_2-glycoprotein	Membrane phospholipids, extracellular-mineral-associated phopholipids

Other NCPs found in dECM include matrix metalloproteinases (MMPs), which are a class of zinc- and calcium-dependent hydrolases with twenty-three family members in total. These enzymes play an important role in matrix remodelling, angiogenesis and wound healing (Hannas et al., 2007) and have been shown to be released during cariogenic attack and during treatment of dentine with ethylenediaminetetraacetic acid (EDTA), citric acid and dentine bonding agents (Pashley et al., 2004, Tay et al., 2006, Mazzoni et al., 2007). Odontoblasts secrete MMP enzymes (Llano et al., 1997, Caron et al., 1998), which catalyse the degradation of matrix macromolecules, such as collagens and proteoglycans. MMPs have been shown to be involved in the initiation and regulation of mineralisation (Fanchon et al., 2004, Beniash et al., 2006) and the processing of DSPP (Yamakoshi et al., 2006). *In vitro,* MMP-2 has been shown to cleave DMP-1 which leads to the formation of a bioactive molecule capable of enhancing differentiation of progenitor pulp cells (Chaussain et al., 2009). Release of MMPs also appears to be important in activating other biological molecules, as adrenomedullin (ADM), insulin-like growth factors (IGFs) and transforming growth factor–β1 (TGF-β1) have all been shown to have their activity modified by such proteolytic enzymes (Dallas et al., 2002, Martinez et al., 2004, Miyamoto et al., 2004). These data suggest that MMPs, released along with the other molecules from the dECM, have the potential to orchestrate reparative events by promotion and attenuation of key cellular events (Smith et al., 2012a).

1.2.2 Growth factors and cytokines in dECM

Growth factors and cytokines are key signalling molecules that control and regulate cellular events involved in tissue development, homeostasis and repair. They are known to play a central role in initiating and regulating events in wound repair in the dental pulp (Smith et

al., 2012a). Indeed, their roles and activities are being explored to identify new biological repair and tissue engineering approaches for treatment of pulpal and periradicular disease (Kim et al., 2010). Growth factors are potent peptide signalling molecules, which can elicit autocrine, paracrine and endocrine effects at very low concentrations (picogram range) (Lazar-Molnar et al., 2000, Smith et al., 2012a). Some growth factors are highly specific in their activity, while others have broader effects. These molecules act by binding to specific cell surface receptors and initiating a cascade of intracellular events, which lead to transduction of the signal to the cell nucleus; this, in turn, may lead to gene expression changes which ultimately influence cell behaviour and activity.

During tooth development, epithelial-mesenchymal interactions are responsible for initiating the differentiation of ameloblasts and odontoblasts, which then begin to secrete enamel and dentine respectively. In particular, TGF-β family members have been shown to be important in facilitating signalling leading to odontoblast differentiation (Begue-Kirn et al., 1992, Begue-Kirn et al., 1994, Ruch et al., 1995). During mineralisation of dECM, growth factors secreted by odontoblasts (Smith and Lesot, 2001) interact with extracellular matrix or mineral components and become 'fossilised' or sequestered within it (Smith et al., 1998, Sloan et al., 2002). These interactions with other matrix components are important in protecting these signalling molecules from degradation as their half-lives are often of the order of only a few minutes if not protein bound (Wakefield et al., 1990). The precise nature of the association of these molecules with the dECM is not yet fully understood (Tziafas et al., 2000, Smith et al., 2001, Cassidy et al., 1997, Roberts-Clark and Smith, 2000), however, a group of heparan sulphate proteoglycans present within the dECM are thought to be involved. Decorin and biglycan are two such proteoglycans / GAGs, which have been shown to bind TGF-β1 in dentine (Smith et al., 1998, Baker et al.,

2009). The heparan sulphate binding proteoglycans have also been shown to interact with numerous other proteins in dECM which, importantly, include the growth factors: fibroblast growth factors (FGF), vascular endothelial growth factor (VEGF), placental growth factor (PlGF), platelet-derived growth factor (PDGF) and hepatocyte growth factor (HGF) (Dreyfuss et al., 2009). Some growth factors, such as the IGFs, are bound to specific binding proteins (BPs), which support and attenuate the bioactivity of their signalling activity (Arai et al., 1996, Kuang et al., 2006). Some growth factors, such as HGF, are known to bind to glycoproteins including fibronectin and vitronectin and these molecular complexes have been shown to enhance biological activity to promote neovascularisation during health and disease (Rahman et al., 2005). In other tissues, signalling molecules such as the bone morphogenetic proteins (BMPs) and interleukin-2 (IL-2) are able to bind to collagen type I and III directly (Paralkar et al., 1990, Paralkar et al., 1991, Somasundaram et al., 2000), whereas collagen type II and IV have been shown to have binding domains for both BMP and TGF-β family members (Zhu et al., 1999, Larrain et al., 2000). Brain-derived neurotrophic factor (BDNF) has been shown to bind to a number of different GAGs in tissues of the central nervous system (Kanato et al., 2009). Although relatively little is directly known about how growth factors and cytokines are bound to dECM, there is enough evidence to suggest that the mechanism of binding is similar to how these molecules bind to the ECM of other tissues (Smith et al., 2012a).

To date, several different growth factors have been identified in dECM including TGF-β1 (Finkelman et al., 1990, Cassidy et al., 1997, Smith et al., 1998), IGF-I, IGF-II (Finkelman et al., 1990), BMP (Bessho et al., 1991) PDGF-AB, VEGF, PlGF, FGF-2 and epidermal growth factor (EGF) (Roberts-Clark and Smith, 2000). Pro- and anti-inflammatory cytokines including IL-1α, IL-1β, IL-4, IL-6, IL-8, IL-12 and granulocyte macrophage

colony stimulating factor (GM-CSF) have also been reported as being present in dECM (Cooper et al., 2010, Graham et al., 2007). Although this rich cocktail of growth factors and cytokines present in dECM has been identified, it is likely that there are many more key signalling molecules sequestered in dentine that are yet to be identified. The role of the TGF-β1 growth factor is, however, well documented in tooth development and repair and it is thought to play a key role in initiating the differentiation of odontoblasts at the periphery of the dental papilla (Ruch et al., 1995). In addition, TGF-β1 has been shown to be a chemoattractant for dental papilla-derived cells (Kwon et al., 2010) and other less well differentiated cells (Macdonald et al., 2007, Brenmoehl et al., 2009). The application of TGF-β1 and its other isoforms has been shown to induce odontoblast-like cell differentiation and dentinogenesis *in vitro* (Sloan and Smith, 1999, Melin et al., 2000) and *in vivo* (Hu et al., 1998). While TGF-β1 has demonstrable key biological activities, it is likely that the effects of dECM components when released are not due to one bioactive molecule alone. Indeed, extracts of whole dECM components have been shown to induce increased proliferation of stem / progenitor cells *in vitro* at relatively low concentrations, however, it appeared that relatively high concentrations inhibit proliferation (Musson et al., 2010, Zhang et al., 2011).

While the dECM is known to be a rich source of bioactive molecules, research thus far has concentrated on characterisation of specific growth factors, which have been identified using more conventional enzyme-linked immunosorbent assays (ELISAs). The principle underpinning this technique is based on the formation of an antigen (target protein) / antibody complex which has a direct or indirect reporting system which indicates the concentration of the target protein compared with a standard (Engvall and Perlmann, 1971, Van Weemen and Schuurs, 1971). During the 1990s, antibody array technology was

developed to enable high-throughput analysis of multiple targets simultaneously using small sample volumes (Ekins and Chu, 1991, Ekins, 1998). This technology allows a more rapid and in-depth approach to protein analysis and it has previously been applied to characterise dECM components for inflammatory cytokine content (Graham et al., 2007, Cooper et al., 2011), but it has yet to be used for growth factor analysis in dECM.

Application of such a high-throughput approach has the potential to better characterise growth factor presence within the dECM and identify new molecules, which could contribute to dentine-pulp complex development and repair. Indeed, one particular candidate is the multifunctional growth factor, HGF, which has previously been demonstrated to act as a powerful mitogen, morphogen, motogen and chemotactic agent in multiple tissue types; it is involved in a variety of physiological processes, including tissue development and regeneration (Trusolino et al., 2010). HGF signalling is mediated by binding to its transmembranous tyrosine kinase receptor encoded by the proto-oncogene c-Met (Bottaro et al., 1991). Expression of c-Met in various developing and mature organs indicates that HGF is a mesenchymal-derived factor that acts on neighbouring developing epithelia which express c-Met, thus playing a key role in tissue development where epithelial-mesenchymal interactions occur (Birchmeier and Gherardi, 1998). Interestingly, expression of HGF and c-Met has been localised in developing tooth germs, implicating potential signalling roles in dental tissue development (Sonnenberg et al., 1993, Kajihara et al., 1999). Studies conducted using an *ex vivo* mouse tooth germ model have demonstrated that HGF translation arrest results in abnormal tooth development, with the enamel organs being surrounded by a thin layer of dentine and dental papilla thus appearing “inside-out” compared with that of the normal tooth germ (Tabata et al., 1996).

1.2.3 Mobilisation of dECM components

The hypothesis that mobilisation of bioactive molecules from dECM initiates a sequence of events leading to pulp repair and regeneration is well established (Smith et al., 2012a), however, the mechanism(s) by which dECM components are released is far less well understood. Different solutions have been used to release soluble dECM components, including EDTA (Smith and Leaver, 1979), lactic acid (Dung et al., 1995), citric acid (Mazzoni et al., 2007), phosphoric acid (Smith and Smith, 1998, Ferracane et al., 2010) and calcium hydroxide (Graham et al., 2006). Interestingly, although the pH of these solutions ranges from acidic through to alkaline, they are all still capable of extracting ECM molecules from dentine, so it therefore appears that the process is not entirely pH dependent (Goldberg and Smith, 2004). In terms of yield, EDTA has been shown to be the most effective and is therefore considered to be a valuable control agent for *in vitro* studies in this area. Understanding the mechanisms by which dECM components are released by such agents would open new avenues for research into the development of novel biologically-based treatment modalities for dental tissue regeneration.

1.3 Dental pulp

The dental pulp lies at the core of the tooth encased by the dentine. The loose connective tissue of the dental pulp is surrounded at its periphery by a highly specialised single layer of cells called odontoblasts. A network of capillaries, known as the terminal capillaries, exists in close proximity to this layer of odontoblasts, providing nutrients and performing homeostatic functions. In addition, free nerve endings pass between odontoblasts to form the terminal axons of the plexus of Raschkow, which provides the nervous supply (Okiji,

2012). Also within this layer, dendritic cells can be found which detect transdentinal antigenic stimuli (Jontell et al., 1998) and perform an immune defensive role. Beneath the odontoblasts is a relatively sparse area, which contains few cells and is known as the cell free zone or zone of Weil (Nanci, 2013). This zone is not always possible to distinguish when the odontoblasts are highly active, but it is generally rich in unmyelinated nerve fibres, capillaries and processes of fibroblasts. More centrally to the cell free zone is the cell rich zone of Höhl, which is densely populated with fibroblasts, undifferentiated mesenchymal stem cells and immune defence cells (macrophages and lymphocytes). More central to this zone is the pulp core, which has similar content to the cell rich zone, however, the cells here are less densely packed and there is a higher density of larger blood vessels and collagen bundles (Nanci, 2013) (Figure 1.3).

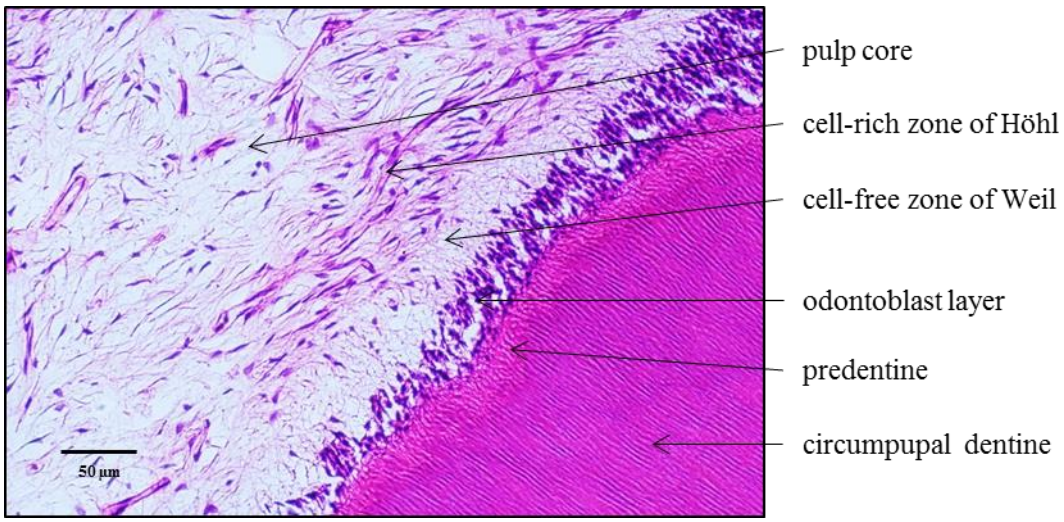

Figure 1.3 Histological section showing the structure of the dentine-pulp complex in a human third molar with H&E staining. (Histological processing was performed by Sue Finney and image captured by the author at x20 magnification)

To enable the study of the homeostatic and reparative events of the dental pulp *in vitro*, numerous different pulp-derived cell lines have been utilised. Immortalised cell lines such

as murine odontoblast-like cells (MDPC-23) (Hanks et al., 1998a) and undifferentiated murine dental pulp cells (OD-21) (Hanks et al., 1998b) have been used extensively. MDPC-23 cells are derived from mouse dental papilla and express odontoblast phenotypic markers such as DPP, DSP, type I collagen, alkaline phosphatase, osteopontin and osteocalcin (Hanks et al., 1998a). Although experiments with these cells have been published widely, cultures tend to comprise of a homogeneous cell type and thus may not provide a true representation of pulp tissue. More recently, heterogeneous populations of primary rat dental pulp cells have been characterised in detail (Patel et al., 2009) and maintenance at a low passage enables the potential for cells to differentiate into those with a phenotypic profile similar to that of odontoblasts.

1.3.1 Cells of the dental pulp

This section reviews the individual specialised cells found within the pulp and which have functions related to tertiary dentine formation.

1.3.1.1 Odontoblasts

Odontoblasts are highly differentiated, post-mitotic cells developmentally derived from the neural crest and whose functions include secretion of dECM during tooth development, tissue homeostasis and responsiveness to noxious stimuli. They have a life-span the same as the viable tooth. Coronal odontoblasts differ from those found in the root canal in terms of their morphology; those lining the crown are elongated and more columnar with a polarised nucleus, whereas those found in the root canal exhibit a more pyramidal morphology. This difference in cell shape may, however, be artefactual due to the density with which odontoblasts are packed into the coronal aspect of the pulp chamber compared with the root (Smith, 2008). The morphology of the odontoblast very much reflects the stage within its life cycle and thus its functional activity (Couve, 1986). In general, odontoblasts characteristically are elongated with a nucleus polarised towards the basal compartment of the cell and a high nuclear to cytoplasmic ratio, especially during cell development. The organelles in an actively secreting odontoblast are prominent; as is typical of a secretory cell, there are extensive rough endoplasmic reticula, numerous golgi apparatus and mitochondria scattered throughout the main cell body. The quiescent odontoblast is shorter and described as being “stubby” with a less polarised nucleus. The numbers of organelles, including rough endoplasmic reticulum, golgi apparatus and mitochondria, are significantly

reduced in quiescent cells and they are located in a more perinuclear arrangement (Smith, 2008).

The odontoblast process is a direct extension of the main cell body beyond the junctional complex. It is sparsely filled with organelles compared with the cell body, which reflects its decreased secretory activity. The process is not a single isolated smooth projection from the cell body as it has numerous lateral branches which may contact other branches from neighbouring processes. The odontoblast process is comprised predominantly of a well-developed cytoskeleton with microfilaments running along its long axis (Holland, 1985, Frank and Steuer, 1988). The extent to which the process extends into the tubule has generated some debate over the years, however, with the use of more sophisticated techniques, it now seems probable that the process only extends to peripheral dentine during development (Byers and Sugaya, 1995, Yoshiba et al., 2002).

The cell bodies of odontoblasts are joined together laterally by desmosomes, which form gap junctions and occluding zones (tight junctions) (Sasaki et al., 1982, Calle, 1985). The inter-odontoblast space allows transfer of intracellular ions and water soluble metabolites and this may act as a communication system leading to changes in secretory activity of the odontoblast (Okiji, 2012). As yet, however, the degree of permeability and the mechanisms, which control flow within this space are not fully understood. Tight junctions around the neck of odontoblasts have been shown to be impenetrable (Turner et al., 1989, Bishop and Yoshida, 1992), however, following cavity preparation a tracer was shown to permeate into predentine and dentine (Turner et al., 1989, Izumi et al., 2001). This suggests that the change in permeability may be a defensive action and increasing fluid outflow towards dentine may prevent inward diffusion of any noxious or infecting agent.

1.3.1.1.1 Odontoblast differentiation

In the early stages of odontogenesis, cells that originate from the neural crest migrate towards the first branchial arch. Differential growth between epithelial cells of the dental lamina and the underlying mesenchyme initiates the formation of a tooth bud. As the dental organ becomes more developed, the most peripheral cells of the dental papilla start to differentiate and become odontoblasts (Smith, 2008). All cells within the dental papilla of the developing enamel organ have the potential to become odontoblasts, however, it is only those that contact the basement membrane of the internal dental epithelium which receive the relevant signals to initiate this process (Ruch et al., 1995). These cells undergo several cycles of cell division and during the last cycle of mitosis, the cells contacting the basement membrane become pre-secretory, pre-polarised odontoblasts. Those dental papilla cells which do not receive this signal form the cells in the subodontoblastic Höhl's layer. During this cycle, the cells move from a position, which is roughly parallel to the basement membrane, to a new orientation, lying perpendicular to it. The pre-odontoblast undergoes major cellular changes and restructuring to develop into a functional cell (Goldberg et al., 2011).

1.3.1.1.2 Secretory activity of odontoblasts

Radiolabelled ^{3}H-proline has been used to demonstrate a pathway of collagen synthesis and secretion in odontoblasts which follows a course typical of cells present in connective tissues. *In vivo* animal experiments have shown that, once taken up into the odontoblast cell bodies, the radiolabelled isotope followed a course from the rough endoplasmic reticulum to the golgi apparatus and was finally exocytosed into the predentine via pre-secretory and

secretory granules (Weinstock and Leblond, 1974, Frank, 1979). Notably, while other matrix components, such as phosphoproteins, glycoproteins and proteoglycans, are secreted along a similar pathway (Weinstock et al., 1972, Weinstock and Leblond, 1973), their route is more rapid and occurs in minutes rather than days. It has been suggested (Linde, 1984) that odontoblasts secrete different components from different surface sites on the cell. Collagen and proteoglycans are secreted from the proximal end of the odontoblasts, whereas specific NCPs are secreted at the distal level close to the mineralisation front. Although this is hypothetical, it may explain why peritubular dentine is collagen poor but rich in NCPs (section 1.2). Indeed, it has also been suggested that NCPs act as nucleators for hydroxyapatite formation (Linde, 1989) at the mineralisation front. It is likely that this is where growth factors, secreted from the active odontoblast, become sequestered in the dentine, however, this is currently only a suggesion and their precise location in dentine is unclear (Smith et al., 1998).

Dentinogenesis does not simply relate to matrix deposition, but rather entails a process of complex remodelling from the transition of predentine to dentine (section 1.2.1). One of the major differences between bone and dentine is the difference in turnover rate and remodelling of the extracellular matrix. It had traditionally been thought that dentine was inert and was not modified once it had matured, however, there is now some evidence of limited endocytosis by odontoblasts (Linde and Goldberg, 1993). Indeed, the odontoblast communicates intimately with its extracellular matrix via its processes and their lateral branches, which form a canalicular network; exchange and remodelling may occur at a level that is undetected, however, this is currently hypothetical.

In order for dentine to be mineralised, significant quantities of mineral ions have to be transferred from the vasculature to the mineralisation front. Although the capillary plexus penetrates the odontoblastic layer, there are still only two routes for this transfer to take place; it can occur either through the inter-odontoblast space or via direct transfer through the odontoblast itself. As previously discussed (section 1.3.1.1), tight junctions exist at the proximal end of the odontoblast and this results in it being a relatively impervious layer, however, it has been demonstrated that calcium ions can pass through this space (Nagai and Frank, 1974). It has also been shown that a transmembranous phosphate and calcium ion transport mechanism exists through the odontoblast (Linde and Lundgren, 1995, Lundquist, 2002). Mineralisation is achieved via the production of matrix vesicles during the formation of mantle dentine; these are rich in adenosine triphosphatase and phosphohydrolytic enzymes and contain a high concentration of mineral ions (Eisenmann and Glick, 1972). It has been suggested that once the mature odontoblast is formed, circumpulpal dentine is mineralised by a process in which extracellular matrix components, secreted by odontoblasts, act as nucleation factors. Recently, it has been shown that hydroxyapatite crystal formation is directed by such secreted components (Qin et al., 2007).

1.3.1.2 Fibroblasts and multipotent cells

Fibroblasts constitute the largest proportion of cells within the pulp and are most densely located in the cell-rich zone, although they can be found throughout the pulp. Their function is to secrete extracellular matrix; when they are active, this secretory function is reflected in their cellular morphology, with numerous rough endoplasmic reticulum and golgi apparatus. When they are quiescent, they appear considerably smaller, spindle shaped and contain far fewer of those organelles involved in the synthesis and secretion of collagen

type I and III, and NCPs. Fibroblasts have been shown to express osteonectin, BSP (Garcia et al., 2003, Martinez and Araujo, 2004) and OPN (Yokota et al., 1992), which are functionally involved in hard tissue formation, as well as growth factors such as isoforms from the TGF-β superfamilies (Sloan et al., 2000, Nakashima et al., 1994, Gu et al., 1996).

A number of different populations of mesenchymally derived stem cells have been identified within the pulp and associated tissues. Any true stem cell is undifferentiated and has the ability to differentiate into several different phenotypes, for instance, into osteoblasts, chondrocytes or adipocytes (Augello et al., 2010). Amongst fibroblasts, within the cell-rich zone and central core of the pulp, undifferentiated mesenchymal cells have been identified and are reported as being multipotent. When isolated by enzymatic digestion *in vitro* from human dental pulps and implanted into immunocompromised mice *in vivo,* these cells were shown to develop into a tissue with a dentine-like structure lined with odontoblast-like cells. The isolated cells were termed 'dental pulp stem cells' (DPSCs) (Gronthos et al., 2000). It has recently been proposed that these cells within pulp tissue act as progenitors and contribute to reparative dentinogenesis (Tecles et al., 2005) (section 1.5.2). Other isolated dental stem cell populations from the pulp include those from human exfoliated deciduous teeth, termed 'stem cells from human exfoliated deciduous teeth' (SHED) (Miura et al., 2003) and those identified in the apical papilla, called 'stem cells from apical papilla' (SCAP) (Sonoyama et al., 2006). It has been proposed that SCAP cells may lead to continued root formation following a treatment procedure called pulp revascularisation, which is performed on an immature tooth that has undergone pulp necrosis (Iwaya et al., 2001, Banchs and Trope, 2004, Thibodeau and Trope, 2007). A more recent study has suggested there is another source of progenitor cells that may originate as pericytes from perivascular tissue (Feng et al., 2011). Although it is established that

progenitor cells are required to participate in reparative dentinogenesis, many questions still remain unanswered with regard to the origin of these cells and whether they are even derived from a pulpal source (section 1.5.2).

1.3.1.3 Immunocompetent cells

For any tissue with a blood supply, the defence system to protect that tissue is supported by immunocompetent cells, recruited from the bloodstream, which become transient inhabitants of the tissue. These cells will respond to foreign antigens and infectious agents, initiating and modulating immune and inflammatory reactions, whilst supporting other cellular processes. Dendritic cells are resident in the pulp and they rapidly accumulate at the odontoblast layer if stimulated by an antigen (Jontell et al., 1988, Yoshiba et al., 1996). It has been proposed that TGF-β1, released from dentine during its degradation by bacteria or iatrogenic agents, may act as a chemotactic factor for dendritic cells and initiate the immune response (Farges et al., 2003). T-lymphocytes would be considered normal residents of the healthy dental pulp, however, B-lymphocytes are rarely found and a specific role in the dental pulp's response during disease has not been identified. T-lymphocytes require specific antigen presentation to activate a response and this is likely to be undertaken by dendritic cells. Once the antigen has been recognised, T-helper cells will orchestrate the immune response, whilst cytotoxic T-cells act directly and attempt to destroy the antigen. Macrophages are found in the dental pulp during health and they reportedly accumulate around the blood vessels, especially in the pulp core. Their primary function is immuno-surveillance and phagocytosis, especially of invading bacteria (Okiji et al., 1992), and they act opportunistically. The inflammatory and immune response associated with the dentine-pulp complex is considered in more detail in section 1.6.2.

1.3.2 Pulp extracellular matrix

Collagen is the major organic constituent of pulp tissue, as it is for dentine. It contributes, by dry weight, 26% in human premolars and 32% in third molars; most of this is collagen type I and III (van Amerongen et al., 1983). The proportion of type III collagen is greater in the pulp than it is in dentine; odontoblasts almost exclusively secrete type I collagen, however, pulp fibroblasts have the ability to secrete both types. Throughout the pulp tissue, there are intensely hydrophilic proteoglycans which create the gel-like consistency of the pulp tissue. Proteoglycans are three dimensional structures, which can be schematically represented as an interdental brush (Okiji, 2012); the proteoglycan core forms the central spine with GAG chains sprouting off the core, represented by the bristles. Many extracellular proteins, including growth factors such as TGF-β1, have binding sites for GAGs, which may regulate the activity of these bioactive molecules. NCPs, such as fibronectin, are distributed throughout the pulp and have been shown by immunolocalisation to form corkscrew fibres that run parallel to odontoblasts, passing from the pulp into predentine (van Amerongen et al., 1984, Yoshiba et al., 1994). Notably, fibronectin has been implicated in the terminal differentiation of odontoblasts during primary dentinogenesis (Lesot et al., 2001). *In vitro,* isolated pulp extracellular matrix and its breakdown products have been shown to act as a chemoattractant for primary pulp cells, suggesting that, during disease, degradation of the pulp extracellular matrix may play an important role in stimulating pulp repair (Smith et al., 2012c).

1.4 General processes in wound healing

The stages of pulpal repair follow a very similar pattern to the wound healing processes described for other tissues within the human body. For a tissue to repair itself following injury, a complex cascade of precisely timed and co-ordinated physiological processes must be initiated; this ultimately leads to tissue regeneration or scar formation if ideal environmental conditions predominate. These overlapping stages are classically divided into four phases: haemostasis, inflammation, cell proliferation and tissue remodelling (Gurtner et al., 2008, Velnar et al., 2009).

1.4.1 Haemostatic phase

When a tissue is punctured in some form and the integrity of the blood supply is breached, a complex clotting cascade is initiated to prevent exsanguination and ensure continuity of the body's vascular supply. Initially, platelets aggregate and form a plug, whilst the affected blood vessels immediately constrict to reduce blood flow to the site of injury. EGF, IGFs, PDGF and TGF-β1 are immediately released from the cytoplasm of platelets at the site of injury (Pool, 1977) and act as chemotactic factors for other cellular process involved in wound healing. The formation of fibronectin amongst the platelet plug provides a provisional matrix, which allows adhesion of leukocytes, fibroblasts and endothelial cells (Laurens et al., 2006); this creates a dynamic environment for subsequent modification and maturation.

1.4.2 Inflammatory phase

Following formation of the initial wound, the surrounding tissue may start to necrose and is at risk of bacterial invasion and infection. To prevent this, early in the healing process (within 24 – 36 hours), neutrophils are recruited through the activation of complement, the exocytosis of platelets and the release of products through the degradation of bacteria (Grose and Werner, 2004). Neutrophils are necessary for the removal and destruction of bacteria and damaged tissue by the process of phagocytosis. Macrophages appear later (approximately 48 – 72 hours) and are formed by the differentiation of monocytes at the wound site. Apart from playing a role in phagocytosis, macrophages provide a pool of growth factors, especially TGF-β family members and others including EGF, FGF and TGF-α, which activate fibroblasts and endothelial cells to initiate tissue repair (Velnar et al., 2009).

1.4.3 Proliferative phase

This subsequent phase occurs between 2 – 10 days post-injury and is characterised by cell proliferation and migration where the fibrin matrix is replaced by granulation tissue. In order for the tissue to mature it needs a nutrient supply, so the development of blood vessels (angiogenesis) in the new tissue is one of the initial steps. Key regulators of angiogenesis include PDGF, VEGF and FGF-2, which are secreted into the wound during the haemostatic phase (Takeshita et al., 1994, Baum and Arpey, 2005).

In vitro, numerous different techniques have been used to mimic these wound healing events and to determine the rate at which mesenchymal cell numbers (e.g. fibroblasts and

stem cells) increase. Traditionally, in monolayer cultures, cell numbers are determined using a counting chamber such as a haemocytometer. However, for large experiments, this can be time consuming so colorimetric assays are commonly used; these utilise a surrogate marker, such as metabolic activity, to calculate cell number from a standard curve produced in a parallel experiment. Examples of these techniques include the MTT assay [3-(4,5-dimethylthiazol-2-yl)-2,5-diphenyltetrazolium bromide] and the WST-1 assay (water soluble tetrazolium salts). Assays to test the ability of agents to act as chemotactic factors include transwell assays, scratch wound assays and 3D matrix invasion assays, amongst others (Eccles et al., 2005).

1.4.4 Remodelling phase

The final phase of wound healing may last for several years and frequently will involve specialised cells, depending on the complexity of the tissue being reformed. For this phase to take place, appropriate signals are required for intracellular signalling to initiate differentiation of progenitor cells. It is not fully understood if these cells originate from local tissue or are recruited from other sources. More recently, circulating mesenchymal stem cells (MSCs) have been shown to enhance reparative mechanisms in a variety of tissue types including the lung (Wong et al., 2009), skin (Sasaki et al., 2008) and gut (Okamoto et al., 2006). The remodelling phase relies on establishing a fine balance between controlling degradation of provisional matrix and synthesising a new, more developed matrix to replace it. Maturation of extracellular matrix includes removing fibronectin and hyaluronic acid, which are replaced with new collagen fibrils, and increasing the diameter of those collagen fibrils initially secreted (Baum and Arpey, 2005). MMPs, produced by neutrophils, macrophages and fibroblasts, are responsible for the breakdown of unwanted

extracellular matrix; this process is regulated by inhibitory factors (Mulder and Vande Berg, 2002, Toy, 2005). As the old matrix is replaced with new, the drivers for controlling these processes are removed and the metabolic activity of this healing / healed tissue decreases until the wound has completely matured.

1.5 Response of the dental pulp to injury

The oral cavity is a hostile environment and the dental pulp comes under attack from a number of different challenges, such as caries, periodontal disease, trauma, iatrogenic damage and anachoresis. In response to some of these noxious agents, the pulp will lay down tertiary dentine in an attempt to protect itself. Tertiary dentine has been sub-classified, based on the mechanism by which it is deposited, into reactionary dentine and reparative dentine (Lesot H. et al., 1993, Smith et al., 1995). Reactionary dentine is defined as, "tertiary dECM secreted by surviving post-mitotic odontoblasts in response to an appropriate stimulus" (Smith, 2012). This stimulus tends to be mild and slowly progressing, such as wear, erosion or slowly developing caries. This response consists of an up-regulation in odontoblastic activity compared with what is normally expected for secretion during secondary dentinogenesis (Figure 1.4). Reparative dentine is defined as, "tertiary dentine secretion by a new generation of odontoblast-like cells in response to an appropriate stimulus, after the death of the original post-mitotic cells responsible for primary and secondary dentine secretion" (Smith, 2012). If favourable environmental conditions prevail, reparative dentinogenesis may occur after a stimulus, such as rapidly progressing caries, trauma or an iatrogenic intervention. Both reactionary and reparative pulpal responses represent repair of a wound and thus will follow the basic outline of events associated with repair of any other connective tissue (section 1.4).

1.5.1 Reactionary dentinogenesis

Although it cannot be accurately determined, the amount of reactionary dentine laid down by the pulp is likely to correlate with the severity and duration of the stimulus. The molecular basis by which this increased odontoblast secretory activity is initiated, or indeed halted, is not fully understood. It has been shown that, in ferrets, lining unexposed cavities with solubilised dECM following very careful cavity preparation resulted in increased reactionary dentine formation (Smith, 1994). The processes leading to upregulation of this odontoblast activity are not known, however, it is proposed that in the case of caries, bacterial acids may cause release of growth factors that initiate intracellular pathways leading to increased secretory activity of odontoblasts (Dung et al., 1995, Cooper et al., 2010).

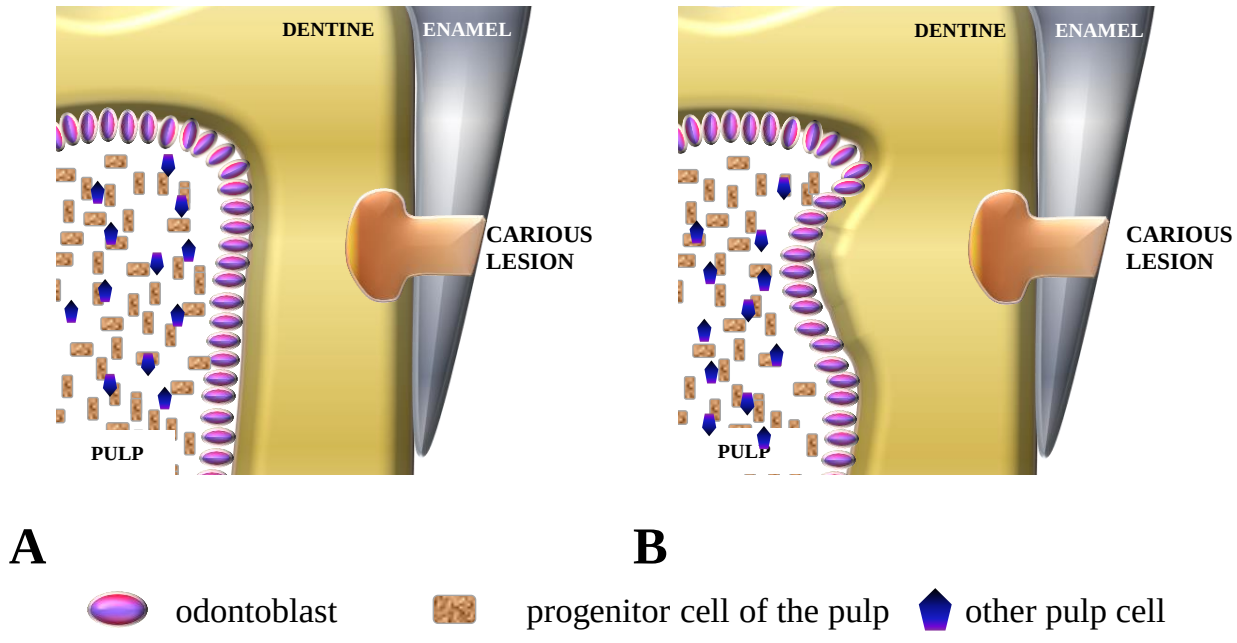

Figure 1.4 A diagram representing a cross-section of the tooth illustrating reactionary dentinogenesis. **A**) A slowly progressing carious lesion presents a relatively mild challenge to the dentine-pulp complex. **B**) The pulp responds by odontoblast up-regulation of their synthetic and secretory activity resulting in a focal deposition of dECM beneath the lesion.

Iatrogenic invention causes tertiary dentine to be laid down; this can be clearly demonstrated in patients through routine sequential radiographs which are taken over a time-course of years. The remaining dentine thickness (RDT) is defined as the thickness of dentine between the base of a cavity and the underlying pulp and is frequently used when describing pulpal responses to iatrogenic interventions. An *in vivo* study of young patients (217 teeth) (Murray et al., 2000) who experienced standardised buccal class V cavities, on teeth that were due to be extracted for orthodontic reasons, showed that the amount of reactionary dentine secretion was greater in younger patients and in those who had deeper and wider cavities. In addition, it was found that the greatest secretion of reactionary dentine occurred when the deepest part of the cavity was between 0.25 - 0.5 mm away from the pulp. If RDT was less than 0.25 mm, no reactionary dentine was secreted suggesting that not all the odontoblasts in this region had survived the iatrogenic intervention. In these cases odontoblast survival was approximately 50% (Murray et al., 2002).

1.5.2 Reparative dentinogenesis

When odontoblasts are injured and subsequently die, it is not possible for odontoblasts adjacent to the wound to migrate, divide and replace the lost functional activity as these cells are fully differentiated and are post-mitotic. Reparative dentinogenesis relies on a much more complex series of events compared with that of reactionary dentinogenesis. This process requires recruitment and proliferation of stem / progenitor cells, their migration, signalling of odontoblast-like cell differentiation and initiation of dentine secretion at the site of tissue injury (Figure 1.5). It is thought that these events are closely aligned with those which occur during embryonic development of teeth (Smith and Lesot, 2001), however, these reparative events remain incompletely understood.

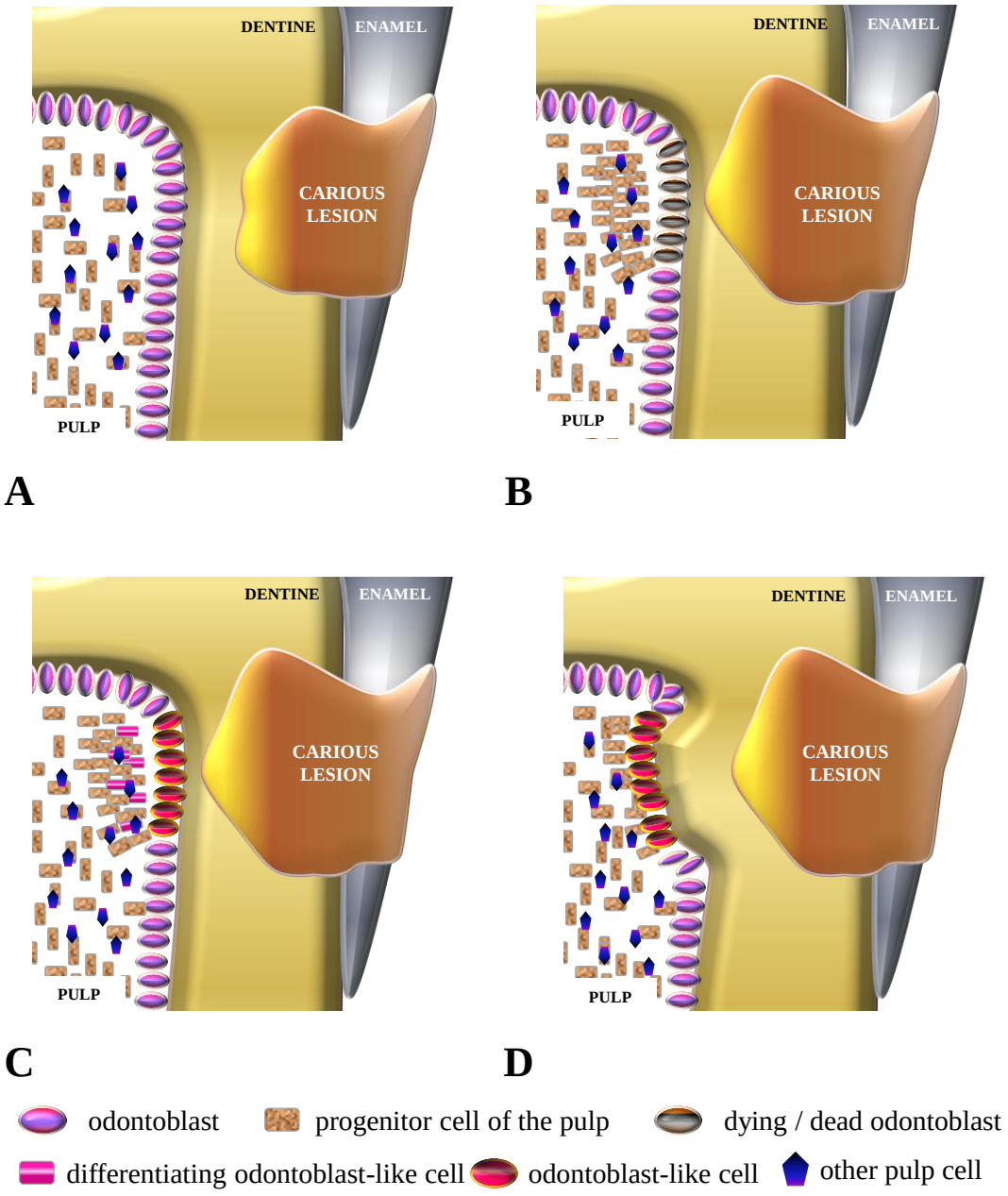

Figure 1.5 A diagram illustrating the process of reparative dentinogenesis. **A**) A rapidly progressing carious lesion presents a more severe challenge to the dentine-pulp complex, and **B**) this results in odontoblast death. However, if the disease process is arrested, a wound repair reaction can occur if favourable environmental conditions prevail. This process will include cell proliferation and migration of progenitor cells. **C**) Progenitor cells differentiate into odontoblast-like cells. **D**) Odontoblast-like cells secrete dECM beneath the lesion which increases the distance between the pulp and the source of assault.

If the odontoblast layer loses its integrity, there may be an initial non-specific response paralleling that seen in normal connective tissue wound healing (section 1.4). The earliest specific response that can be seen is the secretion of a fibrodentine matrix by far less well developed cuboidal cells (Baume, 1980). It is thought that this fibrodentine matrix may contain the relevant signalling molecules for odontoblast differentiation, mirroring the role of the dental basement membrane in primary dentinogenesis (Ruch et al., 1995). However, it is possible that exposure of such molecules on the surface of the existing dECM may provide the necessary stimulus for odontoblast-like cell differentiation. For some time, it was thought that the progenitor cells, which ultimately differentiate into odontoblast-like cells, were recruited from the pulp itself (Fitzgerald, 1979, Fitzgerald et al., 1990) and most likely from the cell rich zone of Höhl (Ruch et al., 1995). More recently, that hypothesis has been questioned and it has been suggested that these cells may originate from pericytes (Feng et al., 2011) or from circulating mesenchymal stem cells / haematopoietic cells (Frozoni et al., 2012). In order for the progenitor cells to localise to the site of injury, there must be appropriate signalling to attract these cells; the molecules responsible for this signalling process are termed chemokines. Recently, both pulp and dentine extracellular matrix have been shown to contain chemotactic factors capable of inducing pulp cell migration *in vitro* (Smith et al., 2012c). Notably, TGF-β1, which has been shown to be present in the dECM, has been shown to be a chemoattractant for inflammatory and repair cells (Pierce et al., 1992) and mitogenic for cells in the subodontoblastic layer (Melin et al., 2000).

Following chemotaxis and recruitment of progenitor cells to the site of injury, appropriate signals are required to initiate differentiation. *In vitro* culture of embryonic dental papillae cells with solubilised dECM components induced a physiological gradient of odontoblast

differentiation, which was inhibited by neutralising antibodies for TGF-β1 (Begue-Kirn et al., 1992). Similarly, in ferrets, treatment of exposed pulps with similar solubilised dECM components led to reparative dentine formation with regular tubular structure (Smith et al., 1990). Combined, these observations suggest that signalling molecules involved with initiating developmental differentiation of odontoblasts are also involved in similar events during reparative dentinogenesis in postnatal teeth. Interestingly, microarray analysis of odontoblasts in early stage (primary dentinogenesis) and late stage (secondary dentinogenesis) has shown that genes involved in the p38 mitogen-activated protein (MAP) kinase pathway were down-regulated in secondary dentinogenesis suggesting that this pathway is critical for regulation of odontoblast secretory activity (Simon et al., 2009). Indeed, during tertiary dentinogenesis when odontoblasts are more active, the p38 MAP kinase pathway was reactivated (Simon et al., 2010) and interestingly, this signalling has been shown to be regulated by TGF-β1 (Ning et al., 2002, Zhao et al., 2004). Clearly, a precise understanding of these events will help to inform dental pulp regenerative strategies in the future.

1.6 Managing the injured pulp

The vitality of the dental pulp can be challenged in many ways, including carious tissue loss, non-carious tooth surface loss, trauma and iatrogenic damage; this can lead to reversible or irreversible changes (Burke and Samarawickrama, 1995). The extent of injury to the pulp is very difficult to determine and clinicians rely on weak empirical evidence, since there is a poor correlation between clinical signs and symptoms and the true histological state of the pulp (Dummer et al., 1980). Ironically, in 1922, not long after the pioneering thesis of Herman (1920), the exposed pulp was described as a "doomed organ" (Rebel, 1922). Unfortunately, that dogma still blights our approach and anecdotally appears to be followed in many undergraduate teaching programmes even though our understanding of the reparative mechanisms of the dentine–pulp complex is now so much greater and maintaining vitality of the dental pulp is known to be advantageous to the patient in many ways. Following pulpal injury, the vitality of the pulp can be maintained therapeutically in one of three ways: indirect pulp cap, direct pulp cap and pulp amputation / pulpotomy. Classically, a definition of indirect pulp capping would include "the stepwise excavation of caries", however, more pragmatically, it would be defined simply as a procedure during which a lining material is placed in a deep cavity close to the pulp in order to encourage a favourable response. A direct pulp cap is defined as a procedure in which the pulp is covered with a protective dressing or base placed directly over the pulp at the site of exposure [European Society of Endodontology (2006)]. Pulp amputation or pulpotomy is when part of the exposed pulp is removed, leaving some intact undisturbed tissue in which a therapeutic agent is placed in order to maintain its vitality. Pulpectomy, included here for completeness only, is total removal of the pulp when it is considered irreversibly inflamed

and root canal treatment is subsequently required [European Society of Endodontology (2006)].

Successful maintenance of pulp vitality following injury has numerous benefits. It preserves the tooth's defence system, avoids pulpectomy and subsequent root canal treatment (costly and likely to weaken the tooth), avoids extraction of the tooth with its subsequent disadvantages, and ensures continued development of the dento-alveolar complex particularly in younger patients. With an increasing understanding of pulp biology, the precision of operative techniques improving (Stanley, 1989, Simon et al., 2013) and patients' expectations growing, it is likely that procedures to maintain pulp vitality will become increasingly commonplace; this, in turn, should lead to more predictable results.

As already discussed, vital pulp treatment has sometimes been viewed with scepticism (Rebel, 1922); this has probably been compounded by the lack of evidence that exists due to the paucity of good quality clinical research (Miyashita et al., 2007, Olsson et al., 2006). Numerous different techniques and procedures have been investigated during the last ninety years (Miyashita et al., 2007), however, inconsistencies in the study conditions and the techniques used means that robust comparisons cannot readily be drawn. From a biological standpoint, there are three key issues to consider when undertaking pulp treatment - the microbial challenge, the inflammatory challenge and the choice of pulp capping agent. These three factors are explored in more detail below.

1.6.1 The microbial challenge

It was not until 1965, when the classic study by Kakehashi et al. was performed on germ-free rats, that microorganisms were shown unequivocally to play a role in the aetiology of pulpal and periradicular disease. Prior to this, there had, however, been suggestions that this might be the case and that the microbial challenge could be the primary cause of pulpal and periradicular disease (Miller, 1894). Kakehashi et al. (1965) exposed the pulps of a group of germ-free rats, which were maintained in sterile conditions, and a group of conventional rats, which were maintained in standard laboratory conditions for the test period of up to 42 days. Histological analysis, performed on the exposed teeth of both groups, showed that the exposed teeth of normal rats had signs of gross inflammation, pulp necrosis and periradicular disease. However, in the germ-free rats there was little inflammation and in those sacrificed later in the study, there was evidence of pulp healing and dentine bridge formation. Under normal conditions, the dentine-pulp complex is sterile and it is only subject to microbial challenge if breached by trauma, periodontal disease, an operative intervention or, most commonly, carious disease. The vital pulp is often able to resist this microbial challenge by laying down peritubular dentine and reactionary dentine, whilst also increasing the release of host defence molecules, such as antibodies and complement, in dentinal fluid (Ackermans et al., 1981, Okamura et al., 1980, Okamura et al., 1979, Pashley, 1996); however, even if the carious process only reaches the peripheral dentine, pulpal inflammation may still be present (Brannstrom and Lind, 1965). Furthermore, increasing the duration of the microbial contamination of the pulp is known to decrease the chance of successful pulpal healing (Masterton, 1966, Torneck et al., 1983, Kakehashi et al., 1969, Cox et al., 1982). It is very difficult to determine the degree of microbial load and the duration of the microbial challenge, and there are few clinical studies which attempt to

address this issue (Olsson et al., 2006). It is clear, however, that minimising the microbial challenge, posed by caries or due to microleakage around restorations, remains the most important determinant of success in preventing pulpal disease progression and indeed, in achieving a predictable treatment outcome once the pulp is injured (Kakehashi et al., 1965, Brannstrom and Nyborg, 1973, Bergenholtz, 1977, Bergenholtz et al., 1982).

1.6.2 The inflammatory and immune challenge

The odontoblast process acts like an outpost to the cellular defence system of the dental pulp; from its strategic position, it can identify early bacterial invasion and initiate mediation of various host defence mechanisms (Fouad, 2012). Although the odontoblast is a terminally differentiated cell, it plays an important role in mediating the interplay between immune and reparative responses of the dental pulp when exposed to an injurious challenge (Cooper et al., 2011, Cooper et al., 2010). Odontoblast cell surface receptors, including members of the Toll-like family (TLR 1-6 and 9), have been shown to sense bacterial components, such as lipoteichoic acid (LTA) and lipopolysaccharide (LPS), which are present in the cell wall of gram positive and negative bacteria. The odontoblasts then release chemokines that recruit immune cells such as dendritic cells and T-lymphocytes, which subsequently propagate the immune response (Durand et al., 2006, Farges et al., 2003, Nomiyama et al., 2007, Veerayutthwilai et al., 2007). Dendritic cells have been shown to establish a close spatial relationship with odontoblasts which are under carious attack; they can induce odontoblast differentiation and increased activity in terms of secretion of dECM (Ohshima et al., 1995). Notably, pro-inflammatory cytokines are involved in this process and include interleukin-1α (IL-1α), interleukin-2α (IL-2α) and tumor necrosis factor (TNF-α) and these regulate the inflammatory reaction in response to

bacterial components (Hosoya et al., 1996, Matsuo et al., 1994, McLachlan et al., 2004, Pezelj-Ribaric et al., 2002). Interestingly, amongst other pro-inflammatory cytokines, IL-1α has been shown to be solubilised *in vitro* from dECM by lactic acid and calcium hydroxide (Cooper et al., 2010).

Bacterial infection of the dental pulp leads to the activation of complex inflammatory processes. This response is originally initiated, as discussed earlier, by odontoblasts and subsequently by pulp fibroblasts (Staquet et al., 2008) via signalling through TLRs; this leads to the further release of pro-inflammatory cytokines and chemokines. This complex cocktail is supplemented by other pro-inflammatory cytokines from the dECM, which may initiate wound healing events driving either reactionary or reparative dentinogenesis, depending on the severity of the assault (Cooper et al., 2010). Longstanding chronic inflammation, however, will tend to lead to pulpal death. There is therefore a fine balance between the positive drivers from the inflammatory and immune response, which lead to pulp regeneration, and the negative ones, which are detrimental to the pulp's vitality (Goldberg et al., 2008, Smith et al., 2012b).

1.7 Pulp capping – material selection

Numerous different materials have been used as direct pulp capping agents; these have included gold foil (Pfaf, 1756, Dammaschke, 2008), aqueous calcium hydroxide (Heys et al., 1981), commercial preparations of calcium hydroxide (Stanley and Lundy, 1972), glycyrrhetinic acid / antibiotic mixture (Shovelton et al., 1971), resin bonding agents (Horsted-Bindslev et al., 2003), corticosteroid / antibiotic mixture (Cowan, 1966), isobutyl cyanoacrylate (Bhaskar et al., 1972), resin modified glass ionomer (do Nascimento et al.,

2000) and more recently, calcium silicate cements such as mineral trioxide aggregate (MTA) (Aeinehchi et al., 2003, Nair et al., 2008). The aim of using these materials in pulp capping is to induce a hard tissue barrier between the injured pulp and the restoration being placed in the tooth, thus maintaining the tooth's vitality. The properties of a direct pulp capping agent should ideally include [adapted from (Cohen and Combe, 1994)]:

- Antibacterial activity
- Creation of a bacterial tight seal and prevention of microleakage
- Promotion of tertiary dentinogenesis and controlled hard tissue barrier formation
- Biocompatibility – prevention of 'over' irritation and avoidance of induction of a severe inflammatory response
- Radiopacity
- Ease of clinical handling
- Resistance to forces of displacement of any subsequent material placed over the pulp capping agent

No material is known to demonstrate all of these properties, however, there is clinical and laboratory evidence to show that calcium hydroxide and the calcium silicate cement, MTA, satisfactorily meet these requirements, at least in part. Evidence is increasingly emerging that MTA induces a more predictable pulp healing response than calcium hydroxide (Aeinehchi et al., 2003, Nair et al., 2008); this is clearly illustrated in Figure 1.6.

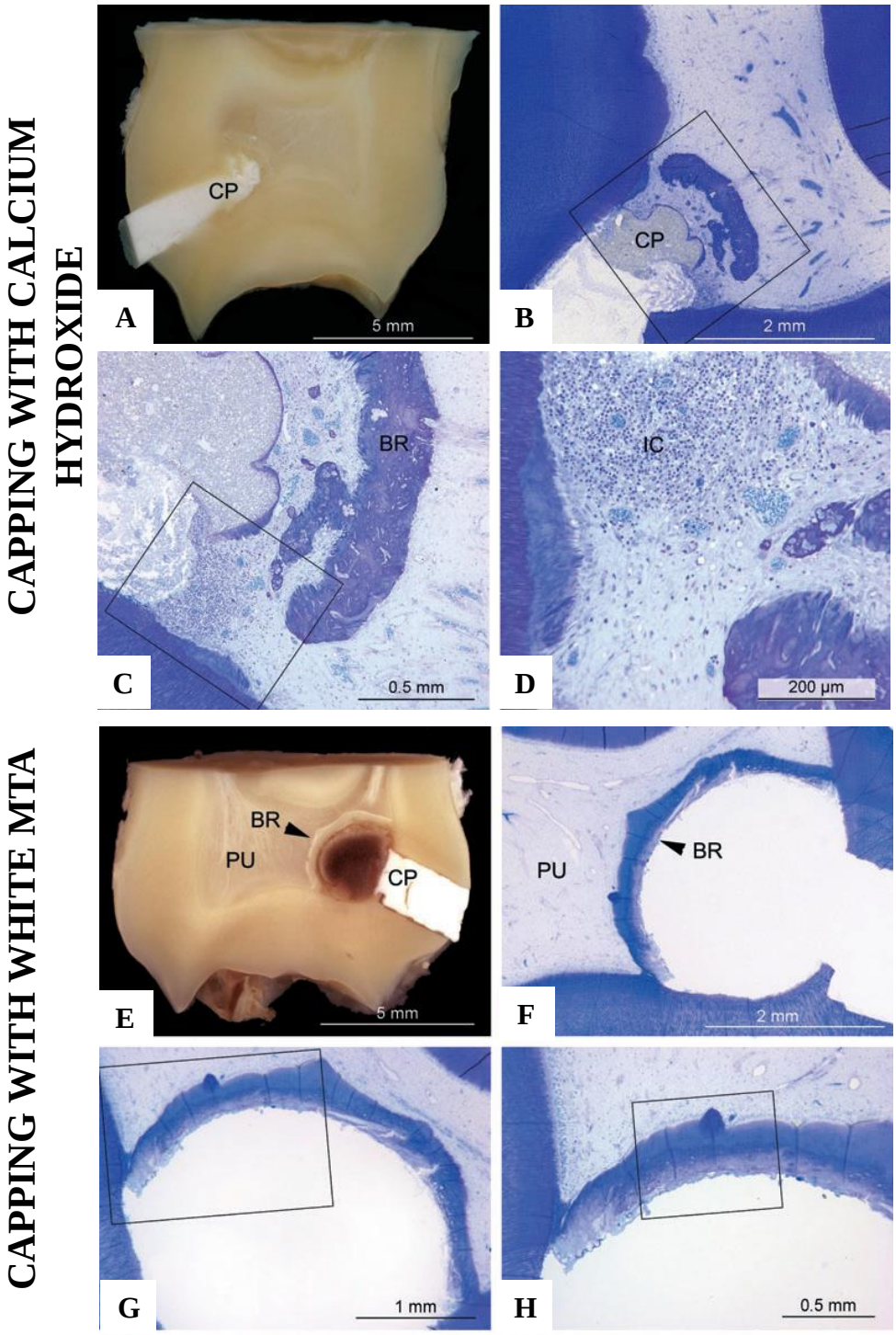

Figure 1.6 Pulpal response 3 months after inducing an iatrogenic pulp exposure in aseptic conditions in human third molars and capping with calcium hydroxide or white MTA. **A**) Macrophotographic view of mesial half of third molar showing calcium hydroxide (CP) placed into pulp with hard tissue response. **B, C and D**) Histological section of (**A**) showing incomplete dentine bridge (BR) (tunnel defect) with chronic inflammatory cell infiltrate (IC). **E**) Macrophotographic view of mesial half of third molar showing white MTA (CP) placed into pulp with hard tissue response. **F, G and H**) Histological section of (**E**) showing complete hard tissue barrier (BR) organisation of pulp tissue and no evidence of inflammatory cell infiltrate. (Histological sections embedded in epoxy resin and stained with periodic acid-Schiff and methylene blue-azur II). Images reproduced from Nair et al., 2008, with permission (John Wiley and Sons) and thanks to H.F.Duncan.)

1.7.1 Calcium hydroxide

Numerous different materials have been used as pulp capping agents over the years with varying degrees of success, however, generations of clinicians have returned to using calcium hydroxide, which is considered the 'gold standard' (Goldberg et al., 2008). This agent has been in use for over ninety years (Hermann, 1920) and has been intensively researched during this time (Glass and Zander, 1949, Schroder, 1972, Stanley and Lundy, 1972, Schroder, 1973, Tronstad, 1974, Pitt Ford, 1979, Schroder, 1985, Pitt Ford and Roberts, 1991). Indeed, direct pulp capping studies using calcium hydroxide on non-experimental pulp exposures that were carious or induced by trauma have demonstrated clinical success rates of 80–90% (Baume and Holz, 1981, Ravn, 1982, Matsuo et al., 1996).

There is still considerable debate about the mode of action of calcium hydroxide; numerous animal studies have shown histological dentine bridge formation in 50-87% of teeth treated (Brannstrom et al., 1979, Heys et al., 1981, Cox et al., 1982, Cox et al., 1985, Pitt Ford, 1985) but this is, however, less predictable in humans (Aeinehchi et al., 2003, Chacko and Kurikose, 2006, Nair et al., 2008). It has been suggested that its action is related to its caustic nature; it has a high pH of 11-12, which initially induces tissue irritation and superficial necrosis, known as a zone of coagulation necrosis (Glass and Zander, 1949). For clinical application, calcium hydroxide is either mixed as a pure powder with an aqueous solution (water or saline) or is more commonly used as a commercially available hard setting wound dressing / lining material, such as Life® (Kerr, Boggio, Switzerland) or Dycal® (Denstply Caulk, Milford, DE, USA), with a number of different types of vehicles (Fava and Saunders, 1999). Aqueous suspensions have been shown to induce wider zones of necrosis compared with commercial preparations (Heys et al., 1981). In a histological

study using rhesus monkeys by Heys et al. (1981), wound healing occurred at the material interface when commercial preparations were used, however, for calcium hydroxide paste formed with saline, the reparative tissue formation was some distance from the material itself, leaving a persistent vacant zone. The hard setting materials resulted in less evidence of caustic damage and it appears that the necrotic zone was removed by phagocytosis and replaced with granulation tissue (Stanley and Lundy, 1972). In a more recent study in humans (Lu et al., 2008), one week of pulp capping with calcium hydroxide resulted in a moderate inflammatory infiltrate, disorganised tissue with hyperaemia and no evidence of a hard tissue barrier. At one month, the majority of samples showed a reduced inflammatory response with evidence of dECM secretion and partial hard tissue repair. This is consistent with earlier reports, which suggested that hard tissue healing next to calcium hydroxide was unpredictable and not complete across the wound, with numerous tunnel defects being present (Cox et al., 1996).

The mechanisms by which calcium hydroxide induces hard tissue repair are not entirely understood (Smith, 2002). However, it has been suggested that the superficial necrotic layer acts to separate the vital tissue from the wound so that the pulp can repair itself (Schroder, 1985). Others have postulated that it is the creation of a supersaturated environment of calcium ions adjacent to the pulp that induces hard tissue healing. This latter hypothesis was, however, subsequently disproved when it was demonstrated that the calcium ions, which were incorporated into the mineralised dentine bridge, originated from the underlying tissues rather than the pulp capping material itself (Pisanti and Sciaky, 1964, Sciaky and Pisanti, 1960). It has also been proposed that the tissue may respond favourably to the high pH environment, which is created by the release of hydroxyl ions (Kardos et al., 1998). Without doubt, the bactericidal nature of calcium hydroxide brought about by its

high pH, provides an environment which is conducive to pulp survival (Kakehashi et al., 1969, Kakehashi et al., 1965). In studies in which exposed pulps were purposely infected with bacteria prior to pulp capping with calcium hydroxide, dentine bridges were still formed in a high percentage of cases (Pitt Ford, 1985, Cox et al., 1985). These findings suggest that the bactericidal nature of calcium hydroxide is an important property of the material. More recently, it has been shown that calcium hydroxide can solubilise growth factors sequestered in dentine; this is thought to initiate the sequence of reparative events which leads to tertiary dentine formation (Graham et al., 2006).

Although numerous studies have demonstrated successful pulp healing with calcium hydroxide, many clinicians view its use in pulp capping with scepticism. A 5 and 10 year retrospective analysis of 123 calcium hydroxide pulp capping procedures performed on carious exposures showed that 45% had failed in the 5 year group and 80% had failed in the 10 year group (Barthel et al., 2000). In another retrospective analysis of 248 teeth, with follow up of 0.4-16.6 years (mean 6.1 ±4.4 years), overall survival rate was found to be 76.3% after 13.3 years (Dammaschke et al., 2010). Pulp capping in patients that were over 60 years showed a considerably less favourable outcome than in patients younger than 40 years old. All forms of calcium hydroxide, including the hard setting variants, are easily solubilised; this poses a challenge for long term restorative success when it is used as a lining material or pulp capping agent, because even the best restorative materials available will inevitably undergo some form of microleakage. Under amalgam restorations, Dycal has been shown to be relatively soft in 70% of cases (Pereira et al., 1990) and furthermore, it undergoes significant wash out (Novickas et al., 1989) so although it is bactericidal, it does not maintain a durable seal against bacterial microleakage (Cox and Suzuki, 1994).

1.7.2 Mineral trioxide aggregate

MTA was developed in the 1990s by Mahmoud Torabinejad (Lee et al., 1993) and is now widely thought of as the first choice material for managing endodontic problems which require a material to interface with the pulp (Nair et al., 2008) or periradicular tissues (Saunders, 2008). It was approved by the U.S. Food and Drugs Administration (FDA) in 1998 as ProRoot MTA Original (Dentsply Tulsa Dental, Oklahoma, USA). The original grey version was ostensibly developed as an agent to seal the root canal from the periradicular tissues, however, it was also found to be biocompatible when interfacing with pulpal tissue and showed promise as a therapeutic pulp capping agent. The original grey variety caused issues in terms of aesthetics when it was used for pulp treatment in anterior teeth; a white variety was therefore developed and subsequently, in 2001, FDA approval was granted for this version, ProRoot MTA (Dentsply Tulsa Dental, Oklahoma, USA). It has since become apparent that both varieties of MTA cause discolouration and it is recommended that neither should be used in the aesthetic zone (Lenherr et al., 2012, Ioannidis et al., 2013). MTA is presented as a fine hydrophilic powder, which is mixed with water, at a specific powder to water ratio, to obtain a workable "sandy" consistency. The composition is complex and predominantly based on ordinary Portland cement (OPC). The original patent (Torabinejad and White, 1995) says that "Portland cement should remain as its principle embodiment" and even suggests the preferred brand (Figure 1.7). Comparisons of OPC and ProRoot MTA using sophisticated methodologies, such as energy dispersive X-ray analysis (EDXA) (Dammaschke et al., 2005, Camilleri et al., 2005, Asgary et al., 2009), X-ray diffraction (XRD) (Camilleri et al., 2005) and X-ray photoelectron spectroscopy (XPS) (Dammaschke et al., 2005), demonstrate the basic similarities between the materials, however, the absence of bismuth oxide, the radiopaque agent in ProRoot MTA, is noted.

Broadly, MTA contains calcium oxide (50-75 mass%), silicone dioxide (15-25 mass%) and aluminium oxide (2-5 mass%) (Darvell and Wu, 2011). The original grey form of MTA contains ferric oxide, however, this is absent in the white version. Calcium sulphate is also added to modify handling and setting characteristics.

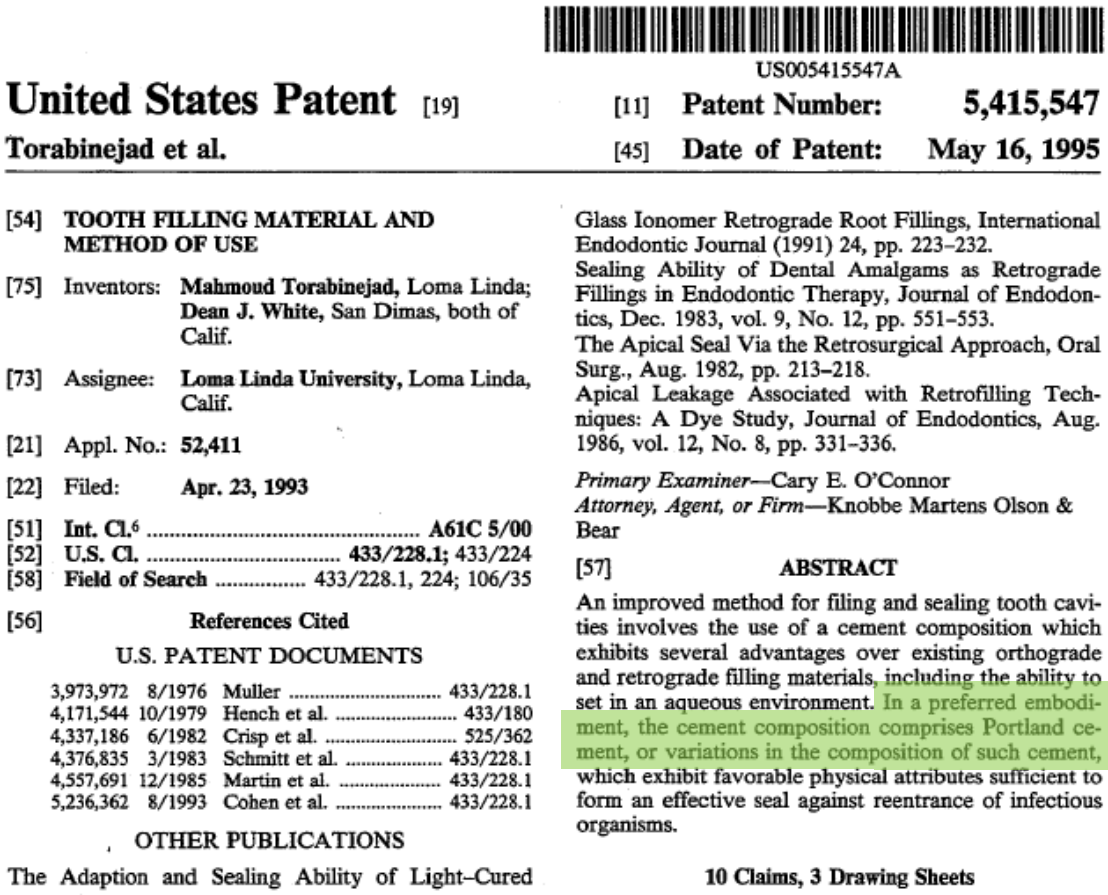

US005415547A

United States Patent [19]

Torabinejad et al.

[11] **Patent Number: 5,415,547**

[45] **Date of Patent: May 16, 1995**

[54] **TOOTH FILLING MATERIAL AND METHOD OF USE**

[75] Inventors: **Mahmoud Torabinejad,** Loma Linda; **Dean J. White,** San Dimas, both of Calif.

[73] Assignee: **Loma Linda University,** Loma Linda, Calif.

[21] Appl. No.: **52,411**

[22] Filed: **Apr. 23, 1993**

[51] **Int. Cl.**[6] **A61C 5/00**
[52] **U.S. Cl.** **433/228.1;** 433/224
[58] **Field of Search** 433/228.1, 224; 106/35

[56] **References Cited**

U.S. PATENT DOCUMENTS

3,973,972	8/1976	Muller	433/228.1
4,171,544	10/1979	Hench et al.	433/180
4,337,186	6/1982	Crisp et al.	525/362
4,376,835	3/1983	Schmitt et al.	433/228.1
4,557,691	12/1985	Martin et al.	433/228.1
5,236,362	8/1993	Cohen et al.	433/228.1

OTHER PUBLICATIONS

The Adaption and Sealing Ability of Light–Cured Glass Ionomer Retrograde Root Fillings, International Endodontic Journal (1991) 24, pp. 223–232.
Sealing Ability of Dental Amalgams as Retrograde Fillings in Endodontic Therapy, Journal of Endodontics, Dec. 1983, vol. 9, No. 12, pp. 551–553.
The Apical Seal Via the Retrosurgical Approach, Oral Surg., Aug. 1982, pp. 213–218.
Apical Leakage Associated with Retrofilling Techniques: A Dye Study, Journal of Endodontics, Aug. 1986, vol. 12, No. 8, pp. 331–336.

Primary Examiner—Cary E. O'Connor
Attorney, Agent, or Firm—Knobbe Martens Olson & Bear

[57] **ABSTRACT**

An improved method for filing and sealing tooth cavities involves the use of a cement composition which exhibits several advantages over existing orthograde and retrograde filling materials, including the ability to set in an aqueous environment. In a preferred embodiment, the cement composition comprises Portland cement, or variations in the composition of such cement, which exhibit favorable physical attributes sufficient to form an effective seal against reentrance of infectious organisms.

10 Claims, 3 Drawing Sheets

Figure 1.7 A copy of the original patent for MTA. Highlighted in the abstract is the suggestion that the preferred embodiment of the cement is Portland cement. Later in the patent a preferred brand of Portland cement is suggested, "Colton Fast-Set brand (California Portland Cement Company, USA)".

1.7.2.1 Other calcium silicate cements

As MTA gained in popularity, it was inevitable that other manufacturers would begin to develop similar materials, particularly because the commercial patent was relatively weak. MTA Angelus (Angelus Soluções Odontológicas, Londrina, Brazil) was recently developed and is available in grey and white forms; it does not contain calcium sulphate (Oliveira et al., 2007, Camilleri et al., 2012), which may explain its shorter setting time of 10-15 minutes (Song et al., 2006, Santos et al., 2008). As ProRoot MTA and MTA Angelus are based on OPC and thus manufactured from naturally occurring raw materials, it is conceivable that they contain traces of heavy metals such as arsenic, lead and chromium (Duarte et al., 2005, De-Deus et al., 2009, Camilleri et al., 2012). In an attempt to prevent this contamination, other manufacturers use pure laboratory grade materials. More recently, the dental materials Bioaggregate (Innovative Bioceramix Inc. Vancouver, Canada) and Biodentine® (Septodont, Saint Maur des Fosses, France) have been manufactured using this approach. Bioaggregate is composed predominantly of calcium silicate oxide and calcium silicate. Hydroxyapatite, calcium phosphate silicate and calcite are also present, with tantalum oxide used as the radiopacifier (Park et al., 2010). Biodentine® powder predominantly consists of tri-calcium silicate as the core material with di-calcium silicate, calcium carbonate (filler), iron oxide (shade) and zirconium oxide (radiopacifier). It differs from other materials in this restorative category because its liquid phase has active components, for example, calcium chloride (accelerator) and a hydrosoluble polymer (reducing agent) (Richard, 2010). As a result, the powder to liquid ratio is more precise than other brands of MTA and it is mixed in an encapsulated form.

Given that there are now a number of dental materials, which are chemically related to MTA, it would seem pertinent to introduce a generic name to describe this group, particularly because MTA is not an accurate description of the material itself and has developed more into a brand / trade name. For standardisation purposes and to prevent confusion for teaching and research, a generic class name should be used. All of these materials primarily consist of calcium silicates and therefore, it would appear prudent to call them calcium silicate cements, however, this does not accurately distinguish them from acid-base calcium silicates that were used in dentistry previously (Johnson, 1908, Voelker, 1916). Darvell and Wu (2011) recently proposed the generic term hydraulic silicate cements (HSC) for this new group of materials. Although this term more accurately reflects the chemical composition of these materials, it appears from recent scientific literature that the term calcium silicate cements is preferred and therefore, this term will be used henceforth in this text.

1.7.2.2 Manufacture and setting reaction

Patented in 1824 (Aspdin, 1824), Portland cement has been used consistently in civil engineering since 1850 (Blezard, 1998); surprisingly, despite its considerable role in construction, its precise setting reaction still remains unclear.

Both OPC and MTA are produced via a basic manufacturing process, which generates a fine powder that, when hydrated, sets to form solid cement. The manufacturing process includes blending the various constituents and heating them to 1400-1500 °C; this is known as ‘clinkering’ and the resultant product as the ‘clinker’. Darvell and Wu (2011) have recently outlined the chemical reactions that occur both during the manufacture of calcium

silicate cements (Figure 1.8) and during their subsequent hydration when used clinically (Figure 1.9). During the manufacture of MTA, the sintering of the raw materials predominantly forms tri- and di- calcium silicates (Figure 1.8 ①). Limestone (calcium carbonate), which is found in OPC, will produce calcium oxide and carbon dioxide gas (Figure 1.8 ②). Depending on the purity of the initial materials used, oxides of their related metal may be formed, for example sodium, potassium and magnesium oxide, as in the case of ProRoot MTA Original. Those materials containing aluminium will also form tri-calcium aluminate (Figure 1.8 ③) Subject to the blend of initial materials used, it is likely that unreacted calcium oxide will remain. The clinker, which will be fused as blocks or large particles, is ground into fine particles. With some forms of calcium silicate cements, a modifier such as calcium sulphate (gypsum) is added; this is the case for ProRoot MTA.

$$CaO + MO.SiO_2.xH_2O \rightarrow 3CaO.SiO_2 + 2CaO.SiO_2 + MO + H_2O\uparrow \quad ①$$

$$CaCO_3 \rightarrow CaO + CO_2 \quad ②$$

$$CaO + Al_2O_3 \rightarrow 3CaO.Al_2O_3 \quad ③$$

Figure 1.8 Outline of chemical reactions and resultant products formed during the clinkering process in the manufacture of calcium silicate cements [adapted from Darvell and Wu (2011)].

The hydration reaction is complex and dependent upon the proportions of each reactant, the presence of impurities and the temperature (varies as the reaction is exothermic). This chemical reaction is summarised in Figure 1.9. In brief, the presence of water will cause calcium oxide to react immediately and produce calcium hydroxide (Figure 1.9 ④). If tri-calcium aluminate is present, this also reacts rapidly to form a succession of hydrates (Figure 1.9 ⑤). The resultant products can produce a diffusion barrier which may inhibit further downstream reactions. If a sulphate is present (e.g. modifier - calcium sulphate), opposing reactions will dictate (Figure 1.9 ⑥). This will prevent further reactions until all

of the sulphates are consumed, acting somewhat like a retardant. The core reaction is the formation of calcium silicate hydrate from the hydration of tri- and di- calcium silicates (Figure 1.9 ⑦). In summary, once set, calcium silicate cements form a hydrated calcium silicate matrix interspersed with calcium hydroxide crystals. If other reactants are present, such as aluminium oxide or calcium sulphate, crystalline products of hydrated calcium aluminate and sulphate aluminates will also be present.

$$CaO + H_2O \rightarrow Ca(OH)_2 \quad ④$$

$$3CaO.Al_2O_3 \rightarrow 2CaO.Al_2O_3.8H_2O \rightarrow 4CaO.Al_2O_3.19H_2O \rightarrow 3CaO.Al_2O_3.6H_2O \quad ⑤$$

$$3CaO.Al_2O_3 + SO_4^{2-} + H_2O \rightarrow 3CaO.Al_2O_3.3CaSO_4.32H_2O \rightarrow 3CaO.Al_2O_3.CaSO_4.12H_2O \quad ⑥$$

$$3CaO.SiO_2\ ,\ 2CaO.SiO_2 + H_2O \rightarrow 9CaO.5SiO_2.11H_2O \quad ⑦$$

Figure 1.9 Outline of chemical reactions and resultant products formed during hydration of calcium silicate cements for clinical use [adapted from Darvell and Wu (2011)].

The setting time for ProRoot MTA and other similar materials is considered to be between 2-4 hours according to manufacturers' instructions, however, like OPC, these materials mature over a long period of time depending on their environment. Hardened OPC and calcium silicate cements have a continuous pore system with hydraulic radii (defined as the ratio of the volume to the surface area of a pore faction), between <1 – 1000 nm (Odler, 1993). The initial water to powder ratio affects total pore space. Generally, the total pore space is equivalent to the initial water to powder ratio; therefore, increasing the water to powder ratio increases pore space (Odler, 1993, Fridland and Rosado, 2003). As a result, this means that if the set cement is in a moist or aqueous environment, the fluid is likely to penetrate the surface of the cement and there will be ionic exchange between the cement

surface and the fluid surrounding it. Reports regarding the degree of solubility of MTA have not been consistent, with most indicating low or no solubility (Poggio et al., 2007, Shie et al., 2009) whilst others have suggested that the material is soluble over a longer period of time (Fridland and Rosado, 2005). Inconsistencies are likely to be due to the different methodologies used and the variable interpretations of the term solubility (Parirokh and Torabinejad, 2010). Due to the complex chemical composition of calcium silicate cements, it is not surprising that a number of different leachable ions are liberated from the cement surface in an aqueous environment (Table 1.2).

Table 1.2 Summary of ions leached from white and grey ProRoot MTA. * Presence confirmed but concentration not reported.

Type of calcium silicate cement	Chemical component determined as present	Concentration	Reference
Grey MTA (ProRoot - Tulsa Dental, Dentsply, USA)	Calcium (Ca^{2+}) Potassium (K^{+}) Sodium (Na^{+}) Iron (Fe^{3+}) Sulphate (SO_4^{2-})	482.00 (mg/L) 45.20 (mg/L) 21.40 (mg/L) 4.96 (mg/L) 5.20 (mg/L)	(Fridland and Rosado, 2003)
White MTA (ProRoot - Tulsa Dental, Dentsply, USA)	Chromium(Cr) Arsenic (As) Lead (Pb)	0.84 (mg/Kg) 0.39 (mg/Kg) 0.02 (mg/Kg)	(Schembri et al., 2010)
White MTA (ProRoot - Tulsa Dental, Dentsply, USA)	Calcium Potassium Sodium Magnesium Silicone Bismuth Phosphorous Aluminium Iron	12368 (µg/g) * * * * 3.62 (µg/g) * * *	(Camilleri, 2010)

1.7.2.3 Biological properties of calcium silicate cements

In order for a material to be regarded as clinically successful as a pulp capping agent, it should demonstrate a number of important properties (section 1.7). Since its introduction, MTA has undergone extensive *in vitro* and *in vivo* analysis as a clinical material that interfaces with the pulpal and periradicular tissues and subsequently, it has been described as "one of the least cytotoxic dental materials commercially available" (Torabinejad and Parirokh, 2010).

The antimicrobial and antifungal effects of MTA have been extensively analysed, with conflicting results reported. MTA was shown to have an antibacterial effect on some facultative bacteria, but no effect on any strict anaerobes, while in contrast, this study showed that zinc oxide-eugenol based materials that were tested in parallel showed inhibition of growth amongst both types of bacteria (Torabinejad et al., 1995c). An assessment using unimicrobial and polymicrobial broths of bacteria and fungi showed that MTA inhibited fungal and microbial growth in both types of culture (Estrela et al., 2000). Interestingly, grey MTA was shown to inhibit similar amounts of growth of *S. sanguis* and *E. faecalis* at lower concentrations than white MTA suggesting that it may have greater antibacterial activity (Al-Hezaimi et al., 2006). Attempts have been made to enhance the antibacterial properties of MTA by combining it with chlorhexidine instead of water, at concentrations of 0.12% (Stowe et al., 2004) and 2% (Holt et al., 2007), both of which proved successful, however, other authors have expressed doubts about its utility in terms of biocompatibility (Hernandez et al., 2005) and deterioration of physical characteristics (Holt et al., 2007). Although *in vitro* micro-leakage studies are frequently viewed with scepticism (Rechenberg et al., 2011, Wu and Wesselink, 1993, De-Deus, 2008), they are

the main means of determining the ability of a material to create a barrier to prevent bacterial penetration in a given clinical scenario. Numerous different *in vitro* techniques have been used to compare the sealing ability of MTA to other materials used in the same clinical situation. MTA has been shown to be superior to amalgam, super EBA (ethoxy benzoic acid) and intermediate restorative material (IRM) using different techniques including dye leakage (Torabinejad et al., 1994, Martell and Chandler, 2002), fluid filtration (Wu et al., 1998, Karlovic et al., 2005) and bacterial penetration studies (Torabinejad et al., 1995d, Fischer et al., 1998, Tang et al., 2002). Notably, MTA is recognised as providing a good seal when used for a number of different clinical applications.

The biocompatibility of MTA has been tested rigorously *in vitro* and *in vivo*. Early studies in dogs showed that the histological response of the periradicular tissues was more favourable when MTA, rather than amalgam, was used as a root end filling material (Torabinejad et al., 1995a); similarly, the histological response was better when MTA rather than a calcium hydroxide based sealer (Sealapex, SybronEndo, California, USA) was used to repair root perforations (Holland et al., 2001). Numerous studies have used monolayer cell culture experiments with different cell types, including primary pulp cells (Yasuda et al., 2008), cementoblasts (Hakki et al., 2009), periodontal ligament fibroblasts (Keiser et al., 2000), osteoblasts (Camilleri et al., 2004) and gingival fibroblasts (Pistorius et al., 2003), to assess the cytotoxicity of MTA. The consensus view expressed in these papers is that MTA demonstrates minimal cytotoxicity to these cell types in monolayer culture (Torabinejad and Parirokh, 2010).

MTA has been shown to exhibit excellent biocompatibility when it is in contact with pulp wounds in animals (Ford et al., 1996, Keiser et al., 2000, Faraco and Holland, 2001, Asgary et al., 2008, Kuratate et al., 2008) and in humans (Aeinehchi et al., 2003, Accorinte Mde et al., 2008, Min et al., 2008, Nair et al., 2008). Histological studies of iatrogenic exposures in human teeth, managed in aseptic conditions, compared teeth that were capped with MTA with those capped with calcium hydroxide. Notably, the teeth capped with MTA demonstrated greater reparative dentine formation in terms of thickness and quality, less inflammation and more predictable healing (Aeinehchi et al., 2003, Min et al., 2008, Nair et al., 2008). The precise mechanism by which MTA works, however, is not well understood. It has been shown to induce key stages in pulp repair, namely pulp cell proliferation (Moghaddame-Jafari et al., 2005), migration (Kuratate et al., 2008) and differentiation (Masuda-Murakami et al., 2010). Immunohistochemical analysis of pulp wounds, which had been capped with MTA for up to 11 weeks, showed expression of DSPP and collagen type I in those odontoblasts in direct contact with the MTA. There was also evidence of dentine secretion by these cells (Simon et al., 2008). The surface of MTA has been reported to form hydroxyapatite when it is in contact with synthetic body fluids (Sarkar et al., 2005, Reyes-Carmona et al., 2009). It is suggested that this biologically accepted surface layer allows for excellent cell / material adhesion and enables superior sealing characteristics when compared with other materials.

MTA displays many of the properties expected of an ideal pulp capping agent (section 1.7). It has been clearly demonstrated that MTA is biocompatible and there is an indication that it may also be bioinductive, however, a clear biological mechanism of action is yet to be determined. MTA is now widely accepted to be the material of choice for pulpotomy and vital pulp capping; gaining a better understanding of its biological mechanism of action is

essential in order to improve our understanding of pulp tissue repair so that novel dental tissue regenerative strategies can be developed.

1.8 Regenerative endodontics

The ultimate goal for pulp biologists would be to regenerate the dental pulp following injury, or to engineer a whole tooth. The dental pulp has a natural ability to protect itself and does so by secreting tertiary dentine in response to noxious attack. Herman (1920) demonstrated that it was possible to use a simple iatrogenic intervention to manipulate the pulp tissue into secreting dECM, thus showing that pulp regeneration was possible. Since that time, our knowledge of the biological mechanisms underpinning these events has developed to such an extent that the principles of pulp tissue engineering can now be demonstrated (Cordeiro et al., 2008).

The basis of regenerative tissue therapy follows the basic principles of tissue engineering; there are three core components, as outlined below:

i) a **scaffold** to act as an initial matrix for tissue development

ii) **stem or progenitor cells** that have the ability to differentiate into other specialised cells with functional activity

iii) the correct **extra- and intra-cellular signalling induction** necessary to orchestrate the complex events required for tissue development

The regenerative capacity of other oral tissues has already been demonstrated; for example, the use of enamel matrix protein from porcine fetal teeth (Emdogain®, Strauman) has been

used for periodontal tissue regeneration (Heijl et al., 1997) and recombinant BMPs have been used for bone augmentation (Fujimura et al., 1995). The dentine-pulp complex is an elaborate tissue, which is highly developed; therefore, unravelling the signalling cues that lead to its regeneration following injury, or even necrosis, presents enormous challenges. In terms of cell signalling, the key events that lead to reparative dentine formation are: proliferation, migration, differentiation and mineral secretion**.** There have been huge advances in biological research methods to analyse such processes, some of which have already been discussed (section 1.2.2). An exciting recent development utilises adenoviral vector transfection. This technique, initially conceived by Goff and Berg (1976), enables the incorporation of specific genetic instructions into the target cells, leading to over-expression of selected proteins. In this way, it is possible to test the specific effect of signalling molecules in key reparative events such as those described above.

The exploitation of chemotaxis and cell homing, in developing novel treatment modalities to harness the natural reparative mechanism of the pulp, shows exciting potential (Laird et al., 2008, Mao et al., 2010). Successful engineering of dental pulp tissue using chemotaxis-induced cell homing has recently been reported (Kim et al., 2010) and in this analysis, several cytokines were studied including FGF, VEGF and PDGF alone or in combination with nerve growth factor (NGF) and BMP-7. While the optimum combination of cytokines required to induce the necessary cellular organisation remains to be determined, these data clearly indicated that synergistic signalling interactions are likely to occur during wound repair.

Recently, the debate about undertakng more conservative pulp treatments, such as pulpotomy rather than pulpectomy, has been reintroduced (Simon et al., 2013). Greater

understanding of the various biological events associated with pulp wound healing will facilitate the development of novel therapeutic strategies. As MTA is known to promote profound tissue regenerative responses, an understanding of the mechanisms by which it does so, will help to ensure that regenerative endodontics ultimately becomes a clinical reality.

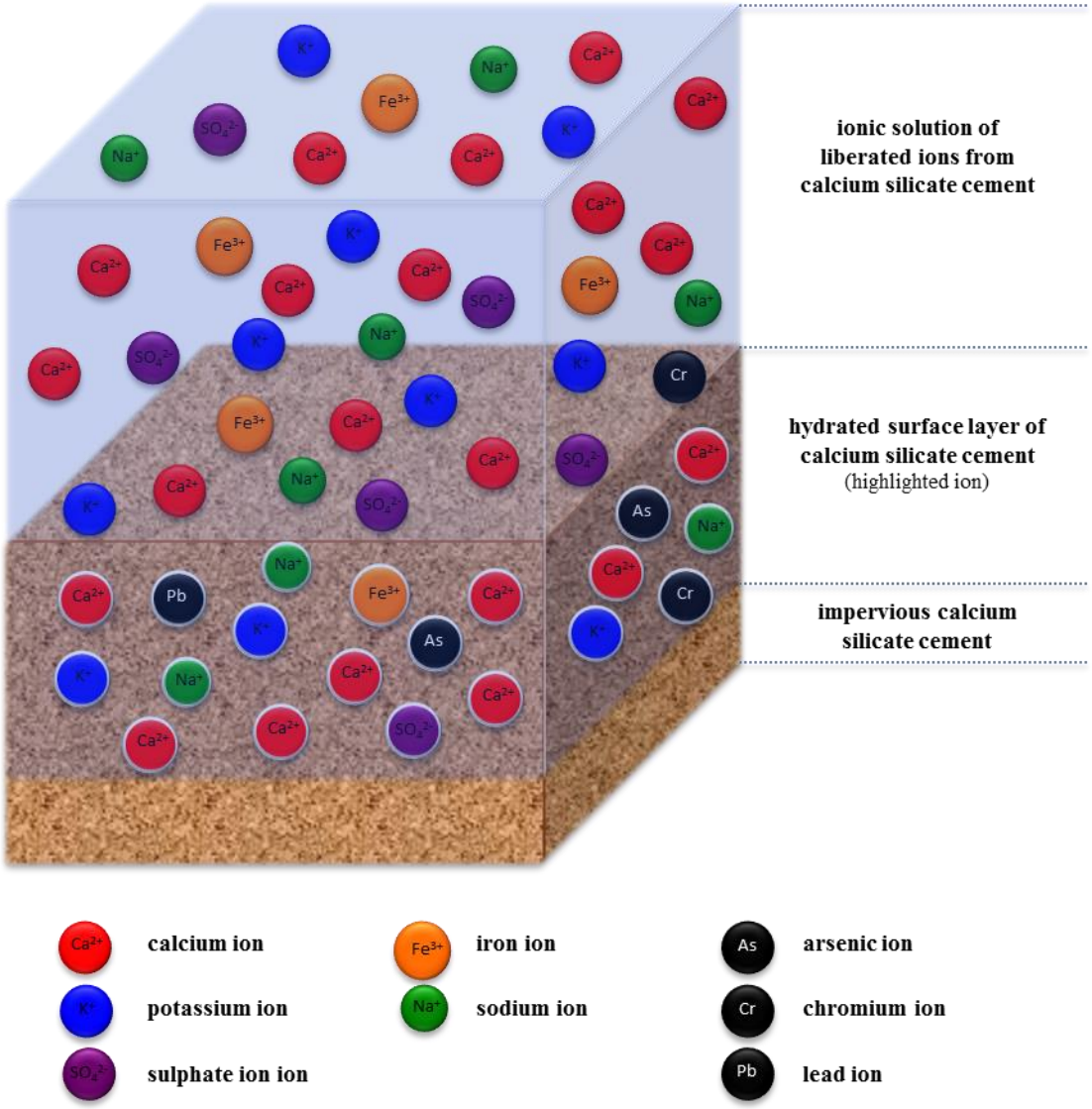

Figure 1.10 Ionic interactions at the surface of calcium silicate cements. *In vivo* the surface of calcium silicate cement will be infiltrated by tissue fluid and extracellular exudate which will liberate soluble ions from the cement. The fluid immediately surrounding the cement will have a unique ionic composition.

1.9 Project aims

This project aimed to examine the interaction of calcium silicate cements with dECM and assess their role in the events leading to tertiary dentinogenesis. The following hypotheses were investigated:

1) The interaction of calcium silicate cements, in both their set and setting phases, with tissue fluid (substituted with water *in vitro*) results in the formation of a unique ionic solution (Figure 1.10 opposite) which causes disruption of dECM, leading to the release of bioactive molecules.

2) The soluble constituents of therapeutic pulp capping agents liberate dECM components, which contain a rich cocktail of growth factors, some of which have not previously been identified in dECM (Figure 1.11 A-D overleaf).

3) The components of dECM released by therapeutic pulp capping agents, including those released by calcium silicate cements, promote regenerative events such as proliferation and chemotaxis in dental pulp cells.

4) HGF is solubilised from dECM by the soluble products of calcium silicate cements and plays an important role in the repair-associated processes of chemotaxis, differentiation and mineralisation during dental pulp repair.

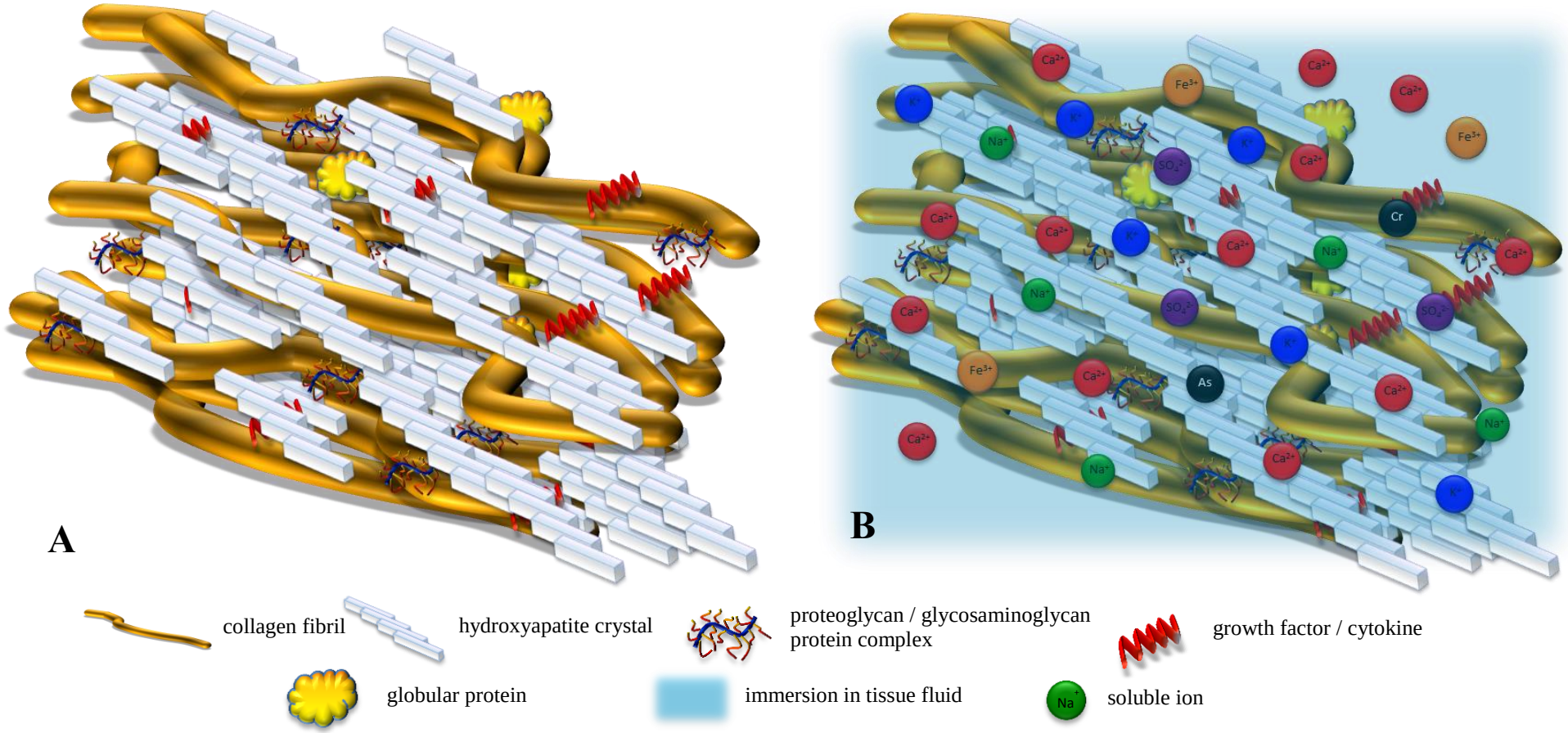

Figure 1.11 A) Diagrammatic representation of dentine, including inorganic and organic components, at a nanometre scale. **B**) Dentine represented in **A)** immersed in tissue fluid or extracellular exudate that has interacted locally with calcium silicate cement and has a unique ionic composition (components in diagram are not to scale).

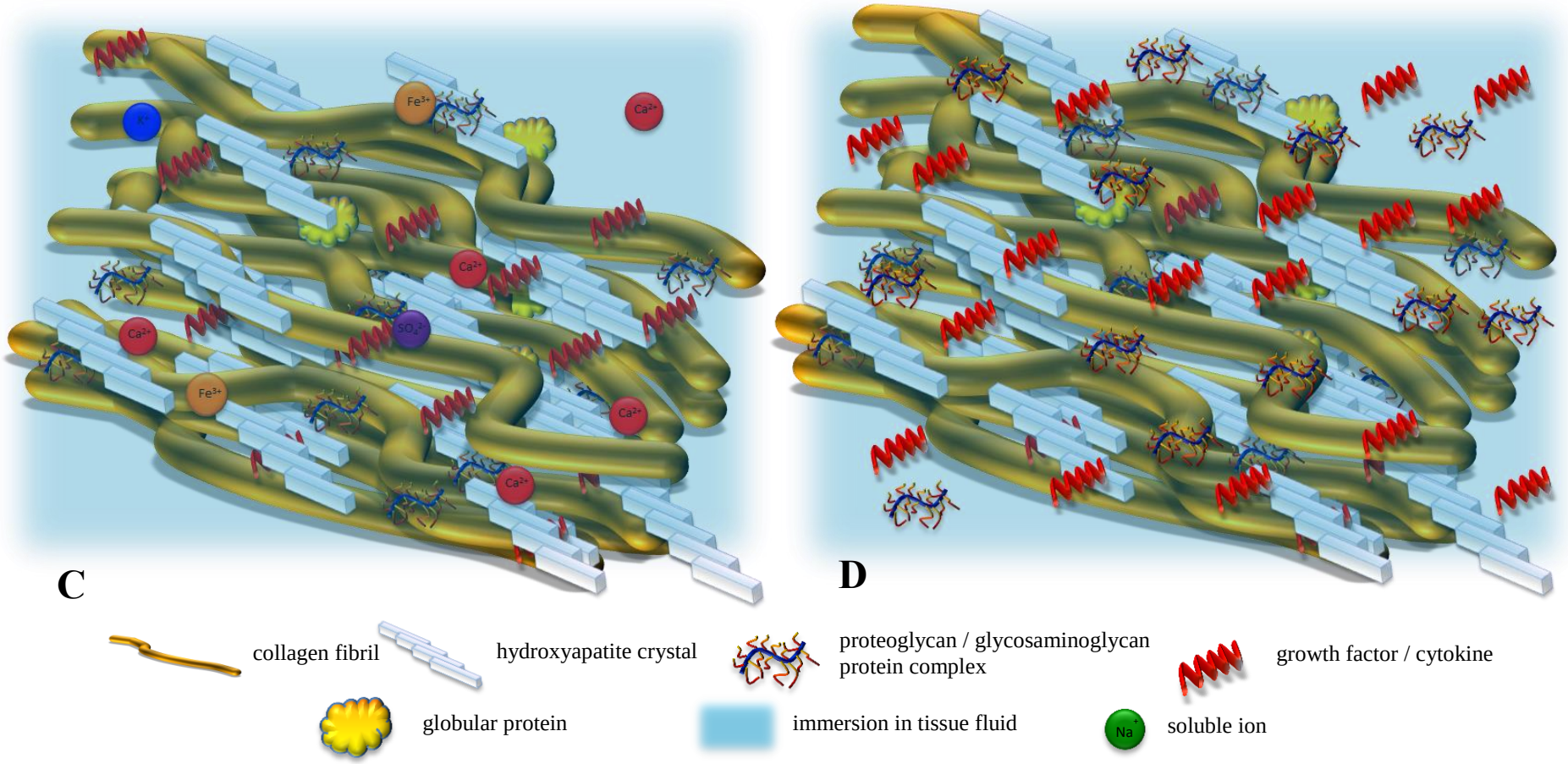

Figure 1.11 C) Ionic exchange between dentine and soluble components of calcium silicate cements has resulted in disruption of hydroxyapatite crystals leading to **D**) solubilisation and release of bioactive molecules from dECM including non-collagenous proteins, glycosaminoglycans and growth factors (components in diagram are not to scale).

2.0 MATERIALS AND METHODS

2.1 Isolation of dentine extracellular matrix components

2.1.1 Preparation of dentine extracellular matrix extractant solutions

Solutions of 10% EDTA (control) (pH 7.2) (Sigma-Aldrich, UK), 0.02M calcium hydroxide (pH 11.9) (Sigma-Aldrich, UK), the solubilised components of white MTA (pH 11.7) (Dentsply Tulsa Dental, USA), grey MTA (pH 11.7) (Dentsply Tulsa Dental, USA) and Biodentine® (pH 11.2) (Septodont, France) were prepared by dissolving solids in distilled water. The solutions of MTA were prepared by mixing 1.72 g of white or grey MTA with 1 litre of distilled water with constant agitation at 37 °C for 72 hours. The solution of Biodentine® was prepared by mixing the encapsulated material as per the manufacturer's instructions in an amalgamator (Kerr Optimix, CA, USA) at 4000 rpm for 30 seconds and allowing it to set in a plastic weigh boat at 37 °C for 24 hours with a thickness no greater than 2 mm. The set material was crushed to a fine powder in a ceramic mortar and pestle and graded using a 44 mesh sieve ($\leq$0.354 mm^2). 1.72 g of Biodentine® powder was subsequently suspended in 1 litre of distilled water with constant agitation at 37 °C for 72 hours. Insoluble particles were subsequently removed by filtration from all solutions.

2.1.2 Atomic absorption spectroscopic analysis of extraction solutions

To determine the concentration of calcium, aluminium, magnesium, sodium, potassium and iron in control and experimental extraction solutions[1], flame atomic absorption spectroscopy was employed. Standard solutions were prepared for calcium, aluminium, magnesium, sodium and potassium from the following salts: calcium chloride dehydrate (Sigma-Aldrich, UK), aluminium nitrate (Sigma-Aldrich, UK), magnesium chloride hexahydrate (Sigma-Aldrich, UK), sodium phosphate tribasic hexahydrate (Sigma-Aldrich, UK) and potassium phosphate monobasic (Sigma-Aldrich, UK), at a concentration of 1000 ppm. For iron, a proprietary standard solution (1000 ppm) was used (Fisher Scientific, UK). Each standard solution was diluted to concentrations of 40, 20, 10, 5 and 1 ppm. These standards, a control (EDTA) and the experimental solutions (calcium hydroxide, white MTA and grey MTA) as described above (section 2.1.1), were analysed using an atomic absorption spectrophotometer (AAS; Model 751, Instrumentation Laboratory, USA). Solutions were aspirated, mixed with acetylene and air and atomised in a flame. A light beam from a hollow cathode lamp with a filament specific to the element of interest was passed across the atomised sample to a monochronometer and intensity was determined with a detector. As each element absorbs at a specific wavelength of light, the decrease in intensity of the light determines the concentration of the sample. The experimental set up is illustrated in Figure 2.1. Concentrations of each element in control and experimental solutions were calculated from standard curves generated from the solutions, as described above (Figure 2.2).

[1] Analyses were not performed for Biodentine® as it was not commercially available when this experiment was undertaken.

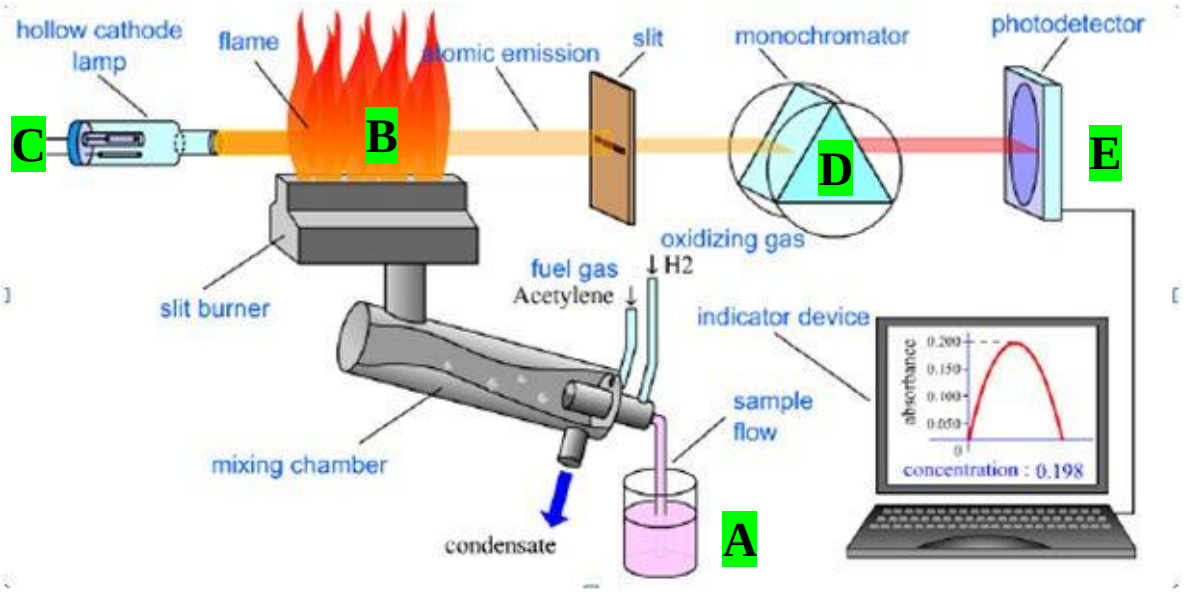

Figure 2.1 A schematic diagram of flame atomic absorption spectroscopy. (**A**) Sample is aspirated and mixed with acetylene and air; (**B**) it is atomised in a flame in gas phase, (**C**) a beam of light from a hollow cathode lamp (filament specific to element of interest) is passed through the atomised sample into (**D**) a monochronometer, then intensity was determined with a detector (**E**). (Reproduced with permission from http://lawrencekok.blogspot.co.uk/2012/10/ib-chemistry-on-atomic-absorption.html).

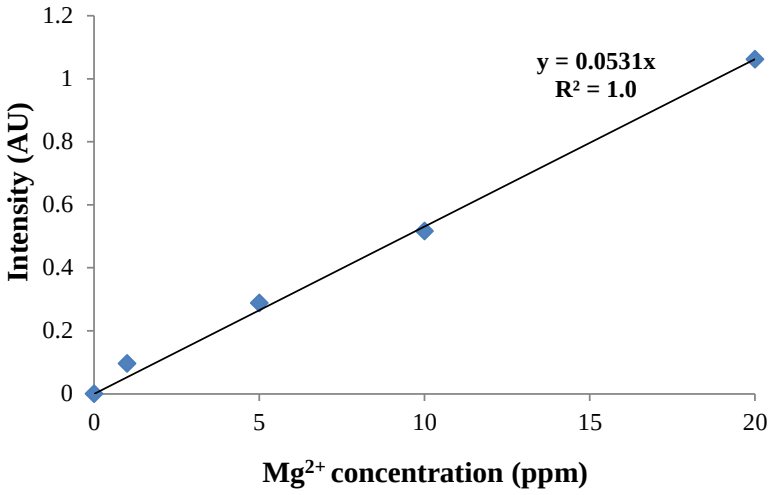

Figure 2.2 A representative example of a standard curve generated using atomic absorption spectroscopy, showing flame intensity (absorbance units) plotted against solutions containing a range of concentrations of magnesium ions as described in section 2.1.2. The R^2 coefficient (>0.9) and linear regression equation are displayed next to the line of best fit.

2.1.3 Isolation of dentine extracellular matrix components

To assess the ability of therapeutic pulp capping agents to release dentine extracellular matrix components (dECM), the solutions produced in section 2.1.1, containing the soluble components of EDTA, calcium hydroxide, white MTA, grey MTA and Biodentine®, were applied in a well-established and recognised extraction technique (Smith and Leaver, 1979). The root surfaces of a total of 572 non-carious intact human extracted molars and premolars (predominantly third molars and premolars) obtained from Birmingham Dental Hospital's Tooth Bank[2], were prepared; remaining attached soft tissue and cementum were removed using both a scalpel blade and a rotating brush with dental prophylactic paste (Nupro®, Dentsply, UK). Cleaned teeth were dissected into 1 mm longitudinal sections using a diamond edged rotary disc saw (TAAB, UK) cooled with distilled water. Pulp tissue was subsequently extirpated and the pulp chamber surface scraped clean with a large excavator (Ash, Dentsply, UK). Enamel was removed using bone clippers and the remaining dentine was crushed into a fine powder using a percussion mill (Spex 6700 Freezer/Mill, Glen Creston Ltd, UK) cooled with liquid nitrogen to prevent protein denaturation. The powdered dentine was graded using a 60 mesh sieve ($\leq$0.251 mm^2).

dECM components were extracted from the powdered dentine using the solutions previously described (section 2.1.1) (EDTA, calcium hydroxide, white MTA, grey MTA and Biodentine®) with the addition of the protease inhibitors, 10 mM n-ethylmaleamide (Sigma, UK) and 5 mM phenyl-methyl-sulphonyl fluoride (Sigma, UK) to prevent protein denaturation. Extractions were performed with constant agitation at 4 °C for 14 days.

[2] Approval for the use of human tooth tissue was obtained from the UK National Research Ethics Service (09/H0405/33).

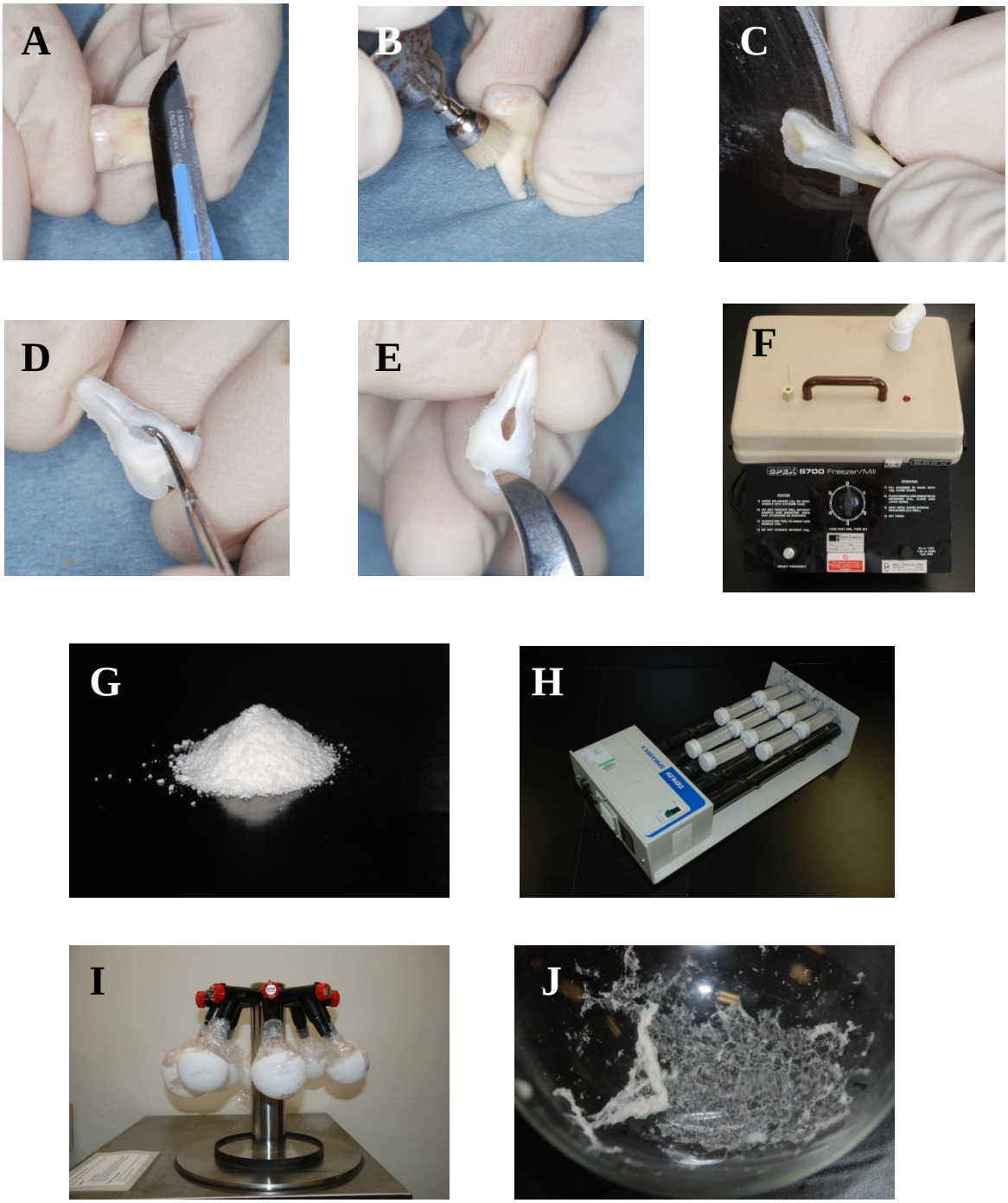

Figure 2.3 Photographic images of processing stages applied in the isolation of dentine extracellular matrix components. **A-B**) Removal of soft tissue and cementum from tooth roots, **C**) sectioning teeth into 1 mm sections, **D**) careful removal of pulp tissue, **E**) removal of enamel, **F**) pulverisation of dentine into powder using a percussion mill cooled with liquid nitrogen, **G**) graded dentine powder, **H**) extraction of dECM components in 30 mL polystyrene universals (Appleton Woods, UK) from dentine powder (5 g), using different extraction solutions (20 mL) constantly agitated at 4 °C, **I**) following dialysis, extraction supernatants were freeze dried, and **J**) close up of freeze dried dECM components in round bottom flask.

Each day, the solution was centrifuged (Jouan B4i, Thermo scientific, UK) at 3000 rpm for 10 minutes and supernatants were decanted prior to measurements being obtained for pH and absorbance. These absorbance values were obtained at 280 nm using a spectrophotometer (UV/VIS spectrophotometer, Philips UK), to monitor protein dissolution. The pooled supernatants were exhaustively dialysed for 14 days at 4 °C with repeated changes of distilled water, at least once daily, to remove salts and impurities. The resultant dialysates were shell frozen in round bottom flasks using liquid nitrogen and lyophilised using a freeze dryer (Modulyo, Edwards, UK). The lyophilised dECM component preparations were stored at -20 °C prior to use. The extraction process is illustrated in Figure 2.3.

2.2 Characterisation of dECM preparations

2.2.1 One dimensional sodium dodecyl sulphate polyacrylamide gel electrophoresis (1D SDS PAGE)

Prior to loading, 0.5 mg of extracted lyophilised dECM components were dissolved in 10 µL of LDS buffer (Invitrogen, UK), 26 µL of deionised water and 4 µL of reducing agent (Invitrogen, UK). Following denaturation at 105 °C for 10 minutes, loading volume was optimised by repeated attempts and it was determined that 2 µL of the solution was loaded onto either a 3-8% Tri-Acetate (NuPAGE, Invitrogen, UK) or a 10% Bis-Tris (NuPAGE, Invitrogen, UK) pre-cast polyacrylamide gel to separate higher and lower molecular weight proteins, respectively. 2 µL of molecular weight marker (Mark12, Invitrogen, USA) was included within the gel. Gels were electrophoresed at 150 V and 45 mA for 1 hour using SDS running buffer (Invitrogen, UK). Protein banding was visualised using Coomassie blue or silver staining techniques as described below. Throughout both staining procedures, glassware was ultra-clean, high quality water was used and gels were handled with care.

2.2.1.1 Coomassie blue staining

Gels were fixed in a solution of 50% methanol (BDH laboratory supplies, Poole, England) 10% acetic acid (BDH laboratory supplies, Poole, England) and 40% deionised water overnight. Gels were then rinsed with copious volumes of deionised water twice and immersed in a staining solution containing 0.5% Coomassie blue R-250 (BDH laboratory supplies, Poole, England) for 2 hours. Each gel was transferred to a destaining solution containing 5% methanol, 7.5% acetic acid and 87.5% deionised water for approximately 1-2 hours until the background appeared clear. Images of the stained gels were captured using a Nikon Coolpix 950 (Nikon, Japan) under illumination from a white light box (Hancocks, England).

2.2.1.2 Silver staining

Tri-Acetate and Bis-Tris gels were stained with SilverXpress silver staining kit (Invitrogen, UK) as per the manufacturer's instructions. Protein gels were fixed using a solution containing 50% methanol, 10% acetic acid and 40% deionised water for 10 minutes. Gels were immersed in a solution of 50% methanol and 2.5% of the propriety sensitising agent; Tris-Acetate for 10 minutes and Bis-Tris for 30 minutes. Each gel was washed twice with ultrapure water for 5 - 10 minutes and stained for 15 minutes with the silver solution. Each gel was washed a further two times in ultrapure water. Gels were immersed in developer and gently agitated until bands reached an appropriate visible intensity at which point 5 mL of stop solution was added. Finally, the gels were washed a further three times in ultrapure water to remove background stain and images were captured under illumination from a light box using a Nikon Coolpix 950 (Nikon, Japan). The molecular weight of each migrated protein

band was determined by comparison with the known weight of the molecular weight markers (Mark12, Invitrogen, USA). The number of bands separated and their respective molecular weight for each extract was determined using GeneTools image acquisition software (Syngene, Cambridge, UK).

2.2.2 Dye binding assays for total NCPs and glycosaminoglycan quantification

To determine the total amount of non-collagenous protein (NCPs) recovered from dECM preparations extracted by the different solutions, two dye binding assays sensitive to microgram levels were employed: the Bradford assay (Bradford, 1976) and Bicinchoninic acid (BCA) protein assay (Smith et al., 1985).

2.2.2.1 Dye binding assay for NCPs - Bradford assay

The Bradford assay is based on an absorbance shift of the dye Coomassie Brilliant Blue G-250 from its unbound form (cationic – green/red) to its bound form (anionic – blue), which can be detected spectrophotometrically at a wavelength of 595 nm. Bovine serum albumin (BSA) (Sigma-Aldrich, UK) was dissolved in dH_20 to give a stock concentration of 1 mg/mL. From this, a serial dilution was generated to produce 5 samples with the following concentrations: 2, 4, 6, 8, 10 µg/mL, to provide a standard curve. Lyophilised dECM components were dissolved in dH_20 at a concentration of 2 mg/mL. 50 µL of standard, experimental sample or blank were aliquoted into a cuvette; to this, 1.5 mL of Bradford reagent (Sigma-Aldrich, UK) was added, gently vortexed and incubated for 5 minutes at room temperature. Absorbance was measured using a spectrophotometer (UV/VIS

spectrophotometer, Philips UK) at 595 nm for three replicates of sample and standard; sample concentration of NCP content was calculated from the standard curve (Figure 2.4).

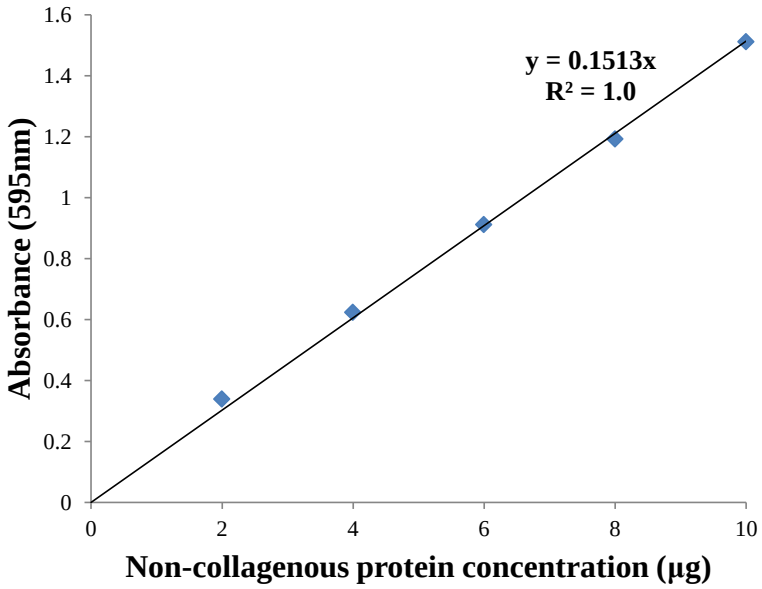

Figure 2.4 Representative example of standard curve used to determine concentration of non-collagenous proteins, generated using BSA as a standard in the Bradford assay, as described in section 2.2.2.1. The R^2 coefficient (>0.9) and linear regression equation are displayed next to the line of best fit.

2.2.2.2 Dye binding assay for NCPs - Bicinchoninic acid protein assay

The principle of the Bicinchoninic acid assay (BCA) is the formation of a Cu^{2+}/protein complex in alkaline conditions, which causes a reduction of Cu^{2+} to Cu^{+}. BCA forms a blue / purple complex with Cu^{+}, and the reduction of Cu^{2+} ions can be determined by absorbance changes detected at a wavelength of 562 nm (Smith et al., 1985). This assay was performed in parallel with the Bradford assay (section 2.2.2.1) using the same concentrations of BSA to create a standard curve and the same experimental samples were analysed. 2 mL of BCA

working reagent (Sigma-Aldrich, UK) was added to 100 µL of standard, experimental sample or blank in a plastic cuvette and vortexed gently. The resulting solution was incubated at 37 °C for 2 hours and absorbance measured at a wavelength of 562 nm using a spectrophotometer (UV/VIS spectrophotometer, Philips UK). Three replicates were generated for each standard and experimental sample and measured within 5 minutes of each other. Concentration of NCP was calculated from the standard curve generated (Figure 2.5).

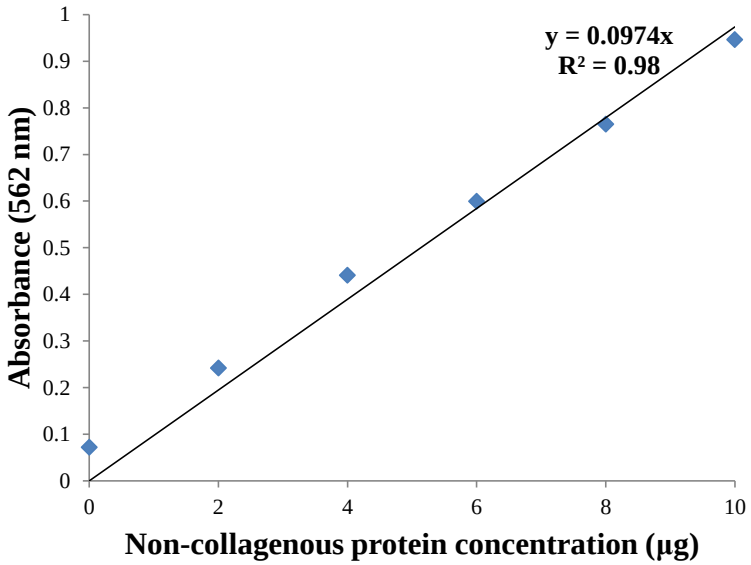

Figure 2.5 Representative example of a standard curve used to determine concentration of non-collagenous protein using BSA as a standard in the Bicinchoninic acid assay as described in section 2.2.2.2. The R^2 coefficient (>0.9) and linear regression equation are displayed next to the line of best fit.

2.2.2.3 Dye binding assay for GAGs – Farndale assay

Quantification of glycosaminoglycans (GAGs) in dECM preparations extracted by different reagents was determined using the Farndale assay (Farndale et al., 1986). The assay utilises the ability of GAGs to bind to dimethylmethylene blue (DMMB) which will result in a change in absorbance of of the GAG/DMMB complex at 525 nm.

The Farndale reagent was prepared with 46 μM of 1, 9 dimethylmethylene blue (Sigma, UK), 40 mM glycine (Sigma, UK) and 40 mM sodium chloride (Sigma, UK), and stored at room temperature and protected from light prior to use. To produce a standard curve, 2 mg of chondroitin-4-sulphate (Type A, whale cartilage, Fluka Biochemika, Germany) was dissolved in 20 mL of 0.5 M acetic acid; from this stock solution, serial dilutions of 2, 4, 6, 8, and 10 μg/mL were generated. Lyophilised dECM preparations were dissolved in 0.5 M acetic acid at a concentration of 2 mg/mL. 1 mL of prepared Farndale reagent was added to 100 μL of the standard, experimental sample or blank in a cuvette and gently mixed. Absorbance was measured at a wavelength of 525 nm using a spectrophotometer (UV/VIS spectrophotometer, Philips UK). All samples and standards were analysed in triplicate. Concentrations of GAGs were calculated by extrapolation from the standard curve produced (Figure 2.6).

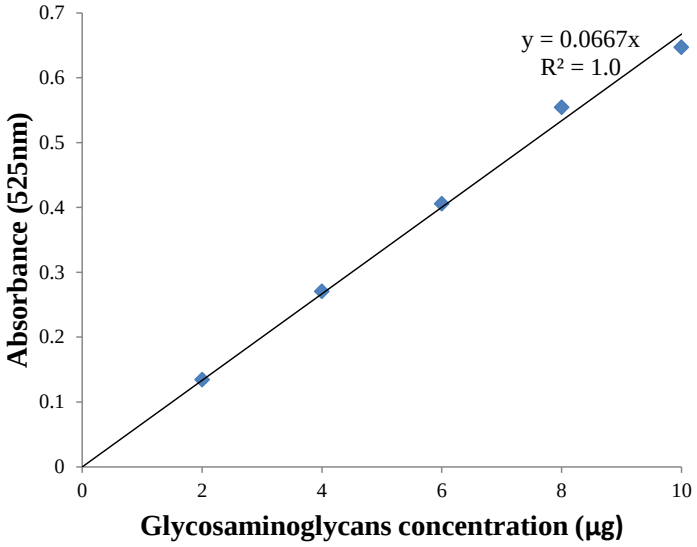

Figure 2.6 Representative example of a standard curve used to determine concentration of glycosaminoglycans using chondroitin-4-sulfate as a standard in the Farndale assay as described in section 2.2.2.3. The R^2 coefficient (>0.9) and linear regression equation are displayed next to the line of best fit.

2.2.3 Immunoassays

To determine the presence and the concentrations of specific growth factors in dECM preparations extracted by control and test reagents, a sandwich-type immunoassay for transforming growth factor-β1 (TGF-β1) and adrenomedullin (ADM) was employed.

2.2.3.1 Preparation of phosphate buffered saline

Phosphate buffered saline (PBS) was prepared by dissolving 7.8 g sodium chloride (Sigma-Aldrich, UK), 1.5 g dipotassium phosphate (Sigma-Aldrich, UK) and 0.2 g monopotassium phosphate (Sigma-Aldrich, UK) in 1 L of distilled water and it was adjusted to pH 7.4.

2.2.3.2 TGF-β1 Enzyme-linked immunosorbent assays (ELISA)

The TGF-β1 ELISA applied here was a modification of that previously described (Danielpour, 1993). In total, 2 mg of each sample of lyophilised dECM components were dissolved in 150 μL of PBS prior to addition of 30 μL of 1 M hydrochloric acid (Sigma-Aldrich, UK); this was then incubated at room temperature for 10 minutes to activate the TGF-β1. The reaction was neutralised with 30 μL of 1.2 M sodium hydroxide (Sigma, UK) and 0.5 M HEPES (Sigma-Aldrich, UK); 50 μL of the resultant solution was assayed in triplicate using the Quantikine Human TGF-β1 ELISA kit (R & D Systems, UK) according to the manufacturer's instructions. A serial dilution of TGF-β1 was created from a stock solution of 2000 pg/mL with the following concentrations: 1000, 500, 250, 125, 62.5, 31.25 pg/mL, to create a standard curve. 200 μL of standard, sample or blank was added to a well of the prepared 96-well plate, which was then sealed and incubated at room temperature for 3 hours. After incubation, wells were washed with wash buffer in an automated plate washer (Bio-Tek Instruments, USA). Visual inspection was used to ensure that the wash buffer was completely removed prior to advancing to the next step. 100 μL of TGF-β1 conjugate was added to each well, sealed and incubated for 2 hours at room temperature. The washing procedure was repeated and then 100 μL of substrate solution was added to each well and incubated for 30 minutes at room temperature in the dark. To terminate the reaction, 100 μL of the stop solution (R & D Systems, UK) was added and the absorbance was read using an ELX800 Universal Microplate Reader (Bio-Tek Instruments, USA) at 450 nm with correction set at 540 nm to reduce optical interference. Concentrations of TGF-β1 in dECM preparations extracted using different reagents were calculated from the standard curve produced (Figure 2.7).

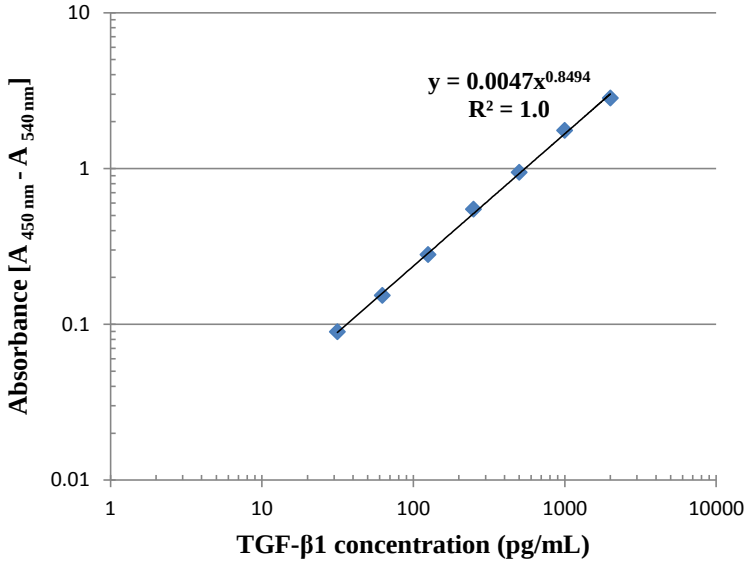

Figure 2.7 Representative example of a standard curve used to determine concentration of TGF-β1 using ELISA analysis as described in section 2.2.3.2. The R^2 coefficient (>0.9) and linear regression equation are displayed next to the line of best fit.

2.2.3.3 Adrenomedullin enzyme immunoassay (EIA)

Quantification of ADM in each dECM preparation was determined using an adrenomedullin EIA Kit (Phoenix Pharmaceuticals, Inc. California, USA) according to the manufacturer's instructions. A solution with a concentration of 10 mg/mL was made for each lyophilised sample of dECM preparation with assay buffer (Phoenix Pharmaceuticals, Inc. California, USA). A serial dilution with assay buffer of rehydrated ADM was generated from a stock to produce the following concentrations of standard: 0.01, 0.1, 1.0, 10, 100 and 1000 ng/mL. 50 µL of sample, standard or blank were added to wells of the prepared 96-well plate with internal controls. 25 µL of rehydrated primary antiserum and 25 µL of rehydrated biotinylated peptide were added to each well apart from the internal controls; the plate was then sealed and incubated at room temperature for 2 hours with gentle agitation on an orbital shaker (Denley orbital mixer, ThermoFisher Scientific, UK). After incubation, the plate was washed, as

described above, using assay buffer. 100 µL of streptavidin-horseradish peroxidase was added to each well apart from internal controls; the plate was sealed and incubated for 1 hour. The plate was then washed and 100 µL of substrate solution was added to each well and incubated for 1 hour in the dark. Following incubation, 100 µL of 2N HCl was added to each well to terminate the reaction. Absorbance readings at 450 nm were measured using an ELX800 Universal Microplate Reader (Bio-Tek Instruments, USA). Concentrations of ADM in each sample were calculated using XLFit4 statistical software (IDBS, UK) by comparison with the standard curve produced (Figure 2.8).

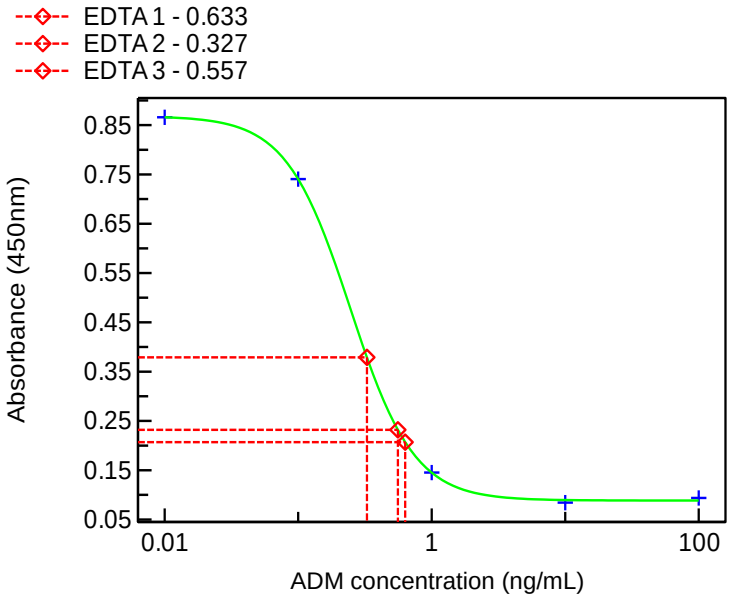

Figure 2.8 A graph generated on XLFit4 statistical software to determine the concentration of ADM in samples of dECM preparations using a standard curve. In this example, calculation of the concentration of ADM in three samples of EDTA (EDTA 1-3) extracted dECM components is made on the *x-axis* illustrated with red dotted lines determined from absorbance on the *y-axis*.

2.2.4 Human cytokine antibody array

To analyse the range of growth factors sequestered within dECM and solubilised by control and test reagents, a human cytokine antibody array AAH-GF-1 (RayBiotech, Norcross, GA, USA) was utilised. This approach enabled relative expression levels of multiple proteins (Table 2.1) to be determined at high throughput using a sandwich ELISA technique.

Table 2.1 Proteins analysed in dECM components extracted by EDTA, calcium hydroxide, white and grey MTA using the human cytokine antibody array AAH-GF-1 (RayBiotech, Norcross, GA, USA). Key to abbreviations is provided on page xii.

AR	FGF-6	HGF	IGF-I	NT-4	PlGF	TGF-β3
FGF-2	FGF-7	IGFBP-1	IGF-I SR	PDGF R a	SCF	VEGF
NGF	G-CSF	IGFBP-2	IGF-II	PDGF R b	SCF R	VEGF R2
EGF	GDNF	IGFBP-3	M-CSF	PDGF-AA	TGF-α	VEGF R3
EGF R	GM-CSF	IGFBP-4	M-CSF R	PDGF-AB	TGF-β1	VEGF-D
FGF-4	HB-EGF	IGFBP-6	NT-3	PDGF-BB	TGF-β2	

Lyophilised dECM preparations extracted by EDTA, calcium hydroxide, white and grey MTA were dissolved in PBS to a concentration of 200 µg/mL of total protein as determined by the Bradford assay using BSA as a standard (section 2.2.2.1). Nitrocellulose membranes labelled with specific antibodies (Table 2.1) were prepared according to the manufacturer's instructions. Membranes were placed in the well tray provided and immersed in 2 mL 1X blocking buffer to block any nonspecific binding sites, then incubated at room temperature for 30 minutes. The blocking buffer was decanted and 1 mL of dECM dissolved in PBS was placed on the surface of the membrane and incubated at room temperature for 2 hours. Any antigen targets would bind to specific capture antibodies at this point. The sample was removed and each membrane was immersed in 1X wash buffer I and agitated for 5 minutes using an orbital shaker; this washing procedure was repeated three times. Each membrane was

then washed a further two times using 1X wash buffer II using the same technique. The wash solution was removed and 1 mL of diluted biotin-conjugated antibody was added to each membrane to bind to the target antigen-antibody complexes and incubated further at room temperature for 2 hours. The membranes were washed again with wash buffer I and II as previously described above to remove any unbound antibody-enzyme conjugates. 2 mL of diluted HRP-conjugated streptavidin was added to each membrane to label antigen-antibody complexes and incubated at room temperature for 2 hours. The wash procedure using wash buffer I and II was repeated.

To detect immunosorbed antigen-antibody complexes, the membrane was removed from its carrier, drained of wash buffer and placed face up on a clean plastic sheet. A total of 500 μL of a solution of 50% 1X detection buffer C and 50% 1X detection buffer D was added to the membrane surface and incubated at room temperature for 2 minutes. Excess detection agent was removed, and the membrane was sandwiched between two plastic sheets and air bubbles were carefully removed. Under dark room safe light conditions, the membrane was exposed to X-ray film (Carestream Kodak X-OMAT, Sigma-Aldrich, UK) for 3 minutes, which was then manually processed. Each film was immersed in GBX developer / replenisher (Carestream, Kodak, Sigma-Aldrich, UK) for approximately 5 minutes with moderate agitation. It was then transferred to a stop bath (Carestream Kodak, Sigma-Aldrich, UK) for 30 seconds and fixed in GBX fixer / replenisher (Carestream Kodak, Sigma-Aldrich, UK) for 60 seconds. Finally, the film was washed in running water for 5 minutes. An image of each membrane was captured using the G:BOX gel imaging system (Syngene, Cambridge, UK) and transferred to GeneSnap image acquisition software (Syngene, Cambridge, UK) for volume density quantification. RayBio® Analysis Tool (RayBiotech, Norcross, GA, USA) was used to

calculate relative expression levels of each protein for dECM preparations extracted by EDTA, calcium hydroxide, white and grey MTA.

2.2.5 Multiplex sandwich ELISA analysis

To determine the concentration and confirm the presence of specific growth factors, surface receptors and a binding protein in dECM, extracted by control and experimental reagents, a quantitative multiplex sandwich ELISA service (Quantibody® RayBiotech, Norcross, GA, USA) was utilised. Using parallel internal standard controls, this system allowed quantitative measurement of the concentration of multiple proteins in an array format. The technique is performed on a glass slide with multiple spots of specific antibodies related to the proteins of interest (Figure 2.9).

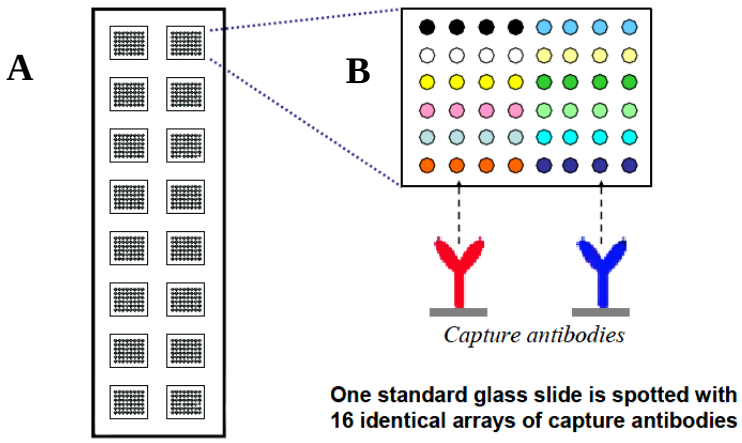

Figure 2.9 A schematic diagram showing the glass slide layout for detection of multiple proteins simultaneously using a sandwich ELISA technique. **A**) Glass slide spotted with 16 wells of identical antibody arrays **B**) Close-up of a well shows that each capture antibody, together with the positive and negative control is arrayed in quadruplicate.

Lyophilised dECM preparations were dissolved in PBS at a concentration of 190 µg/mL total protein as determined from the Bradford assay using BSA as a standard (section 2.2.2.1). 100 µL of sample diluent was added to each well and incubated at room temperature for 30 minutes whilst agitated gently on an orbital shaker to block the slides. The buffer was then decanted from each well. 100 µL of sample or serial dilutions of standard were added to each well of the activated prepared glass slide containing spots of antibody for the targets listed in Table 2.2. Samples and standard were incubated for 2 hours at room temperature and then washed five times with the 1X wash buffer I under gentle agitation. The same process was repeated twice with wash buffer II. 80 µL of the detection antibody was added to each well and incubated at room temperature for 2 hours. Following five sequential washes with the appropriate wash buffer I, 80 µL of cyanine 3 dye-conjugated streptavidin was added to each well and incubated for a further 1 hour at room temperature without light, to bind to any cytokine-antibody-biotin complexes. The slide was washed and the fluorescence was measured at a wavelength of 532 nm using a microarray scanner (Agilent G2505B, Cheshire, UK) at a resolution of 2 µm. Three biological replicates were assessed for each sample of dECM preparation. Concentrations of each growth factor, binding protein or surface receptor were calculated from standard curves (Figure 2.10).

Table 2.2 A list of the proteins analysed in dECM components extracted by EDTA, calcium hydroxide, white MTA, grey MTA and Biodentine® using the customised Quantibody human cytokine array QAH-CUST service. Key to abbreviations is provided on page xii.

TGF-β1	EGF	PDGF-AA	SCF
IGF-I SR	IGF-I	HGF	NGF
BMP-4	IGF-II	G-CSF	NT-3
BMP-7	IGFBP-1	GM-CSF	NT-4
FGF-2	VEGF	M-CSF	GDNF

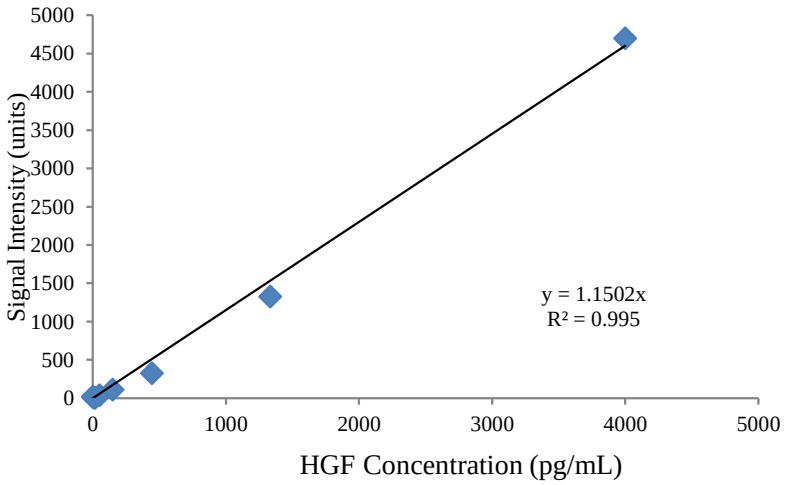

Figure 2.10 Representative example of a standard curve used to determine concentration of HGF in samples of dECM using multiplex ELISA analysis as described in section 2.2.5. The R^2 coefficient (>0.9) and linear regression equation are displayed next to the line of best fit.

2.3 Tissue isolation

2.3.1 Human pulp tissue

Human pulps were obtained from freshly extracted healthy premolar teeth which were removed for orthodontic reasons[3]. The teeth were immersed in RNA Later (Qiagen, West Sussex, UK) immediately after extraction. Within one hour of removal, the crown was sectioned with a needle diamond bur (166-017M, MDT, Israel) in a dental turbine (Synea, W&H, UK) at the cementoenamel junction to expose the most coronal point of the pulp chamber. The pulp tissue was carefully extirpated from the root canal system using a size 40

[3] Approval for the use of human tooth tissue was obtained from the UK National Research Ethics Service (09/H0405/33).

K Flexofile (Dentsply, Maillefer, Switzerland) and re-immersed in RNA Later prior to RNA isolation (section 2.6.2).

2.3.2 Rat pulp tissue

For rat dental pulp cell (RDPC) cultures and rat pulp tissue isolation, maxillary and mandibular incisor teeth were dissected from 100-120 g body weight freshly sacrificed male Wistar Hannover rats (Charles River Laboratories, Aston University, Pharmaceutical Sciences Animal House, UK) using a scapel. Teeth were washed in sterile PBS (pH 7.5) and placed in sterile αMEM medium (Biosera, UK), containing 2 mM L-glutamine (Sigma-Aldrich, UK) supplemented with 1% penicillin / streptomycin (10 000 units/mL of penicillin with 10 mg/mL streptomycin) (Sigma-Aldrich, UK). In a laminar flow hood, teeth were carefully sectioned along their long axis; pulp tissue was carefully removed using fine forceps and placed in sterile αMEM medium. Pulps were washed three times in sterile αMEM medium prior to isolation of RDPCs (section 2.4.2).

2.3.3 Rat non-dental tissue isolation

RNA was isolated from different rat tissues, including tongue, palatal mucosa, bone marrow and lung from a freshly sacrificed 100-120 g male Wistar Hannover rat. The tongue was detached from its base and approximately 20-30 mg removed from the tip. Palatal mucosa was dissected from the hard palate and a representative section approximately 20-30 mg in weight detached. Bone marrow was removed whole and pooled from the central core of four femoral bones after longitudinal sectioning with a scalpel. Lung tissue was dissected from the thoracic cavity and approximately 20-30 mg separated from the inferior lobe. Upon removal,

each tissue was finely minced with a scalpel and placed in a 1.5 mL microcentrifuge tube containing 600 μL of Buffer RLT (Qiagen, West Sussex, UK) and 0.01% β-Mercaptoethanol (Promega, Madison, WI, USA). The resulting suspension was disrupted with a Turrax Homogenizer (IKA, Staufen, Germany) for 30 seconds. RNA isolation was subsequently performed as outlined in section 2.6.2.

2.4 Cell culture

To study pulp cell responses *in vitro,* an immortalised cell line, murine MDPC-23 isolated from foetal mouse dental papillae (Hanks et al., 1998a) and primary RDPCs isolated from male freshly sacrificed 100-120 g male Wistar Hannover rat were used (section 2.3.2). The MDPC-23 cell line was kindly donated by Professor Jacques Nör, University of Michigan School of Dentistry, USA.

2.4.1 Culture media and processes

2.4.1.1 MDPC-23 culture medium

Dulbecco's modified Eagle's medium (DMEM) (Biowest, Nuaillé, France), containing 2 mM L-glutamine (Sigma-Aldrich, UK) supplemented with 1% penicillin / streptomycin (10 000 units/mL of penicillin with 10 mg/mL streptomycin) (Sigma-Aldrich, UK) and 10% foetal bovine serum (FBS) (Biowest, Nuaillé, France), was used as standard medium for MDPC-23 cell culture.

2.4.1.2 Primary pulp cell culture medium

Alpha minimum essential medium (αMEM) (Biosera, UK), containing 2 mM L-glutamine (Sigma-Aldrich, UK) supplemented with 1% penicillin / streptomycin (10 000 units/mL of penicillin with 10 mg/mL streptomycin) (Sigma-Aldrich, UK) and 10% FBS (Biosera, UK), was used for the culture of RDPCs (maintenance medium).

2.4.1.3 Optimisation of mineralising medium

To determine the ability of growth factors to induce mineralisation in RDPC cultures, an optimal medium supplementation regime was determined to enable sensitive detection of differences in *in vitro* mineralisation induction (Gronthos et al., 1994, Maniatopoulos et al., 1988). Each well of a 6-well plate (Corning, Tewksbury, MA, USA) was seeded with 5×10^4 RDPCs (passage 2) and grown to 60-80% confluence. Medium described in section 2.4.1.2 containing 5% FBS (instead of 10% FBS) was used to decrease growth rates for the extended culture periods with further inclusion of one of the following combination of supplements: 1) PBS (control) 2) 50 μg/mL ascorbic acid (Sigma-Aldrich, UK) + 10 mM beta-glycerophosphate disodium salt hydrate (BGP) (Sigma-Aldrich, UK), 3) 10 mM BGP, 4) 5 mM BGP, 5) 10 mM BGP + dexamethasone 10^{-8} (Dex) (Sigma-Aldrich, UK) and 6) 5 mM BGP + Dex 10^{-8}. This culture medium was replaced every 48 hours. Three replicates for each group were assayed for mineral content using the alizarin red assay (section 2.5.3) at days 5, 12 and 16. The optimum mineralisation medium identified for future experimental analysis was determined to be maintenance medium supplemented with 5% FBS instead of 10% FBS with 5 mM BGP.

2.4.1.4 Cell counting

To ensure correct seeding densities, viable cells were counted using a Neubauer haemocytometer. 50 μL of cell suspension was mixed with 50 μL of 0.4% Trypan blue solution (Sigma-Aldrich, UK). 10 μL of the resultant mixture was pipetted into the Neubauer chamber and Trypan blue negative cells were counted under a variable relief contrast (VAREL) microscope (Zeiss Axiovert 25, Germany). A minimum of three counts were performed per sample and mean values were used to calculate the number of cells in the solution per mL. Cell suspensions were diluted accordingly and seeded at the required densities.

2.4.2 Primary pulp cell preparation

RDPCs were isolated using the Trypsin / EDTA enzyme digestion method (Patel et al., 2009). Pulp tissue obtained from one rat (four incisors) (section 2.3.2) was combined and mechanically minced using a scalpel on a sterile glass slide to give fine pieces no greater than 1 mm^3. The pulp tissue was placed in a 15 mL Falcon® tube with 2 mL of 0.25% (w/v) Trypsin 1 mM EDTA.4Na (Gibco, Paisley, UK) and constantly agitated at 37 °C in 5% CO_2 for 30 minutes. To terminate enzymatic activity, two volumes of supplemented α-MEM containing 10% FBS were added. The resultant tissue suspension was passed through a cell strainer of pore size 70 μm (Becton Dickenson, Oxford, UK) into a 50 mL Falcon® tube to obtain a single cell suspension and centrifuged (Jouan B4i, Thermo scientific, UK) at 900 g for 3 minutes. The supernatant was removed, the cell pellet was re-suspended in 1 mL of medium and cells were seeded in a 25 cm^2 flask (Corning, Tewksbury, MA, USA). Medium was refreshed every 48 hours and cells were passaged once they had reached 80% confluence

by detachment using 0.25% (w/v) Trypsin 1 mM EDTA.4Na (Gibco, Paisley, UK). 1 x 10^5 cells were seeded in a 75 cm^2 flask (Corning, Tewksbury, MA, USA) for expansion. All subsequent experiments were performed at culture passage two.

2.4.3 MDPC-23 cell preparation

MDPC-23 cells were revived from cryogenic storage. Cryovials were heated to 40 °C for 1-2 minutes until thawed and the cell suspension was transferred to 1 mL of fresh medium and centrifuged (Jouan B4i, Thermo scientific, UK) at 900 g for 2 minutes. The supernatant was removed and cells were resuspended in 1 mL of fresh medium and plated in 25 cm^2 flasks. The cells were cultured for 2 hours at 37 °C in 5% CO_2 to enable cell attachment to the culture plasticware prior to addition of 4 mL of medium. Medium was refreshed every 24 hours and cells were passaged once they had reached 80-90% confluence by detachment using 0.25% (w/v) Trypsin 1 mM EDTA.4Na (Gibco, Paisley, UK). 1 x 10^5 cells were seeded in a 25 cm^2 flask for expansion. All subsequent experiments were performed at passage two.

2.4.4 Adenoviral transfection of rat dental pulp cells

Adenoviral vectors (Ad) are commonly used as a means for delivering gene supplementation into cells. This technique (Goff and Berg, 1976) was used to induce expression of hepatocyte growth factor (HGF) and its antagonist NK4 in RDPCs.

2.4.4.1 Optimisation of adenoviral transfection rate

RDPCs were seeded at a density of 2 x 10^3 cells in a 25 cm^2 flask and grown to 80% confluence. Medium was removed and cells were washed with 1 mL of PBS. Cells were then infected with EGFP (enhanced green fluorescent protein) AdNK4 (provided by Dr M. Y. Alexander, University of Manchester and manufactured by the Vector Core, Gene Therapy Program, Department of Medicine, University of Pennsylvania, USA) at a multiplicity of infection (MOI) of 0 – 400 particles / cell in 1 mL of PBS and incubated for 40 minutes. Medium was then added to a volume of 5 mL. A MOI of zero was used as control. Infection rates were determined on days 1, 3 and 5 by analysis of images observed under a Nikon Eclipse TE300 microscope using phase contrast and fluorescent light (Super high pressurised mercury lamp, Nikon, Japan). In five representative areas of the culture, cells were counted within the field of view at a magnification of x400 under phase contrast and fluorescent light. The mean percentage of EGFP positive cells was determined for each flask.

2.5 Functional response assays

2.5.1 WST-1 Cell proliferation assay

The WST-1 assay utilises the reduction of tetrazolium salt WST-1 [2-(4-iodophenyl)-3-(4-nitrophenyl)-5-(2,4-disulfophenyl)-2H-tetrazolium] to a coloured formazan compound, which occurs when it is exposed to a cell surface of metabolically active cells (Mosmann, 1983). When WST-1 reagent is added to cell cultures, it is metabolised and a colorimetric measurement can be obtained to determine the amount of formazan produced; subsequently, an estimated cell number can be determined from a standard curve. The number of cells can

be extrapolated from the standard curve based on the resultant change in absorbance providing an estimate of number of viable cells present in the culture.

To determine cell number, 20 µL of WST-1 (Roche Applied Biosciences, Mannheim, Germany) was added to 180 µL of medium in each well. Plates were kept in the dark for precisely 1 hour and incubated in standard culture conditions. The absorbance of the reduced compound was measured at a wavelength of 450 nm with a reference filter at 630 nm using an ELx800 Absorbance Microplate Reader (Biotek, Winooski, VT, USA). Cell number was calculated from a standard curve (Figure 2.11 and 2.12).

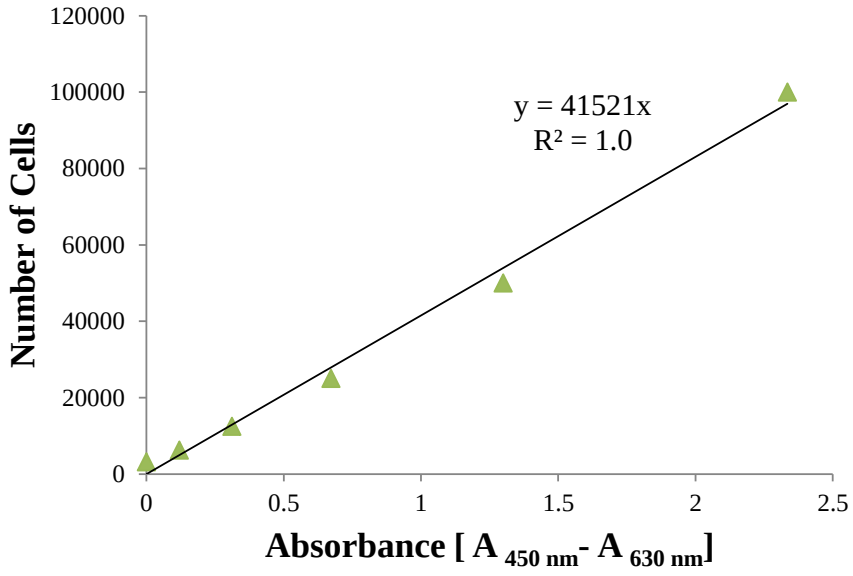

Figure 2.11 Representative example of standard curve used to estimate cell number with WST-1 cell proliferation assay in a 48-well plate using RDPCs as described in section 2.5.1. The R^2 coefficient (>0.9) and linear regression equation are displayed next to the line of best fit.

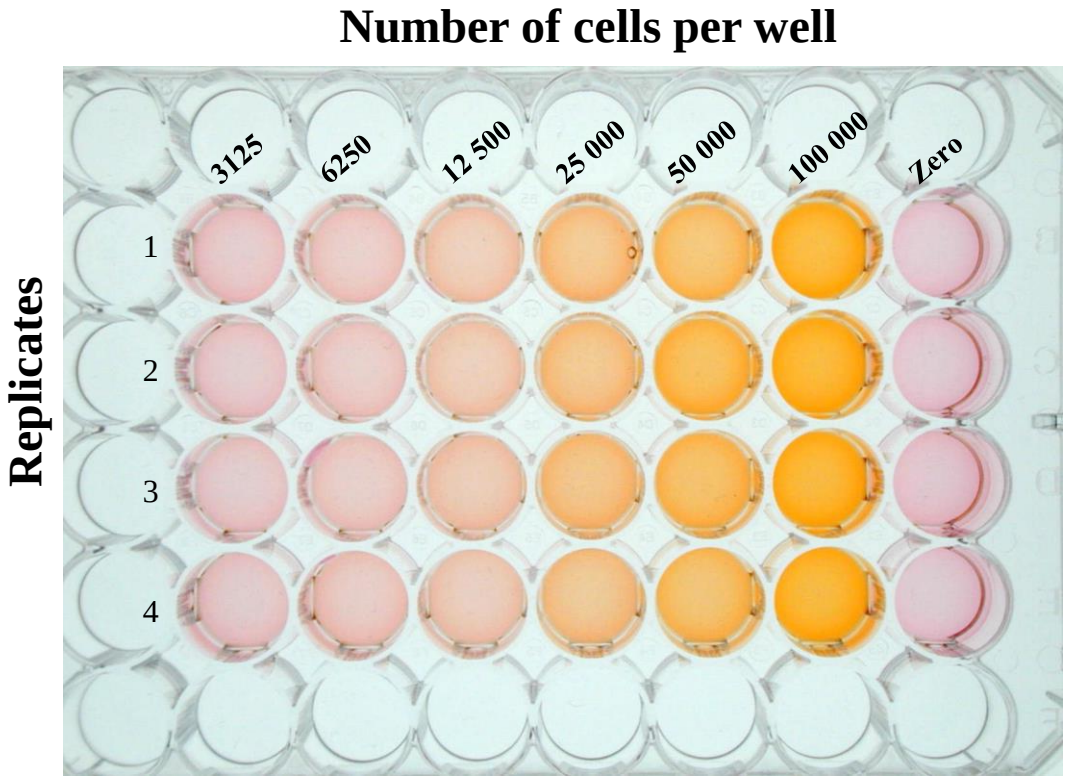

Figure 2.12 Photographic representation of a 48-well plate seeded with RDPCs of different seeding densities (0-100 000 cells) with four replicates of each following 1 hour incubation with WST-1 reagent. The image shows visibly the difference in colours for each seeding density. The plate was read using an optical plate reader at a wavelength of 450 nm with a reference filter at 630 nm in order to generate a standard curve and subsequently extrapolate cell number for each well.

2.5.1.1 Analysis of RDPC cell growth following supplementation with dECM preparations

To determine the optimal seeding density of RDPCs and MDPC-23 cells in a 48-well plate, different initial seeding densities were used and growth was monitored over a 7 day time period. Data indicated that the optimal seeding density for RDPCs was 1.0×10^4 per well and for MDPC-23 cells it was 7.5×10^3 per well in a 48-well plate (IWAKI, Chiba, Japan). Cells were seeded in 30 µL of medium in the centre of the well and allowed to attach for 2 hours prior to addition of 170 µL of the appropriate medium without FBS. Twenty-four hours later, medium was replaced with a dECM preparation supplemented medium. Preparations of dECM were previously extracted using EDTA, calcium hydroxide, white MTA and grey

MTA (section 2.1.3) and supplemented in medium at concentrations of zero (control), 0.1, 1.0, 10.0 and 100.0 μg/mL. To generate a standard curve of absorbance against cell number (Figure 2.11), 48-well plates were seeded at the following densities: 3125, 6250, 12500, 25000, 50000 and 100000 for RDPCs and 1250, 2500, 5000, 10000 and 20000 for MDPC-23 cells. Cultures were maintained for up to 7 days and 4 replicates for each control and experimental condition were analysed. At each time point (1, 3, 5, and 7 days for RDPCs and 1, 2, 3, 4, and 5 days for MDPC-23 cells), an assay of cell number was performed using the WST-1 assay (section 2.5.1).

2.5.1.2 Analysis of RDPC cell growth following HGF supplementation

RDPCs were seeded at a density of 1.0×10^4 in each well of a 48-well plate using standard medium and allowed to equilibrate for 24 hours. The medium was then replaced with mineralisation medium, which comprised α-MEM containing 5% FBS, 5 mM BGP, 2 mM l-Glutamine and 1% penicillin / streptomycin (section 2.4.1.3). Cultures were infected with the recombinant adenovirus for either AdHGF or AdNK4 at a MOI of 250 particles / cell as previously described in section 2.4.4.1 or supplemented with recombinant human HGF (Sigma Life Sciences, St Louis, USA) at concentrations of 5 to 20 ng/mL. To generate a standard curve of absorbance against cell number, 48-well plates were seeded at the following densities: 3125, 6250, 12500, 25000, 50000 and 100000. Four biological replicates for each group were analysed and medium was replenished every 48 hours; cultures were maintained for up to 15 days. At each time point (6, 8, 12, 13, 14 and 15 days), 20 μL of WST-1was added to the 180 μL of medium in each well. Cell number was calculated using a standard curve as described previously in section 2.5.1.

2.5.2 Chemotaxis transwell assay

To determine the chemotactic ability of HGF, migration assays were performed using a two chamber, 96-well plate assay system with 8 μm pore size and hydrophilic membrane (ChemoTx, Neuro Probe, Gaithersburg, MD, USA). Quiescence was induced in RDPCs by culture in maintenance medium (section 2.4.1.2) with 1% FBS 24 hours prior to the assay to induce a quiescent non-mitogenic state. Following this, cells were released as described previously and suspended at a concentration of 2.5 x 10^5 per mL. To fluorescently label cells, 5 μg/mL of calcein AM (Biotium Inc, Hayward CA, USA) was added to the cell suspension prior to incubation at 37 °C in 5% CO_2 for 30 minutes. Cells were pelleted by centrifugation at 800 g for 3 minutes, washed three times with PBS and re-suspended at a concentration of 1.0 x 10^6 per mL in medium containing no FBS. The lower chamber was prepared with either medium containing 30 μL of 10% FBS (positive control), 0% FBS (negative control) or dECM preparations extracted by EDTA, calcium hydroxide, white MTA and grey MTA at concentrations between 0.1 and 100 μg/mL or the following concentrations of recombinant HGF: 5, 10, 15 or 20 ng/mL. 30 μL of labelled (calcein AM) cell suspension was pipetted carefully onto the upper chamber and the plate was incubated for 45 minutes at 37 °C in 5% CO_2. The number of cells which had migrated to the lower chamber was determined using a microplate fluorometer (Twinkle LB970, Berthold Technologies, Harpenden, UK) at an excitation wavelength of 494 nm and emission 517 nm. Cell number was calculated from a standard curve (Figure 2.13) and four biological replicates were used for each condition.

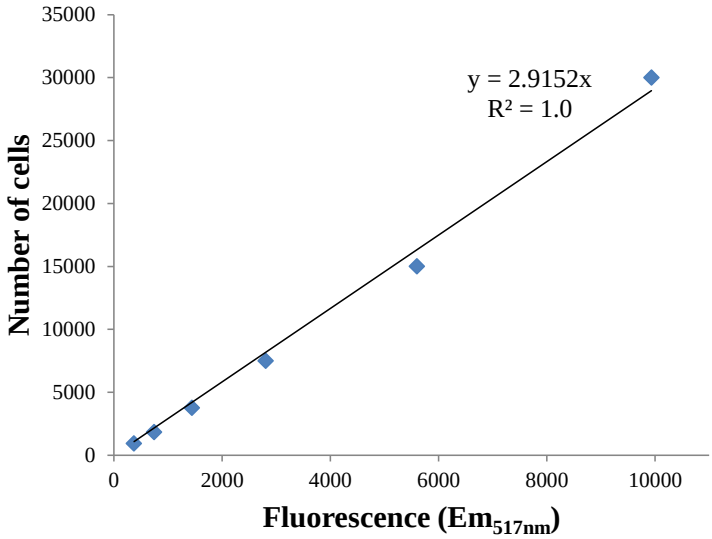

Figure 2.13 Representative example of standard curve used to determine cell number with calcein AM fluorescent label as described in section 2.5.2. The R^2 coefficient (>0.9) and linear regression equation are displayed next to the line of best fit. Em refers to emission wavelength.

2.5.3 Alizarin red staining in RDPC cultures exposed to ADNK4, AdHGF and recombinant HGF

To determine the ability of HGF to induce mineralisation of RDPCs, a semi-quantitative alizarin red staining (ARS) method was applied (Gregory et al., 2004). Alizarin red forms a complex with calcium through a chelation process and extraction of this complex produces an orange red solution whose absorbance can be quantified at 405 nm. The concentration of calcium can then be extrapolated from a standard curve; see Figure 2.14 for a representative example.

At each time point, cultures were washed with excess PBS and fixed with 10% paraformaldehyde (VWR, UK) for 15 minutes at room temperature. Cultures were washed again, twice with distilled water and incubated with 200 µL of 40 mM alizarin red (BDH

Laboratory Supplies, UK) at room temperature for 20 minutes with gentle agitation using an orbital shaker. Wells were gently washed four times with distilled water and stained cultures were captured under illumination from a light box using a Nikon Coolpix 950.

To enable quantification of staining, 200 µL 10% (v/v) acetic acid was added to each well and incubated at room temperature for 30 minutes with gentle agitation. Monolayers were subsequently removed from plates using a cell scraper and transferred to 1.5 mL microcentrifuge tubes. After vortexing for 30 seconds, the slurry was overlaid with 100 µL mineral oil (Sigma–Aldrich, UK), heated to 85 °C for 10 minutes and transferred to ice for 5 minutes. The slurry was then centrifuged at 20,000 g for 15 minutes and 500 µL of the supernatant was transferred to a new 1.5mL microcentrifuge tube. 200 µL of 10% (v/v) ammonium hydroxide was added to neutralise the acid. The absorbance values of aliquots (150 µL) of the supernatant were read in triplicate at a wavelength of 405 nm in 96-well format in a Biotek ELx800 microplate reader (Biotek, Winooski, VT USA) for each biological replicate.

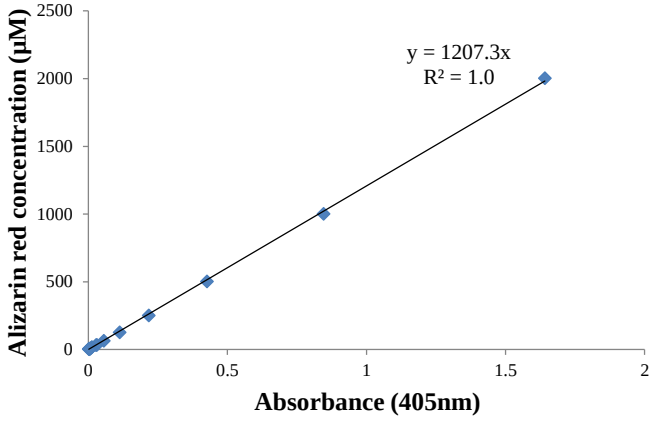

Figure 2.14 Representative example of standard curve used to determine mineral deposition by RDPCs using alizarin red staining as described in section 2.5.3. The R^2 coefficient (>0.9) and linear regression equation are displayed next to the line of best fit.

2.6 Gene expression analysis

2.6.1 RDPC exposure to HGF for gene expression analysis

RDPCs were seeded at a density of 5 x 10^4 in 500 μL culture medium in the centre of each well of a 6-well plate (Appleton Woods, UK). Following cell attachment after 6 hours, a further 2.5 mL of standard medium was added to each well. Twenty four hours after seeding the cells, the medium was replaced with optimised mineralisation medium (section 2.4.1.3) supplemented with PBS (control) or 5 ng/mL or 20 ng/mL of recombinant HGF. Medium was replaced every 48 hours and cells were cultured for up to 12 days. At days 1, 7 and 12, RNA was isolated as described in section 2.6.2. Three biological replicates for each control and experimental group were analysed.

2.6.2 RNA isolation from mammalian tissue and cell cultures

Total RNA was extracted using the same approach for all tissues or monolayer cell cultures using the RNeasy® minikit (Qiagen, West Sussex, UK) as per the manufacturer's instructions. For mammalian tissues, 20 mg of tissue was coarsely minced with a scalpel blade and placed in 500 μL of lysis buffer containing 1% (v/v) beta-mercaptoethanol (β-ME) (Promega, Wisconsin, USA) and disrupted with a Turrax Homogenizer (IKA, Staufen, Germany). For RDPCs, medium was removed and the cells were washed with warmed sterile PBS. RDPCs were then directly lysed *in situ* using 500 μL of lysis buffer (Qiagen, West Sussex, UK) containing 1% β-ME and then passed through a 25G gauge needle three times to aid cellular disruption. The resultant lysates were mixed with 500 μL 70% molecular grade ethanol (Sigma-Aldrich, UK) and transferred to a spin column assembly provided in the

RNeasy® minikit. The spin column was centrifuged for 15 seconds at 8,000 g (5415D Microcentrifuge, Eppendorf, UK) and the eluate discarded. Total RNA binds to the membrane and additional steps were used to aid removal of genomic DNA. The membrane was initially washed with 350 μL of wash buffer RW1 (RNeasy® minikit) and centrifuged for 15 seconds at 8,000 g prior to a DNase digestion step.

Digestion of contaminating genomic DNA was performed by treating the membrane with 80 μL of DNase 1 (RNase-Free DNase Set, Qiagen, UK) for 15 minutes at room temperature. Further wash steps were undertaken according to the manufacturer's instructions and the membrane finally dried by centrifugation of the spin column assembly at 11,000 g for 1 minute. The RNeasy® spin column was transferred to a collection tube and 40 μL of RNase free water was added directly to the membrane; this was centrifuged at 8,000 g for 1 minute to elute the RNA.

RNA concentration was estimated using a spectrophotometer (BioPhotometer, Eppendorf, UK) which measured absorbance at 260 nm and the purity determined from the ratio of absorbance at 260 and 280 nm with pure RNA has a A_{260}/A_{280} ratio of 1.9-2.1. RNA integrity was further analysed by agarose gel electrophoresis (section 2.6.6) and inspection whereby the ratio of 28s ribosomal RNA band to the 18s band should be approximately 2:1 (Figure 2.15).

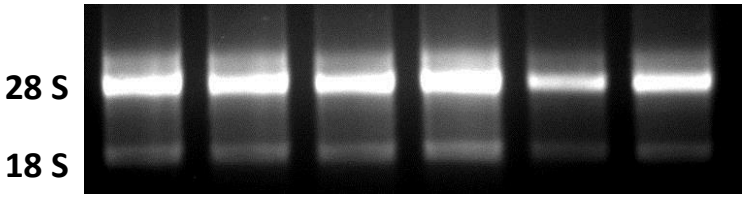

Figure 2.15 Representative image of total RNA extracted from RDPCs exposed to different concentrations of recombinant HGF with the RNeasy® mini kit and visualised using a SYBR gold 1.5% agarose gel separated by electrophoresis.

2.6.3 Reverse transcription

To generate single stranded DNA complementary to the mRNA samples isolated above (section 2.6.2), a reverse transcription (RT) step using a High Capacity RNA-to-cDNA Kit™ (Applied Biosystems, Paisley, UK) was used. 1-2 μg of RNA was added to the reaction mixture detailed in Table 2.3 according to the manufacturer's instructions. This mix was incubated in a thermal cycler (Mastercycler® Gradient, Eppedorf, UK) at 37 °C for 60 minutes to enable extension of transcription product and finally, at 95 °C for 5 minutes to denature the reverse transcriptase enzyme. The mix was then rapidly cooled to 4 °C prior to purification.

Table 2.3 The components and volumes for each constituent of a 20 µL reverse transcription reaction to convert RNA to single stranded cDNA.

Component	Component Volume (µL)
2✕ RT Buffer	10.0
20✕ RT Enzyme Mix	1.0
Sample RNA	≤ 5
Nuclease-free water	Made up to 20
Total volume per reaction	**20.0**

2.6.4 Concentration and purification of cDNA

To purify and concentrate cDNA, the unincorporated RT reaction components were removed as they could interfere or inhibit downstream analyses. Samples of cDNA were diluted with 480 µL of RNA-free water and added to the membrane of a Microcon YM-30 filter device (Millipore, UK), which was centrifuged at 10,000 g for 6 minutes. Single stranded cDNA molecules less than 60 nucleotides in length are removed and eluted with the water using this approach. Samples were washed with a further 500 µL of RNA-free water and centrifuged at 10,000 g for 8 minutes. The volume was measured with a pipette and further centrifugation was performed until a volume of less than 50 µL was obtained. To collect the cDNA, the Microcon device was inverted and placed in a 1.5 mL microcentrifuge tube and the assembly was centrifuged at 1,000 g for 3 minutes. The concentration of cDNA was established in a cuvette with a dilution of 1 µL in 69 µL of Nuclease-free water (Ambion, CA, USA) using a spectrophotometer (A_{260}) (BioPhotometer, Eppendorf, UK).

2.6.5 Polymerase chain reaction

2.6.5.1 Preparation and reaction conditions

Preparation for all polymerase chain reactions (PCRs) was performed on ice to prevent primer dimer formation and premature initiation of the reactions. Lyophilised oligonucleotide primers (Invitrogen, UK) specific to human and rat species were dissolved in DNase free water according to manufacturer's instructions. These were further diluted to a concentration of 25 µM and stored at -20 °C as working stocks. PCR assays were performed using the REDTaq® PCR system (Sigma-Aldrich, UK) according to manufacturer's instructions. The REDTaq system contains: 20 mM Tris-HCl, pH 8.3, with 100 mM KCl, 3 mM MgCl2, 0.002% gelatin, 0.4 mM dNTP mix (dATP, dCTP, dGTP, TTP), stabilizers, and 0.06 unit/µL of Taq DNA Polymerase. For each set of primers (Table 2.4 provides primer sequences and cycling conditions), a master mix was prepared (Table 2.5) and placed in a 200 µL PCR tube (Appleton Woods, UK).

Table 2.4 PCR primer sequences, accession number, product size and assay conditions for human and rat primers. (GAPDH, glyceraldehyde 3-phosphate dehydrogenase; HGF, Hepatocyte growth factor; DMP-1, dentine matrix phosphoprotein-1; ALP, alkaline phosphatase; Col-Iα, collagen type I alpha).

	Gene	Primer sequence (5′ to 3′)	Accession Number	Product Size (bp)	Tm (°C)	Cycle Number
Human	GAPDH	F-TCT AGA CGG CAG GTC AGG TCC R-CCA CCC ATG GCA AAT TCC ATG	NM001256799.1	598	60	30
	HGF	F – ACC ACA CGA ACA CAG CTT TTT GCC R – CCC CAG AGG GAT GTC TCA GGC AG	NM001010934	408	60	40
	c-Met	F – GCT GGT CCA GGC AGT GCA GC R – AGC ACG CCA AAG GAC CAC ACA	NM001127500.1	633	60	36
Rat	GAPDH	F – CCC ATC ACC ATC TTC CAG GAG C R – CC AGT GAG CTT CCC GTT CAG C	XM576394.4	473	60	23
	HGF	F – TCA CAC AGA ATC AGG CAA R – TGC ATT TGA AGT TCT CGG	NM017017.2	368	55	45
	c-Met	F – ACC CAG ATT GTT TTC CTT R – AAT GCA ATG AAT AAT CGG	NM031517.1	366	55	45
	DMP-1	F – CGG CTG GTG GTC TCT CTA AG R – CAT CAC TGT GGT GGT CCT TG	NM_203493.3	248	60.5	31
	Nestin	F – CAT TTA GAT GCT CCC CAG GA R – AAT CCC CAT CTA CCC CAC TC	NM_012987.1	285	60.5	35
	ALP	F – CTC CGG ATC CTG ACA AAG AA R – ACG TGG GGG ATG TAG TTC TG	J03572.1	499	60.5	28
	Col-Iα	F – GGGCAAGACAGTCATCGAAT R – TTGGTTTTTGGTCACGTTCA	BC133728	336	60	30
	Osteopontin	F – AAG CCT GAC CCA TCT CAG AA R – GCA ACT GGG ATG ACC TTG AT	NM_012881.1	445	60.5	24
	Osterix	F – GCT GCC TAC TTA CCC GTC TG R – TGT GAA TGG GCT TCT TCC TC	NM001037632.1	302	60	30
	Osteocalcin	F – TCC GCT AGC TCG TCA CAA TTG G R – CCT GAC TGC ATT CTG CCT CTC T	J04500.1	699	60	28
	Runx2	F – GCC ACC GAG ACC AAC CGA GTC R – GAA ACT CTT GCC TCG TCC GCT CC	NM053470.2	736	60	28

Table 2.5 Reagents and volumes used for each PCR analysis.

Reagent	Volume (µL)	Concentration
REDTaq® ReadyMix™	12.5	1 x
Forward Primer(25 mM)	0.5	25 mM
Reverse Primer (25 mM)	0.5	25 mM
RNase Free Water	make up to 25	N/A
cDNA	≤ 2	50 ng

Based on spectrophotometer readings, 50 ng of cDNA was added to the master mix in the PCR tube with a gentle pipetting action to agitate the mixture. Reactions were amplified in a thermal cycler (GeneAmp PCR system 2700 Applied Biosystems, Foster City CA, USA) according to the conditions in Table 2.5 and Table 2.6 for each target. 6 µL of product was removed from the PCR tube once the relevant cycle number had been reached for subsequent visualisation using gel electrophoresis (section 2.6.6).

Table 2.6 Typical temperature and timings for each stage of the PCR performed in a thermal cycler (GeneAmp PCR system 2700 Applied Biosystems, Foster City CA, USA).

Reaction stage	Temperature (°C)	Time (minutes)	
Denaturation	94	5	
Denaturation	94	30 seconds	cycle number dependent upon gene assay
Annealing	Primer specific (See Table 2.4)	30 seconds	
Polymerisation	72	30 seconds	
Polymerisation	72	7	

2.6.5.2 Sample normalisation

To compare gene expression changes between control and experimental samples, band intensity of the target gene was normalised against the housekeeping gene, glyceraldehyde 3-phosphate dehydrogenase (GAPDH) (McKinney and Robbins, 1992, Robbins and McKinney, 1992). To ensure that the amount of amplified product was comparable in each subsequent PCR for test genes, volumes of each control and experimental sample to be compared were adjusted until the intensity of each GAPDH product [calculated using image analysis software (section 2.6.6)] was within 10%.

2.6.6 Gel electrophoresis and imaging

Isolated RNA and PCR products were visualised using non-denaturing agarose gel electrophoresis. Agarose gels were prepared using 1.0% (for RNA) or 1.5% (for DNA) (w/v) agarose (WebScientific, UK) in 1xTris-acetate EDTA (TAE) buffer (Helena Biosciences, UK) by boiling in a microwave (M1714 Samsung, Korea) for approximately 2 minutes at 850 W until the agarose had dissolved. Once the gel had cooled, 10 mg/mL of SYBR gold (Molecular probes, UK) for RNA gels or 10 mg/mL ethidium bromide (Helena Bioscience, UK) for PCR product analysis were added to the gel solution. The gel was poured into an appropriate gel casting tray and a comb added to create wells within the gel. All air bubbles were removed. Prior to loading RNA, 6X bromophenol blue loading dye (Merck, UK) was added to each sample. 5 µL of RNA with loading dye (Bioline, UK), PCR product or Hyperladder IV (Bioline, UK) as a nucleic acid standard were loaded into the wells of the gel prior to electrophoresis at 80-120 v for 25-35 minutes. Gel imaging was performed using the G:BOX gel imaging system (Syngene, Cambridge, UK) for image capture under UV

illumination. The resultant image was analysed with GeneSnap image acquisition software (Syngene, Cambridge, UK) to determine the band density for control and experimental targets. Semi-quantitative gene expression changes were conveyed as a percentage increase or decrease compared with control.

2.7 Statistical analysis

The individual experiments were performed with at least 3 biological replicates per control or experimental group. Normal distribution was tested for using the Shapiro-Wilk test. Statistical differences between the experimental and control groups were determined using one way ANOVA with Bonferroni post hoc analysis or Student's t test for normally distributed data. Statistical analysis was performed using Microsoft Excel (Microsoft Corporation, USA) or SPSS software (SPSS Inc, USA) with $p<0.05$ deemed to be statistically significant from control.

3.0 RESULTS CHAPTER 1

Analysis of dentine extracellular matrix (dECM) liberated by the soluble components of therapeutic pulp capping agents

Although tissue repair and regeneration of the dental pulp via iatrogenic material induction has been recognised since the early twentieth century (Hermann, 1920), the underlying biological repair mechanisms remain poorly understood. Numerous different therapeutic agents have been used to create an environment in which pulpal repair will occur and until recently, calcium hydroxide was deemed to be the gold standard. The effects of calcium hydroxide were originally attributed to three mechanisms: i) hydroxyl ion release and maintenance of a high pH (Kardos et al., 1998), ii) bactericidal activity (Horsted-Bindslev et al., 2003), and iii) chemical injury initiating a superficial layer of necrosis (Goldberg et al., 2003b, Schroder and Granath, 1971, Schroder and Sundstrom, 1974). Recently, our laboratory postulated that calcium hydroxide released growth factors sequestered in the dentine which subsequently stimulate pulpal healing (Graham et al., 2006). Little is yet known about the ability of more contemporary and predictable therapeutic pulp capping agents, such as MTA (Nair et al., 2008), to solubilise dECM components.

In this study, dECM components were isolated from powdered sound human dentine using solutions prepared from a routinely used agent 10% EDTA (control) and the soluble products from recognised therapeutic pulp capping agents, including calcium hydroxide and the calcium silicate cements of white MTA, grey MTA and Biodentine®. Notably, previous studies have shown that 10% EDTA and a super saturated solution of 0.02M calcium hydroxide are effective at solubilising dECM from powdered dentine using a well characterised *in vitro* extraction technique (Smith and Leaver, 1979, Graham et al., 2006).

This chapter investigates the soluble components of MTA using atomic absorption spectroscopy (AAS) and includes an analysis of liberated dECM components using biochemical techniques, gel electrophoretic separation, conventional and multiplex ELISA.

3.1 Spectroscopic analysis of extraction solutions

To characterise the solubilised metallic ion composition of solutions of EDTA, calcium hydroxide, white MTA and grey MTA prior to their use in dECM extraction, atomic absorption spectroscopy (AAS) was employed (Table 3.1). All ions analysed, including aluminium, calcium, iron, magnesium, potassium and sodium, were potentially able to be liberated from MTA as identified by the manufacturer's (Dentsply Tulsa Dental, USA) contents list.

Notably, the EDTA solution had a high concentration of sodium ions due to the addition of sodium hydroxide, which was used to neutralise the pH to 7.2. White and grey MTA liberated similar amounts of each metallic ion assessed, with calcium being the most abundant. No iron was detectably solubilised by the grey MTA using this method of dissolution, although aluminoferrite is described as one of its constituents. The calcium ion concentration in the calcium hydroxide solution was four times greater than that detected in white or grey MTA solutions. Potassium and sodium ions were detected in both white and grey MTA at similar concentrations.

Table 3.1 Data for the mean concentrations (mg/L) of ions present in each of the extraction solutions of EDTA, calcium hydroxide [$Ca(OH)_2$], white MTA (WMTA) and grey MTA (GMTA), as determined by atomic absorption spectroscopy. (All experiments were performed in triplicate and data are expressed as mean values ±SD).

Ion	EDTA (mg/L)	$Ca(OH)_2$ (mg/L)	WMTA (mg/L)	GMTA (mg/L)
Aluminium	0.00	0.00	25.42 (±2.29)	21.48 (±3.67)
Calcium	0.00	1725.49 (±160.50)	405.23 (±274.74)	444.44 (±114.89)
Iron	0.00	0.00	0.00	0.00
Magnesium	0.00	0.00	0.00	0.00
Potassium	0.00	0.00	10.41 (±0.64)	10.04 (±0.64)
Sodium	46727.00 (±910.0)	12.30 (±2.62)	10.94 (±0.52)	12.46 (±0.78)

3.2 Extraction profile analysis

dECM components were extracted over a 14 day period as described in section 2.1.3. In order to monitor changes in extraction conditions during this period and determine the rate at which dECM components were released, pH and protein content was measured daily.

3.2.1 pH of supernatant over 14 day extraction

The addition of protease inhibitors n-ethylmaleimide and phenyl-methyl-sulphonylfluoride resulted in the therapeutic pulp capping agent solutions becoming mildly acidic (pH 5.1-5.5) compared to their initial pH values which were: calcium hydroxide (11.9), white MTA (11.7), grey MTA (11.7) and Biodentine® (11.5) respectively. However, after one day of contact with dentine powder in solution, this acidity was neutralised (Figure 3.1) and the pH of the pulp capping agents ranged from 7.5 to 8.2. Over the 14 day extraction period, the pH of recovered supernatant for the EDTA solution varied minimally with the lowest pH on day 7 being 6.7; it returned to 7.2 by day 14. All pulp capping materials demonstrated a similar trend over the 14 day period (apart from calcium hydroxide) and the recovered supernatants showed a general decline in pH after day 1 for white MTA, grey MTA and Biodentine®. After incubation with dentine powder, the calcium hydroxide recovered supernatant decreased in pH after day 1 to 6.7 by day 3; from that point in time there was a gradual daily increase in pH, reaching 11.2 by day 14.

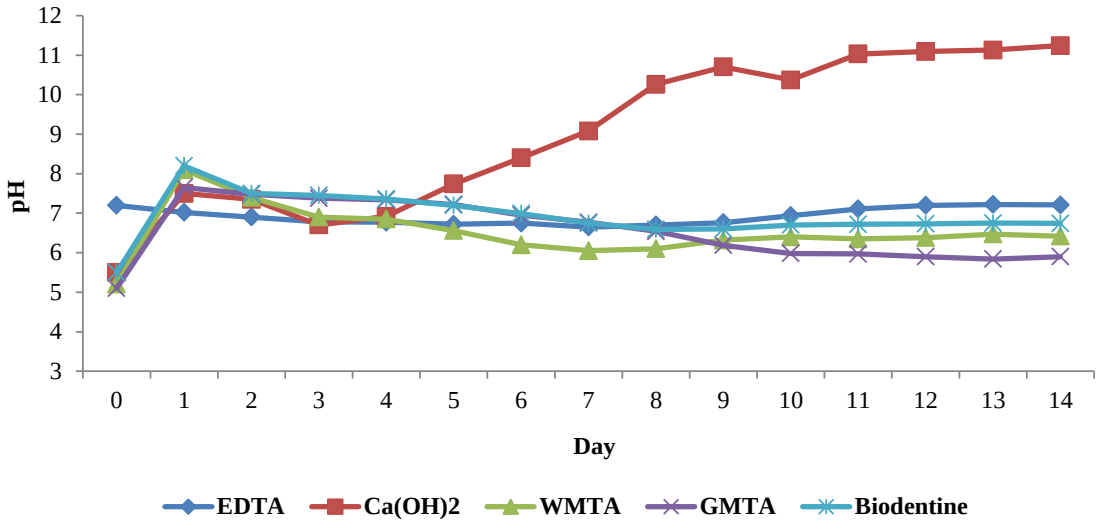

Figure 3.1 pH of extraction solutions for EDTA, calcium hydroxide [$Ca(OH)_2$], white MTA, grey MTA and Biodentine®, prior to isolation (day 0) with supernatant from dentine dissolution and profiled over the 14 day extractant period.

3.2.2 Protein release over 14 day extraction period of recovered supernatants

Protein content of recovered supernatant for each extraction was determined on a daily basis throughout the extraction period by measuring absorbance at 280 nm as a surrogate marker (Figure 3.2). The pattern of protein release from dentine by the control, EDTA during the extraction period, was comparable with that of previous in-house and published data (Graham et al., 2006), whereby absorbance was relatively high on the first day of extraction (3.51 units) and this gradually declined throughout the extraction period, in this case to 1.77 units by day 14. The pulp capping agents demonstrated analogous protein profile release with each other, apart from grey MTA where daily protein release was similar throughout the extraction period. Calcium hydroxide, white MTA and Biodentine® solutions demonstrated that protein release from powdered human dentine decreased between day 1 and 2 and plateaued for the remaining extraction period. Only calcium hydroxide demonstrated a slight deviation from this pattern, with a sharp decrease in absorbance detected between day 13 (1.90 units) and day

14 (1.44 units). In contrast, the protein release in the extractant supernatant for grey MTA showed a gradual increase over the 14 day extraction period with the absorbance value rising gradually from 1.53 units on day 1 to 2.30 units on day 12. There was a slight decrease over the final two days of the extraction period to 2.12 units.

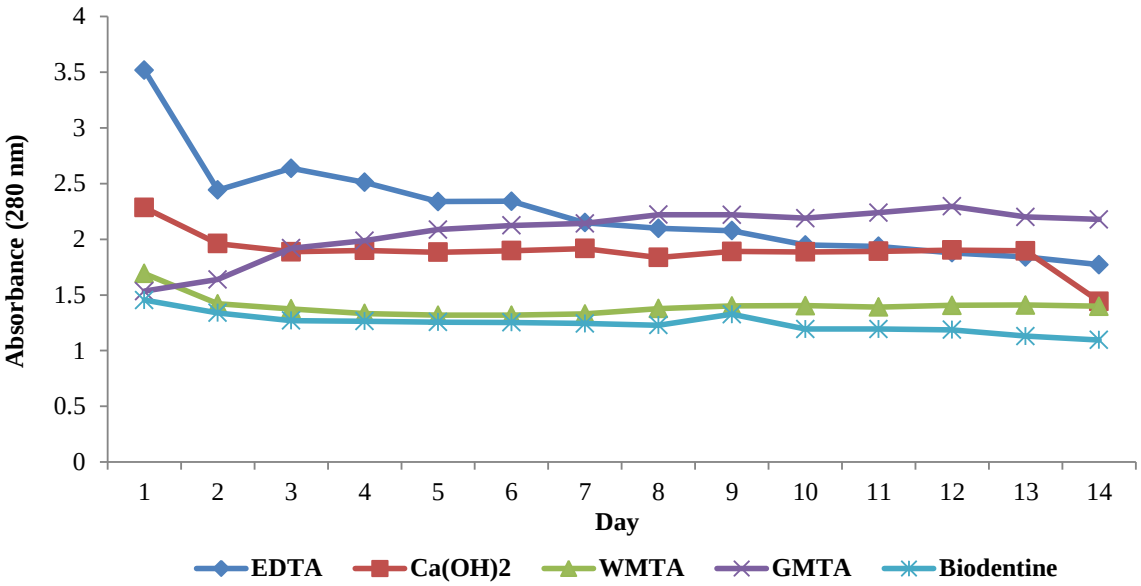

Figure 3.2 Estimation of protein content using absorbance profile at 280 nm as a surrogate marker, over the 14 day extraction period, for dissolution of dECM by EDTA, calcium hydroxide, white and grey MTA and Biodentine® solutions.

3.2.3 Percentage yield of recovered dECM components following extraction with EDTA, calcium hydroxide, white MTA, grey MTA and Biodentine® solutions

The total yield of dECM components was calculated as a percentage of the total weight of dentine powder originally used in the extraction, as shown in Table 3.2. The highest yield of dECM resulted from the EDTA extraction solution, with 4.35% of human dentine powder solubilised and recovered as ECM components. Of the remaining solutions, white MTA produced the second highest yield (0.91%) followed by grey MTA (0.64%) calcium hydroxide (0.32%) and Biodentine® (0.16%).

Table 3.2 Percentage yield of recovered extracted dECM components following extraction for 14 days with EDTA, calcium hydroxide, white and grey MTA and Biodentine®.

Extraction Solution	Weight of powdered dentine (g)	Weight of recovered extract (g)	Yield (%)
EDTA	10.07	0.439	4.35
$Ca(OH)_2$	25.05	0.081	0.32
WMTA	25.05	0.228	0.91
GMTA	25.10	0.162	0.64
Biodentine®	20.01	0.033	0.16

3.3 Characterisation of dECM components

dECM composition includes collagenous and non-collagenous proteins (NCPs), glycosaminoglycans (GAGs) and proteoglycans (Linde, 1985). To characterise solubilised dECM components extracted by each control and test agent, several methodological approaches were applied, including biochemical analysis using dye binding assays, separation by molecular weight using 1D SDS PAGE and cytokine antibody array analysis for different growth factor content.

3.3.1 Non-collagenous protein (NCP) and glycosaminoglycan (GAG) analysis of dECM extracts

Dye binding assays based on the Bradford assay (Bradford, 1976) and Bicinchoninic acid (BCA) assay (Smith et al., 1985) were used to determine the concentration of NCPs in dECM extracts. The Farndale assay (Farndale et al., 1986) was used to determine the concentration of GAGs in each sample of dECM components. Data are summarised in Table 3.3

Table 3.3 Table showing a comparison of total weight (per mg of extract or per gram of dentine) of non-collagenous proteins (NCPs) and glycosaminoglycans (GAGs) extracted by EDTA, calcium hydroxide, white and grey MTA and Biodentine®, as determined by the Bradford, Bicinchoninic acid (BCA) or Farndale assays, respectively.

Extraction Solution	Bradford assay		BCA assay		Farndale assay	
	µg NCP per mg of extract	µg NCP per gram of dentine	µg NCP per mg of extract	µg NCP per gram of dentine	µg GAGs per mg of extract	µg GAGs per gram of dentine
EDTA	53.96	2350	62.14	2703	50.10	2180
Calcium Hydroxide	49.48	160	66.54	210	48.39	154
WMTA	27.49	250	66.54	610	32.90	299
GMTA	36.75	235	96.52	616	39.74	254
Biodentine®	30.18	48	84.70	136	32.70	52

When comparing the quantity of NCP per gram of dentine released using the Bradford and BCA assays, the results demonstrated a similar trend, however, the BCA assay demonstrated greater amounts of NCPs released, suggesting it may be a more sensitive detection method for

NCPs. EDTA solubilised the greatest amount of NCPs from dentine as determined by the Bradford (2350 μg per gram of dentine) and the BCA (2703 μg per gram of dentine) assays. The proportion of NCPs in samples solubilised by white and grey MTA was the greatest for all of the pulp capping agents tested, as detected by the Bradford assay [WMTA (250 μg per gram of dentine) and GMTA (235 μg per gram of dentine)] and the BCA assay [WMTA (610 μg per gram of dentine) and GMTA (616 μg per gram of dentine)]. Biodentine® solubilised the least amount of NCPs of all extraction agents used: Bradford assay (48 μg per gram of dentine) and the BCA assay (136 μg per gram of dentine).

The release of GAGs, as determined by the Farndale assay, by the extraction solutions demonstrated a similar pattern of results to those obtained with the NCP dye binding assays. The EDTA extraction solution solubilised the most GAGs (2180 μg per gram of dentine) and Biodentine® solubilised the least (52 μg per gram of dentine). The ratio of NCPs (Bradford) to GAGs for each solution was as follows: EDTA (1:1.07), calcium hydroxide (1:1.03), white MTA (1:0.84), grey MTA (1:0.93) and Biodentine® (1:0.92).

3.3.2 One dimensional polyacrylamide gel electrophoretic analysis of dECM extracts

1D SDS PAGE analysis was performed to compare the profile of proteins that were solubilised by solutions of EDTA, calcium hydroxide, white MTA and grey MTA, based on molecular weight. Figures 3.3 to 3.5 show representative images of Tris-Acetate and Bis-Tris gels, which separate high and low molecular weight proteins, visualised using the Coomassie blue and silver staining methods. GeneTools software (Syngene, Cambridge, UK) analysis enabled automatic determination of the number of bands separated along with their individual molecular weights; these data are summarised in Table 3.4.

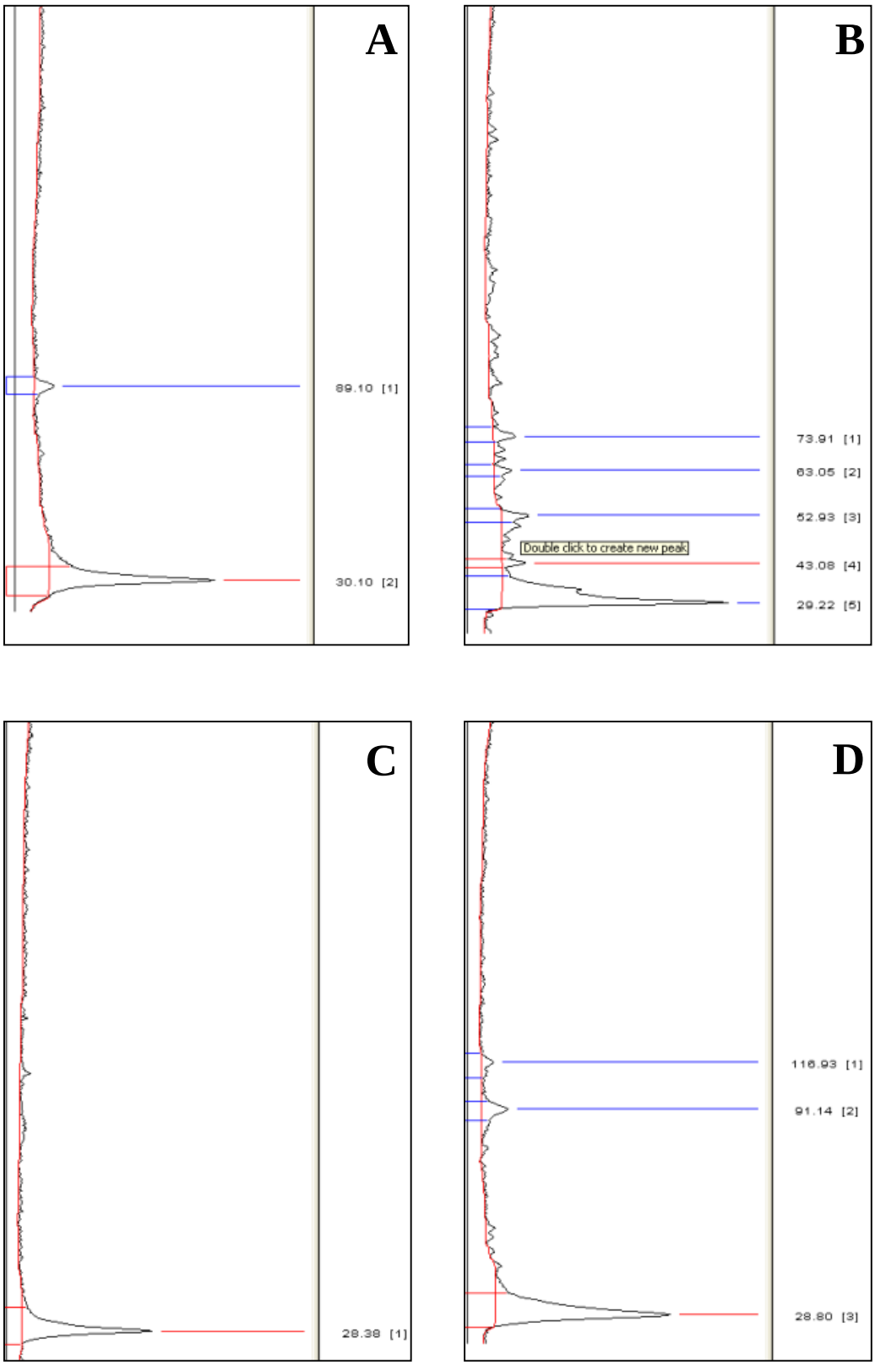
A
89.10 [1]
30.10 [2]
B
73.91 [1]
63.05 [2]
52.93 [3]
Double click to create new peak
43.08 [4]
29.22 [5]
C
28.38 [1]
D
116.93 [1]
91.14 [2]
28.80 [3]

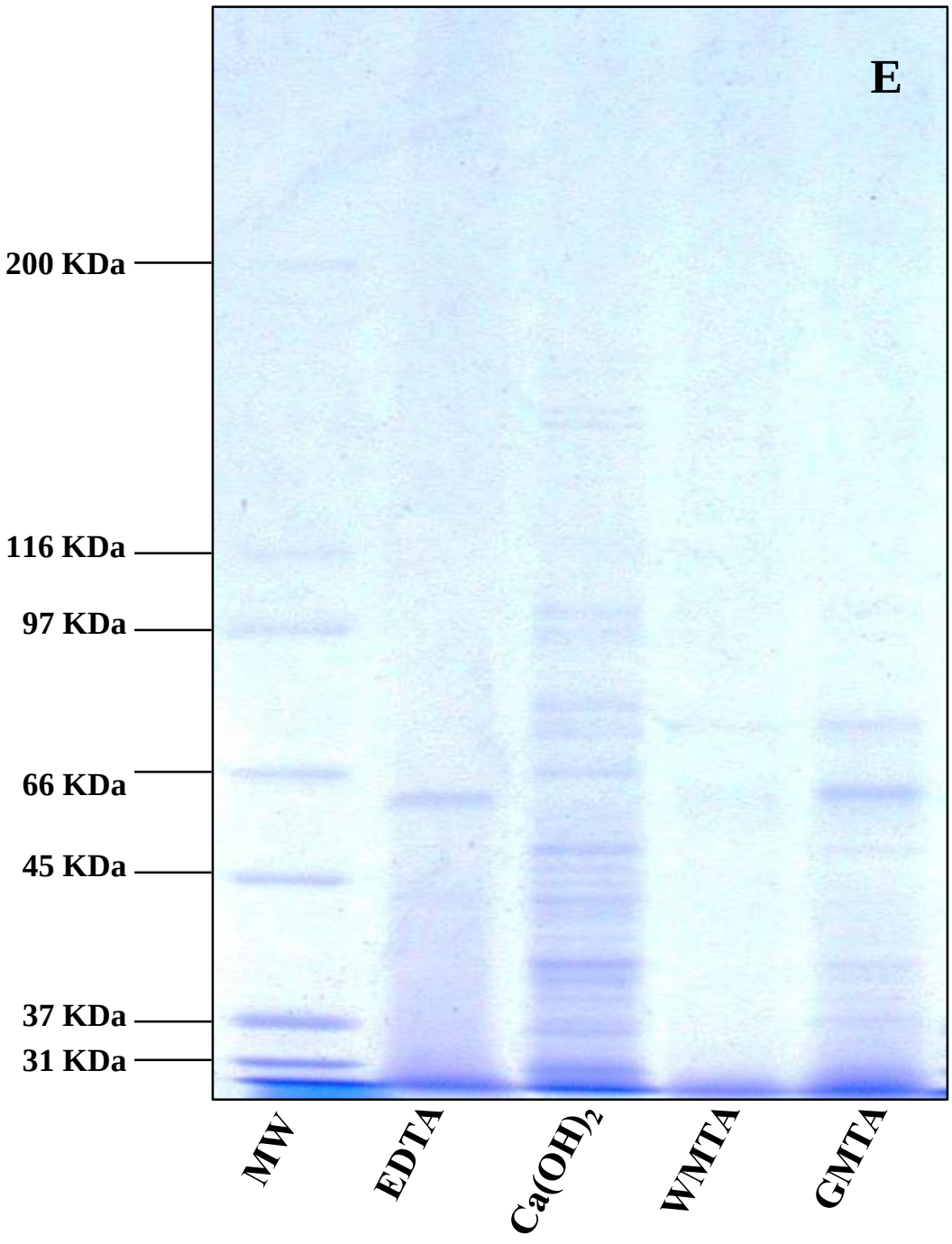

Figure 3.3 *(opposite*) Histogram analysis of gel above using GeneTools software (Syngene, UK) to automatically identify peaks and molecular weight of bands separated in dECM components extracted by: **A)** EDTA, **B)** calcium hydroxide, **C)** white MTA and **D)** grey MTA. *(above)* **E)** SDS PAGE protein separation of dECM components extracted by EDTA, calcium hydroxide ($Ca(OH)_2$), white MTA (WMTA) and grey MTA (GMTA) with Tris-Acetate 3-8% gel stained using Coomassie blue. MW=molecular weight marker MARK 12 (Invitrogen,UK).

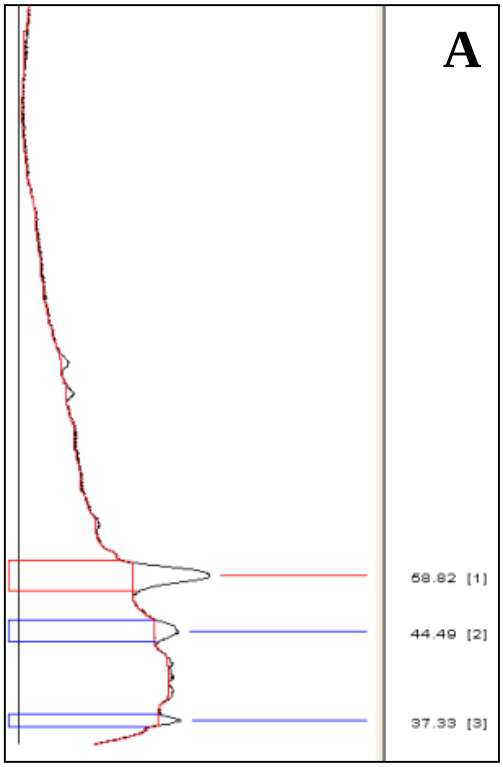
A
68.82 [1]
44.49 [2]
37.33 [3]

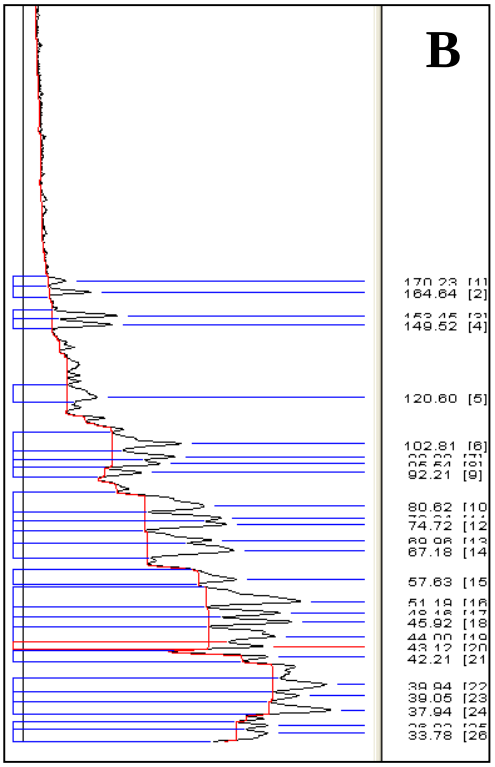
B
170.23 [1]
164.64 [2]
149.52 [4]
120.60 [5]
102.81 [6]
92.21 [9]
80.62 [10]
74.72 [12]
67.18 [14]
57.63 [15]
45.92 [18]
42.21 [21]
39.05 [23]
37.94 [24]
33.78 [26]

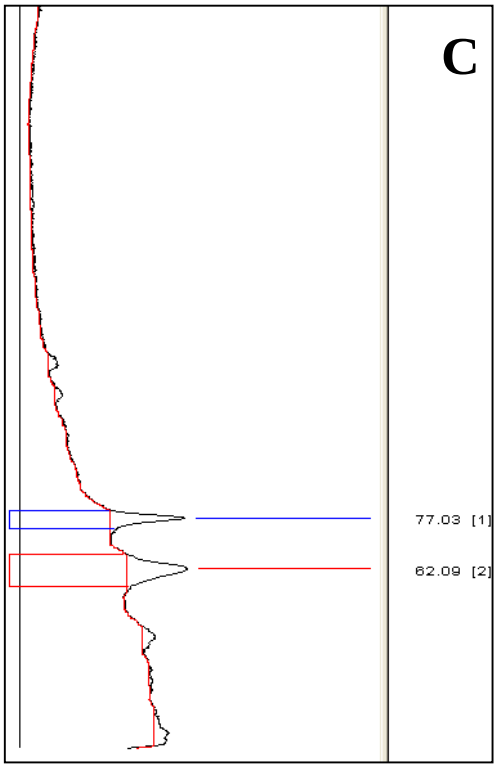
C
77.03 [1]
62.09 [2]

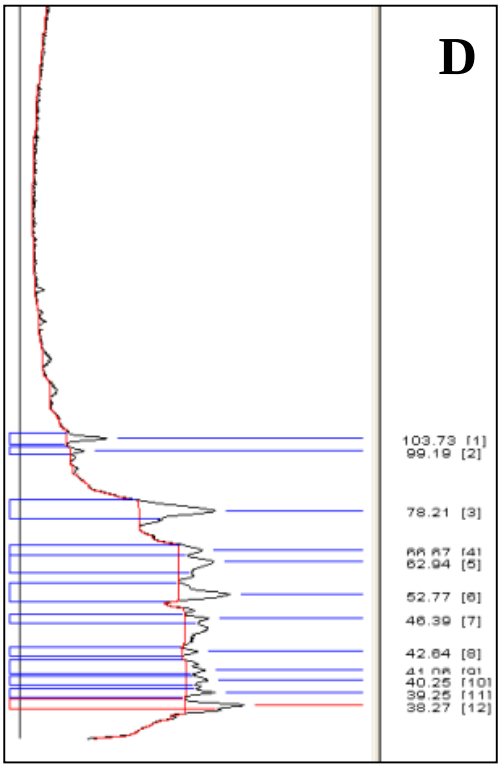
D
103.73 [1]
99.19 [2]
78.21 [3]
62.94 [5]
52.77 [6]
46.39 [7]
42.64 [8]
40.25 [10]
39.25 [11]
38.27 [12]

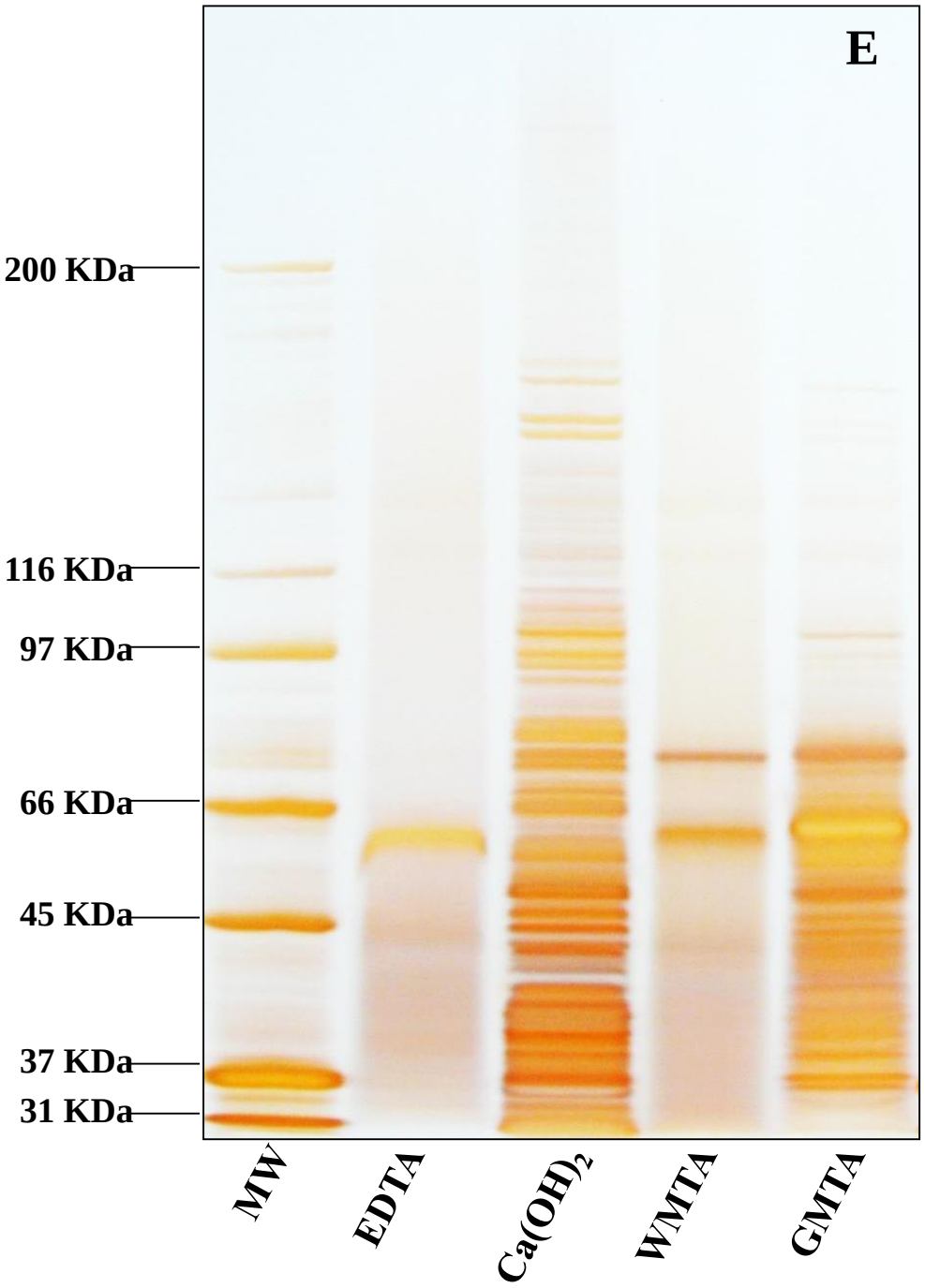

Figure 3.4 *(opposite*) Histogram analysis of gel above using GeneTools software (Syngene, UK) to automatically identify peaks and molecular weight of bands separated in dECM components extracted by: **A)** EDTA, **B**) calcium hydroxide, **C)** white MTA and **D)** grey MTA. *(above)* **E)** SDS PAGE protein separation of dECM components extracted by EDTA, calcium hydroxide ($Ca(OH)_2$), white MTA (WMTA) and grey MTA (GMTA) with Tris-Acetate 3-8% gel stained using silver stain. MW=molecular weight marker MARK 12 (Invitrogen,UK).

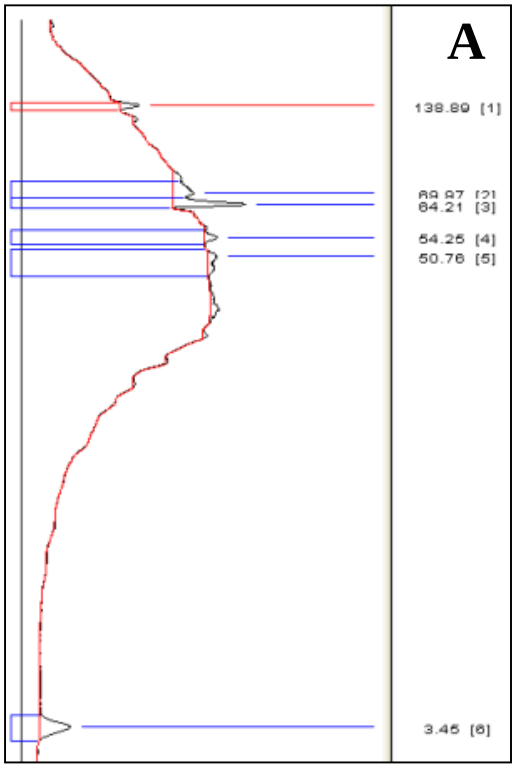
A
138.89 [1]
84.21 [3]
54.25 [4]
50.76 [5]
3.45 [6]

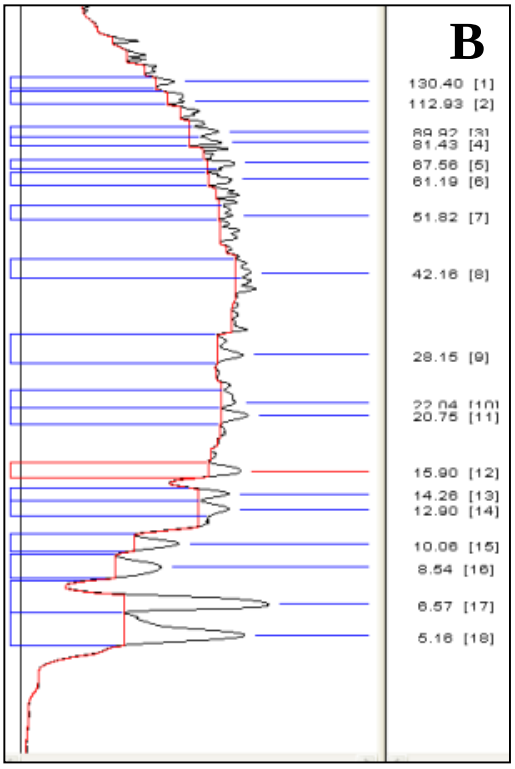
B
130.40 [1]
112.93 [2]
67.56 [5]
61.19 [6]
51.82 [7]
42.16 [8]
28.15 [9]
20.75 [11]
15.90 [12]
14.26 [13]
12.90 [14]
10.06 [15]
8.54 [16]
6.57 [17]
5.16 [18]

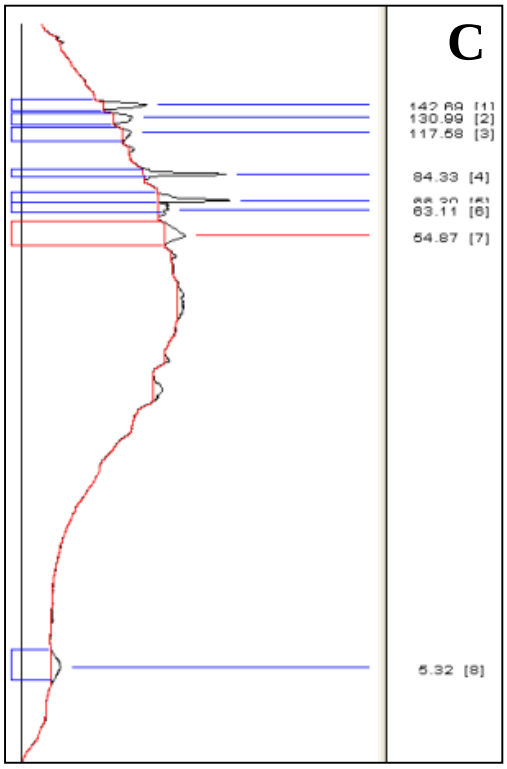
C
130.99 [2]
117.58 [3]
84.33 [4]
63.11 [6]
54.87 [7]
5.32 [8]

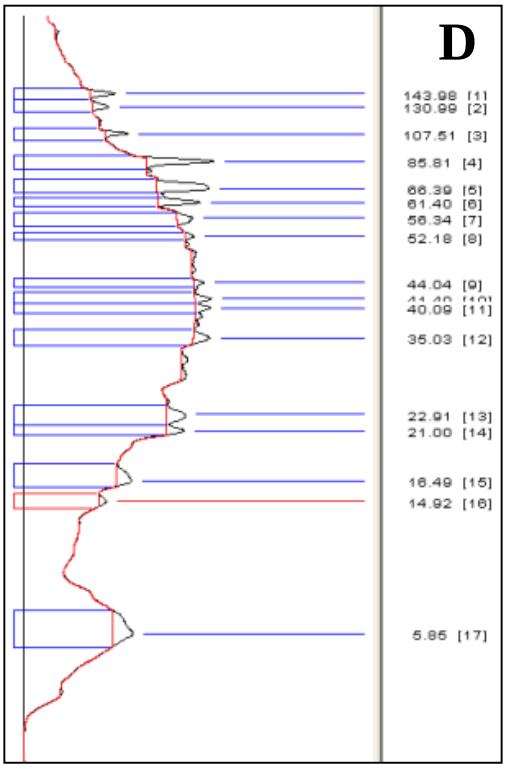
D
143.98 [1]
130.99 [2]
107.51 [3]
85.81 [4]
66.39 [5]
61.40 [6]
56.34 [7]
52.16 [8]
44.04 [9]
40.09 [11]
35.03 [12]
22.91 [13]
21.00 [14]
16.49 [15]
14.92 [16]
5.85 [17]

.

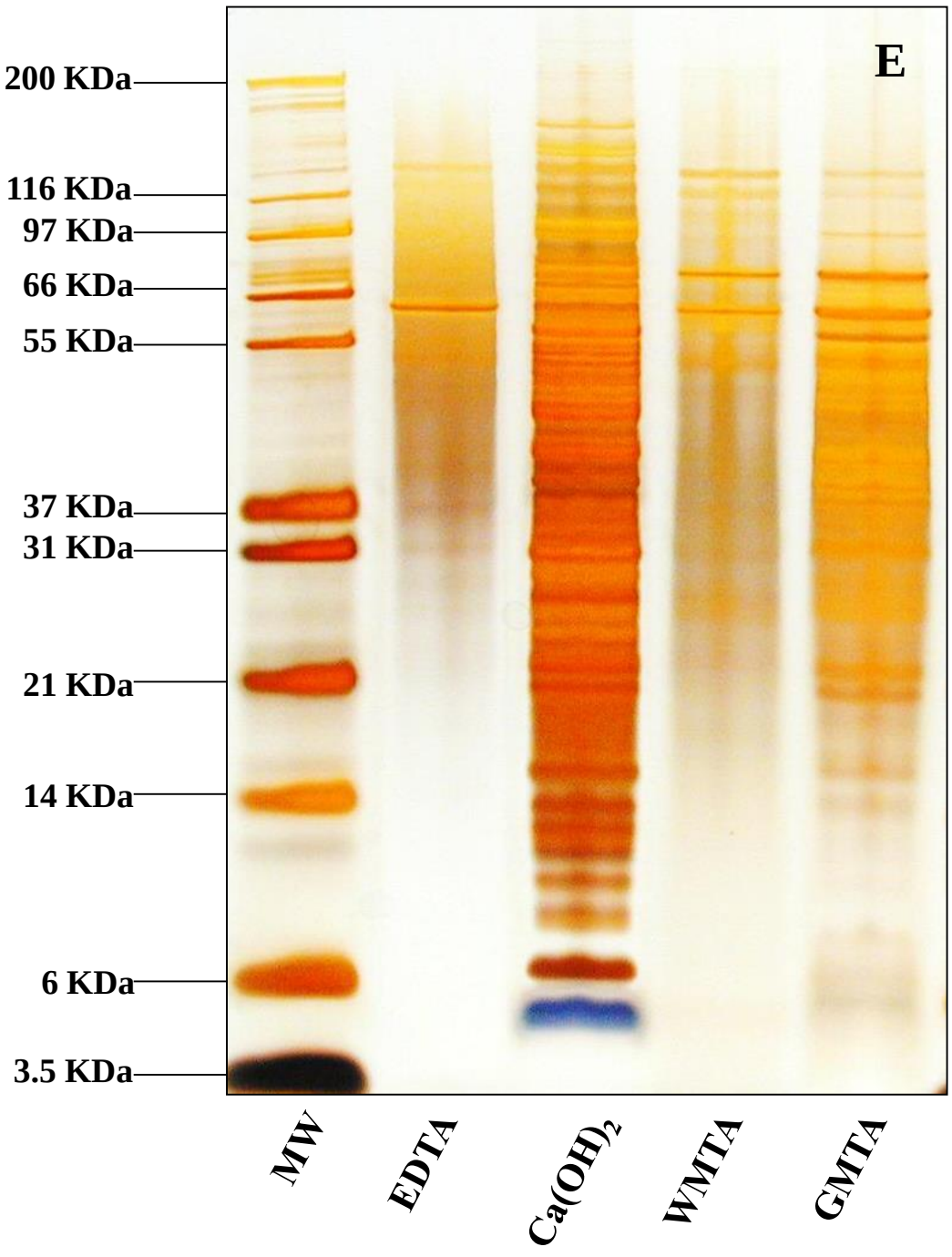

Figure 3.5 *(opposite)* Histogram analysis of gel above using GeneTools software (Syngene, UK) to automatically identify peaks and molecular weight of bands separated in dECM components extracted by: **A)** EDTA, **B)** calcium hydroxide, **C)** white MTA and **D)** grey MTA. *(above)* **E)** SDS PAGE protein separation of dECM components extracted by EDTA, calcium hydroxide ($Ca(OH)_2$), white MTA (WMTA) and grey MTA (GMTA) with 10% Bis-Tris gel stained using silver stain. MW=molecular weight marker MARK 12 (Invitrogen, UK).

Table 3.4 Summary of analysis using GeneTools software (Syngene, Cambridge, UK) of 1D SDS PAGE separation of solubilised dECM components by EDTA, calcium hydroxide, white and grey MTA. Molecular weights of each individual band rounded to the nearest whole value.

		EDTA	Calcium Hydroxide	White MTA	Grey MTA
Coomassie Blue Tris-Acetate	No. of bands detected	2	5	1	3
	Molecular weight of identified bands (KDa)	89, 30	74, 63, 53, 43, 29	28	117, 91, 28
Silver Stain Tris-Acetate	No. of bands detected	3	26	2	12
	Molecular weight of identified bands (KDa)	59, 44, 37	170, 165, 153, 150, 121, 103, 98, 96, 92, 81, 77, 75, 70, 67, 58, 51, 48, 46, 44, 43, 42, 40, 39, 38, 36, 34	77, 62	104, 99, 78, 67, 63, 53, 46, 43, 41, 40, 39, 38
Bis-Tris	No. of bands detected	6	18	8	17
	Molecular weight of identified bands (KDa)	139, 70, 64, 54, 51, 3	130, 113, 90, 81, 68, 61, 52, 42, 28, 22, 21, 16, 14, 13, 10, 9, 7, 5	143, 130, 118, 84, 66, 63, 55, 5	144, 131, 108, 86, 66, 61, 56, 52, 44, 41, 40, 35, 23, 21, 16, 15, 5

Visual inspection of the gels indicated that each extractant solubilised a different protein profile of dECM components, although some similarities existed. The same pattern of protein separation was resolved using both staining techniques, although it was possible to see more bands within the gel stained with silver. Comparisons of different staining techniques under the same conditions indicated that the silver staining method allows greater discrimination between protein bands than the Coomassie blue staining technique with visual inspection and using GeneTools software. Indeed, for the calcium hydroxide sample of dECM components,

it was possible to distinguish 26 bands using the silver staining method; however, only 5 bands could be identified with Coomassie blue (Figure 3.3) using the automated GeneTools software analysis approach (Table 3.4).

Six distinct bands were identified in the sample extracted by EDTA separated in the Bis-Tris gel ranging from 3 - 139 KDa (Figure 3.5). The histogram for EDTA and white MTA (Figure 3.5 A and C) shows similar characteristics with most of the dECM components extracted being in the higher molecular weight range (greater than 20 KDa). The calcium hydroxide and grey MTA samples of dECM components contained protein bands resolved at high and low molecular weights, showing similar characteristics in histogram profiles in the Tris-Acetate (Figure 3.4) and Bis-Tris gels (Figure 3.5).

3.3.3 Growth factor cytokine array analysis of extracted dECM components

A cytokine array, which employed a sandwich ELISA technique, was used to analyse dECM components extracted with EDTA, calcium hydroxide, white MTA and grey MTA (section 2.2.4). This approach enabled a broad characterisation of growth factors, their binding proteins and some soluble receptors to be evaluated within samples of solubilised dECM components. A total of forty-one different cytokines were analysed and an autoradiographic image for each sample of dECM components assessed was produced using this technique. A representative negative autoradiographic image is displayed in Figure 3.6. Image analysis was subsequently used to determine the relative radiographic intensity for each cytokine in each sample of dECM components and this is shown in Figures 3.7 to 3.9. The cytokines analysed have been grouped together as follows: transforming growth factor-β (TGF-β) family members, angiogenic growth factors including related soluble receptors, insulin-like growth

factor (IGF) family members including their binding proteins (BP), fibroblast growth factor (FGF) family members, epidermal growth factor (EGF) family members including related soluble receptor, neurotrophic growth factor family members, colony stimulating growth factor (CSF) family members and hepatocyte growth factor (HGF).

Radiographic intensities of the dECM components tested ranged from 5.0 to 2791.5 units for all forty-one cytokines analysed. The mean intensities of the positive and negative controls were 39666 (±1119) and 3.25 (±0.323) units, respectively. Figure 3.6 shows the cytokine antibody array map and representative negative autoradiographic images for each sample of dECM components tested.

RayBio® Human Growth Factors Antibody Array G series 1

	A	B	C	D	E	F	G	H	I	J	K	L	M
1	Pos 1	Pos 2	Pos 3	Neg	Neg	AR	bFGF	b-NGF	EGF	EGF R	FGF -4	FGF-6	FGF -7
2	Pos 1	Pos 2	Pos 3	Neg	Neg	AR	bFGF	b-NGF	EGF	EGF R	FGF -4	FGF-6	FGF -7
3	GC SF	GDNF	GM-CSF	HB-EGF	HGF	IGFBP -1	IGFBP -2	IGFB P-3	IGFB P-4	IGFB P-6	IGF-I	IGF-I SR	IGF-II
4	GC SF	GDNF	GM-CSF	HB-EGF	HGF	IGFBP -1	IGFBP -2	IGFB P-3	IGFB P-4	IGFB P-6	IGF-I	IGF-I SR	IGF-II
5	M-CS F	M-CSF R	NT-3	NT-4	PDGF R a	PDGF R b	PDGF-AA	PDGF -AB	PDGF -BB	PIGF	SCF	SCF R	TGF -a
6	M-CS F	M-CSF R	NT-3	NT-4	PDGF R a	PDGF R b	PDGF-AA	PDGF -AB	PDGF -BB	PIGF	SCF	SCF R	TGF -a
7	TG F-b	TGF-b 2	TGF-b 3	VEG F	VEGF R2	VEGF R3	VEGF-D	neg	IC 1	IC 2	IC 3	Neg	Neg
8	TG F-b	TGF-b 2	TGF-b 3	VEG F	VEGF R2	VEGF R3	VEGF-D	neg	IC 1	IC 2	IC 3	Neg	Neg

A

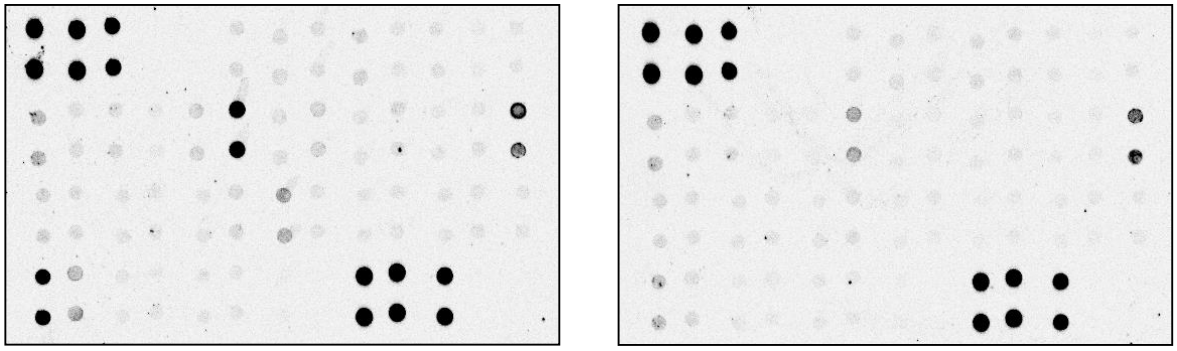

B

C

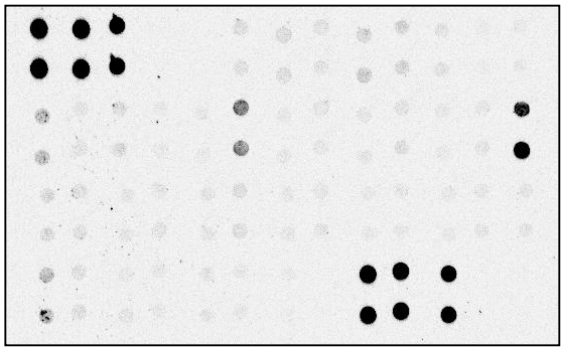

D

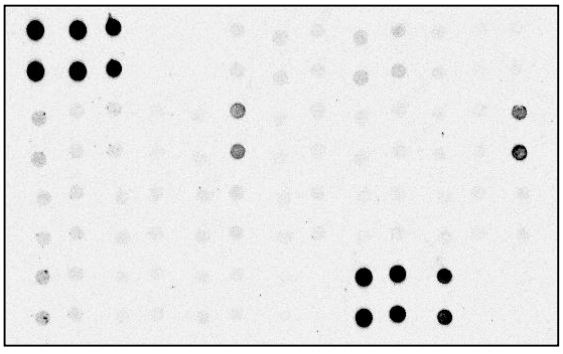

E

Figure 3.6 A) Cytokine antibody array map. **(B-E)** Negative autoradiographic images of cytokine array membranes following exposure with dECM components extracted by **B)** EDTA, **C)** calcium hydroxide, **D)** white MTA and **E)** grey MTA.

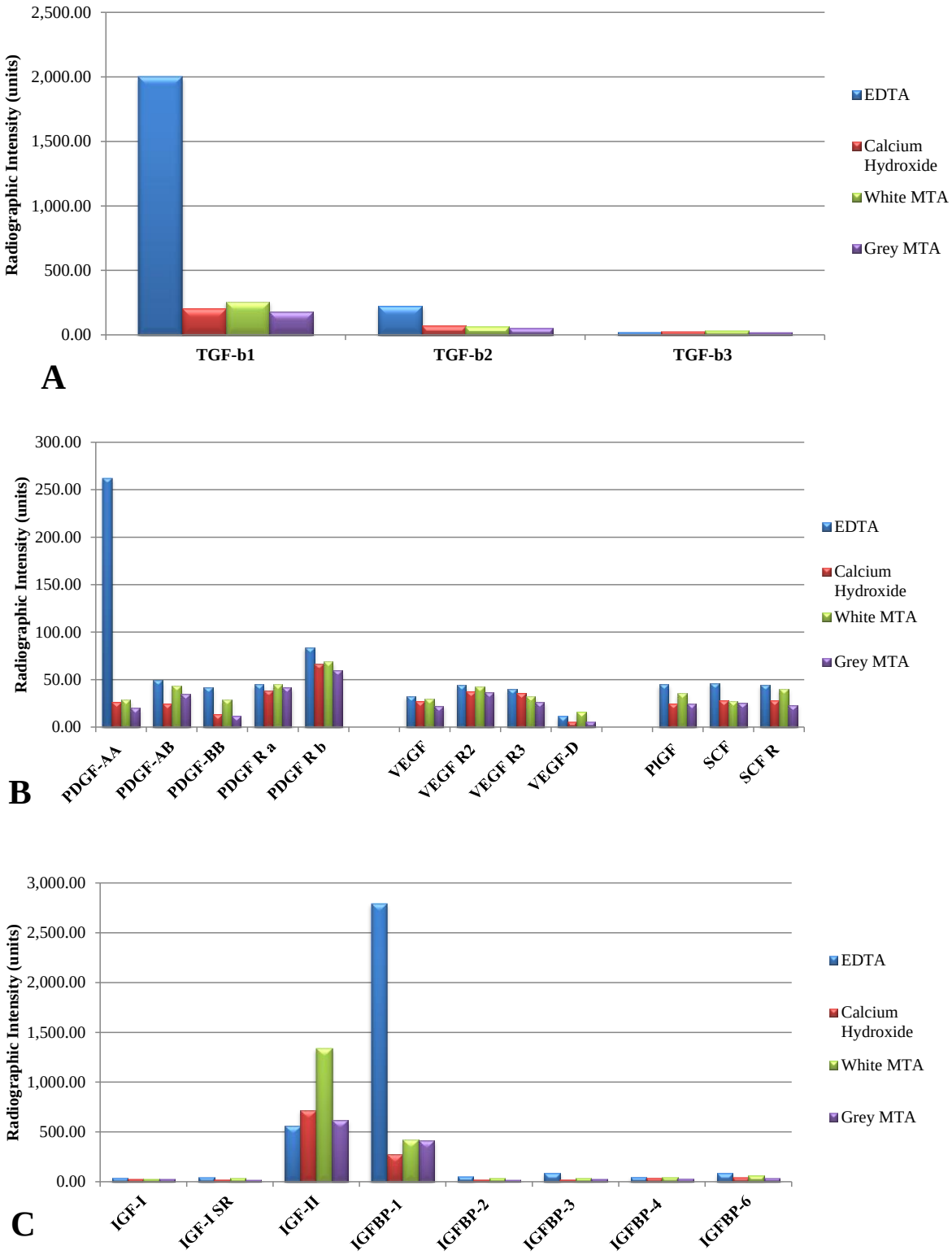

Figure 3.7 Relative intensity levels of cytokines found in dECM extracted by EDTA, calcium hydroxide, white and grey MTA. Members of **A**) transforming growth factor-β family (TGF-β), **B)** angiogenic growth factors including related soluble receptors (PDGF = platelet derived growth factor, VEGF = vascular endothelial growth factor, PlGF = placental growth factor, SCF = stem cell factor, R = receptor) and **C)** insulin-like growth factor family (IGF, SR = surface receptor, BP = binding protein).

Figure 3.7A shows the relative intensities for TGF-β1, -β2 and -β3 in dECM components extracted by EDTA, calcium hydroxide, white and grey MTA. The signal intensity for TGF-β1 extracted by EDTA was relatively high (2001 units) when compared with the detected intensity for other cytokines and the intensity for TGF-β1 in dECM extracted by the other agents. The signal intensity for TGF-β2 was highest in the dECM components extracted by EDTA (223.5 units). Signal intensity for TGF-β3 was relatively low for each sample of dECM components tested and ranged between 19.5 (grey MTA) to 32.6 units (white MTA).

Levels of eight of the angiogenic growth factors including PDGF-AA, PDGF-AB, PDGF-BB, VEGF, VEGF-D, PlGF and SCF were assessed using this array together with five of their respective receptors (PDGF R a and b, VEGF R2 and 3, and SCF R). Data generated are shown in Figure 3.7B. The signal intensity for PDGF-AA in dECM components extracted by EDTA was relatively high (262 units) in comparison with the other growth factors and samples in which signal intensity ranged from 5.3 to 49.5 units. For all growth factors except SCF, the relative intensity followed the same pattern whereby signal intensity was highest in dECM components extracted by EDTA, followed by white MTA, calcium hydroxide and grey MTA, respectively. The relative intensities of receptors identified in dECM components followed the same rank order as described above apart from VEGF R3 whose relative intensity was greatest for EDTA followed by calcium hydroxide, white MTA and grey MTA, respectively.

Assessment of the relative intensity levels for insulin-like growth factor family members is shown in Figure 3.7C including IGF-I and -II, IGFBP-1, -2, -3, -4, 6 and IGF-I SR. The intensity for IGFBP-1 in dECM components extracted by EDTA was relatively high (2791.5 units); it was ~10-fold greater than that observed for the dECM extract obtained using

calcium hydroxide and ~6.5-fold greater than that observed for white and grey MTA extracted samples of dECM components. Intensity of signal for IGF-II (561.5 to 1337.5 units) was considerably greater than IGF-I (25.5 to 39.5 units) for all samples. The intensity for IGF-II was greatest in dECM components extracted by white MTA. For all IGFBPs, the relative intensity was the greatest for the EDTA followed by white MTA extracts.

Four members of the twenty-two members of the fibroblast growth factor family were analysed using the cytokine array including FGF-2, -4, -6 and -7. The relative intensities for each cytokine are shown in Figure 3.8A. The radiographic intensity for FGF-2 was greatest in the white MTA sample (67.3 units) of dECM components and lowest in the grey MTA sample (55 units). The pattern of intensity for FGF-4 was similar to that for a number of other growth factors tested in the array, whereby EDTA showed greatest intensity followed by white MTA, calcium hydroxide and grey MTA. The patterns for FGF-6 and -7 intensities were the same where ranking was as follows from highest to lowest intensity: EDTA > calcium hydroxide > white MTA > grey MTA.

The relative radiographic intensities for four members of the epidermal growth factor family including AR, EGF, HB-EGF and TGF-α, generated from the dECMs solubilised by the four extractants, are shown in Figure 3.8B. The radiographic intensities ranged from 13 - 109 units amongst all growth factors and samples. AR and HB-EGF followed a pattern frequently detected in the array whereby EDTA extracts showed greatest intensity followed by white MTA, calcium hydroxide and grey MTA. The greatest relative intensities for EGF and TGF-α were detected in dECM components solubilised by white MTA compared with the other extraction agents.

Four members of the neurotrophic growth factor family were analysed using these arrays including NGF, GDNF, NT-3 and NT-4 (Figure 3.8C). EDTA solubilised dECM components demonstrated the greatest radiographic intensity for all neurotropic growth factor studied. The overall range for radiographic intensity was relatively narrow for all extracted samples and cytokines (32 - 63 units).

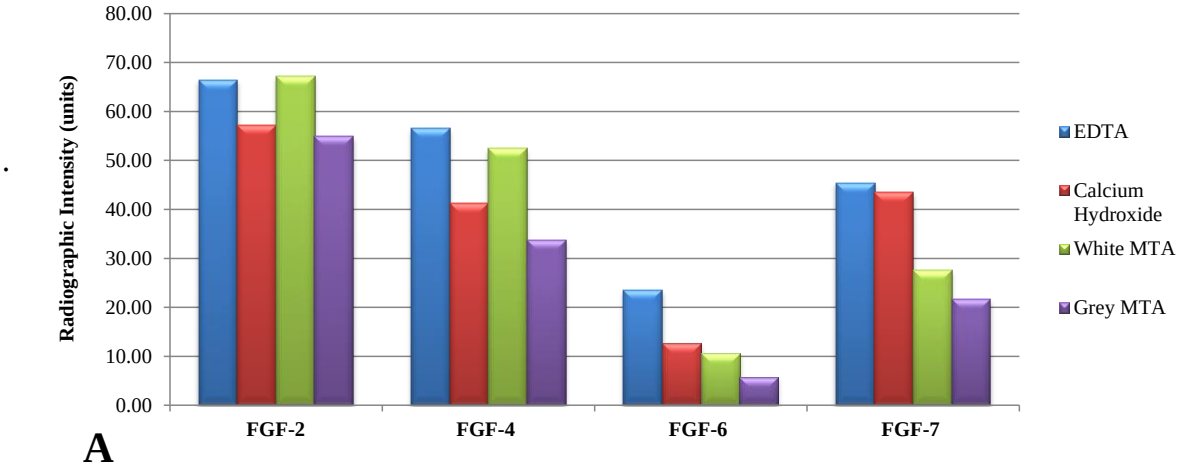

A

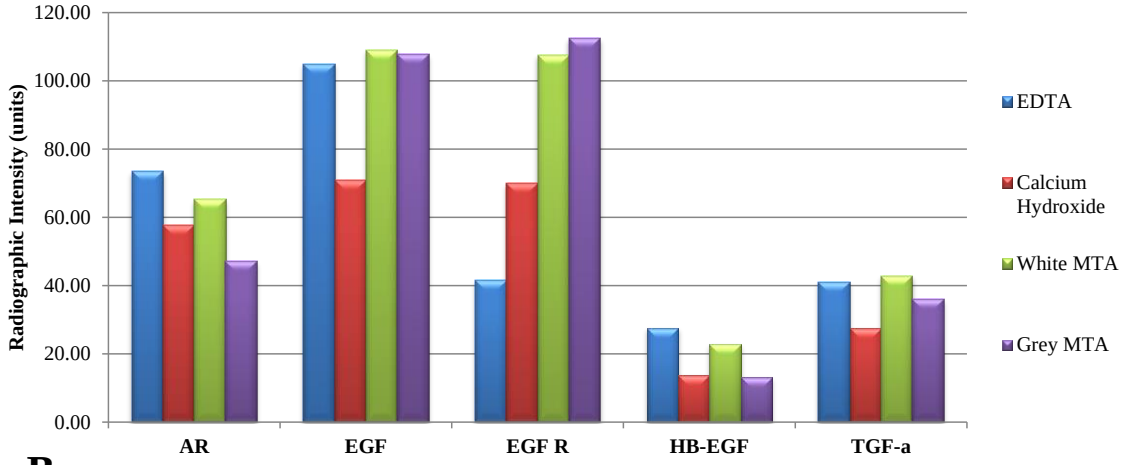

B

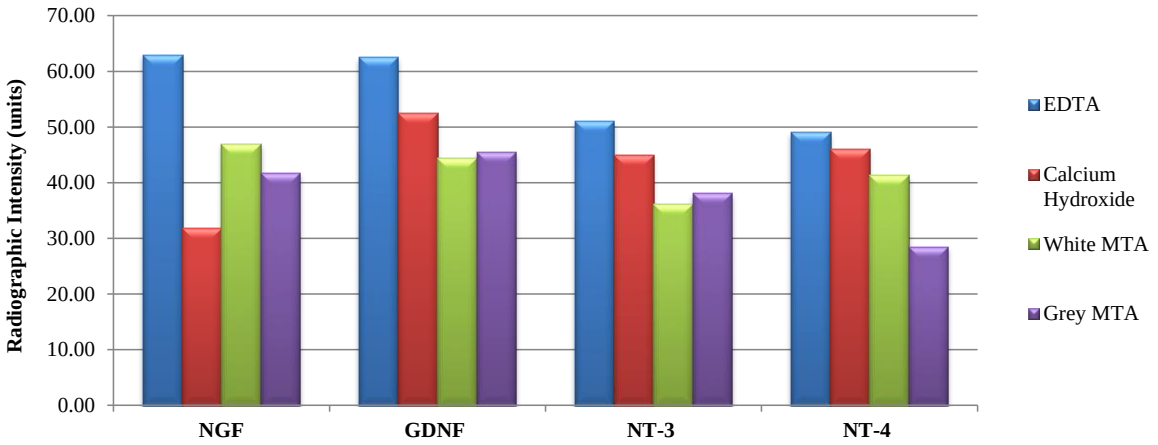

C

Figure 3.8 Relative signal intensity levels for **A)** fibroblast growth factor family (FGF), **B)** epidermal growth factor family (EGF, AR = amphiregulin, HB = heparin-binding, TGF-a = transforming growth factor-α) including related soluble receptor and **C)** neurotrophic factors (NGF = nerve growth factor, GDNF = glial cell line-derived neurotrophic factor, NT = neurotrophin), found in dECM extracted by EDTA, calcium hydroxide, white and grey MTA.

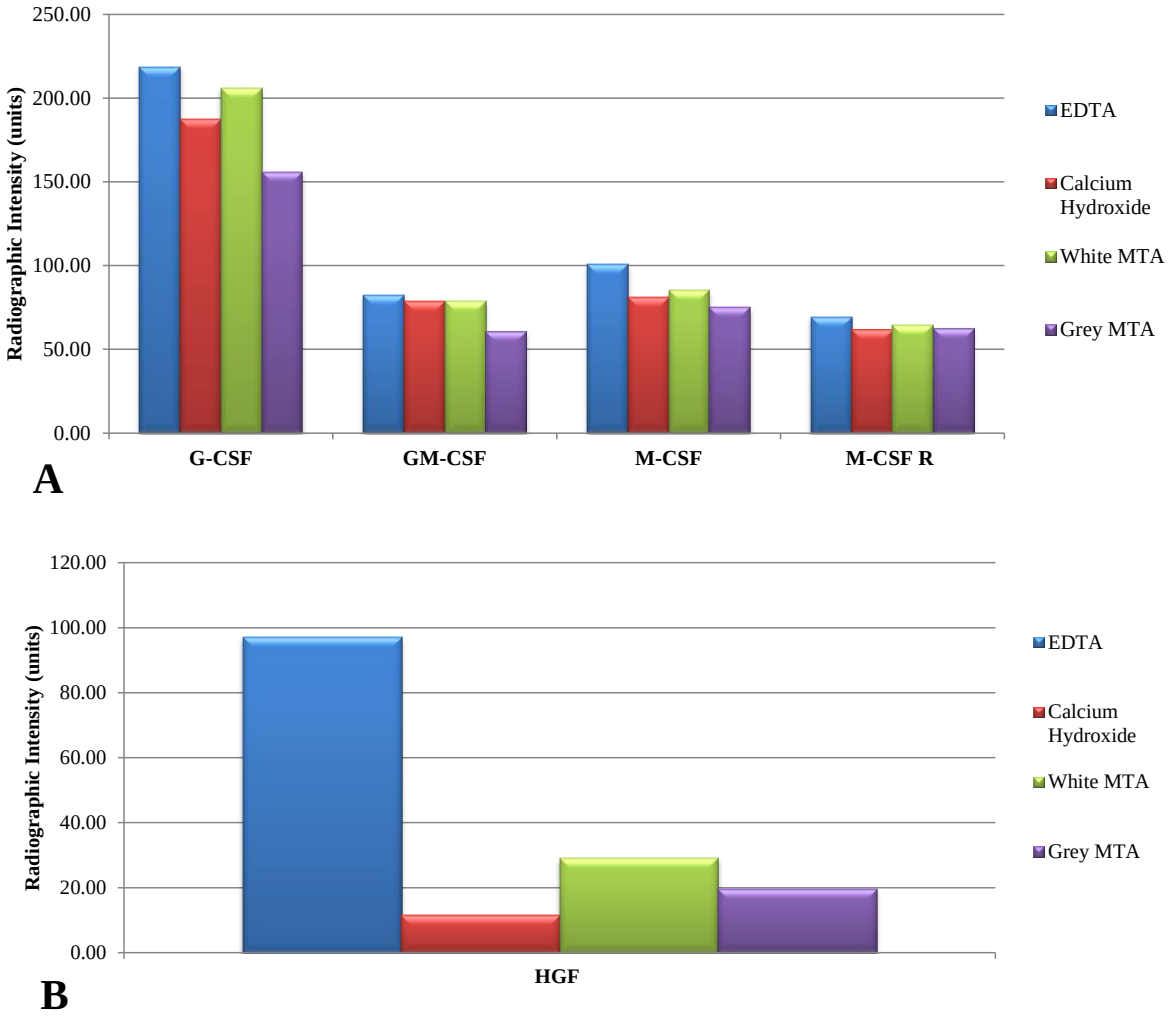

Figure 3.9 Relative signal intensity levels for **A)** colony stimulating growth factor family (CSF, G = granulocyte, GM = granulocyte macrophage, R = receptor) and **B)** hepatocyte growth factor (HGF), found in dECM extracted by EDTA, calcium hydroxide, white and grey MTA.

Assessment of relative signal intensity levels for three colony stimulating factors (CSFs) and one respective receptor were performed using the arrays and included G-CSF, GM-CSF, M-CSF and its receptor. Results from this analysis are presented in Figure 3.9A. The relative pattern for each of these growth factors was as follows: EDTA extract demonstrated highest radiographic intensity followed by white MTA, calcium hydroxide and grey MTA extracts.

Relative signal intensity levels for hepatocyte growth factor (HGF), which does not reportedly belong to a specific growth factor family, were assessed using the cytokine array and results are provided in Figure 3.9B. The radiographic intensity detected for the extracts was greatest for EDTA (97.0 units) followed by white MTA (29.1 units) grey MTA (19.6 units) and calcium hydroxide (11.6 units), respectively.

3.4 Characterisation of individual growth factors in dECM extracts

The aim of this study was to more accurately characterise individual growth factors TGF-β1 and Adrenomedullin (ADM) that were solubilised from the dECM by EDTA, calcium hydroxide, white MTA, grey MTA and Biodentine®.

TGF-β1 is well documented as a mediator of pulpal repair and regeneration (Smith, 2003) and has previously been shown to be present in dECM components solubilised by EDTA (Cassidy et al., 1997, Smith et al., 1998). ADM has been implicated in pulpal repair (Cooper et al., 2011) through its multiple roles as an initiator and regulator of inflammation (Wong et al., 2005), its broad antimicrobial properties (Allaker et al., 1999), its expression in the dental pulp (McLachlan et al., 2005) and its promotion of pulp cell proliferation and mineralisation (Musson et al., 2010). Release of TGF-β1 and ADM by control and test agents was determined using conventional well plate ELISA.

To further explore the findings of the antibody array data, a bespoke multiplex ELISA was also undertaken to determine the concentrations of previously reported and novel growth factors identified in each sample of dECM extracted by control and test agents.

3.4.1 Concentration of TGF-β1 and ADM in dECM extracts

To determine the specific concentrations of TGF-β1 and ADM in dECM components released by EDTA, calcium hydroxide, white MTA and grey MTA, sandwich ELISAs were performed (section 2.2.3.2 and 2.2.3.3). TGF-β1 was detected in all extracts of dECM (Figure 3.10) with the mean concentration of dECM components extracted by EDTA (209.09 ±3.36 pg/mg) being significantly greater than that extracted by calcium hydroxide (77.31 ±4.99 pg/mg), white MTA (121.47 ±8.64 pg/mg) or grey MTA (90.99 ±3.48 pg/mg), $p<0.0001$. White MTA dECM components contained significantly more TGF-β1 than grey MTA ($p=0.01$) and calcium hydroxide ($p<0.0001$); grey MTA dECM components contained significantly more TGF-β1 than calcium hydroxide dECM components ($p=0.002$).

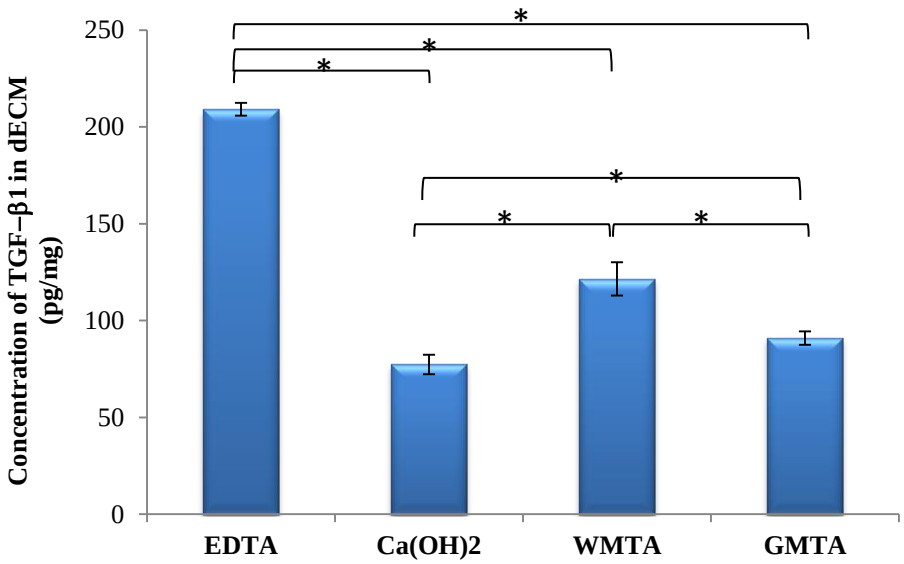

Figure 3.10 Mean concentration of TGF-β1 in dECM extracted by EDTA, calcium hydroxide, white or grey MTA. Error bars represent one standard deviation from the mean for triplicate analyses. *$p \leq 0.005$ when compared using one-way ANOVA.

ADM was also detected in all extracts of dECM analysed (Figure 3.11) with the greatest amount present in calcium hydroxide liberated samples (420.83 ±175.27 pg/mg); this was significantly greater than the amount released by EDTA (50.57 ±15.93 pg/mg, $p=0.029$) or

white MTA (57.4 ±35.4 pg/mg, p=0.032). Grey MTA released dECM components contained 278.3 ±152.5 pg/mg of ADM.

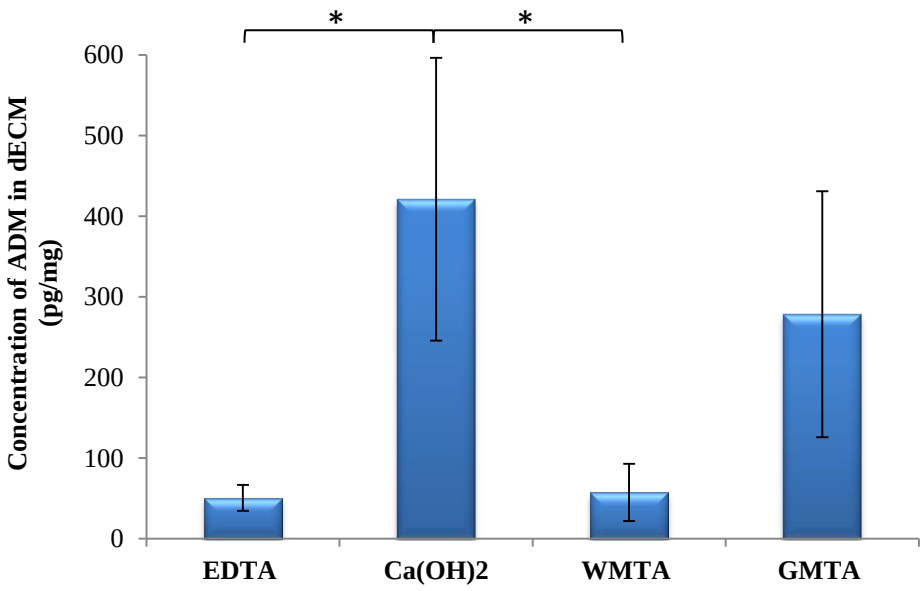

Figure 3.11 Mean concentration of ADM in dECM extracted by either EDTA, calcium hydroxide ($Ca(OH)_2$), white (W) or grey (G) MTA. Error bars represent one standard deviation from the mean for triplicate analyses. *p≤0.05 when compared using one-way ANOVA.

3.4.2 Multiplex sandwich ELISA of dECM extracts

Further to the growth factor cytokine array analysis (section 2.2.5), confirmation of the presence of newly identified growth factors in dECM was sought and their concentrations determined. Given the relatively high cost of individual ELISAs and the precious nature of recovered dECM components, a multiplex sandwich ELISA technique was performed to concomitantly assess levels of several cytokines. This approach allowed specific concentrations of each target protein to be determined in dECM extracts using relatively low volumes analysed on a customised glass slide array. The slide was spotted with specific test antibodies and provision was made to assay cytokine standards in parallel to enable calculation of concentrations of each cytokine. Figure 3.12 shows a photographic

representation of a glass slide under fluorescent light with a close up view of the array capture for one dECM sample, with key provided.

A

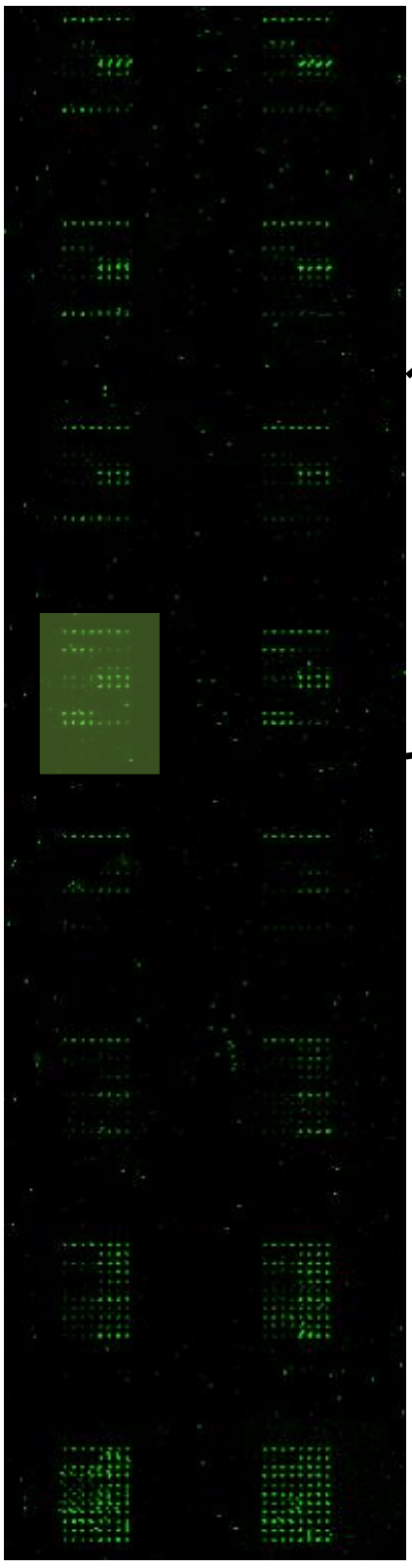

B

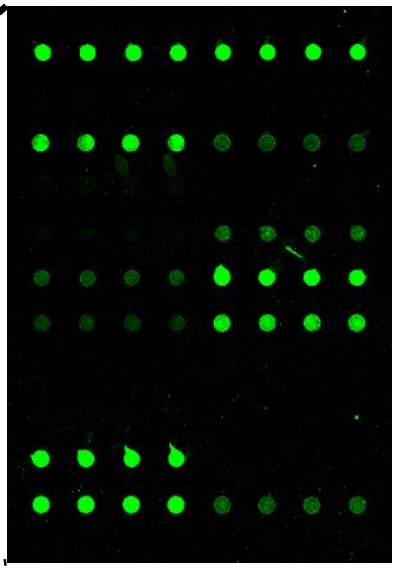

C

POS 1	POS 2
FGF	BMP-4
BMP-7	NGF
EGF	G-CSF
GDNF	GM-CSF
HGF	IGF-BP1
IGF-I	IGF-II
IGF-1SR	M-CSF
NT-3	NT-4
PDGF-AA	SCF
TGF-β1	VEGF

Figure 3.12 Multiplex sandwich ELISA array system showing: **A**) representative laser scanned image of whole glass chip, **B)** close up of array captured for one EDTA dECM component sample, and **C)** cytokine array key for image **B)**.

The levels of twenty proteins were analysed, including the angiogenic growth factors (VEGF, PDGF – AA, SCF), colony stimulating factors (G-CSF, GM-CSF, M-CSF), insulin-like growth factors, surface receptor and binding protein (IGF-I, IGF-II, IGF-I SR, IGFBP-1), neurotrophic growth factors (NGF, NT-3, NT-4, GDNF) and bone morphogenetic proteins (BMP-4, BMP-7) as well as several others (TGF-β1, EGF, FGF-2, HGF). The results are presented in groups, where possible, to aid interpretation (Figures 3.13 and 3.14).

All angiogenic growth factors (VEGF, PDGF-AA, SCF) assessed were detected in the dECM extracts (Figure 3.13A). VEGF was present in all extracts, with white and grey MTA extracts containing the highest concentrations, 107.27 ±17.79 pg/mL and 189.47 ±14.33 pg/mL, respectively. These concentrations were significantly greater ($p \leq 0.0001$) than those detected for extracts obtained using EDTA (53.93 ±8.19 pg/mL), calcium hydroxide (26.8 ±6.26 pg/mL) and Biodentine® (81.23 ±4.07 pg/mL). The mean concentration of VEGF detected in Biodentine® extracts was significantly greater than that for the calcium hydroxide extracts ($p=0.04$). PDGF-AA was extracted by EDTA (4386.6 ±224.15 pg/mL) with trace amounts detected in white MTA (7.9 ±0.59 pg/mL) and grey MTA (2.63 ±1.69 pg/mL) extracts. Only grey MTA was able to extract significant quantities of SCF (25.05 ±0.17 pg/mL).

The concentrations of the colony stimulating factors, including G-CSF, GM-CSF, M-CSF, were assayed by multiplex ELISA (Figure 3.13B) and data indicated that for all dECM extracts, G-CSF levels were below the level for accurate detection. M-CSF was detected in the dECM components extracted by white MTA (5.75 ±1.56 pg/mL) and grey MTA (4.1 ±1.99 pg/mL) only and there was no statistical difference between groups. GM-CSF was detected in dECM components extracted by EDTA (15.3 ±0.46 pg/mL), calcium hydroxide

(20.95 ±7.8 pg/mL), white MTA (17.33 ±8.7 pg/mL) and Biodentine® (37.85 ±4.33 pg/mL). There were no statistically significant differences between concentrations detected.

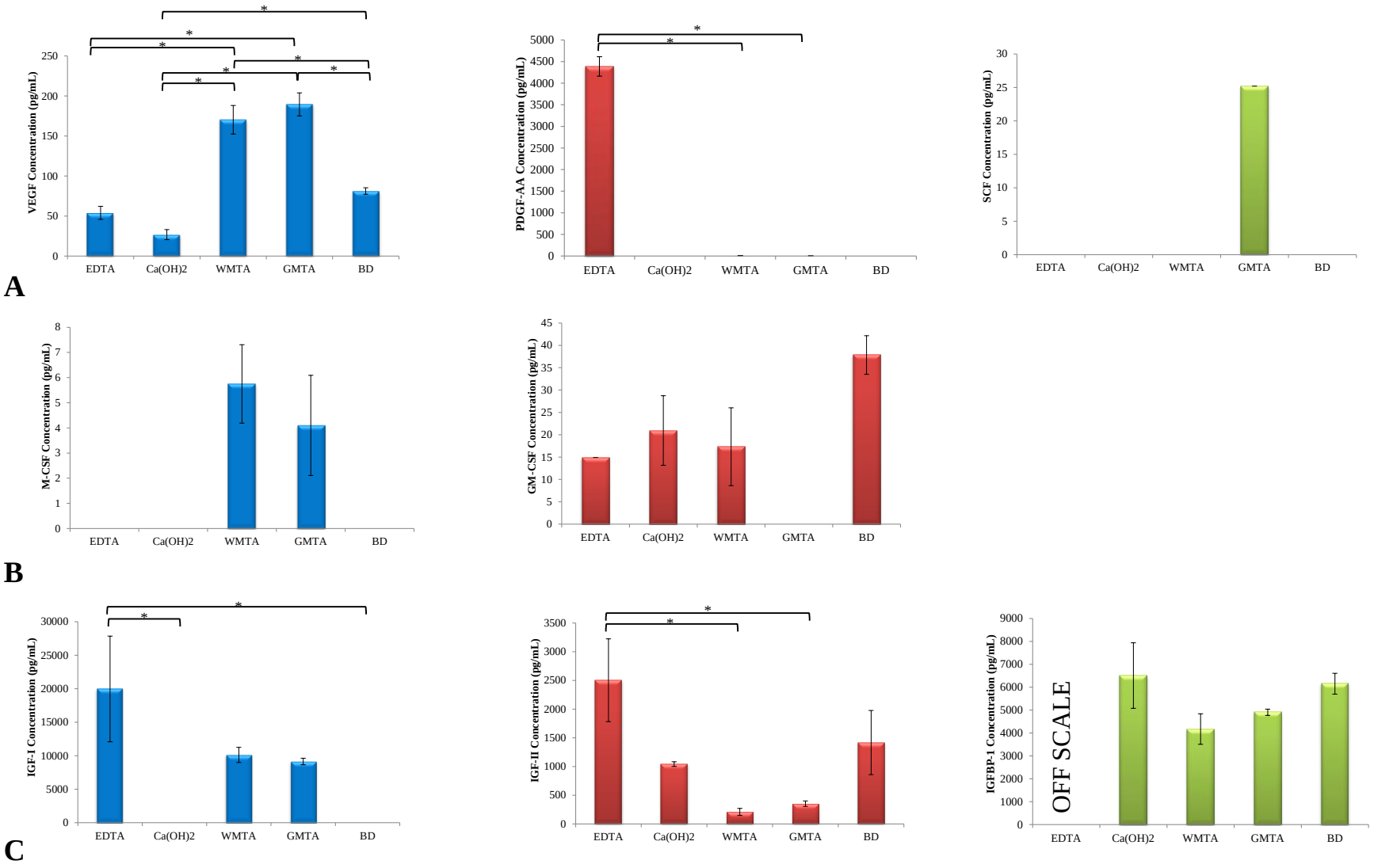

Figure 3.13 Mean concentrations of **A)** angiogenic growth factors, **B)** colony stimulating factors and **C)** insulin-like growth factors and binding protein (pg/mL) present in dECM components released from human dentine by solutions of EDTA, calcium hydroxide, white MTA, grey MTA and Biodentine®, as determined by multiplex ELISA (±SD, n=3). * indicates statistically significant difference ($p<0.05$) using one way ANOVA.

Proteins involved in signalling along the IGF axis, including IGF-I, II, IGFBP-1 and IGF-I SR, were analysed for their presence in dECM extracts (Figure 3.13C). IGF-I SR was not detected in any of the extracts of the dECM components. IGF-I was detected in dECM components extracted by EDTA (19963 ±7890.10 pg/mL), white MTA (10119 ±1122.40 pg/mL) and grey MTA (9128.7 ±483.93 pg/mL). IGF-II was extracted by all agents; EDTA (2502.9 ±720.04 pg/mL), calcium hydroxide (1042.6 ±39.78 pg/mL), white MTA (210.3 ±61.08 pg/mL), grey MTA (353.07 ±47.70 pg/mL) and Biodentine® (1417.4 ±559.52 pg/mL). The concentration of IGF-II was statistically significantly higher in dECM components extracted by EDTA when compared with white MTA ($p=0.012$) and grey MTA ($p=0.009$). The concentration of IGFBP-1 in EDTA extracted dECM components was demonstrably greater than 100000 pg/mL and this intensity of fluorescence was beyond the upper limits for accurate quantitative detection. Other extracting agents extracted similar levels of IGFBP-1 to each other with no statistical differences found; calcium hydroxide (6507 ±1431.3 pg/mL), white MTA (4107.5 ±667.86 pg/mL), grey MTA (4903.1 ±137.02 pg/mL) and Biodentine® (6105.5 ±457.96 pg/mL).

Analysis of neurotrophic growth factors (GDNF, NGF, NT-3, NT-4) showed that NT-3 and NT-4 were not detected in any samples using this methodology. GDNF was detected in all samples of dECM components (Figure 3.4.5A); the highest concentration of which was found in the dECM extract released by calcium hydroxide (233.43 ±55.4 pg/mL), which was significantly greater than EDTA (53.53 ±17.50 pg/mL) ($p<0.0001$), white MTA (98.3 ±3.85 pg/mL) ($p=0.02$) and grey MTA (63 ±2.92 pg/mL) ($p<0.0001$). Biodentine® released the second highest concentration of GDNF (155.7 ±6.30 pg/mL), which was significantly greater than EDTA ($p=0.016$) and grey MTA ($p=0.031$). NGF was detected in dECM components

released by EDTA (23.63 ±3.12 pg/mL), white MTA (1.15 ±0.4 pg/mL) and grey MTA (2.05 ±0.06 pg/mL).

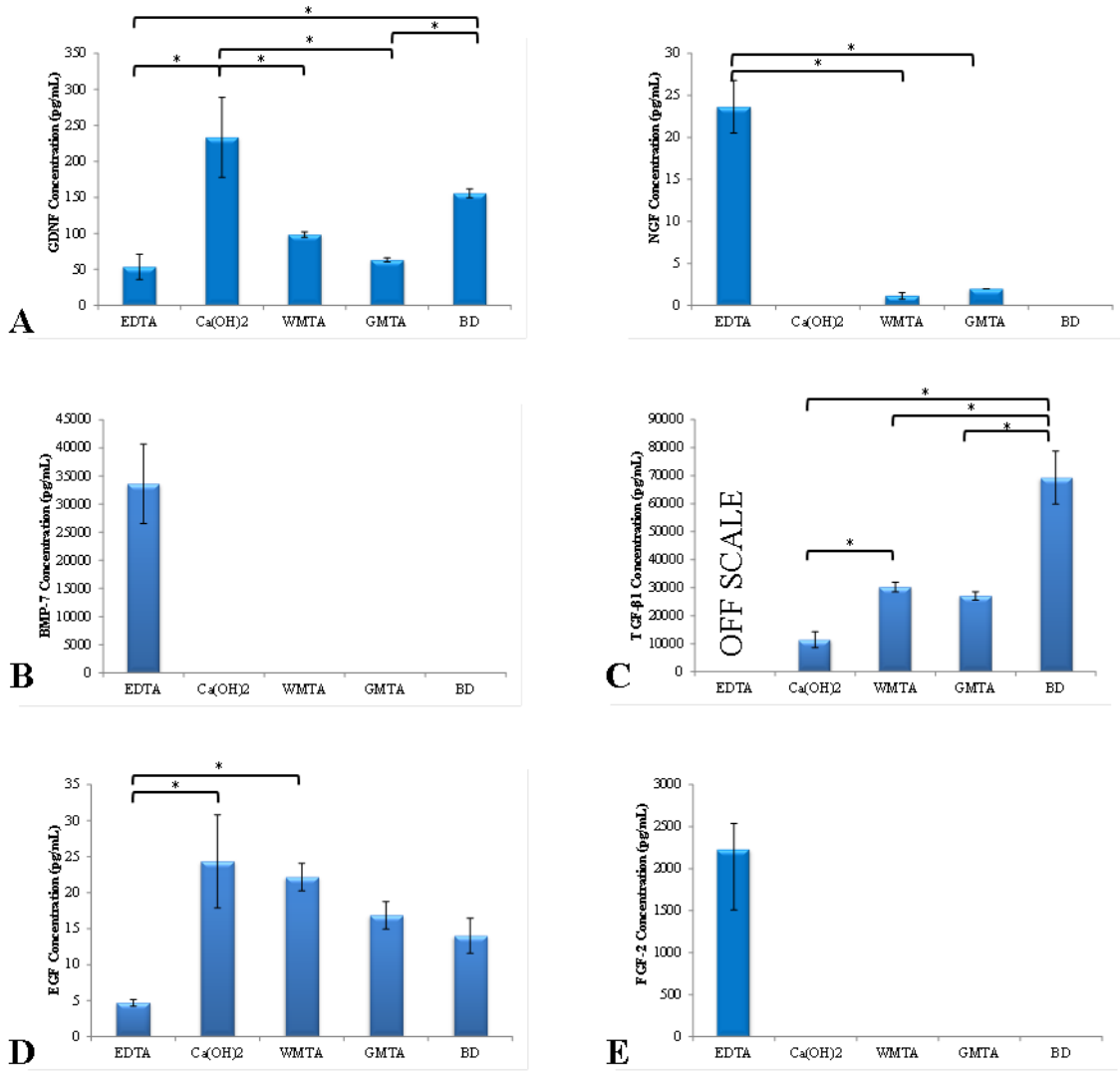

Figure 3.14 Mean concentration of **A)** neurotrophic growth factors, **B)** BMP-7, **C)** TGF-β1, **D)** EGF and **E)** FGF-2 (pg/mL) in dECM components released from human dentine by solutions of EDTA, calcium hydroxide, white MTA, grey MTA and Biodentine®, as determined by multiplex ELISA (±SD, n=3). * indicates statistically significant difference ($p<0.05$) using one way ANOVA.

The BMP-4 and -7 growth factors associated with mineralised tissue formation and repair were also assessed using multiplex ELISA and results are shown in Figure 3.14B. Only BMP-7 was detected in dECM released by EDTA (33584 ±7086.2 pg/mL). TGF-β1 analysis showed that dECM extract for EDTA was beyond the upper limit for accurate quantitative detection, indicating that the concentration was greater than 100000 pg/mL. Biodentine® extracts exhibited the highest concentration of TGF-β1 (69256 ±9470 pg/mL), which was significantly greater than those detected for calcium hydroxide (11427 ±2802.2 pg/mL) ($p<0.0001$), white MTA (30203 ±1700.3 pg/mL) ($p<0.0001$) and grey MTA (27066 ±1500.8 pg/mL) ($p<0.0001$) (Figure 3.14C). EGF was detected at relatively low levels in all samples of dECM components (Figure 3.14D): EDTA (4.7 ±0.46 pg/mL), calcium hydroxide (24.33 ±6.48 pg/mL), white MTA (22.17 ±1.9 pg/mL) and Biodentine® (14 ±2.43 pg/mL). There were significantly lower concentrations of EGF detected in EDTA extracted samples compared with those extracted by calcium hydroxide ($p=0.004$) and white MTA ($p=0.009$). Using this methodology, FGF-2 was only detected in dECM extracted by EDTA (2227.9 ±308.48 pg/mL) (Figure 3.14E).

4.0 RESULTS CHAPTER 2

Effects of dentine extracellular matrix (dECM) components on dental pulp cells

Following tissue injury, a complex series of events is initiated, involving various intra- and extra-cellular signalling pathways, which aim to facilitate tissue repair if favourable environmental factors predominate (Gurtner et al., 2008). Wound repair follows a sequence of overlapping stages that include cell homing of progenitor cells to the site of injury, cellular differentiation, proliferation and deposition of extracellular matrix (Kang et al., 2012). The necessary cues and signals required for progenitor cell recruitment, proliferation and differentiation in pulpal tissue remain poorly understood. In 3.0 Results Chapter 1, it was demonstrated that the soluble products of therapeutic pulp capping materials could release dECM components that comprised a complex cocktail of non-collagenous proteins. Further analysis showed that these dECM components contained a broad range of signalling molecules and growth factors, some of which have not been previously reported in this dental tissue. These molecules may play key roles in regulating the process of wound repair during pulp healing and regeneration. The interaction of pulp capping agents with the dECM may initiate the release of cytokines and growth factors, which could induce reparative processes leading to dentine-pulp complex repair.

The aim of the work documented in this chapter was to investigate the effect of dECM components, released by therapeutic pulp capping agents, on two important processes which occur during wound healing and tissue regeneration, namely chemotaxis and proliferation.

4.1 The influence of dECM components on rat dental pulp cell (RDPC) migration

The chemotactic potential of dECM components was assessed using a transwell plate assay (section 2.5.2). The number of RDPCs moving towards medium supplemented with dECM components was determined and compared with appropriate positive and negative controls.

4.1.1 Chemotactic analysis of RDPCs in response to EDTA soluble dECM components

Within 45 minutes of cells being exposed to stimulus, 88% of RDPCs in the positive control group had migrated to the medium containing 10% FBS while, in contrast, for the negative control, a significantly lower proportion ($p<0.0001$) of the RDPCs (36%), had migrated to the medium without FBS. These data indicated that FBS exerted a strong chemotactic influence and served as an appropriate positive control (Figure 4.1). All concentrations of EDTA soluble dECM components studied attracted more RDPCs to the lower chamber of the transwell plate than the medium containing no FBS supplementation, however, this was only statistically significant for the following concentrations: 1.0 µg/mL ($p=0.04$), 10 µg/mL ($p=0.01$) and 100 µg/mL ($p=0.02$). No statistically significant differences were detected between the different concentrations of EDTA dECM components in terms of the number of RDPCs that migrated when compared between groups.

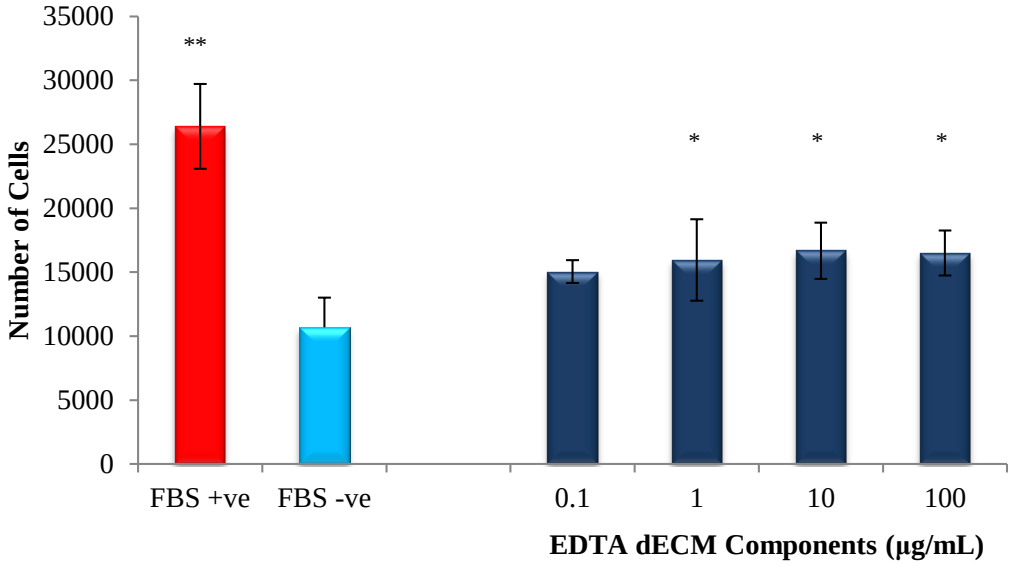

Figure 4.1 RDPC migration induced by EDTA extracted dECM components at concentrations between 0.1 - 100 µg/mL. Positive control (FBS +ve) included 10% FBS and negative control was medium without FBS (FBS -ve). All experiments were performed in quadruplicate and data are expressed as mean values ±SD. *$p\leq0.05$, **$p\leq0.001$ when compared with negative control using one-way ANOVA.

4.1.2 Chemotactic analysis of RDPCs in response to calcium hydroxide soluble dECM components

Figure 4.2 shows data demonstrating that all concentrations of dECM components extracted by calcium hydroxide induced significantly ($p<0.05$) more cell migration compared with FBS unsupplemented medium. A comparison of different concentrations of calcium hydroxide extracted dECM components showed that both 1.0 µg/mL and 10 µg/mL induced significantly more RDPC migration compared with the lower concentration of 0.1 µg/mL ($p=0.022$ and $p=0.004$, respectively).

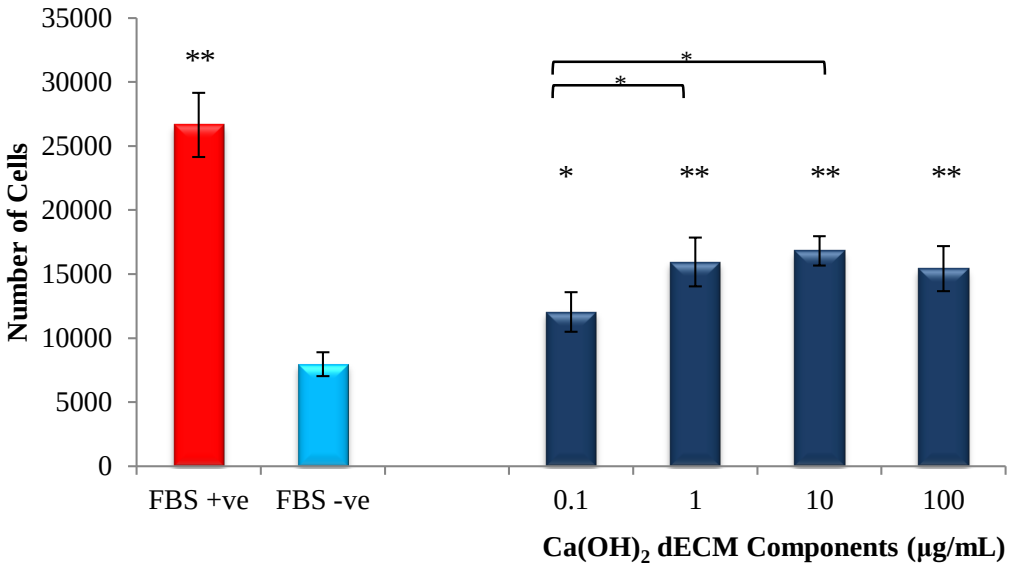

Figure 4.2 RDPC migration induced by calcium hydroxide extracted dECM components at concentrations between 0.1 - 100 µg/mL. Positive control (FBS +ve) included 10% FBS and negative control was medium without FBS (FBS -ve). All experiments were performed in quadruplicate and data are expressed as mean values ±SD. *$p\leq0.05$, **$p\leq0.001$ when compared with negative control using one-way ANOVA.

4.1.3 Chemotactic analysis of RDPCs in response to white MTA soluble dECM components

Figure 4.3 shows that all concentrations of dECM components extracted by white MTA induced significantly more RDPC migration compared with medium alone, $p \leq 0.001$ for all assay groups analysed. The highest concentration tested (100 µg/mL) induced significantly more cell migration than the 0.1 µg/mL ($p=0.04$) exposure. Combined data for all concentrations show that, on average, within the 45 minute assay period, 55% of RDPCs migrated to dECM components extracted by white MTA compared with 21% for the negative control.

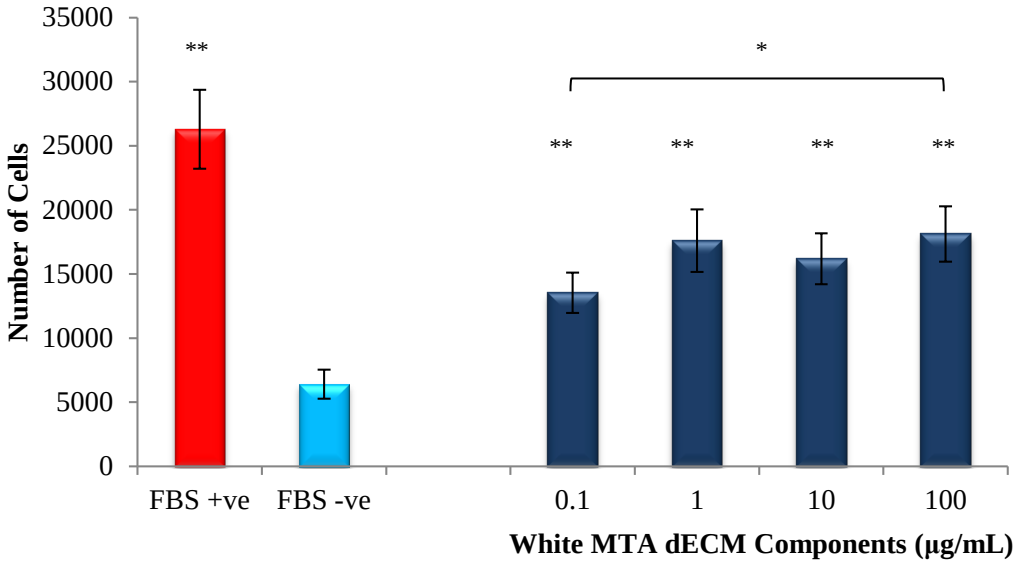

Figure 4.3 RDPC migration induced by white MTA extracted dECM components at concentrations between 0.1 - 100 µg/mL. Positive control (FBS +ve) included 10% FBS and negative control was medium without FBS (FBS -ve). All experiments were performed in quadruplicate and data are expressed as mean values ±SD. *$p \leq 0.05$, **$p \leq 0.001$ when compared with negative control using one-way ANOVA.

4.1.4 Chemotactic analysis of RDPCs in response to grey MTA soluble dECM components

Figure 4.4 demonstrates that all concentrations of grey MTA extracted dECM components induced significantly more RDPC migration compared with negative control ($p<0.0001$). Data combined for all dECM concentrations analysed showed that, on average, 54% of RDPCs migrated towards the lower chamber of the transwell plate. For medium with no additional supplement, only 17% of cells were found to migrate across the membrane.

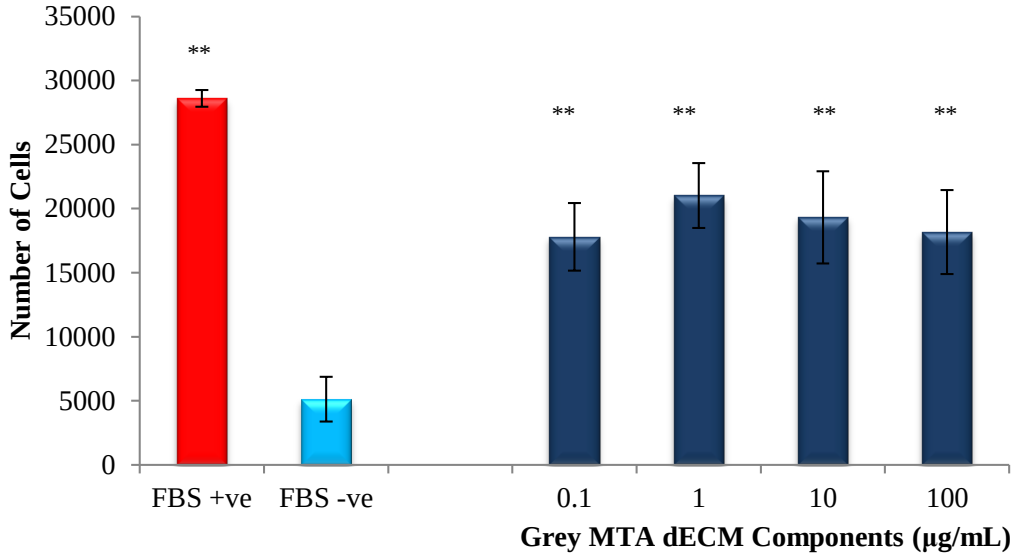

Figure 4.4 RDPC migration induced by grey MTA extracted dECM components at concentrations between 0.1 - 100 µg/mL. Positive control (FBS +ve) included 10% FBS and negative control was medium without FBS (FBS -ve). All experiments were performed in quadruplicate and data are expressed as mean values ±SD. *$p\leq0.05$, **$p\leq0.001$ when compared with negative control using one-way ANOVA.

4.2 The influence of dECM components on pulp cell proliferation

To determine the effect of solubilised dECM components on pulp cells in terms of their capacity to potentially enhance the proliferative phase of wound healing processes, the WST-1 (Roche Applied Biosciences, Mannheim, Germany) assay was applied. Primary RDPCs and the odontoblast-like cell line (MDPC-23 cells) were utilised for comparison and exposed to a range of concentrations of dECM components extracted by EDTA, calcium hydroxide, white MTA or grey MTA (section 2.5.1). Medium was changed every 48 hours. Two different types of pulp cells were used in this experiment as the primary RDPC cultures provide a heterogeneous pulp cell population (Patel et al., 2009) whereas MDPC-23 cells are regarded as being homogeneous and more highly differentiated along an odontoblast-like lineage (Hanks et al., 1998a).

4.2.1 Growth of RDPCs exposed to EDTA extracted dECM components

On days 5 and 7, the cell counts for RDPCs exposed to dECM components extracted by EDTA at concentrations of 0.1, 1.0 and 10 µg/mL were greater than unstimulated controls, however, this was not statistically significant ($p>0.05$) (Figure 4.5). There appeared to be minimal difference in numbers of RDPCs in the control group compared with those exposed to dECM components at a concentration of 100 µg/mL, at each time-point analysed. EDTA extracted dECM components at this concentration therefore appeared to have minimal effect on primary RDPC growth.

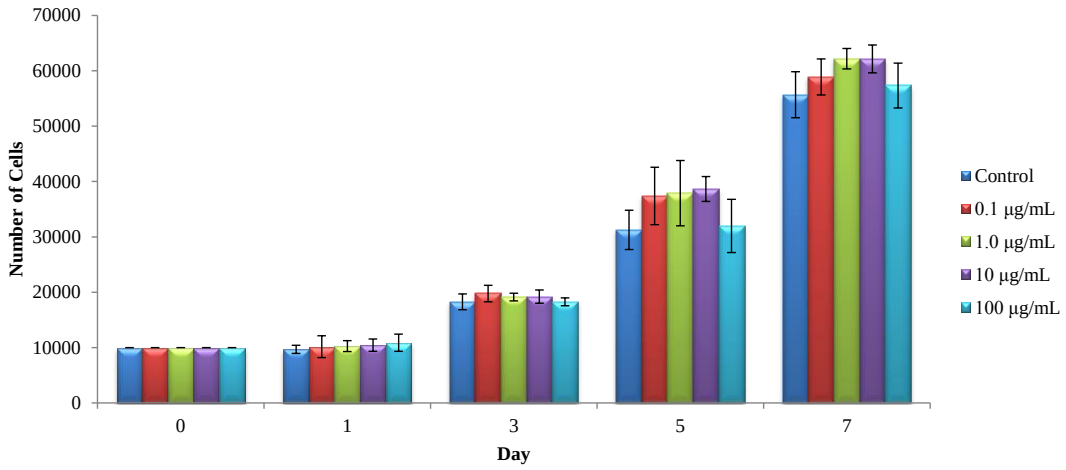

Figure 4.5 RDPC growth over 7 days following exposure to a range of concentrations of dECM components extracted by EDTA as determined by the WST-1 assay. Error bars represent one standard deviation from the mean for quadruplicate analyses. *$p \leq 0.05$ when compared with control using one-way ANOVA.

4.2.2 Growth of RDPCs exposed to calcium hydroxide extracted dECM components

During the first three days of culture, there was minimal difference in cell number when experimental groups were compared (Figure 4.6). At day 5, however, mean cell numbers were greater for cultures exposed to dECM components extracted by calcium hydroxide at concentrations of 0.1 µg/mL (36,000 cells), 1.0 µg/mL (40,000 cells), 10 µg/mL (41,000 cells) and 100 µg/mL (41,000 cells) compared with control (32,000 cells). These differences were not statistically significant ($p>0.05$). On day 7, mean numbers of RDPCs were greatest for cultures exposed to dECM components at a concentration of 10 µg/mL (62,200 cells). There were no statistically significant differences detected between any of these groups when compared ($p>0.05$). The highest concentration of dECM components, 100 µg/mL exerted minimal effect when compared with control at all time-points analysed.

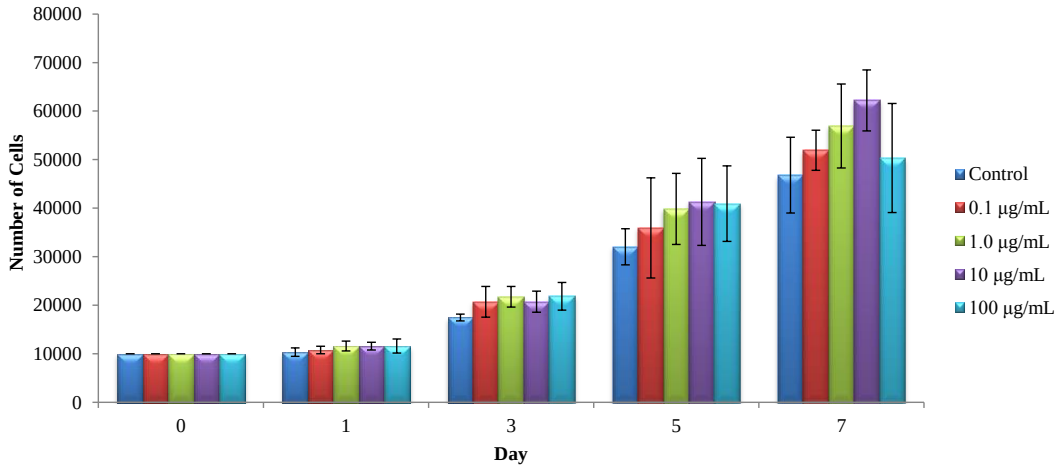

Figure 4.6 RDPC growth over 7 days following exposure to a range of concentrations of dECM components extracted by calcium hydroxide as determined by the WST-1 assay. Error bars represent one standard deviation from the mean for quadruplicate analyses. *$p \leq 0.05$ when compared with control using one-way ANOVA.

4.2.3 Growth of RDPCs exposed to white MTA extracted dECM components

RDPCs exposed to all concentrations of dECM components extracted by white MTA demonstrated no significant differences to the control over the first three days of the culture period (Figure 4.7). However, data from day 5 of culture demonstrated that RDPC numbers were increased by all concentrations when compared with control. The mean difference between control (31,000 cells) and 0.1 µg/mL (37,000 cells) was not statistically significant ($p>0.05$), however, statistically significant differences were detected for all other concentrations applied including 1.0 µg/mL (43,000 cells, $p=0.013$), 10 µg/mL (43,500 cells, $p=0.01$) and 100 µg/mL (42,000 cells, $p=0.027$). On day 7, RDPC numbers increased in a dose dependent manner, with increasing concentrations of white MTA extracted dECM components, up to 10 µg/mL: 0.1 µg/mL (48,500 cells), 1.0 µg/mL (53,000 cells), 10 µg/mL (58,500 cells) versus control (43,000 cells). Comparison with control demonstrated that the 10 µg/mL dECM exposure was statistically significant ($p=0.014$). At the highest concentration (100 µg/mL) of dECM components applied, the cell numbers were similar to those of the control (40,000 cells).

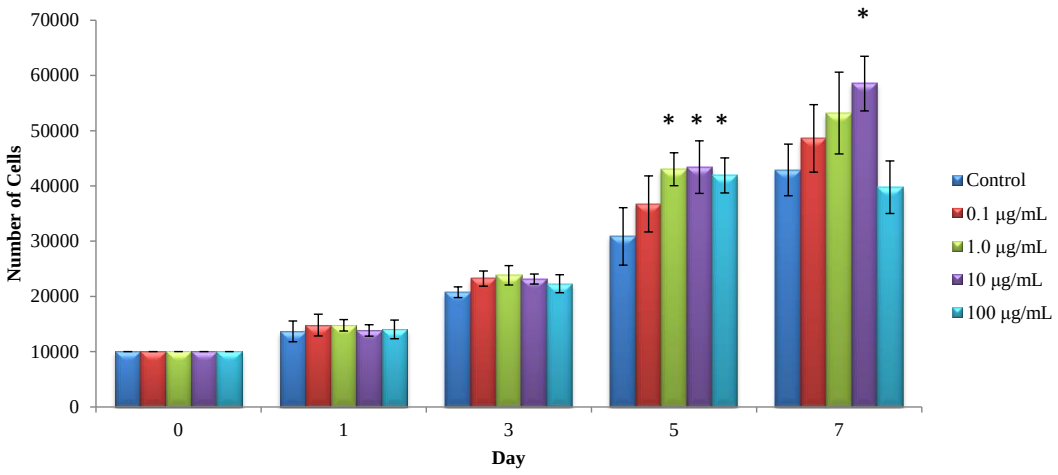

Figure 4.7 RDPC growth over 7 days following exposure to a range of concentrations of dECM components extracted by white MTA as determined by the WST-1 assay. Error bars represent one standard deviation from the mean for quadruplicate analyses. *$p\leq0.05$ when compared with control using one-way ANOVA.

4.2.4 Growth of RDPCs exposed to grey MTA extracted dECM components

During the first three days of culture, RDPCs exposed to the concentrations of dECM components extracted by grey MTA showed minimal variation in cell number compared with control. Day 5 data demonstrated that the mean cell numbers for 1.0 µg/mL (51,000 cells) and 10 µg/mL (50,000 cells) dECM exposure were only marginally greater than control (43,500 cells), and no statistically significant differences were detected ($p>0.05$). On day 7, mean cell numbers were greater for dECM exposures at 0.1 µg/mL (69,000 cells), 1.0 µg/mL (74,000 cells) and 10 µg/mL (72,500 cells) compared with control (60,000 cells). Statistically significant differences were only identified for the concentration of 1.0 µg/mL ($p=0.05$). Mean cell number for the highest concentration (100 µg/mL: 63,000 cells) was similar to that of control.

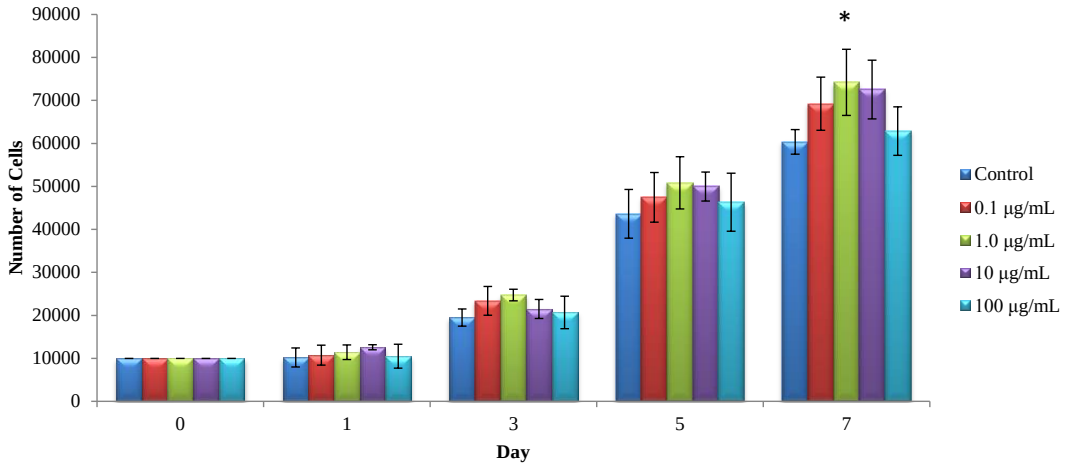

Figure 4.8 RDPC growth over 7 days following exposure to a range of concentrations of dECM components extracted by grey MTA as determined by the WST-1 assay. Error bars represent one standard deviation from the mean for quadruplicate analyses. *$p\leq0.05$ when compared with control using one-way ANOVA.

4.2.5 Growth of MDPC-23 cells exposed to EDTA extracted dECM components

Lower concentrations (0.1 and 1.0 µg/mL) of dECM components extracted by EDTA increased growth of MDPC-23 cells compared with control (Figure 4.9). The differences in means were not statistically significant at earlier time-points, until day 4, when the mean cell number for control was 18,500 and for a concentration of 1.0 µg/mL dECM was 22,300 ($p=0.003$). The higher concentration of dECM components appeared to have a deleterious effect on cell growth; on days 4 and 5, the mean cell numbers for the concentration of 100 µg/mL were significantly lower than control, $p=0.004$ and $p<0.0001$, respectively.

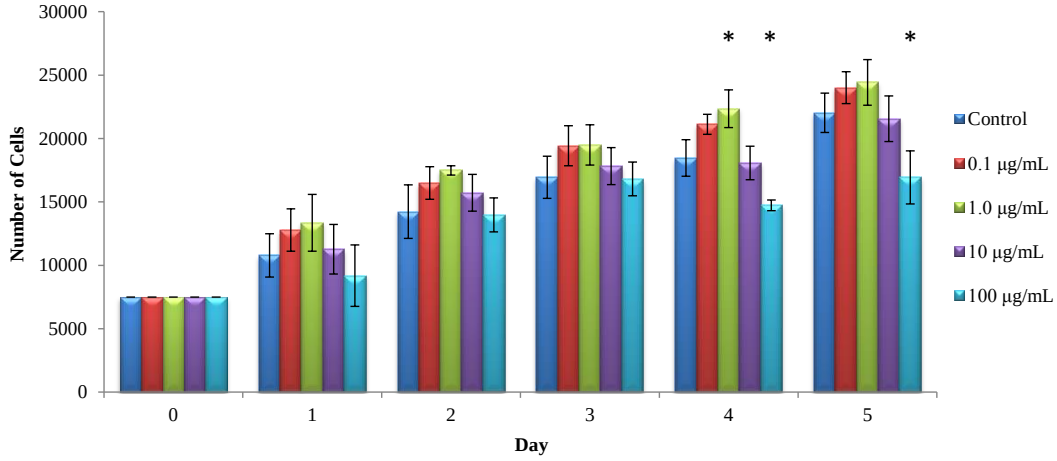

Figure 4.9 MDPC-23 cell growth following exposure to a range of concentrations of dECM components extracted by EDTA over 5 days as determined using the WST-1 assay. Error bars represent one standard deviation from the mean for quadruplicate analyses. *$p\leq0.05$ when compared with control using one-way ANOVA.

4.2.6 Growth of MDPC-23 cells exposed to calcium hydroxide extracted dECM components

Over the first three days of cell culture, there were minimal differences in mean cell numbers of MDPC-23 cells exposed to all concentrations of dECM components extracted by calcium hydroxide (Figure 4.10). Analysis of day 4 and 5 cell counts demonstrated that the highest concentration (100 µg/mL) of dECM inhibited cell growth as mean cell numbers at 100 µg/mL exposure were significantly lower than control, p=0.03 and p=0.015, respectively. On day 5, concentrations of 0.1 and 1.0 µg/mL of dECM, resulted in the mean number of cells increasing above control, however, statistically significant differences were only detected for 1.0 µg/mL dECM exposure (p=0.042).

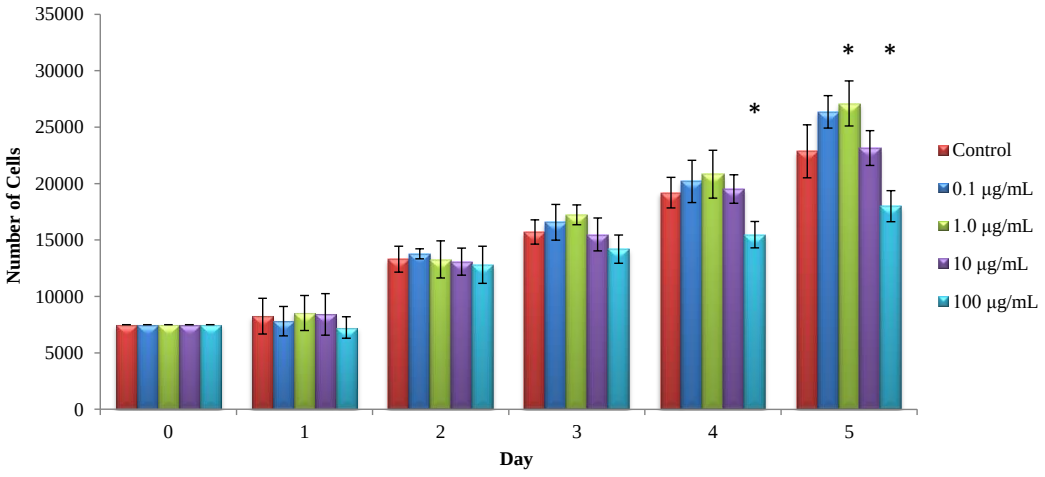

Figure 4.10 MDPC-23 cell growth following exposure to a range of concentrations of dECM components extracted by calcium hydroxide over 5 days as determined using the WST-1 assay. Error bars represent one standard deviation from the mean for quadruplicate analyses. *p≤0.05 when compared with control using one-way ANOVA.

4.2.7 Growth of MDPC-23 cells exposed to white MTA extracted dECM components

Lower concentrations (0.1, 1.0 and 10 µg/mL) of dECM components extracted using white MTA stimulated increases in cell numbers in exposed cultures by day 3 when compared with control (Figure 4.11). Day 4 data demonstrated statistically significant differences in cell numbers when control (17,900 cells) was compared with 1.0 µg/mL (28,200 cells) and 10 µg/mL (28,150 cells) exposures of dECM components liberated by white MTA ($p=0.005$) indicating that these concentrations promoted cell growth. On day 5, cell numbers for the lowest dECM exposure concentrations (0.1 and 1.0 µg/mL) were significantly greater than those for control ($p<0.0001$), while cell numbers for cultures exposed to 100 µg/mL dECM were significantly lower than those of control ($p<0.0001$).

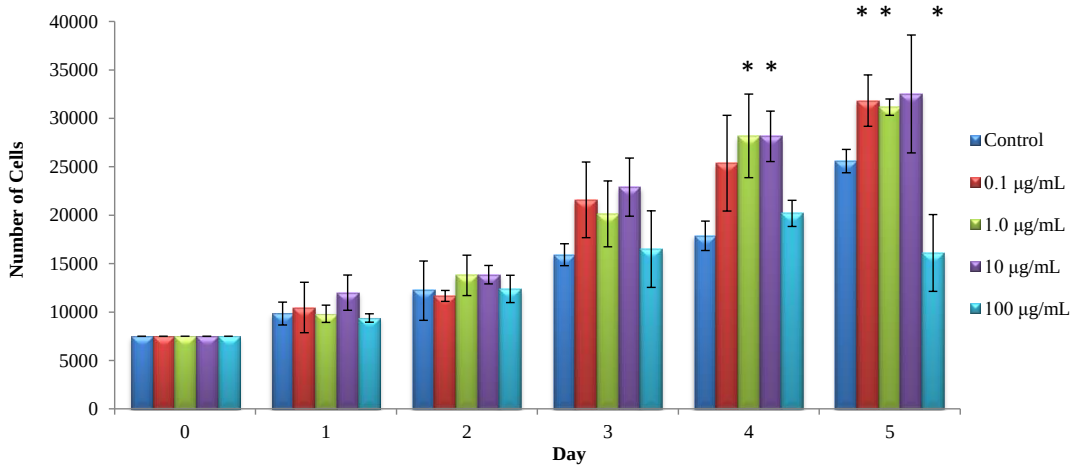

Figure 4.11 MDPC-23 cell growth following exposure to a range of concentrations of dECM components extracted by white MTA over 5 days as determined using the WST-1 assay. Error bars represent one standard deviation from the mean for quadruplicate analyses. *$p \leq 0.05$ when compared with control using one-way ANOVA.

4.2.8 Growth of MDPC-23 cells exposed to grey MTA extracted dECM components

The dECM components extracted by grey MTA at the highest concentration of 100 µg/mL negatively affected cell growth throughout the 5 day culture period, however, differences were only statistically significant on days 2-5 of analysis (Figure 4.12). Mean cell numbers were greater than those for control on day 4 and 5 for medium supplemented with dECM components at concentrations of 0.1, 1.0 and 10 µg/mL. These comparisons were only statistically significant for dECM concentrations of 1.0 µg/mL (p=0.028) and 10 µg/mL (p=0.003) on day 4 and 10 µg/mL (p=0.028) on day 5.

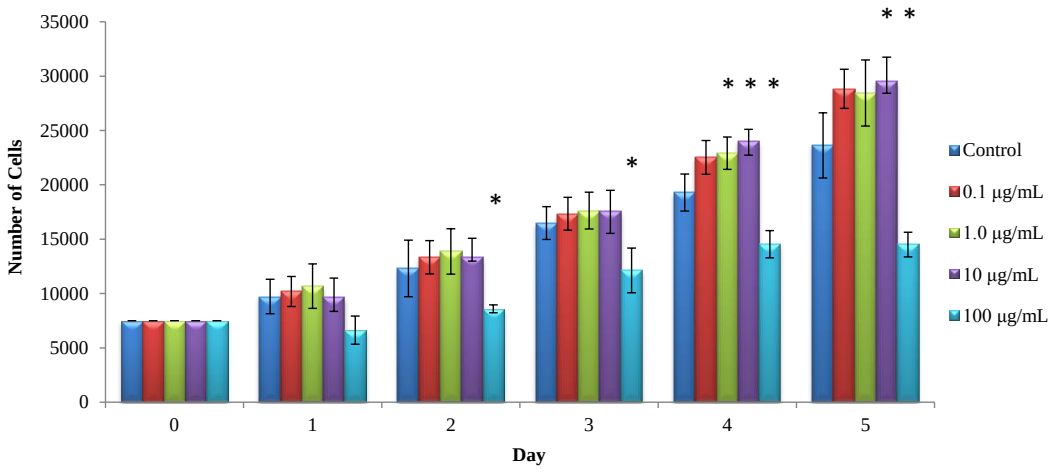

Figure 4.12 MDPC-23 cell growth following exposure to a range of concentrations of dECM components extracted by grey MTA over 5 days as determined using the WST-1 assay. Error bars represent one standard deviation from the mean for quadruplicate analyses. *p≤0.05 when compared with control using one-way ANOVA.

5.0 RESULTS CHAPTER 3

The role of hepatocyte growth factor in cellular processes associated with pulp wound healing

In 3.0 Results Chapter 1, dECM was demonstrated to contain a rich cocktail of growth factors, which could be differentially released from human dentine by different pulp capping agents. Release of many of the molecules from dECM has not been previously reported. Indeed, cytokine array analysis demonstrated for the first time the presence of hepatocyte growth factor (HGF) in extracted dECM components (Figure 3.9B).

The expression of HGF and c-Met has been shown in the developing tooth germs of mice (Sonnenberg et al., 1993, Kajihara et al., 1999) with its deletion in knock-out mice demonstrating abnormal tooth development (Tabata et al., 1996) suggesting it plays an important role in primary dentinogenesis (section 1.2.2). Together with its known functionalities in other tissues, this led to the hypothesis that HGF could play an important role in dental tissue regeneration. Therefore, the aims of the studies described below were to determine: i) the concentration of HGF in dECM components released by relevant pulp therapeutic agents (using quantitative ELISA), ii) if HGF and its receptor c-Met are expressed in RDPC cultures, human and rat pulp tissue, and iii) if HGF is able to activate pulp derived cells in terms of the repair-associated processes of chemotaxis, differentiation and mineralisation.

5.1 HGF analysis in human dentine

To determine the concentration of HGF released from human dentine by solutions of EDTA and the pulp therapeutic agents calcium hydroxide, white MTA, grey MTA and Biodentine®, a multiplex sandwich ELISA was performed, as described previously (section 2.2.5). The presence of HGF was identified in dECM extracted by solutions of EDTA, white MTA and grey MTA (Figure 5.1), however, levels of HGF in dECM extracted by calcium hydroxide and Biodentine® solutions were lower than the detection level limit of this assay. EDTA extracted significantly more HGF (457.8 ±3.3 pg/mL) ($p<0.0001$) than the other extraction solutions of white MTA (28.8 ±4.3 pg/mL) and grey MTA (31.3 ±2.1 pg/mL). There were no significant differences in the amounts of HGF released by white and grey MTA ($p=1.0$).

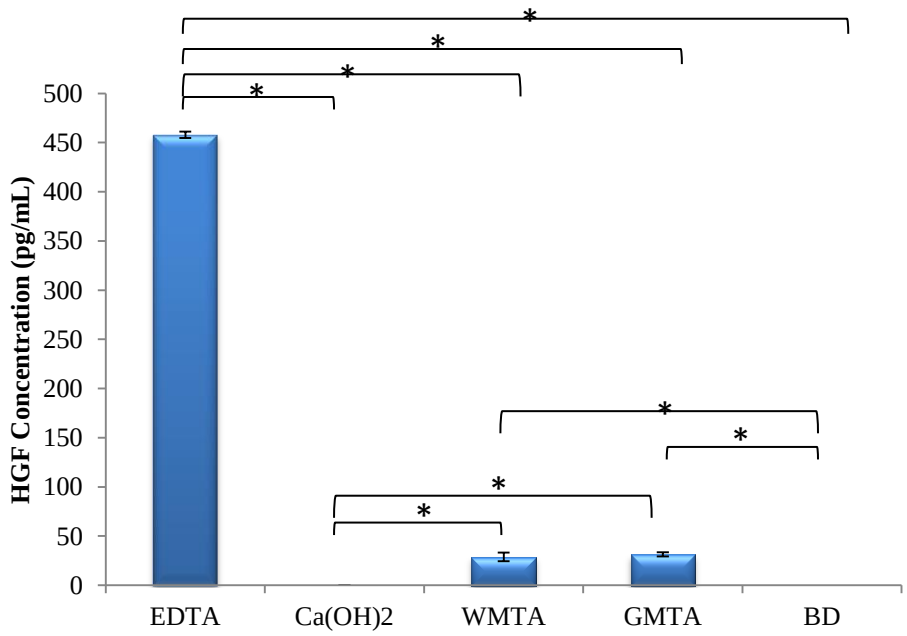

Figure 5.1 Mean HGF concentration (pg/mL) in dECM released from human dentine by solutions of EDTA, calcium hydroxide ($Ca(OH)_2$), white MTA (WMTA), grey MTA (GMTA) and Biodentine® (BD) as determined by ELISA (mean ±SD, n=3) * indicates statistically significant difference ($p<0.05$) using one-way ANOVA**.**

5.2 Expression of c-Met and HGF in human and rat cells and tissues

To determine whether pulpal cells were likely to be able to respond to HGF signalling and therefore, whether HGF could potentially contribute to dental tissue repair and regeneration, the expression of HGF and its receptor c-Met in human pulp tissue was analysed. RNA was isolated from human pulp tissue and control RNA was obtained from commercial sources for a range of other tissues to act as comparators for expression levels. Qualitative RT-PCR analysis was performed to determine relative levels of expression. Both HGF and its receptor c-Met were strongly expressed in human pulp tissue, liver (control) and smooth muscle (control) compared with the other tissues analysed (Figure 5.2).

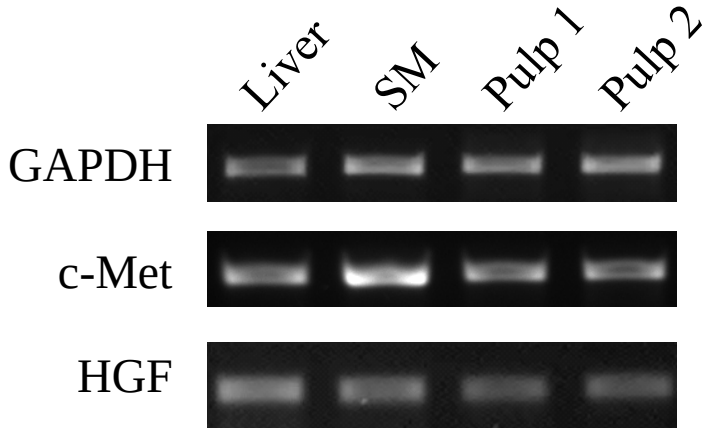

Figure 5.2 Gel images showing relative gene expression levels of c-Met and HGF in human tissues (SM= Smooth Muscle) normalised to the GAPDH housekeeping gene.

To determine whether rat dental pulp cells (RDPCs) in culture were likely to be able to respond to HGF via HGF/c-Met signalling, the expression of the c-Met receptor was analysed. Qualitative RT-PCR analysis was undertaken on several rat tissues including pulp, tongue, palatal mucosa, bone marrow and lung, as well as RDPC monolayer cultures, to

assess the expression of HGF and c-Met. Data demonstrated that both HGF and its receptor c-Met were expressed in a variety of rat tissues as well as RDPCs. Interestingly, it appeared that higher expression levels of c-Met were detected in the RDPCs compared with other tissues while the converse was true for HGF expression (Figure 5.3).

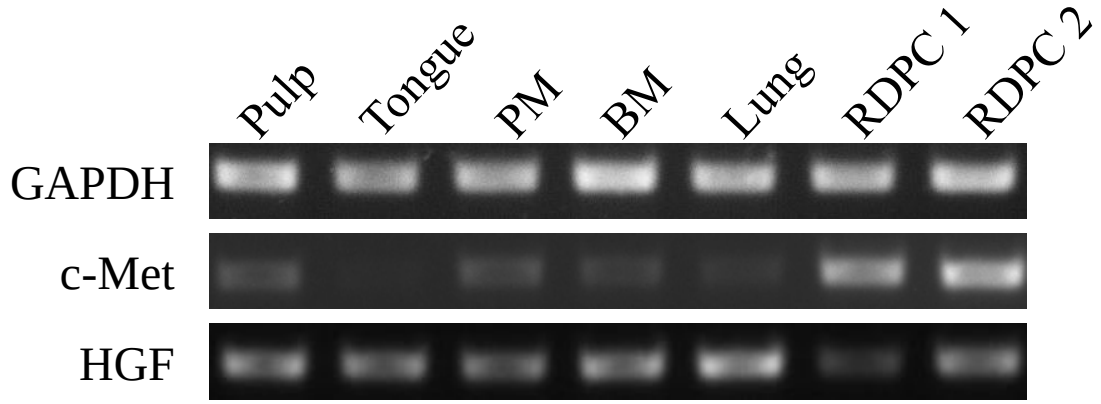

Figure 5.3 Gel images showing relative expression of c-Met and HGF in rat tissues [PM = Palatal Mucosa, BM = Bone Marrow, RDPC = Rat Dental Pulp Cells (two independent cultures were analysed)] normalised to the housekeeping gene GAPDH.

5.3 Chemotactic activity of HGF

To determine the ability of RDPCs to respond chemotactically to HGF, a two chamber transwell assay was employed. In the positive control group (10% FBS), 81% of RDPCs migrated to the lower chamber, whereas with the medium containing no FBS supplement (negative control) only 16% of cells migrated (Figure 5.4). Medium containing recombinant HGF in the concentration ranges of 5-20 ng/mL demonstrated statistically significant migration of RDPCs when compared with control medium with no supplement. Within the 45

minute assay period, the percentage movement of cells ranged from 48-59% for all HGF groups analysed.

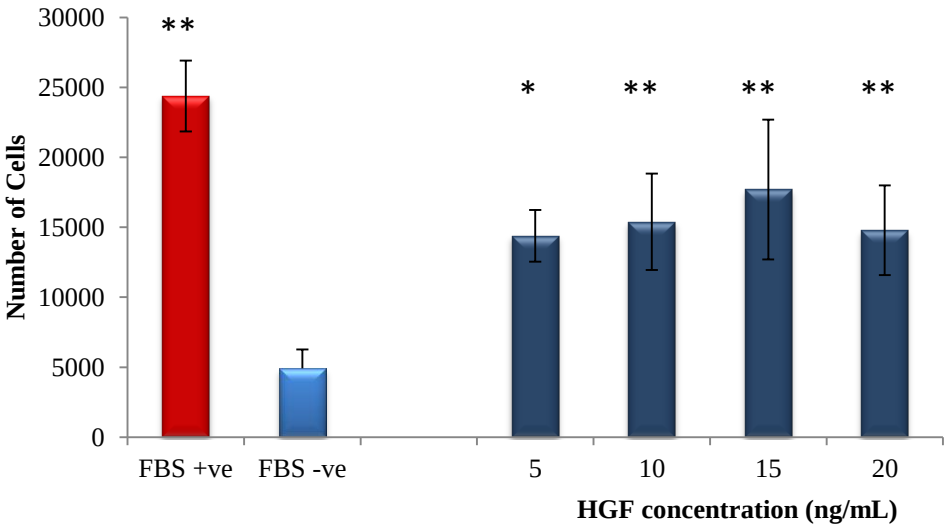

Figure 5.4 RDPC migration, induced by recombinant HGF at concentrations between 5-20 ng/mL, within the 45 minute assay period. Positive control with 10% FBS (FBS +ve) and negative control without FBS (FBS –ve). All experiments were performed in quadruplicate and are expressed as mean values ±SD. *$p \leq 0.05$, **$p \leq 0.005$ when compared with medium containing no supplement using one-way ANOVA.

5.4 Gene expression analysis of RDPCs exposed to HGF

To investigate further the effects of HGF on RDPCs in terms of differentiation, gene expression analyses were performed for several transcripts associated with mineralisation. A panel of markers, that are considered to reflect dentinogenic and osteogenic phenotypic characteristics, were studied. For convenience of analysis, the markers were grouped as being predominantly either odontoblastic (McLachlan et al., 2003) or osteoblastic (Karsenty, 2000) as has been previously described.

RDPCs were cultured for up to 12 days and exposed to a range of concentrations of recombinant HGF (5 or 20 ng/mL). Gene expression analysis using semi-quantitative RT-PCR was performed on days 1, 7 and 12 of culture and normalised against the housekeeping gene (GAPDH) levels. Transcript levels of general markers of mineralisation [alkaline phosphatase (ALP) and collagen 1 alpha (Col1α)], dentinogenic markers [dentine matrix protein-1 (DMP-1) and nestin] and osteogenic markers (osteopontin, osterix, osteocalcin, and Runx2) were compared with control using densitometric analysis.

Figure 5.5 shows the gene expression changes of ALP and Col1α observed in RDPCs that were exposed to HGF (5 or 20 ng/mL) over the 12 day period. Expression levels of ALP in RDPCs did not vary considerably over this time period, nor in response to HGF supplementation. The greatest detectable change in expression of ALP during this period occurred when RDPCs were cultured for 12 days with 20 ng/mL of HGF supplement (8% increase), however, this was not statistically significant ($p=1.0$). Mean expression changes of Col1α appeared greater as there was reduced expression on day 1 [5 ng/mL (-15%), 20 ng/mL (-7%)] and increased expression for RDPCs exposed to 20 ng/mL HGF on day 7 (13%) and day 12 (14%), however, none of these changes were statistically significant.

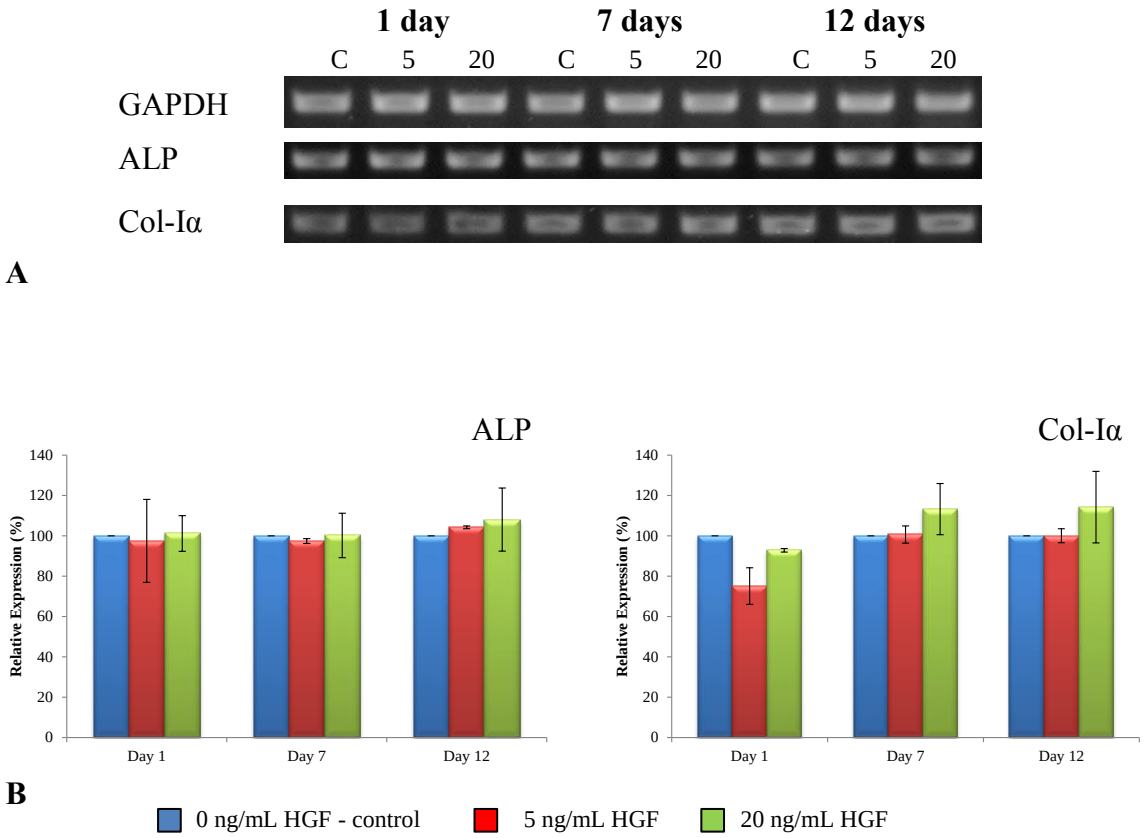

Figure 5.5 RT-PCR analysis of RDPCs following culture for 1, 7 and 12 days in mineralising medium supplemented with recombinant HGF at concentrations of 5 or 20 ng/mL. Control (C) was supplemented with PBS instead of HGF. **A**) Representative gel images showing relative gene expression. **B**) Densitometric analysis of gel images showing differential gene expression of ALP (alkaline phosphatase) and Col-Iα (Collagen type I alpha); levels were normalised to the GAPDH housekeeping gene levels. Data are expressed as a relative increase compared with control cultures (mean ±SD, n = 3) *p≤0.05 when compared to control with one way ANOVA.

Expression changes of dentinogenic-related markers (DMP-1 and nestin) are displayed in Figure 5.6. Relative expression levels of DMP-1 in RDPCs did not change considerably on the first day of culture, however, on day 7, the expression level was statistically significantly ($p=0.001$) increased when the RDPCs were exposed to both the 5 ng/mL (164%) and 20 ng/mL (178%) concentrations of HGF. These differences in expression were maintained until the end of the culture period on day 12, although at this point they were smaller in magnitude [5 ng/mL (65%) and 20 ng/mL (62%)], nevertheless remaining statistically significant ($p \leq 0.002$). HGF exposure exerted minimal effect on the expression levels of nestin in RDPCs during the culture period (Figure 5.6). 20 ng/mL of HGF decreased expression marginally on day 7 (-11%) and day 12 (-22%), however, none of these changes were statistically significant when compared with control.

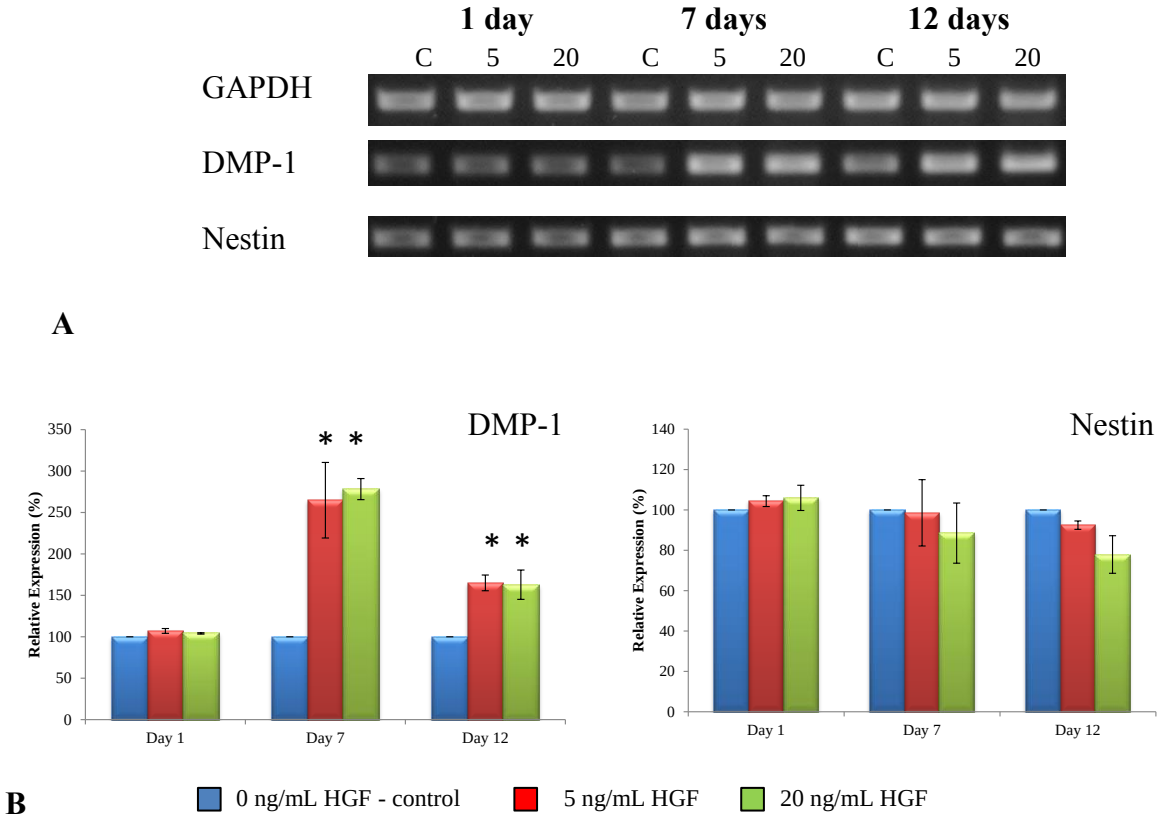

Figure 5.6 RT-PCR analysis of RDPCs following culture for 1, 7 and 12 days in mineralising medium supplemented with recombinant HGF at concentrations of 5 or 20 ng/mL. Control (C) was supplemented with PBS instead of HGF. **A**) Representative gel images showing relative gene expression. **B**) Densitometric analysis of gel images showing differential gene expression of DMP-1 (dentine matrix protein-1) and nestin; levels were normalised to GAPDH housekeeping gene levels. Data are expressed as a relative increase compared with control cultures (mean ±SD, n= 3) *p≤0.05 when compared with control with one way ANOVA.

Gene expression analyses were performed for several transcripts associated with the osteogenic phenotype including osteopontin, osterix, osteocalcin, and Runx2 (Figure 5.7). Data demonstrated varying degrees of elevated cellular expression when RDPCs were exposed to recombinant HGF compared with unstimulated controls over the 12 day period. Mean expression of osteocalcin was up-regulated compared with control on all days, by both concentrations of HGF applied. On day 7, this was statistically significant for 5 ng/mL [49% increase ($p=0.002$)] and 20 ng/mL [67% increase ($p<0.0001$)] exposures. On the final day of analysis, only 5 ng/mL HGF exposure induced a statistically significant increase in expression compared with control [64% ($p=0.002$)].

Runx2 expression was statistically significantly up-regulated following HGF treatment at a concentration of 20 ng/mL [85% increase ($p\leq0.0001$)] on day 1; no changes were detected for 5 ng/mL HGF exposure when compared with control ($p=0.617$). By day 7, both concentrations of HGF (5 and 20 ng/mL) had induced increased expression of Runx2 to levels that were statistically significant, $p=0.002$ and $p<0.0001$, respectively. At the end of the culture period, only a concentration of 20 ng/mL HGF showed a statistically significant difference to control ($p<0.0001$).

Osterix demonstrated considerable changes in transcript level expression (Figure 5.7) in RDPCs; in particular, on day 12 when expression increased significantly ($p\leq0.0001$) for cells exposed to 5 ng/mL (264%) or 20 ng/mL (353%) recombinant HGF. Although transcript levels for osteopontin were up-regulated in comparison with control for RDPCs exposed to 5 and 20 ng/mL HGF on days 7 and 12, the only statistically significant difference detected was in RDPC cultures exposed to 20 ng/mL on day 7 ($p=0.014$).

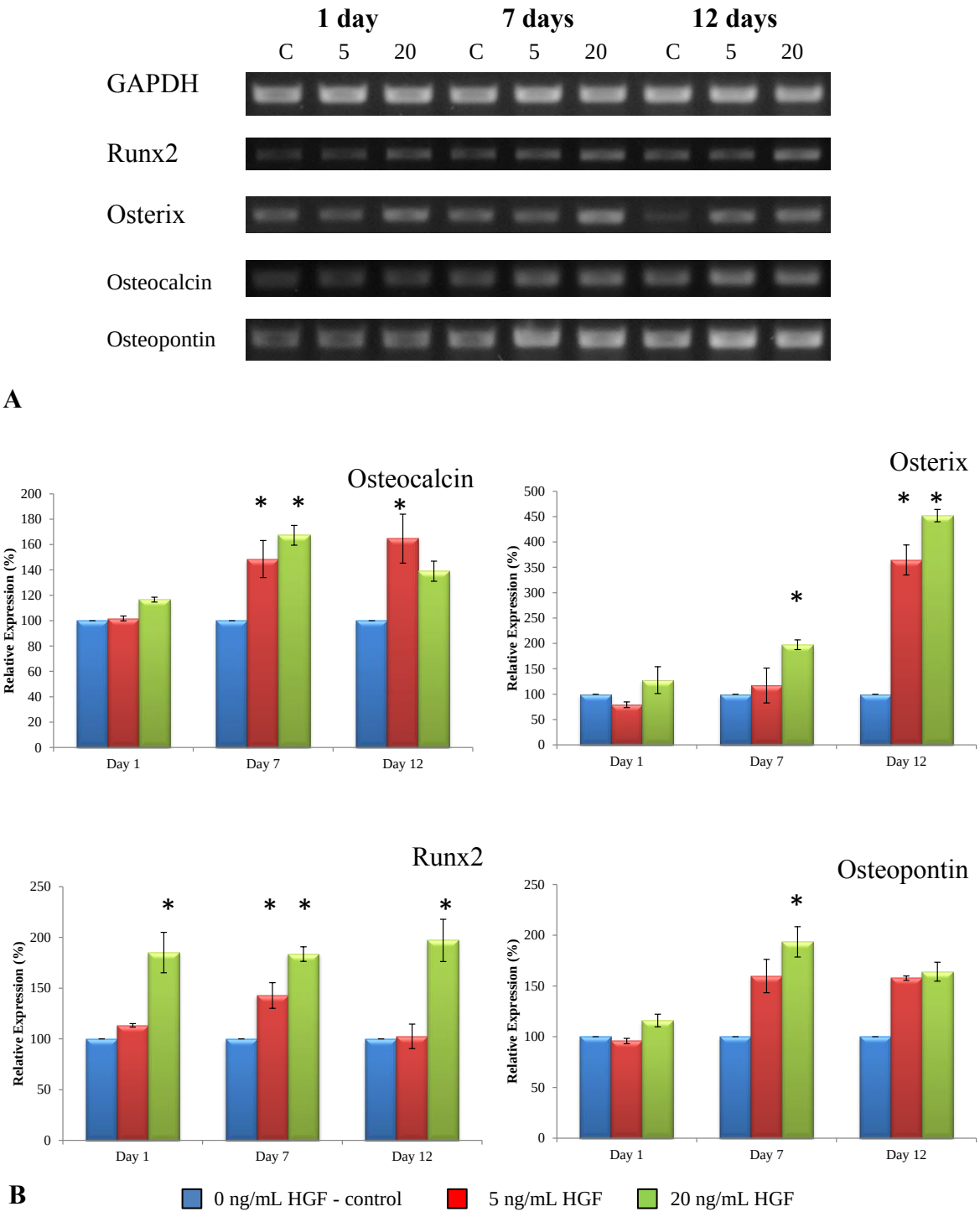

Figure 5.7 RT-PCR analysis of RDPCs following culture for 1, 7 and 12 days in mineralising medium supplemented with recombinant HGF at concentrations of 5 or 20 ng/mL. Control (C) was supplemented with PBS instead of HGF. **A**) Representative gel images showing relative gene expression. **B**) Densitometric analysis of gel images showing differential gene expression of osteocalcin, Runx2, osterix and osteopontin; levels were normalised to the GAPDH housekeeping gene levels. Data are expressed as a relative increase compared with control cultures (mean ±SD, n= 3) *p≤0.05 when compared to control with one way ANOVA.

5.5 HGF induced mineralisation in RDPC cultures

HGF/c-Met signalling has previously been shown to be associated with mineralised tissue formation under pathological conditions (Liu et al., 2007, McKinnon et al., 2006); combined with the expression analyses data, this therefore highlights the potential for HGF involvement in both dental cell differentiation and mineralisation. Alizarin red staining (ARS) of RDPCs was used to determine the ability of HGF to induce mineral production *in vitro*. Adenoviral vectors were used to induce over-expression of HGF and NK4, in parallel with other experimental groups which were exposed to a range of concentrations of recombinant HGF. Prior to studying the effects of mineral production in RDPC cultures using this approach, the optimal adenoviral vector transfection efficiency [multiplicity of infection (MOI)] was determined and the most appropriate mineralisation medium composition for discrimination of experimental group differences was identified.

5.5.1 Optimisation of medium for stimulation of mineralisation in RDPCs

Initial experiments using standard mineralisation medium comprising beta-glycerophosphate disodium salt hydrate (BGP) and dexamethasone (Dex) demonstrated their potent ability to induce mineral production in RDPC cultures. Therefore, in order to discriminate the relative ability of different experimental groups to induce mineralisation, a less potent mineralisation supplement was identified.

RDPCs were cultured for up to 16 days with six different types of media supplement comprising PBS (control); 50 μg/mL ascorbic acid + 10 mM BGP; 10 mM BGP; 5 mM BGP; 10 mM BGP + Dex 10^{-8} and 5 mM BGP + Dex 10^{-8} (section 2.4.1.3). Mineral production was

determined using ARS (section 2.5.3) on days 5, 12 and 16 of culture and results are presented in Figure 5.8. Over the time course of this study, RDPCs supplemented with PBS (control) demonstrated a relatively weak and slow increase in mineral production: day 5 (20.05 ±4.29 µM), day 7 (38.44 ±12.40 µM) and day 16 (51.07 ±4.75 µM). Medium supplemented with both BGP and Dex induced relatively high mineral production by day 5, however, mineral production did not increase significantly during the remaining time period of the experiment. A similar pattern of relatively high mineral production by day 5 was observed for RDPCs exposed to medium containing 50 µg/mL ascorbic acid + 10 mM BGP, however, in this instance, total mineral content continued to rise, reaching its maximum level on day 12 (110.34 ±15.10 µM). Medium supplemented with either 10 mM BGP or 5 mM BGP alone induced a gradually increasing rate of mineral production in RDPCs over the time course of 16 days with total mineral content being greater than control. The 5 mM BGP supplement induced the greatest amount of mineral on day 16 (113.14 ±42.02 µM). It was determined that medium supplemented with 5 mM BGP alone would be used as mineralisation medium.

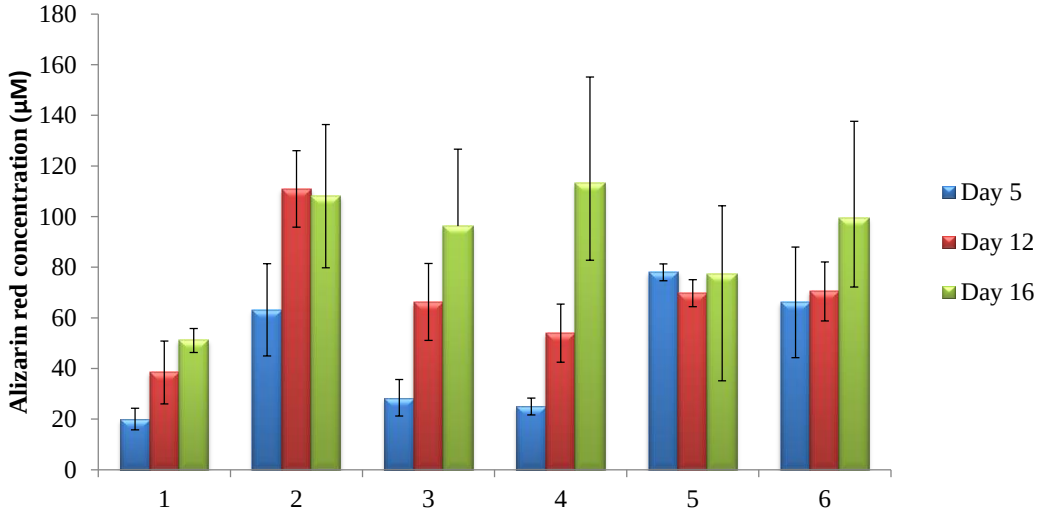

Figure 5.8 Mineral content analysis in RDPC cultures as determined by alizarin red staining following culture for 5, 12 and 16 days in medium supplemented with 1) PBS, 2) 50 µg/mL ascorbic acid + 10 mM BGP, 3) 10 mM BGP, 4) 5 mM BGP, 5) 10 mM BGP + Dex 10^{-8} and 6) 5 mM BGP + Dex 10^{-8}.

5.5.2 Optimisation of adenoviral transfection efficiency using an adenoviral vector expressing enhanced green fluorescent protein

Infecting monolayer cultures of primary cells with adenoviral vectors can have a deleterious effect on cell behaviour, function and viability. To determine the optimal rate of infection, i.e. the ratio of infectious virus particles to the number of cells or multiplicity of infection (MOI), a fluorescently labelled viral vector was utilised. This enabled a high infection rate to be identified, which did not cause detrimental effects on cell viability. The adenoviral vector NK4 (AdNK4) expressed enhanced green fluorescent protein (EGFP); RDPCs were exposed to a range of MOIs (50-400) and cultured for up to 5 days. The percentage of positive EGFP cells viewed under a fluorescent microscope was calculated (section 2.4.4.1). Results are shown in Figure 5.9 and representative images of different MOI rates are also provided in Figure 5.10.

Infection rates using 50 and 100 MOI were relatively low with only 9 ±3% of cells expressing EGFP over the 5 day culture period. MOI of 150, 200 and 300 produced much higher transfection rates with the highest being for a MOI of 250, on day 1 (65.67 ±4.04%), day 3 (84.67 ±3.06%) and day 5 (84 ±7.55%). A MOI greater than 250 resulted in decreased transfection efficiency - this may have been due to the viral vector exerting a toxic effect on cultures. To analyse the effects of transfection with adenoviral vectors, an MOI of 250 was chosen.

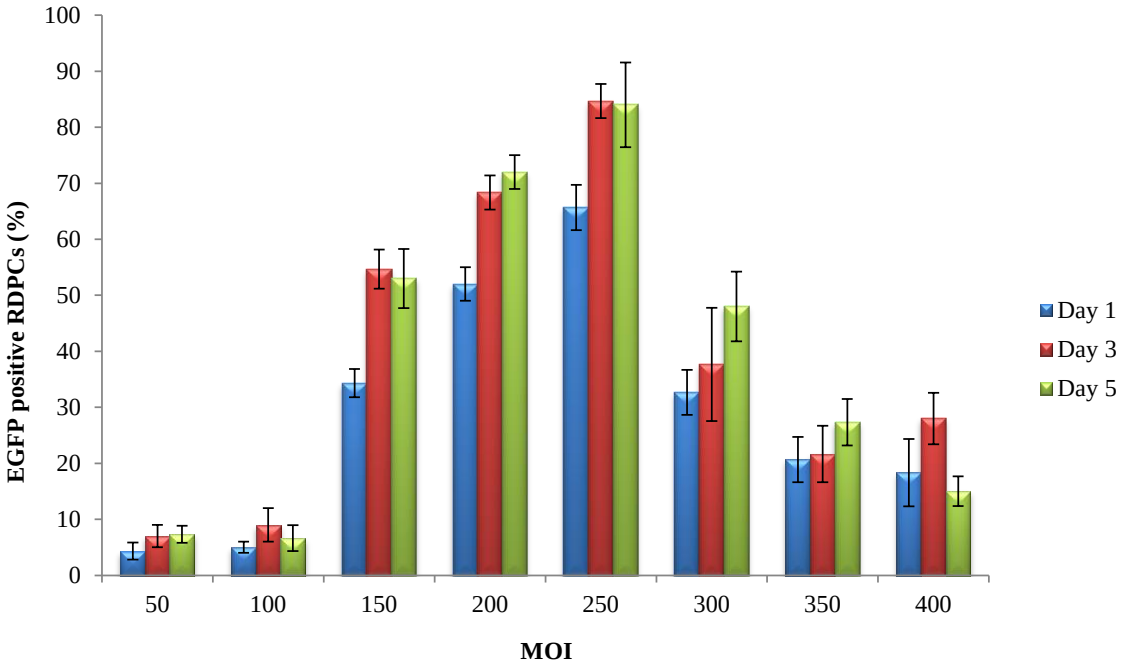

Figure 5.9 Adenoviral transfection rate in RDPCs infected with AdNK4 expressing EGFP at a range of multiplicity of infections (MOIs) from 50-400 and cultured for up to 5 days (n=3).

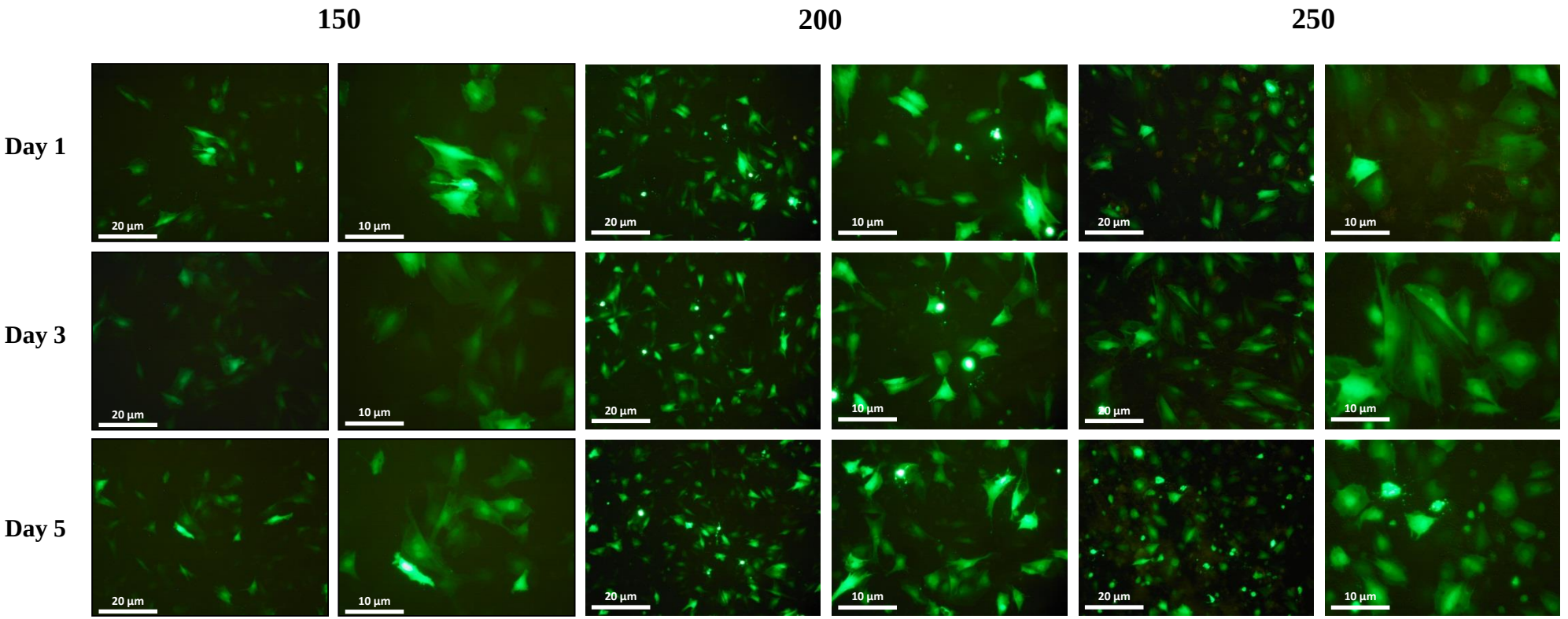

Figure 5.10 Representative photographic image fields of RDPCs infected with EGFP labelled AdNK4 adenoviral vector at MOIs of 150, 200 and 250. RDPCs were cultured for up to 5 days and viewed under a fluorescent microscope (Nikon Eclipse TE300 microscope). Scale bars are shown.

5.5.3 Alizarin red staining of RDPC cultures exposed to AdHGF, AdNK4 and recombinant HGF

To assess the ability of HGF to promote mineralisation in RDPC cultures *in vitro*, alizarin red staining was performed following exposure of cultures to the adenoviral vectors, AdHGF and AdNK4 and recombinant HGF (Figure 5.11). Quantitative measurement of alizarin red staining (Figure 5.12) demonstrated significantly increased levels ($p \leq 0.001$) of mineralisation in RDPC cultures exposed to both AdHGF (63.05 ±17.57 μM) and recombinant HGF: 5 ng/mL (69.82 ±18.43 μM), 10 ng/mL (63.69 ±11.64 μM), 15 ng/mL (56.74 ±8.45 μM) and 20 ng/mL (64.59 ±14.74 μM), from day 8 onwards compared with controls (26.06 ±8.66 μM). This pattern continued until the end of the culture period (day 15); by this time, the differences were even greater: AdHGF (203.63 ±101.0 μM) and recombinant HGF: 5 ng/mL (106.57 ±18.43 μM), 10 ng/mL (198.9 ±47.82 μM), 15 ng/mL (233.01 ±98.98 μM) and 20 ng/mL (324.96 ±118.1 μM), compared with control medium (51.61 ±17.89 μM). RDPCs infected with the AdNK4 control vector showed no significant difference from uninfected control.

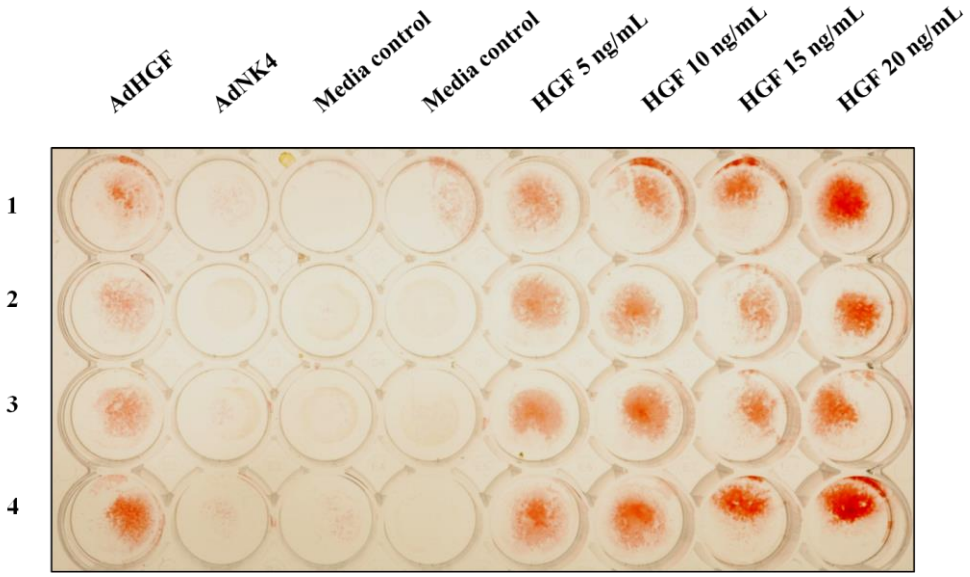

Figure 5.11 Photographic image (n=4) of 48-well plate stained with alizarin red following 15 day culture of RDPCs exposed to adenoviral infection of HGF, NK4 or mineralising medium (5% FBS and 5 mM BGP) supplemented with 5-20 ng/mL of recombinant HGF. Control medium was mineralising medium supplemented with PBS instead of HGF.

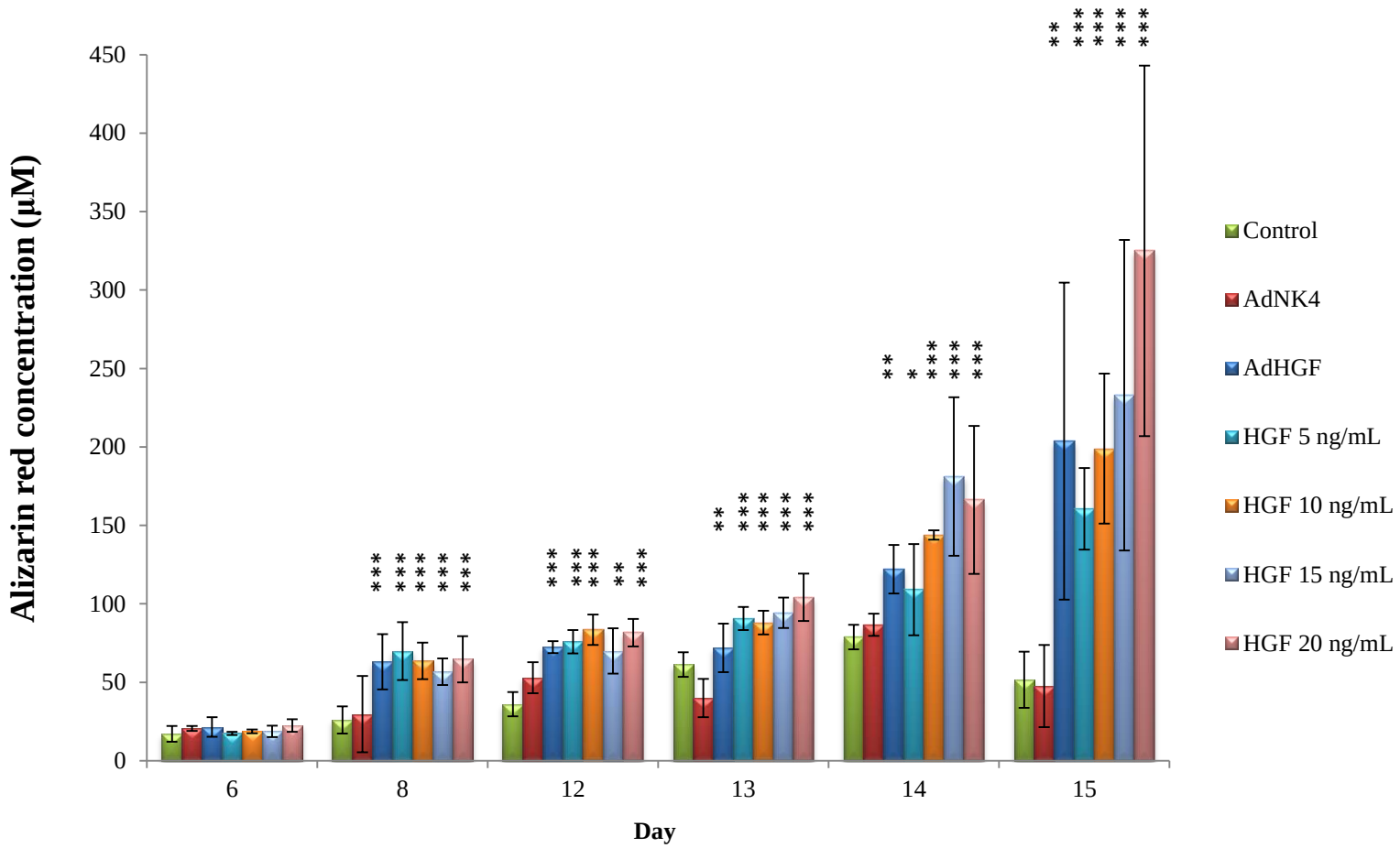

Figure 5.12 Alizarin red staining analysis in RDPC cultures exposed to adenoviral infection of HGF, NK4 or medium supplemented with 5-20 ng/mL of recombinant HGF cultured for up to 15 days. All experiments were performed in quadruplicate and are expressed as mean values ±SD. Experimental groups were compared with control using the students t-test (*p≤0.05, **p≤0.01, ***p≤0.001).

5.5.4 Cell growth analysis in RDPCs exposed to AdHGF, AdNK4 and recombinant HGF

No statistically significant differences in cell growth were detected between control and experimental cultures for any time point studied (Figure 5.13). Cell numbers were greatest for all groups on day 12; control medium (6.6x104 ±2530), AdC (6.2x104 ±3862), HGF 5 ng/mL (6.5x104 ±5090), HGF 10 ng/mL (6.7x104 ±2745), HGF 15 ng/mL (6.8x104 ±4002) and HGF 20 ng/mL (6.6x104 ±3027). Through day 13 to 15, cell numbers decreased each day for control medium (4.0x104 ±4363), AdC (3.7x104 ±3805), HGF 5 ng/mL (4.0x104 ±3451), HGF 10 ng/mL (3.9x104 ±3754), HGF 15 ng/mL (3.7x104 ±5040) and HGF 20 ng/mL (4.0x104 ±4112).

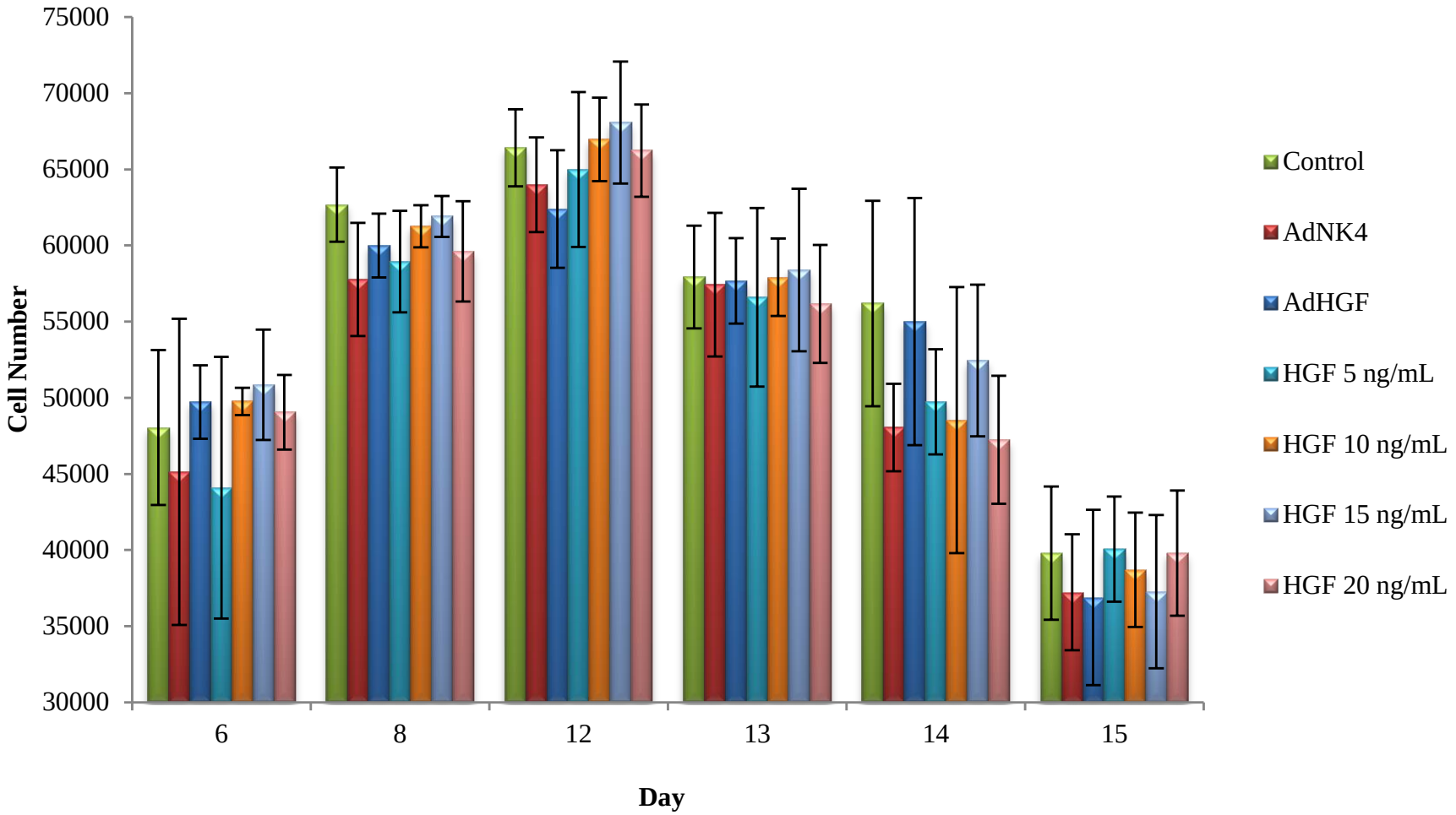

Figure 5.13 Cell growth as determined by WST-1 assay in RDPC cultures exposed to adenoviral infection of HGF, NK4 or medium supplemented with 5-20 ng/mL of recombinant HGF and cultured for up to 15 days. All experiments were performed in quadruplicate and data are expressed as mean values ±SD. Experimental groups were compared with control using one-way ANOVA, no statistical differences were found.

5.5.5 *In vitro* mineralisation in RDPCs exposed to AdHGF, AdNK4 and recombinant HGF

To determine if mineral deposition was increased due to cell number, data were expressed as mineral content per cell (Figure 5.14). Statistically significant higher levels of mineralisation occurred in groups exposed to AdHGF or recombinant HGF from day 8, indicating that the increased mineral production was not simply the result of an increase in cell number. There was a dose-dependent trend of increasing mineralisation with increasing HGF concentration on day 15 in cultures exposed to recombinant HGF (5-20 ng/mL).

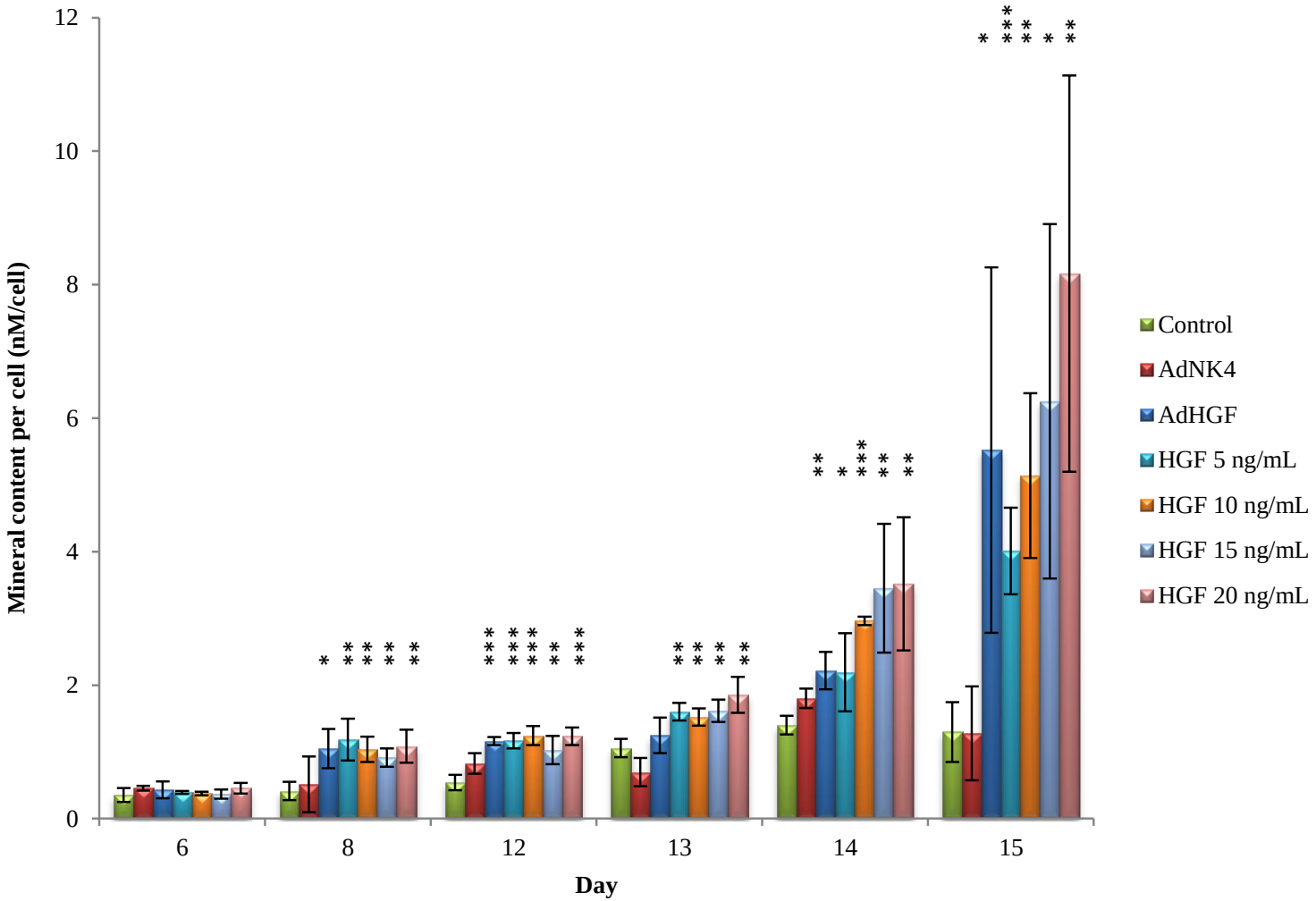

Figure 5.14 Alizarin red staining analysis in RDPC cultures exposed to adenoviral infection of HGF, NK4 or medium supplemented with 5-20 ng/mL of recombinant HGF and cultured for up to 15 days. Data are expressed as mineral production per cell. All experiments were performed in quadruplicate and are expressed as mean values ±SD. Experimental groups were compared with control using the students t-test (*p≤0.05,**p≤0.01,***p≤0.001).

6.0 DISCUSSION

The potential for material-directed regeneration of the wounded dental pulp has been recognised for over ninety years (Hermann, 1920), however, the molecular events leading to the formation of reparative dentine are only just beginning to be understood. Since this pioneering work of Hermann (1920), calcium hydroxide has been considered to be the gold standard material for use in operative procedures for treating the injured pulp. However, more recently, Mineral Trioxide Aggregate (MTA), a calcium silicate cement, has consistently been shown to produce a more predictable hard tissue barrier, create less inflammation and have relatively easier handling characteristics than calcium hydroxide lining materials (Nair et al., 2008, Aeinehchi et al., 2003, Caicedo et al., 2006, Chacko and Kurikose, 2006, Iwamoto et al., 2006). There are a number of hypotheses attempting to explain the regenerative response of the injured pulp when treated with calcium hydroxide. A plausible explanation is that the interaction of calcium hydroxide with the surrounding dentine leads to the liberation of growth factors and bioactive molecules which then provide the necessary signals for pulpal repair (Graham et al., 2006) (section 1.7.1). When a biomaterial is introduced into a vital tissue, it elicits a biological response from the host whether it is desirable or undesirable (Anderson, 2001). The success of the material is dependent both on creating an environment that is conducive to healing, and on initiating the necessary physiological cues which enable wound repair. A broad aim of this study was to determine, in principle, at the molecular level, how calcium silicate cements induce healing and repair of the injured dentine-pulp complex and further investigate any other specific repair mechanisms that became apparent.

6.1 Ionic dissolution of dental materials at the tissue-material interface

Therapeutic materials used in pulp capping (calcium hydroxide, calcium silicates: white MTA, grey MTA and Biodentine®) are soluble to varying degrees. The solubility of calcium hydroxide preparations used in pulp capping is well known (Hwas and Sandrik, 1984). In a clinical situation, calcium hydroxide cements will dissociate into Ca^{2+} and OH^- ions producing a calcium rich and high pH microenvironment, which will interact with local tissues (Glass and Zander, 1949, Schroder and Granath, 1971, Stanley and Lundy, 1972). There is some difference in opinion amongst investigators as to the degree of solubility of MTA (Danesh et al., 2006, Fridland and Rosado, 2005, Islam et al., 2006, Poggio et al., 2007, Shie et al., 2009, Torabinejad et al., 1995b). This is likely to be due to the different methodologies used to assess this and the variation in interpretation of the term 'solubility'. Solubility can be defined as the maximum amount of solute that may be dissolved in a solvent (Parirokh and Torabinejad, 2010). The methodologies used in previously published studies ostensibly determined the percentage weight-loss of the solid material over time in a solvent. These methods do not, however, account for the net increase in weight of the solid due to chemical modification at the surface. It has been established, using techniques such as X-ray diffraction, dispersive X-ray spectroscopy, Fourier transform-infrared spectroscopy and X-ray fluorescence, that calcium phosphates precipitate on the surface of MTA when it is in contact with synthetic physiological solutions and that these calcium phosphates are principally hydroxyapatite (Bozeman et al., 2006, Sarkar et al., 2005, Tay et al., 2007, Tingey et al., 2008). This suggests that there is a natural maturation of the material and a potential net gain in weight, thus explaining some of the variance and potential inaccuracies of solubility testing. The interaction with solvents also indicates that MTA liberates cations and anions from its surface when it contacts an

aqueous environment; this process is known as ionic dissolution. Using atomic absorption spectroscopy (AAS), water soluble components have been reported to include calcium (Ca^{2+}), potassium (K^{+}), sodium (Na^{+}), iron (Fe^{3+}) and sulphate (SO_4^{2-}) ions (Fridland and Rosado, 2003), whilst heavy metals, including chromium, arsenic and lead, are released by water and synthetic body fluid (Schembri et al., 2010).

To model some of the dynamic interactions of therapeutic pulp capping agents (calcium hydroxide, white MTA, grey MTA and Biodentine®) with the dentine-pulp complex, solutions of ionic dissolution products were generated through their interaction with water. An assumption was made that similar products would be released from these pulp capping agents when interacting with tissue fluid in the clinical situation. Therefore, in this present study, EDTA was used as a well characterised positive control, while calcium hydroxide, white MTA, grey MTA and Biodentine® were analysed as known therapeutic pulp capping agents. Solutions of EDTA and calcium hydroxide were produced as reported previously (Smith and Leaver, 1979, Graham et al., 2006). The methodology for generating the MTA solutions was based on these previous studies, but was modified to allow for the fact that these materials undergo a complex setting reaction and have multiple constituents. The manufacturer's data indicated that calcium oxide represented 65% (w/w) of anhydrous MTA and was predicted to react with water to form calcium hydroxide. Based on this, it was determined that, to achieve a final solution containing 0.02 M calcium hydroxide (maximum saturation), 1.72 g of MTA in 1 litre of water was required. To enable comparison with the *in vivo* setting situation, unreacted powdered MTA was solubilised under physiological conditions, i.e. 37 °C for 72 hours, resulting in hydrolysis of the set and setting constituents of MTA. This approach replicates the clinical scenario, in that, the material interfaces with biological tissues, in a setting and set state, under conditions where

local tissue fluids are constantly replenished. A Biodentine® solution could not be produced in exactly the same way because the liquid component of the unreacted material has active ingredients that contribute to its setting reaction. However, given that a precedent had been established here in terms of generating a solution from MTA, the solution of Biodentine® was generated in a similar way by mixing 1.72 g of powdered set material with 1 litre of distilled water under constant agitation at 37 °C for 72 hours. This allowed a direct comparison to be made with MTA solutions and their resultant dECM extracts.

Analyses were undertaken using AAS to investigate the concentration of aluminium, calcium, iron, magnesium, potassium and sodium ions in solutions of EDTA, calcium hydroxide, white MTA and grey MTA only (this was prior to Biodentine® being launched onto the world market in 2010). These ions were selected for investigation as they are reported to be constituents of larger compounds (section 1.7.2) in MTA (Tulsa Dentsply, Oklahoma, USA) and therefore, potentially could be solubilised. In agreement with previous studies, the calcium hydroxide solution demonstrated a high level of calcium ions and the EDTA solution had high levels of sodium ions; the latter was due to use of sodium hydroxide to neutralise pH. The solution of grey MTA, produced here, contained similar proportions of calcium ions and potassium ions as has previously been reported (Fridland and Rosado, 2003, Camilleri, 2008). The studies undertaken here did not, however, detect any Fe^{3+} ions which Fridland and Rosado (2003) had shown to be present in very low concentrations. This unanticipated result may be explained by the different techniques used to treat the MTA in order to produce solutions for analysis with AAS. Indeed, the volume of water used to solubilise MTA was much greater in experiments here, which may have resulted in dilution of the Fe^{3+} ions to undetectable levels. To date, molecules leached from Biodentine® have not been reported.

6.2 Release of dECM components by therapeutic pulp capping agents

When used clinically, therapeutic pulp capping agents have an intimate relationship with the surrounding dentine and actively modify the local environment, thus affecting the dentine structure. EDTA has been used *in vitro* as a standard for extracting dECM (Smith and Leaver, 1979, Cassidy et al., 1997, Lesot et al., 1988, Smith et al., 1990, Tziafas et al., 1995, Zhao et al., 2000) and it has been proposed that it should be used as a therapeutic wash in cavity cleansing (Zhao et al., 2000) in order to expose bioactive molecules from the dentin. Notably, however, this clinical application has never been adopted widely. EDTA is a polyamino carboxylic acid; it is a hexadentate ligand made up of four carboxyl groups and two amino groups (Crouch et al., 2003). Each ligand reacts with a calcium ion in the hydroxyapatite crystalline structure of dentine and this potentially results in the demineralisation and release of sequestered dECM components. Calcium hydroxide is a highly alkaline inorganic compound that is sparingly soluble in water. White and grey MTA release calcium hydroxide when they are combined with water (Fridland and Rosado, 2003, Fridland and Rosado, 2005, Camilleri, 2008, Camilleri, 2010, Camilleri et al., 2011) and have a similarly high alkalinity to calcium hydroxide when solubilised. However, the mechanism(s) by which calcium hydroxide and the calcium silicate cements solubilise dECM components is poorly understood. The total yield of dECM components solubilised by each agent used here varied appreciably and the rank order of total yield was as follows: EDTA > white MTA > grey MTA > calcium hydroxide > Biodentine® (Table 3.2.1). This suggests that the disruption of dECM and its subsequent release of soluble components is more “gentle” with therapeutic capping materials compared to EDTA.

Apatite crystals, which constitute the main inorganic component of dentine and other mineralised tissues, are well known to undergo ionic substitutions and participate in the process of ion exchange. Within dentistry, this ion exchange process is a familiar concept with the interaction between fluoride and hydroxyapatite in dental tissues known to prevent dental caries (Clarkson, 1991, Ten Cate, 2012). Ion exchange is also used in numerous industrial processes, for example, water softening where excess calcium and magnesium ions are removed from hard water (Helfferich, 1995, Carter and Gregorich, 2008). The electrolytic make-up of the ionic dissolution products from pulp capping agents, especially calcium silicates, may create an environment in which ion exchange occurs, such that, bioactive matrix bound non-collagenous proteins are released. This is possible because of the existence of a metastable hydrated layer of loosely bound ions on the crystalline surface of mineralised matrix that readily allows ion exchange (Cazalbou et al., 2005). It is proposed that this mechanism may allow a gradual release of dECM components as seen during *in vitro* extractions by pulp capping agents. Further analysis of these interactions and this hypothesis may produce some interesting findings.

6.3 Major constituents of dECM released by therapeutic pulp capping agents

Apart from type I collagen, the organic phase of dECM consists of non-collagenous proteins (NCPs) and proteoglycans. NCPs such as those of the SIBLING family, which are phosphorylated, include dentine sialoprotein (DSP), dentine phosphoprotein (DPP), bone sialoprotein (BSP), dentine matrix protein-1 (DMP-1), osteopontin, and matrix extracellular phosphoglycoprotein (MEPE) (Fisher and Fedarko, 2003); these play an important role in the regulation of dentine regeneration, as do non-phosphorylated small leucine-rich proteoglycans (SLRPs) such as decorin, byglycan fibromodulin, lumican, and osteoadherin

(Embery et al., 2001) (section 1.2.1). Dye binding assays to determine the amount of NCPs and GAGs in dECM preparations released by the pulp capping agents showed that, although the total yield of dECM components extracted by EDTA was the greatest, the total amount of NCPs and GAGs (w/w) in the EDTA extract was similar to those extracted by the pulp capping agents (Table 3.3). These data suggest that the extracts derived by treatment with the therapeutic pulp capping agents have greater concentrations of components that are NCPs or GAGs compared with the control agent, EDTA. The ratio of NCPs to GAGs for each extraction agent, determined as a proportion of recovered dECM preparation, was approximately equal. It is clear that the compositions of dECM preparations, extracted by EDTA and the other therapeutic pulp capping agents, vary; this was demonstrated visually by one dimensional sodium dodecyl sulphate polyacrylamide (1D SDS PAGE) analysis (excluding Biodentine®) and by the amounts of NCPs and GAGs in each extract. Reassuringly, the 1D SDS PAGE analyses showed that EDTA dECM preparations exhibited a similar profile to that of those previously demonstrated by Graham et al (2006). Profiles resolved from extracts produced by the ionic dissolution products of calcium hydroxide, white MTA and grey MTA showed that, a broad range of proteins were extracted which differed from one another. Therefore, the interaction of the different soluble constituents, from these pulp capping agents, with dentine, appears to differentially release different dECM components. As the ionic make-up of each solution was different, this may lend support to the hypothesis that the release of matrix bound proteins occurs due to ionic exchange between inorganic components of dentine and the ionic dissolution products of pulp capping materials. In this case, as dECM is disrupted differently by each solution, the resultant components that are solubilised will vary.

6.4 Growth factors in dECM released by therapeutic pulp capping agents

Many growth factors are reported to be sequestered in dentine during primary dentinogenesis (Cassidy et al., 1997, Roberts-Clark and Smith, 2000, Musson et al., 2010, Graham et al., 2006, Finkelman et al., 1990) and the principle of their release and induction of cell signalling in tertiary dentinogenesis is well established (Tziafas et al., 2000, Smith and Lesot, 2001, Smith, 2002). Although many growth factors have previously been identified in dentine, including angiogenic growth factors (Roberts-Clark and Smith, 2000), insulin-like growth factors (Finkelman et al., 1990), transforming growth factor-β1 and -2 (Cassidy et al., 1997) and bone morphogenetic proteins (Bessho et al., 1991), there are likely to be many more growth factors which play a vital role in the cell signalling processes which occur during the repair of the dentine-pulp complex.

Protein array technology is increasingly being used on a high-throughput level to screen for proteins, especially those with a limited sample size. The initial semi-quantitative technique used here is well established (Kocaoemer et al., 2007, Dumortier et al., 2008, Ye et al., 2008, Duncan et al., 2009). Analysis revealed that a large number of different growth factors are sequestered within the dECM and can be differentially released by the ionic dissolution products of pulp capping agents. Some of the growth factors identified using this array analysis approach are already known to play an important role in dentine-pulp complex repair, however, several others which were identified here have not previously been reported to be found within the dECM. Notably, many of these growth factors, 'novel' in dentine, are known to play a significant role in the repair and regulation of other tissues. The presence and the concentration of specific growth factors in dECM preparations was confirmed using quantitative sandwich ELISA techniques in both an individual and a novel

multiplex analytical approach (Willingham et al., 2009, El Karim et al., 2009). Transforming growth factor-β1 (TGF-β1), which has been intensively investigated for its role in tooth development (Begue-Kirn et al., 1992, Thyagarajan et al., 2001, Tjaderhane et al., 1998) and repair of the dentine-pulp complex (Dobie et al., 2002, Sloan et al., 2002, Sloan and Smith, 1999), was investigated using all three techniques of protein characterisation and used as a control. Results from these different techniques demonstrated good consistency in levels for the growth factors analysed. Indeed, the rank order of concentration / intensity of TGF-β1 followed the same pattern across all techniques applied: EDTA dECM preparation had the highest concentration / intensity followed by white MTA, grey MTA and calcium hydroxide. In addition, the signal intensity was beyond the detectable scale for the multiplex ELISA, indicating that the TGF- β1 concentration was too great in the samples tested to allow precise concentrations to be determined. This would corroborate data obtained from individual ELISAs where the concentration of TGF-β1 in the EDTA sample was nearly twice as high as that detected in the white MTA extracted samples. In some cases, however, although signal intensity was very low and according to the manufacturer's guidelines the cytokine was regarded as being present, this was not confirmed using multiplex ELISA for NT-3, NT-4, G-CSF and IGF-1 SR and therefore, further analysis would be required to confirm the presence or absence of these cytokines.

Several novel growth factors, which had not previously been reported to exist in human dentine, were shown to be sequestered in this tissue using the approaches applied here. Adrenomedullin (ADM) is a multipotent peptide that is known to play a key role in mammalian development (Ando and Fujita, 2003, Garayoa et al., 2002) and in regulating osteoblast activity and bone growth (Cornish et al., 1997, Naot et al., 2001, Uzan et al., 2008). Previously, it has been shown to be significantly up-regulated during carious disease

(McLachlan et al., 2005, Cooper et al., 2011) and can induce mineralisation processes in pulp-like cells (Musson et al., 2010). Its release by calcium hydroxide, white MTA and grey MTA during pulp capping procedures, as shown here, may also enhance repair of the dentine-pulp complex through its abilities to kill bacteria (Allaker et al., 1999), modulate inflammation (Elsasser and Kahl, 2002) and promote angiogenesis (Ribatti et al., 2007).

The colony stimulating factors (CSFs) are an interesting group of growth factors not previously identified in human dentine. Analysis of CSF family members using the cytokine array suggested that granulocyte colony stimulating factor (G-CSF), macrophage colony stimulating factor (M-CSF) and granulocyte macrophage colony stimulating factor (GM-CSF) were released from the dECM by all agents. This data was not entirely corroborated by the multiplex ELISA studies as G-CSF was not detected, however, it was clear that M-CSF and GM-CSF were present and were released from dECM by pulp capping agents. The CSF group of glycoproteins stimulate the proliferation, differentiation, and survival of haematopoietic cells and also activate mature myeloid cell functions (Hamilton, 2008). Recently, it has been shown that M-CSF induces resident tissue macrophages to differentiate and proliferate in the dental pulp rather than a source of such cells being derived from circulating precursors (Iwasaki et al., 2011). Secretion of GM-CSF and osteopontin, at the pulp-dentine interface, by immunocompetent cells, such as macrophages and dendritic cells, locally induces maturation of dendritic cells, thus encouraging increased activity of odontoblasts and their differentiation from pulpal progenitors (Saito et al., 2011). In addition, G-CSF strongly enhances the production of neutrophils (Bensinger et al., 1993) and their mobilisation from bone marrow during inflammation (Lieschke et al., 1994, Saada et al., 1996). In methotrexate-induced neutropenic rats that underwent pulp exposure, G-CSF was shown to prevent a decrease of

neutrophils at the wound site compared with normal rats and this enabled the immune system to defend against bacterial invasion and reduce necrosis of the pulp (Yamasaki et al., 2008). G-CSF has been shown to be produced by dental pulp fibroblasts and its production is enhanced by inflammatory cytokines, such as tumour necrosis factor-α (TNF-α) (Sawa et al., 2003). Also in this study, it was suggested that pulp fibroblasts, induced by TNF-α, had the ability to produce M-CSF and GM-CSF and that these CSFs contribute to the recruitment of leukocytes and immunological surveillance processes as part of the pulp defence system. Inflammatory cytokines have been shown to be present in dECM components released by lactic acid and calcium hydroxide (Cooper et al., 2010) and there is emerging evidence indicating that low level immune / inflammatory processes, induced by dental injury, may contribute to the regenerative mechanisms leading to pulpal repair (Cooper et al., 2010) (section 1.6.2). The discovery of CSFs in soluble dECM components and their release by pulp capping agents may suggest that they also play a role in the immunomodulating events involved in the wound healing of the pulp.

Insulin-like growth factors (IGFs) are polypeptides which have a sequence similar to that of insulin. They operate within a system often referred to as the IGF-axis, which consists of two cell-surface receptors (IGF-IR and IGF-IIR), two ligands (IGF-I and IGF-II) and a family of six IGF binding proteins (IGFBP 1-6). The IGF-axis reportedly plays an important role in cell growth, differentiation and apoptosis in many different tissues (Jones and Clemmons, 1995). In addition, these molecules have long been of interest in the study of the tooth. Indeed IGF-I has been shown to have autocrine and paracrine effects, both on ameloblasts and odontoblasts, during tooth development (Joseph et al., 1996, Gotz et al., 2006) and can enhance reparative dentinogenesis when applied to injured pulps in rats (Lovschall et al., 2001) and rabbits (Haddad et al., 2003). Both IGF-I and IGF-II have

previously been shown to be present within the dECM (Finkelman et al., 1990), which is consistent with the work presented here. Interestingly, however, IGFBPs have not previously been reported as being sequestered within dentine. Notably IGFBP-1 was found to be released at very high concentrations by all extraction agents, especially EDTA. While IGFBP-2, -3, -4 and -6 were detected by the growth factor array analyses, they were present at a much lower intensity; their presence and their precise concentrations were not, however, confirmed further with ELISA analysis. Interestingly, the activities of IGFs are modulated by the expression of IGFSRs and the binding to IGFBPs, which can act to reduce the activity of IGFs or prolong their half-life (Jones and Clemmons, 1995).

Angiogenesis is a key process in wound repair (Gurtner et al., 2008) and it is vital to ensure sustained development of the tissue by providing a constant supply of nutrients, immunocompetent cells and growth factors to the site of healing. Vascular endothelial growth factor (VEGF) and fibroblast growth factor-2 (FGF-2) are considered to be two of the most important pro-angiogenic growth factors (Werner and Grose, 2003) necessary for wound repair. Indeed, their expression by pulp fibroblasts and odontoblasts is reportedly also likely to be key to angiogenic processes in the repair of the pulp (Tran-Hung et al., 2006). While these growth factors have been shown to have a short half-life (Eppler et al., 2002), these and other pro-angiogenic growth factors [Platelet derived growth factor-AB (PDGF-AB) and placental growth factor (PlGF)], have previously been shown to be sequestered in dentine (Roberts-Clark and Smith, 2000). It has been demonstrated, through *in vitro* analyses, that released dECM components have powerful angiogenic activity which is likely to enhance capillary microvessel formation during repair of the dental pulp (Zhang et al., 2011). More recently, VEGF has been shown to induce differentiation of stem cells from human exfoliated deciduous teeth (SHED) cells into endothelial cells via MEK1/ERK

signalling (Bento et al., 2013). Analysis of growth factors, in this study, supports previous work performed by Roberts-Clark and Smith (2003) and suggests that additional isoforms of PDGF such as PDGF-AA and -BB may be present in dECM. VEGF was detected in all preparations of dECM extracts and interestingly, significantly more was extracted by white and grey MTA than with the other extraction agents.

Innervation of the dental pulp through the neuronal complex, known as the plexus of Raschkow, contributes to the survival and function of the tooth in many ways. Neuronal complexes emit both autocrine and paracrine signals, in the form of neuropeptides, which can be released in response to bacterial components (Brogden et al., 2005, Haug and Heyeraas, 2006) in a process known as neurogenic inflammation. Neuropeptide Y (NPY) is known to have increased expression in pulp inflammation (El Karim et al., 2006, Awawdeh et al., 2002) and more recently, the inflammatory mediators, interleukin-1β and TGF-β1 have been shown to increase the expression of NPY in human primary pulp fibroblasts, suggesting that fibroblasts play a neuro-immunomodulatory role during pulp injury (Killough et al., 2010). Neuropeptides have also been shown to regulate the expression of angiogenic growth factors in human dental fibroblasts, further demonstrating the interaction of these neuronal secreted molecules with other biological systems (El Karim et al., 2009). Neuropeptides and neurotrophic factors are also expressed by odontoblasts, which developmentally originate from cranial neural crest cells; these neuropeptides and neurotrophic factors are thought to contribute to the odontoblast's role in homeostasis and repair of the dentine-pulp complex (Byers et al., 1990, Magloire et al., 2001, Nosrat et al., 1998). Three families of growth factors exist which have significant neurotrophic effects: neurotrophins, glial cell derived neurotrophic factor (GDNF) and neuropoietic cytokines (Boyd and Gordon, 2003). The neurotrophin family consists of four members, which

include nerve growth factor (NGF), brain derived neurotrophic growth factor (BDNF), neurotrophin 3 (NT-3) and neurotrophin 4 (NT-4); these are all expressed with specific temporospatial patterns during rodent tooth development (Nosrat et al., 1998). NGF and BDNF mRNAs were detected in the developing dental papilla, however, NT-3 and NT-4 transcription was predominantly epithelial in origin. This expression was strongest during early developmental stages when the teeth were not yet innervated. NGF, NT-3 and NT-4 were shown to be present in all dECM extracts when analysis was performed using the cytokine array, however, when levels were evaluated using multiplex ELISA, only NGF, at low concentrations, was detected as being present in extracts solubilised by EDTA, white MTA and grey MTA. Notably, NGF has previously been shown to induce mineralisation and increase expression of DSPP and DMP-1 *in vitro* in odontoblast lineage cells (Arany et al., 2009) and TGF-β1 is known to increase expression and secretion of NGF in a dose-dependent manner in human pulp cells (Srisawasdi and Pavasant, 2007). These latter data suggest that, in the event of pulpal injury, the abundance of TGF-β1 may induce increased secretion of NGF (Yongchaitrakul and Pavasant, 2007). The GDNF family consists of four members, of which, GDNF was the first to be characterised; this molecule has previously been shown to promote differentiation and homeostasis of neurons, together with three other trophic factors, namely, neurturin (NTN), persephin (PSP), and artemin (ART) (Airaksinen and Saarma, 2002). Analysis of GDNF knockout mice has shown that ameloblast and odontoblast differentiation is disrupted, suggesting that GDNF is important in tooth cytodifferentiation (de Vicente et al., 2002). Recently, our research group has demonstrated *in vitro* that GDNF may have multi-functionality within the dentine-pulp complex, acting as both a survival factor and mitogen during tooth injury and repair (Gale et al., 2011). In experiments presented here, GDNF was shown to be extracted from dECM by EDTA and all therapeutic pulp capping agents. Following the application of a

therapeutic pulp capping agent to a pulp wound, the solubilisation of NGF, GDNF and potentially neurotrophins, NT-3 and NT-4, may contribute to pulp healing either directly by their effect on pulp cells or indirectly, in terms of mediating immune and inflammatory responses, as previously discussed.

The molecular processes involved in recruitment of progenitor cells which contribute to reparative dentinogenesis, remain poorly understood (Sloan and Smith, 2007, Sloan and Waddington, 2009, Smith and Lesot, 2001). Recently, it has, however, been proposed that non-resident progenitor cells that are haematopoietic or pericyte in origin, are the source of some of the undifferentiated cells in reparative dentinogenesis (Frozoni et al., 2012, Feng et al., 2011). While these are relatively new data, questions have arisen as to how these cells are mobilised and / or recruited. Interestingly, in our study, stem cell factor (SCF) was found to be present in all dECM preparations, at low intensity, when analysed by the cytokine array. Indeed, SCF was detected in grey MTA extracts when analysed using multiplex ELISA. While the mechanisms of controlling the redistribution of haematopoietic stem cells and progenitor cells, between the bone marrow and blood, *in vivo* are not fully understood, early work showed that injection of mice with SCF results in a profound redistribution of primitive haematopoietic cells from the bone marrow into the blood and spleen (Fleming et al., 1993, Yan et al., 1994). Enhancing the release of haematopoietic stem cells has been used as an adjunctive therapy in patients undergoing chemotherapy and / or radiotherapy. SCF is used individually, or in combination, to mobilise haematopoietic stem cells for collection during the process of autologous haematopoietic stem cell transplantation (AHSCT), a technique used to enhance the recovery of immune function following high dose chemotherapy and / or radiotherapy. Used in combination with G-CSF, SCF has been shown to be effective during this process (Herbert et al., 2009, Herbert et al.,

2010). Theoretically, it may therefore be possible that SCF and other factors, released from the dECM by caries and by therapeutic pulp capping agents, initiate the mobilisation and homing of circulating stem cells or pericytes which differentiate and contribute to pulpal repair.

These analyses have identified a number of new growth factor families in dentine, which was already recognised to be a rich reservoir of potent signalling molecules. The ionic dissolution products of inorganic materials have been shown to have direct effects *in vitro* on the homeostasis and repair of human tissues (Hoppe et al., 2011). Rather than these positive biological effects being as a result of direct contact by the ionic solution themselves, it may be more plausible that, these effects are due to the potent growth factors, released locally by the dissolution products. The processes involved in wound repair are numerous and complex and the relatively "gentle" differential release of growth factors and cytokines by therapeutic pulp capping agents, as demonstrated here, may explain how these biological events are initiated and orchestrated.

6.5 Biological effects of dECM components released by therapeutic pulp capping agents

Following tissue injury, once haemostasis has been achieved and an immune response has been initiated, the wound will begin to stabilise to enable the reparative phases of healing to begin (Gurtner et al., 2008, Velnar et al., 2009). Specific cues and signals are required to recruit progenitor cells to the site of injury to undertake the further processes of proliferation and differentiation involved in wound repair. Various growth factors and proteins from different sources, including cementum and bone (Ogata et al., 1997) are thought to play a role in this overall process, however, as yet these have not been

thoroughly characterised. Growth factors known to be present in dECM, including TGF-β1 (Kwon et al., 2010), fibroblast growth factor (FGF) and epidermal growth factor (EGF) (Howard et al., 2010), have also been shown to be effective at inducing pulp cell migration. Interestingly, Howard et al. (2010) reported that the structural ECM proteins, laminin, fibronectin and collagen type-1, also have the ability to act as chemoattractants to dental pulp cells. Other growth factors, such as fibroblast growth factor (FGF), vascular endothelial growth factor (VEGF) and platelet derived growth factor (PDGF), used alone or in combination with nerve growth factor (NGF) and bone morphogenetic protein-7 (BMP-7), were shown to be effective in cell homing to initiate re-cellularisation and re-vascularisation of the pulp chamber in an *in vivo* ectopic implantation model (Kim et al., 2010). Recent work by our research group (Smith et al., 2012c) has shown that dentine chips, pulp ECM and dECM preparations are effective at inducing pulp cell chemoattraction and migration. Notably, when these preparations were degraded by enzymatic or acidic digestion to mimic the carious process, these effects were enhanced.

In the experiments presented here, using a transwell plate assay, all preparations of dECM components induced migration of RDPCs to the homing agent. EDTA solubilised dECM components were previously used by Smith et al. (2012) and similar results were also obtained here. For all extracts assessed (EDTA, calcium hydroxide, white MTA and grey MTA), migration of RDPCs was significantly greater than control. When data for each preparation were combined across all concentrations and the data for the negative control were subtracted (negative control is assumed to be passive movement across the membrane of the transwell plate), grey MTA extracted dECM components induced over twice as much migration of RDPCs, compared with EDTA, and could be considered the most powerful chemotactic agent of those tested. White MTA, calcium hydroxide and EDTA extracted

dECM components would be ranked, second, third and fourth respectively. Although all dECM preparations tested here demonstrated that they were effective at inducing chemotaxis of pulp cells *in vitro,* some appeared more potent than others. As chemotaxis is known to be one of the key processes in wound healing, the potency of the chemotactic effects of dECM components released by pulp capping agents as shown here, may explain at least in part why MTA induces more pulp healing than calcium hydroxide.

Several different growth factors have been shown to increase proliferation of dental pulp cells. In an *ex vivo* culture model, TGF-β1 induced increases in cell numbers in the odontoblastic and subodontoblastic layers adjacent to delivery of the growth factor (Melin et al., 2000). Exposure of human dental pulp cells (DPCs) to VEGF *in vitro* increased proliferation without inducing differentiation towards an endothelial lineage (D' Alimonte et al., 2011) and specific dosages of FGF-2 in *ex vivo* cultures induced cell numbers to increase within the pulp tissue (Ishimatsu et al., 2009, Kikuchi et al., 2007, Kitamura et al., 2012). In studies presented here using *in vitro* monolayer cultures, data demonstrated that a homogeneous population of an immortalised cell line of odontoblast-like cells (MDPC-23) and a heterogeneous population of primary RDPCs, when exposed to different concentrations of dECM components containing a rich cocktail of growth factors, responded similarly. Low to moderate concentrations of dECM components stimulated cell proliferation in a dose-dependent manner, while the highest concentrations decreased cell numbers. These data are also consistent with previous reports (Graham et al., 2006, Musson et al., 2010, Zhang et al., 2011). As has been demonstrated, the solubilised dECM components used here contain numerous biologically active constituents and therefore, the cellular responses studied here cannot be attributed to any single protein. Notably, however,

it has been shown that TGF-β1, a known constituent of liberated dECM components, can alone induce apoptosis in pulp cells at higher concentrations (He et al., 2004).

It has now been demonstrated that dECM components, liberated by the soluble products of therapeutic pulp capping agents, induce migration and proliferation in dental pulp cells, two key processes in reparative dentinogenesis. The interaction of therapeutic pulp capping agents with adjacent dentine has already been suggested for calcium hydroxide (Graham et al., 2006). These functional experiments suggest that the solubilisation of bioactive molecules from dECM by white MTA and grey MTA may promote events involved in reparative dentinogenesis.

6.6 Potential role of hepatocyte growth factor in reparative dentinogenesis

Hepatocyte growth factor (HGF) is considered a multifunctional growth factor and cytokine which is involved in a variety of physiological and pathological processes (Trusolino et al., 2010). The role of HGF / c-Met signalling has been researched intensively in oncogenesis and tumor progression leading to the development of drugs which prevent intracellular signalling along this pathway (Cecchi et al., 2012). The regulation of its expression in oral fibroblasts suggests it may influence local progression of oral squamous carcinoma cells invading underlying stroma (Daly et al., 2008). In terms of tissue healing, an *in vitro* model of wound contraction demonstrated increased levels of HGF in oral fibroblasts compared to skin fibroblasts, suggesting that HGF contributed to accelerated re-epithelialisation of oral wounds compared to skin wounds (Shannon et al., 2006). As discussed in section 1.2.2, expression of HGF and c-Met has been implicated as a potential signalling pathway in tooth development (Sonnenberg et al., 1993, Kajihara et al., 1999). More recently, primary

murine dental papilla cells, exposed to recombinant HGF, demonstrated enhanced proliferation and differentiation, with increased expression of the Pax-9 and Msx-1 genes, which are central to tooth development (Li et al., 2009).

6.6.1 Presence of HGF and its receptor c-Met in dental tissues

The potential for matrix-bound HGF to be released during clinical treatment is highlighted by its solubilisation by EDTA, white MTA and grey MTA. EDTA was a significantly more effective extractant of HGF than the MTA varieties; this was likely to be due to its powerful demineralising and solubilising actions on the dental hard tissues. This pattern of HGF release is consistent with a number of other growth factors analysed here. Interestingly, calcium hydroxide and Biodentine® did not solubilise detectable levels of HGF from dentine; such differences, in terms of bioactive molecules released from dentine, may contribute to differences in biological actions of these materials when applied *in vivo*. The expression of the receptor of HGF and c-Met in isolated rat pulp, as well as in cells of primary cultures derived therefrom, was demonstrated here. This informed the use of primary RDPC cultures in experiments to assess the effects of HGF as this provides a valuable *in vitro* model for analysis of regenerative events in the dentine-pulp complex (Patel et al., 2009). The expression of HGF and c-Met was also confirmed in human pulp tissue to ensure that any conclusions drawn from the *in vitro* analyses were potentially translatable to pulp repair in humans.

6.6.2 Functional effects of HGF in RDPC cultures

The functional responses of RDPCs to HGF, namely chemotactic activity and mineralisation, were clearly demonstrated using the transwell plate assay and alizarin red staining. These results were consistent with a previous report showing HGF to be a mineralisation-inducing agent in human vascular smooth muscle cells (Liu et al., 2007). Notably, HGF was observed to be a powerful chemoattractant in a transwell plate assay over a range of concentrations (5-20 ng/mL). These data may also help to further clarify which active component(s) are responsible for the stimulatory effects of dECM on pulp cell recruitment that have recently been reported (Smith et al., 2012c). Indeed, given that its presence in dentine has been demonstrated and that it is known to be released by control and therapeutic agents, HGF could be a key contributor to the cell recruitment process during dental wound healing. Exploitation of chemotaxis and cell homing processes to develop novel treatment modalities, by which to harness the natural reparative mechanism of the pulp, or engineer pulp tissue, shows exciting potential (Laird et al., 2008, Mao et al., 2010). Recently, successful engineering of dental pulp tissue, using chemotaxis-induced cell homing, has been reported (Kim et al., 2010). In this published study, the role of several cytokines were analysed including FGF, VEGF and PDGF alone or in combination with NGF and BMP-7. While the optimum combination of cytokines remains to be determined, these data clearly indicated that synergistic signalling interactions may be important during the wound repair process. Based on data presented in this thesis, it would appear that HGF may also be a good candidate for further investigation in regeneration and tissue engineering treatment modalities which require cell homing to be induced.

HGF / c-Met signalling has previously been shown to be associated with mineralised tissue formation under pathological conditions (Liu et al., 2007, McKinnon et al., 2006), highlighting the potential for its involvement in mineralised cell differentiation and activation. In this study, we have shown that gene expression changes in RDPCs exposed to HGF are indicative of differentiation of these cells towards dentinogenic and osteogenic lineages. Runx2 and osterix are core osteogenic transcription factors, which regulate expression of numerous mineralisation–associated transcripts including osteocalcin and osteopontin (Ducy et al., 1996, Karsenty, 2000). Notably, runx2, osterix, osteocalcin and osteopontin were all up-regulated in RDPCs following exposure to HGF. While DMP-1 is relatively more abundant in dentine (George et al., 1993), it is also present in bone (D'Souza et al., 1997) and Runx2 is involved in the regulation of DMP-1 during both osteogenic and dentinogenic events. Thus far, however, the regulatory mechanisms involved have been suggested to be different for each cell or tissue type (Fen et al., 2002). Expression of DMP-1 on days 7 and 12 was significantly higher in RDPCs for both concentrations of HGF applied. These data suggest that HGF, via c-Met binding, activates intracellular signalling pathways leading to increased levels of transcriptional signalling for regulation of a mineralising cell phenotype.

To further characterise the effect of HGF on repair-associated responses within the dentine-pulp complex, it was demonstrated that both application of recombinant HGF and induced over-expression of HGF using an adenoviral vector system promoted *in vitro* mineralisation in RDPCs. After 8 days culture, there was significantly greater *in vitro* mineralisation detected independent of the HGF delivery approach. These data concur with those reported by Li et al. (2009), which showed an increase in levels of the marker of mineralisation, alkaline phosphatase, in a developmental pulp cell population exposed to HGF. However, a

significantly longer period of culture of 28 days and a single concentration of 10 ng/mL of recombinant HGF was required to demonstrate this effect. The same group have also indicated that HGF may enhance proliferation and differentiation of primary human pulp cells in culture, potentially via the ERK / MAPK signalling pathway (Ye et al., 2006). The range of exposure conditions and *in vitro* mineralisation assays that were applied in the present study have not previously been documented nor has the potential tissue location of HGF.

While HGF / c-Met signalling is known to play an important role in the repair of many tissues, the identification of HGF sequestration within dentine and the demonstration of its functional role in pulp cell chemotaxis, differentiation and mineralisation, emphasises its potentially important role in signalling repair in the dentine-pulp complex. The release of HGF from the dECM by carious demineralisation or therapeutic pulp capping agents may therefore play an important role in repair-associated events *in vivo*.

6.7 Future work

The work presented here offers a detailed analysis of growth factors found within dECM and suggests an explanation for the well-recognised healing capacity of calcium silicate cements when they are used clinically as pulp capping agents. These studies also provide an opportunity and a sound basis for further investigation along many avenues of research, which should add to our understanding of dentine-pulp repair.

The hypothesis and suggestion that the interaction of calcium silicate cements with surrounding tissue fluids creates an ionic environment that will initiate biological

mechanisms of pulp repair requires further investigation. A broader more detailed analysis of the release of ions from the hydrated layer of calcium silicate cements is necessary to precisely determine the nature of the components released into the surrounding tissue fluid. Although there is only limited knowledge of how growth factors and other bioactive molecules are bound to dECM, the mechanisms by which calcium silicate cements interact with dentine and release these molecules would deepen our understanding. This work has focused on the interaction of these materials with the mineralised component of the dentine-pulp complex, however, it has recently been demonstrated that the ECM of the pulp also contains a plethora of bioactive components that participate in events leading to pulp repair (Smith et al., 2012). In order to provide a more comprehensive picture of how calcium silicate cements interact with the dentine-pulp complex and harness its natural regenerative potential, it would be appropriate to investigate the ability of these materials to release pulp ECM components and then to determine their subsequent cellular and molecular effects.

The work here has identified numerous growth factors, with previously uncharacterised roles in dentine-pulp biology, that are sequestered in dentine. Notably, many have been shown to have potent biological effects in other tissues. Indeed, detailed analysis of the effects of HGF on primary pulp cells *in vitro* has now demonstrated that HGF may play an important role in the wound repair processes of the dentine-pulp complex. Further analysis of these previously uncharacterised growth factors and analysis of their synergistic effects with other molecules should identify exciting opportunities for the development of new biomimetic treatments and pulp tissue engineering strategies for repair of the injured dentine-pulp complex.

7.0 CONCLUSION

With reduced rates of edentulism and people now retaining their teeth for longer (Steele et al., 2012), there is a real need to develop novel biologically based treatment modalities which can protect the pulp, enhance its natural regenerative capacity and enable engineering of new tissue if it becomes irreversibly damaged. This can best be achieved by developing a thorough understanding of the underlying biological repair processes which naturally occur within the dentine-pulp complex. This work aimed to analyse the interaction between what is currently considered to be the most successful pulp capping agent, MTA, and the dentine-pulp complex, in order to understand how a favourable biological response can be induced.

It was shown that grey MTA and white MTA leached multiple different cations from their setting and set phases *in vitro;* these solutions, together with one produced by calcium silicate cement, Biodentine®, were able to solubilise dECM components. This has never previously been reported. When these materials are used as pulp capping agents, they will inevitably interact with dentine at the periphery of the pulp wound and with dentine chips (Seltzer and Bender, 1990) that remain on the open pulp surface and in the surrounding area. Based on the data presented here, it is possible to postulate that tissue fluid originating from the dentinal tubules and the soft tissue of the pulp, hydrates the surface layer of the calcium silicate cement releasing ionic dissolution products. These will interact with the mineral phase of local dentine by ion exchange and liberate sequestered growth factors and bioactive molecules present within it. In turn, these will initiate the events leading to reparative dentine formation.

Each pulp capping agent tested demonstrated liberation of different proportions of NCPs and GAGs in the dECM components obtained. Although dentine is known to be a rich source of bioactive molecules, our growth factor analysis demonstrated the presence of a number of signalling molecules not previously reported, including SCF, M-CSF, GM-CSF, IGFBP-1, GDNF, NGF and HGF. Data from other tissues demonstrate that these molecules mediate biological processes required for tissue repair and homeostasis. The repair processes in a complex tissue, such as the dentine-pulp, are finely balanced between managing the infection, the inflammatory response and the direct tissue healing processes. The subtle release of several of the growth factors, now known to be sequestered in dentine, by the pulp capping agents tested, may orchestrate this complex process.

The dECM components released by therapeutic pulp capping agents (calcium hydroxide, white MTA and grey MTA) were shown to be biologically active and to play a direct role in stimulating chemotaxis and proliferation in pulp cells. Both of these processes are key to the repair and regeneration of the dental pulp. Higher concentrations of dECM components appeared to prevent the proliferation or have a deleterious effect on pulp cells, suggesting that the subtle release of these bioactive components may be more beneficial, which may explain why these agents are successful in pulp capping.

During this work, a more in-depth analysis of HGF was undertaken as this growth factor was shown to be released only by white MTA and grey MTA, which are considered to be the most predictable in terms of pulpal reparative responses when used clinically. HGF was shown to be a chemotactic agent, capable of inducing differentiation of pulp cells along a mineralising lineage, as well as promoting *in vitro* mineralisation processes in dental pulp cell cultures. Both HGF and its receptor c-Met were also detected as being expressed in

human pulp cells. These findings indicate the potential role of HGF in mediating pulpal reparative responses when released during carious demineralisation or following application of pulp capping agents in the clinical situation.

The research presented here suggests a plausible explanation of why MTA and a new generation of calcium silicate cements, based on MTA, induce favourable healing responses of the dental pulp. This knowledge will provide a sound basis for future work investigating molecular processes of pulp repair. It is hoped that such studies will lead to the development of new materials and treatment modalities in the future, thus improving the predictability of treatment outcomes.

REFERENCES

ACCORINTE MDE, L., HOLLAND, R., REIS, A., BORTOLUZZI, M. C., MURATA, S. S., DEZAN, E., JR., SOUZA, V. & ALESSANDRO, L. D. 2008. Evaluation of mineral trioxide aggregate and calcium hydroxide cement as pulp-capping agents in human teeth. *J Endod,* 34**,** 1-6.

ACKERMANS, F., KLEIN, J. P. & FRANK, R. M. 1981. Ultrastructural localization of immunoglobulins in carious human dentine. *Arch Oral Biol,* 26**,** 879-86.

AEINEHCHI, M., ESLAMI, B., GHANBARIHA, M. & SAFFAR, A. S. 2003. Mineral trioxide aggregate (MTA) and calcium hydroxide as pulp-capping agents in human teeth: a preliminary report. *Int Endod J,* 36**,** 225-31.

AIRAKSINEN, M. S. & SAARMA, M. 2002. The GDNF family: signalling, biological functions and therapeutic value. *Nat Rev Neurosci,* 3**,** 383-94.

AL-HEZAIMI, K., AL-SHALAN, T. A., NAGHSHBANDI, J., OGLESBY, S., SIMON, J. H. & ROTSTEIN, I. 2006. Antibacterial effect of two mineral trioxide aggregate (MTA) preparations against Enterococcus faecalis and Streptococcus sanguis in vitro. *J Endod,* 32**,** 1053-6.

ALLAKER, R. P., ZIHNI, C. & KAPAS, S. 1999. An investigation into the antimicrobial effects of adrenomedullin on members of the skin, oral, respiratory tract and gut microflora. *FEMS Immunol Med Microbiol,* 23**,** 289-93.

ANDERSON, D. J., HANNAM, A. G. & MATHEWS, B. 1970. Sensory mechanisms in mammalian teeth and their supporting structures. *Physiol Rev,* 50**,** 171-95.

ANDERSON, J. M. 2001. Biological Responses to Materials. *Annual Reviews in Materials Research,* 31**,** 81-110.

ANDO, K. & FUJITA, T. 2003. Lessons from the adrenomedullin knockout mouse. *Regul Pept,* 112**,** 185-8.

ARAI, T., BUSBY, W., JR. & CLEMMONS, D. R. 1996. Binding of insulin-like growth factor (IGF) I or II to IGF-binding protein-2 enables it to bind to heparin and extracellular matrix. *Endocrinology,* 137**,** 4571-5.

ARANY, S., KOYOTA, S. & SUGIYAMA, T. 2009. Nerve growth factor promotes differentiation of odontoblast-like cells. *J Cell Biochem,* 106**,** 539-45.

ASGARY, S., EGHBAL, M. J., PARIROKH, M., GHANAVATI, F. & RAHIMI, H. 2008. A comparative study of histologic response to different pulp capping materials and a novel endodontic cement. *Oral Surg Oral Med Oral Pathol Oral Radiol Endod,* 106**,** 609-14.

ASGARY, S., EGHBAL, M. J., PARIROKH, M., GHODDUSI, J., KHEIRIEH, S. & BRINK, F. 2009. Comparison of mineral trioxide aggregate's composition with Portland cements and a new endodontic cement. *J Endod,* 35**,** 243-50.

ASPDIN, J. 1824. *Producing an artificial stone*. UK patent application.

AUGELLO, A., KURTH, T. B. & DE BARI, C. 2010. Mesenchymal stem cells: a perspective from in vitro cultures to in vivo migration and niches. *Eur Cell Mater,* 20**,** 121-33.

AWAWDEH, L., LUNDY, F. T., SHAW, C., LAMEY, P. J., LINDEN, G. J. & KENNEDY, J. G. 2002. Quantitative analysis of substance P, neurokinin A and calcitonin gene-related peptide in pulp tissue from painful and healthy human teeth. *Int Endod J,* 35**,** 30-6.

BAKER, S. M., SUGARS, R. V., WENDEL, M., SMITH, A. J., WADDINGTON, R. J., COOPER, P. R. & SLOAN, A. J. 2009. TGF-beta/extracellular matrix interactions in dentin matrix: a role in regulating sequestration and protection of bioactivity. *Calcif Tissue Int,* 85**,** 66-74.

BARTHEL, C. R., ROSENKRANZ, B., LEUENBERG, A. & ROULET, J. F. 2000. Pulp capping of carious exposures: treatment outcome after 5 and 10 years: a retrospective study. *J Endod,* 26**,** 525-8.

BAUM, C. L. & ARPEY, C. J. 2005. Normal cutaneous wound healing: clinical correlation with cellular and molecular events. *Dermatol Surg,* 31**,** 674-86; discussion 686.

BAUME, L. J. 1980. The biology of pulp and dentine. A historic, terminologic-taxonomic, histologic-biochemical, embryonic and clinical survey. *Monogr Oral Sci,* 8**,** 1-220.

BAUME, L. J. & HOLZ, J. 1981. Long term clinical assessment of direct pulp capping. *Int Dent J,* 31**,** 251-60.

BEGUE-KIRN, C., SMITH, A. J., LORIOT, M., KUPFERLE, C., RUCH, J. V. & LESOT, H. 1994. Comparative analysis of TGF beta s, BMPs, IGF1, msxs, fibronectin, osteonectin and bone sialoprotein gene expression during normal and in vitro-induced odontoblast differentiation. *Int J Dev Biol,* 38**,** 405-20.

BEGUE-KIRN, C., SMITH, A. J., RUCH, J. V., WOZNEY, J. M., PURCHIO, A., HARTMANN, D. & LESOT, H. 1992. Effects of dentin proteins, transforming growth factor beta 1 (TGF beta 1) and bone morphogenetic protein 2 (BMP2) on the differentiation of odontoblast in vitro. *Int J Dev Biol,* 36**,** 491-503.

BENIASH, E., SKOBE, Z. & BARTLETT, J. D. 2006. Formation of the dentino-enamel interface in enamelysin (MMP-20)-deficient mouse incisors. *Eur J Oral Sci,* 114 Suppl 1**,** 24-9; discussion 39-41, 379.

BENSINGER, W. I., PRICE, T. H., DALE, D. C., APPELBAUM, F. R., CLIFT, R., LILLEBY, K., WILLIAMS, B., STORB, R., THOMAS, E. D. & BUCKNER, C. D. 1993. The effects of daily recombinant human granulocyte colony-stimulating factor administration on normal granulocyte donors undergoing leukapheresis. *Blood,* 81**,** 1883-8.

BENTO, L. W., ZHANG, Z., IMAI, A., NOR, F., DONG, Z., SHI, S., ARAUJO, F. B. & NOR, J. E. 2013. Endothelial differentiation of SHED requires MEK1/ERK signaling. *J Dent Res,* 92**,** 51-7.

BERGENHOLTZ, G. 1977. Effect of bacterial products on inflammatory reactions in the dental pulp. *Scand J Dent Res,* 85**,** 122-9.

BERGENHOLTZ, G., COX, C. F., LOESCHE, W. J. & SYED, S. A. 1982. Bacterial leakage around dental restorations: its effect on the dental pulp. *J Oral Pathol,* 11**,** 439-50.

BERGMAN, G. 1963. Microscopic demonstration of liquid flow through human dental enamel. *Arch Oral Biol,* 8**,** 233-4.

BESSHO, K., TANAKA, N., MATSUMOTO, J., TAGAWA, T. & MURATA, M. 1991. Human dentin-matrix-derived bone morphogenetic protein. *J Dent Res,* 70**,** 171-5.

BHASKAR, S. N., BEASLEY, J. D., WARD, J. P. & CUTRIGHT, D. E. 1972. Human pulp capping with isobutyl cyanoacrylate. *J Dent Res,* 51**,** 58-61.

BIRCHMEIER, C. & GHERARDI, E. 1998. Developmental roles of HGF/SF and its receptor, the c-Met tyrosine kinase. *Trends Cell Biol,* 8**,** 404-10.

BISHOP, M. A. & YOSHIDA, S. 1992. A permeability barrier to lanthanum and the presence of collagen between odontoblasts in pig molars. *J Anat,* 181 (Pt 1)**,** 29-38.

BLEZARD, R. G. 1998. The history of calcareous cements. *In:* HEWLETT, P. C. (ed.) *Lea's chemistry of cement and concrete.* Elsevier Butterworth Heinemann.

BOSKEY, A. L., DOTY, S. B., KUDRYASHOV, V., MAYER-KUCKUK, P., ROY, R. & BINDERMAN, I. 2008. Modulation of extracellular matrix protein phosphorylation alters mineralization in differentiating chick limb-bud mesenchymal cell micromass cultures. *Bone,* 42**,** 1061-71.

BOSKEY, A. L., MARESCA, M., ULLRICH, W., DOTY, S. B., BUTLER, W. T. & PRINCE, C. W. 1993. Osteopontin-hydroxyapatite interactions in vitro: inhibition of hydroxyapatite formation and growth in a gelatin-gel. *Bone Miner,* 22**,** 147-59.

BOSKEY, A. L., SPEVAK, L., PASCHALIS, E., DOTY, S. B. & MCKEE, M. D. 2002. Osteopontin deficiency increases mineral content and mineral crystallinity in mouse bone. *Calcif Tissue Int,* 71**,** 145-54.

BOTTARO, D. P., RUBIN, J. S., FALETTO, D. L., CHAN, A. M., KMIECIK, T. E., VANDE WOUDE, G. F. & AARONSON, S. A. 1991. Identification of the hepatocyte growth factor receptor as the c-met proto-oncogene product. *Science,* 251**,** 802-4.

BOYD, J. G. & GORDON, T. 2003. Neurotrophic factors and their receptors in axonal regeneration and functional recovery after peripheral nerve injury. *Mol Neurobiol,* 27**,** 277-324.

BOZEMAN, T. B., LEMON, R. R. & ELEAZER, P. D. 2006. Elemental analysis of crystal precipitate from gray and white MTA. *J Endod,* 32**,** 425-8.

BRADFORD, M. M. 1976. A rapid and sensitive method for the quantitation of microgram quantities of protein utilizing the principle of protein-dye binding. *Anal Biochem,* 72**,** 248-54.

BRANNSTROM, M. & LIND, P. O. 1965. Pulpal response to early dental caries. *J Dent Res,* 44**,** 1045-50.

BRANNSTROM, M. & NYBORG, H. 1973. Cavity treatment with a microbicidal fluoride solution: growth of bacteria and effect on the pulp. *J Prosthet Dent,* 30**,** 303-10.

BRANNSTROM, M., NYBORG, H. & STROMBERG, T. 1979. Experiments with pulp capping. *Oral Surg Oral Med Oral Pathol,* 48**,** 347-52.

BRENMOEHL, J., MILLER, S. N., HOFMANN, C., VOGL, D., FALK, W., SCHOLMERICH, J. & ROGLER, G. 2009. Transforming growth factor-beta 1 induces intestinal myofibroblast differentiation and modulates their migration. *World J Gastroenterol,* 15**,** 1431-42.

BROGDEN, K. A., GUTHMILLER, J. M., SALZET, M. & ZASLOFF, M. 2005. The nervous system and innate immunity: the neuropeptide connection. *Nat Immunol,* 6**,** 558-64.

BURKE, F. M. & SAMARAWICKRAMA, D. Y. 1995. Progressive changes in the pulpo-dentinal complex and their clinical consequences. *Gerodontology,* 12**,** 57-66.

BUTLER, W. T. 1998. Dentin matrix proteins. *Eur J Oral Sci,* 106 Suppl 1**,** 204-10.

BYERS, M. R., SCHATTEMAN, G. C. & BOTHWELL, M. 1990. Multiple functions for NGF receptor in developing, aging and injured rat teeth are suggested by epithelial, mesenchymal and neural immunoreactivity. *Development,* 109**,** 461-71.

BYERS, M. R. & SUGAYA, A. 1995. Odontoblast processes in dentin revealed by fluorescent Di-I. *J Histochem Cytochem,* 43**,** 159-68.

CAICEDO, R., ABBOTT, P. V., ALONGI, D. J. & ALARCON, M. Y. 2006. Clinical, radiographic and histological analysis of the effects of mineral trioxide aggregate used in direct pulp capping and pulpotomies of primary teeth. *Aust Dent J,* 51**,** 297-305.

CALLE, A. 1985. Intercellular junctions between human odontoblasts. A freeze-fracture study after demineralization. *Acta Anat (Basel),* 122**,** 138-44.

CAMILLERI, J. 2008. Characterization of hydration products of mineral trioxide aggregate. *Int Endod J,* 41**,** 408-17.

CAMILLERI, J. 2010. Hydration characteristics of calcium silicate cements with alternative radiopacifiers used as root-end filling materials. *J Endod,* 36**,** 502-8.

CAMILLERI, J., CUTAJAR, A. & MALLIA, B. 2011. Hydration characteristics of zirconium oxide replaced Portland cement for use as a root-end filling material. *Dent Mater,* 27**,** 845-54.

CAMILLERI, J., KRALJ, P., VEBER, M. & SINAGRA, E. 2012. Characterization and analyses of acid-extractable and leached trace elements in dental cements. *Int Endod J*.

CAMILLERI, J., MONTESIN, F. E., BRADY, K., SWEENEY, R., CURTIS, R. V. & FORD, T. R. 2005. The constitution of mineral trioxide aggregate. *Dent Mater,* 21**,** 297-303.

CAMILLERI, J., MONTESIN, F. E., PAPAIOANNOU, S., MCDONALD, F. & PITT FORD, T. R. 2004. Biocompatibility of two commercial forms of mineral trioxide aggregate. *Int Endod J,* 37**,** 699-704.

CARON, C., XUE, J. & BARTLETT, J. D. 1998. Expression and localization of membrane type 1 matrix metalloproteinase in tooth tissues. *Matrix Biol,* 17**,** 501-11.

CARTER, M. R. & GREGORICH, E. G. 2008. *Soil Sampling And Methods of Analysis,* USA, CRC Press.

CASSIDY, N., FAHEY, M., PRIME, S. S. & SMITH, A. J. 1997. Comparative analysis of transforming growth factor-beta isoforms 1-3 in human and rabbit dentine matrices. *Arch Oral Biol,* 42**,** 219-23.

CAZALBOU, S., EICHERT, D., RANZ, X., DROUET, C., COMBES, C., HARMAND, M. F. & REY, C. 2005. Ion exchanges in apatites for biomedical application. *J Mater Sci Mater Med,* 16**,** 405-9.

CECCHI, F., RABE, D. C. & BOTTARO, D. P. 2012. Targeting the HGF/Met signaling pathway in cancer therapy. *Expert Opin Ther Targets,* 16**,** 553-72.
CHACKO, V. & KURIKOSE, S. 2006. Human pulpal response to mineral trioxide aggregate (MTA): a histologic study. *J Clin Pediatr Dent,* 30**,** 203-9.
CHAUSSAIN, C., EAPEN, A. S., HUET, E., FLORIS, C., RAVINDRAN, S., HAO, J., MENASHI, S. & GEORGE, A. 2009. MMP2-cleavage of DMP1 generates a bioactive peptide promoting differentiation of dental pulp stem/progenitor cell. *Eur Cell Mater,* 18**,** 84-95.
CLARKSON, B. H. 1991. Caries prevention--fluoride. *Adv Dent Res,* 5**,** 41-5.
COHEN, B. D. & COMBE, E. C. 1994. Development of new adhesive pulp capping materials. *Dent Update,* 21**,** 57-62.
COOPER, P. R., MCLACHLAN, J. L., SIMON, S., GRAHAM, L. W. & SMITH, A. J. 2011. Mediators of inflammation and regeneration. *Adv Dent Res,* 23**,** 290-5.
COOPER, P. R., TAKAHASHI, Y., GRAHAM, L. W., SIMON, S., IMAZATO, S. & SMITH, A. J. 2010. Inflammation-regeneration interplay in the dentine-pulp complex. *J Dent,* 38**,** 687-97.
CORDEIRO, M. M., DONG, Z., KANEKO, T., ZHANG, Z., MIYAZAWA, M., SHI, S., SMITH, A. J. & NOR, J. E. 2008. Dental pulp tissue engineering with stem cells from exfoliated deciduous teeth. *J Endod,* 34**,** 962-9.
CORNISH, J., CALLON, K. E., COY, D. H., JIANG, N. Y., XIAO, L., COOPER, G. J. & REID, I. R. 1997. Adrenomedullin is a potent stimulator of osteoblastic activity in vitro and in vivo. *Am J Physiol,* 273**,** E1113-20.
COUVE, E. 1986. Ultrastructural changes during the life cycle of human odontoblasts. *Arch Oral Biol,* 31**,** 643-51.
COWAN, A. 1966. Treatment of exposed vital pulps with a corticosteroid antibiotic agent. *Br Dent J,* 120**,** 521-32.
COX, C. F., BERGENHOLTZ, G., FITZGERALD, M., HEYS, D. R., HEYS, R. J., AVERY, J. K. & BAKER, J. A. 1982. Capping of the dental pulp mechanically exposed to the oral microflora -- a 5 week observation of wound healing in the monkey. *J Oral Pathol,* 11**,** 327-39.
COX, C. F., BERGENHOLTZ, G., HEYS, D. R., SYED, S. A., FITZGERALD, M. & HEYS, R. J. 1985. Pulp capping of dental pulp mechanically exposed to oral microflora: a 1-2 year observation of wound healing in the monkey. *J Oral Pathol,* 14**,** 156-68.
COX, C. F., SUBAY, R. K., OSTRO, E., SUZUKI, S. & SUZUKI, S. H. 1996. Tunnel defects in dentin bridges: their formation following direct pulp capping. *Oper Dent,* 21**,** 4-11.
COX, C. F. & SUZUKI, S. 1994. Re-evaluating pulp protection: calcium hydroxide liners vs. cohesive hybridization. *J Am Dent Assoc,* 125**,** 823-31.
CROUCH, S., SKOOG, D. A., WEST, D. M. & HOLLER, F. J. 2003. *Fundementals of analytic chemistry,* Philadelphia Saunders College Publishing.
D' ALIMONTE, I., NARGI, E., MASTRANGELO, F., FALCO, G., LANUTI, P., MARCHISIO, M., MISCIA, S., ROBUFFO, I., CAPOGRECO, M., BUCCELLA, S., CAPUTI, S., CACIAGLI, F., TETE, S. & CICCARELLI, R. 2011. Vascular endothelial growth factor enhances in vitro proliferation and osteogenic differentiation of human dental pulp stem cells. *J Biol Regul Homeost Agents,* 25**,** 57-69.
D'SOUZA, R. N., CAVENDER, A., SUNAVALA, G., ALVAREZ, J., OHSHIMA, T., KULKARNI, A. B. & MACDOUGALL, M. 1997. Gene expression patterns of murine dentin matrix protein 1 (Dmp1) and dentin sialophosphoprotein (DSPP) suggest distinct developmental functions in vivo. *J Bone Miner Res,* 12**,** 2040-9.
DALLAS, S. L., ROSSER, J. L., MUNDY, G. R. & BONEWALD, L. F. 2002. Proteolysis of latent transforming growth factor-beta (TGF-beta)-binding protein-1 by osteoclasts. A cellular mechanism for release of TGF-beta from bone matrix. *J Biol Chem,* 277**,** 21352-60.
DALY, A. J., MCILREAVEY, L. & IRWIN, C. R. 2008. Regulation of HGF and SDF-1 expression by oral fibroblasts--implications for invasion of oral cancer. *Oral Oncol,* 44**,** 646-51.
DAMMASCHKE, T. 2008. The history of direct pulp capping. *J Hist Dent,* 56**,** 9-23.

DAMMASCHKE, T., GERTH, H. U., ZUCHNER, H. & SCHAFER, E. 2005. Chemical and physical surface and bulk material characterization of white ProRoot MTA and two Portland cements. *Dent Mater,* 21**,** 731-8.

DAMMASCHKE, T., LEIDINGER, J. & SCHAFER, E. 2010. Long-term evaluation of direct pulp capping--treatment outcomes over an average period of 6.1 years. *Clin Oral Investig,* 14**,** 559-67.

DANESH, G., DAMMASCHKE, T., GERTH, H. U., ZANDBIGLARI, T. & SCHAFER, E. 2006. A comparative study of selected properties of ProRoot mineral trioxide aggregate and two Portland cements. *Int Endod J,* 39**,** 213-9.

DANIELPOUR, D. 1993. Improved sandwich enzyme-linked immunosorbent assays for transforming growth factor beta 1. *J Immunol Methods,* 158**,** 17-25.

DARVELL, B. W. & WU, R. C. 2011. "MTA"-an Hydraulic Silicate Cement: review update and setting reaction. *Dent Mater,* 27**,** 407-22.

DE-DEUS, G. 2008. New directions in old leakage methods. *Int Endod J,* 41**,** 720-1; discussion 721-3.

DE-DEUS, G., DE SOUZA, M. C., SERGIO FIDEL, R. A., FIDEL, S. R., DE CAMPOS, R. C. & LUNA, A. S. 2009. Negligible expression of arsenic in some commercially available brands of Portland cement and mineral trioxide aggregate. *J Endod,* 35**,** 887-90.

DE VICENTE, J. C., CABO, R., CIRIACO, E., LAURA, R., NAVES, F. J., SILOS-SANTIAGO, I. & VEGA, J. A. 2002. Impaired dental cytodifferentiation in glial cell-line derived growth factor (GDNF) deficient mice. *Ann Anat,* 184**,** 85-92.

DO NASCIMENTO, A. B., FONTANA, U. F., TEIXEIRA, H. M. & COSTA, C. A. 2000. Biocompatibility of a resin-modified glass-ionomer cement applied as pulp capping in human teeth. *Am J Dent,* 13**,** 28-34.

DOBIE, K., SMITH, G., SLOAN, A. J. & SMITH, A. J. 2002. Effects of alginate hydrogels and TGF-beta 1 on human dental pulp repair in vitro. *Connect Tissue Res,* 43**,** 387-90.

DREYFUSS, J. L., REGATIERI, C. V., JARROUGE, T. R., CAVALHEIRO, R. P., SAMPAIO, L. O. & NADER, H. B. 2009. Heparan sulfate proteoglycans: structure, protein interactions and cell signaling. *An Acad Bras Cienc,* 81**,** 409-29.

DUARTE, M. A., DE OLIVEIRA DEMARCHI, A. C., YAMASHITA, J. C., KUGA, M. C. & DE CAMPOS FRAGA, S. 2005. Arsenic release provided by MTA and Portland cement. *Oral Surg Oral Med Oral Pathol Oral Radiol Endod,* 99**,** 648-50.

DUCY, P., DESBOIS, C., BOYCE, B., PINERO, G., STORY, B., DUNSTAN, C., SMITH, E., BONADIO, J., GOLDSTEIN, S., GUNDBERG, C., BRADLEY, A. & KARSENTY, G. 1996. Increased bone formation in osteocalcin-deficient mice. *Nature,* 382**,** 448-52.

DUMMER, P. M., HICKS, R. & HUWS, D. 1980. Clinical signs and symptoms in pulp disease. *Int Endod J,* 13**,** 27-35.

DUMORTIER, J., STREBLOW, D. N., MOSES, A. V., JACOBS, J. M., KREKLYWICH, C. N., CAMP, D., SMITH, R. D., ORLOFF, S. L. & NELSON, J. A. 2008. Human cytomegalovirus secretome contains factors that induce angiogenesis and wound healing. *J Virol,* 82**,** 6524-35.

DUNCAN, J. A., GAO, X., HUANG, M. T., O'CONNOR, B. P., THOMAS, C. E., WILLINGHAM, S. B., BERGSTRALH, D. T., JARVIS, G. A., SPARLING, P. F. & TING, J. P. 2009. Neisseria gonorrhoeae activates the proteinase cathepsin B to mediate the signaling activities of the NLRP3 and ASC-containing inflammasome. *J Immunol,* 182**,** 6460-9.

DUNG, S. Z., GREGORY, R. L., LI, Y. & STOOKEY, G. K. 1995. Effect of lactic acid and proteolytic enzymes on the release of organic matrix components from human root dentin. *Caries Res,* 29**,** 483-9.

DURAND, S. H., FLACHER, V., ROMEAS, A., CARROUEL, F., COLOMB, E., VINCENT, C., MAGLOIRE, H., COUBLE, M. L., BLEICHER, F., STAQUET, M. J., LEBECQUE, S. & FARGES, J. C. 2006. Lipoteichoic acid increases TLR and functional chemokine expression while reducing dentin formation in in vitro differentiated human odontoblasts. *J Immunol,* 176**,** 2880-7.

ECCLES, S. A., BOX, C. & COURT, W. 2005. Cell migration/invasion assays and their application in cancer drug discovery. *Biotechnol Annu Rev,* 11**,** 391-421.

EISENMANN, D. R. & GLICK, P. L. 1972. Ultrastructure of initial crystal formation in dentin. *J Ultrastruct Res,* 41**,** 18-28.

EKINS, R. P. 1998. Ligand assays: from electrophoresis to miniaturized microarrays. *Clin Chem,* 44**,** 2015-30.

EKINS, R. P. & CHU, F. W. 1991. Multianalyte microspot immunoassay--microanalytical "compact disk" of the future. *Clin Chem,* 37**,** 1955-67.

EL KARIM, I. A., LAMEY, P. J., LINDEN, G. J., AWAWDEH, L. A. & LUNDY, F. T. 2006. Caries-induced changes in the expression of pulpal neuropeptide Y. *Eur J Oral Sci,* 114**,** 133-7.

EL KARIM, I. A., LINDEN, G. J., IRWIN, C. R. & LUNDY, F. T. 2009. Neuropeptides regulate expression of angiogenic growth factors in human dental pulp fibroblasts. *J Endod,* 35**,** 829-33.

ELSASSER, T. H. & KAHL, S. 2002. Adrenomedullin has multiple roles in disease stress: development and remission of the inflammatory response. *Microsc Res Tech,* 57**,** 120-9.

EMBERY, G., HALL, R., WADDINGTON, R., SEPTIER, D. & GOLDBERG, M. 2001. Proteoglycans in dentinogenesis. *Crit Rev Oral Biol Med,* 12**,** 331-49.

ENGVALL, E. & PERLMANN, P. 1971. Enzyme-linked immunosorbent assay (ELISA). Quantitative assay of immunoglobulin G. *Immunochemistry,* 8**,** 871-4.

EPPLER, S. M., COMBS, D. L., HENRY, T. D., LOPEZ, J. J., ELLIS, S. G., YI, J. H., ANNEX, B. H., MCCLUSKEY, E. R. & ZIONCHECK, T. F. 2002. A target-mediated model to describe the pharmacokinetics and hemodynamic effects of recombinant human vascular endothelial growth factor in humans. *Clin Pharmacol Ther,* 72**,** 20-32.

ESTRELA, C., BAMMANN, L. L., ESTRELA, C. R., SILVA, R. S. & PECORA, J. D. 2000. Antimicrobial and chemical study of MTA, Portland cement, calcium hydroxide paste, Sealapex and Dycal. *Braz Dent J,* 11**,** 3-9.

EUROPEAN SOCIETY OF ENDODONTOLGY 2006. Quality guidelines for endodontic treatment: consensus report of the European Society of Endodontology. *Int Endod J,* 39**,** 921-30.

FANCHON, S., BOURD, K., SEPTIER, D., EVERTS, V., BEERTSEN, W., MENASHI, S. & GOLDBERG, M. 2004. Involvement of matrix metalloproteinases in the onset of dentin mineralization. *Eur J Oral Sci,* 112**,** 171-6.

FARACO, I. M., JR. & HOLLAND, R. 2001. Response of the pulp of dogs to capping with mineral trioxide aggregate or a calcium hydroxide cement. *Dent Traumatol,* 17**,** 163-6.

FARGES, J. C., ROMEAS, A., MELIN, M., PIN, J. J., LEBECQUE, S., LUCCHINI, M., BLEICHER, F. & MAGLOIRE, H. 2003. TGF-beta1 induces accumulation of dendritic cells in the odontoblast layer. *J Dent Res,* 82**,** 652-6.

FARNDALE, R. W., BUTTLE, D. J. & BARRETT, A. J. 1986. Improved quantitation and discrimination of sulphated glycosaminoglycans by use of dimethylmethylene blue. *Biochim Biophys Acta,* 883**,** 173-7.

FAVA, L. R. & SAUNDERS, W. P. 1999. Calcium hydroxide pastes: classification and clinical indications. *Int Endod J,* 32**,** 257-82.

FEN, J. Q., ZHANG, J., DALLAS, S. L., LU, Y., CHEN, S., TAN, X., OWEN, M., HARRIS, S. E. & MACDOUGALL, M. 2002. Dentin matrix protein 1, a target molecule for Cbfa1 in bone, is a unique bone marker gene. *J Bone Miner Res,* 17**,** 1822-31.

FENG, J., MANTESSO, A., DE BARI, C., NISHIYAMA, A. & SHARPE, P. T. 2011. Dual origin of mesenchymal stem cells contributing to organ growth and repair. *Proc Natl Acad Sci U S A,* 108**,** 6503-8.

FENG, J. Q., HUANG, H., LU, Y., YE, L., XIE, Y., TSUTSUI, T. W., KUNIEDA, T., CASTRANIO, T., SCOTT, G., BONEWALD, L. B. & MISHINA, Y. 2003. The Dentin matrix protein 1 (Dmp1) is specifically expressed in mineralized, but not soft, tissues during development. *J Dent Res,* 82**,** 776-80.

FERRACANE, J. L., COOPER, P. R. & SMITH, A. J. 2010. Dentin matrix proteins solubilized by solutions relevant to dentin adhesives. *J Dent Res,* 89B**,** 148.

FINKELMAN, R. D., MOHAN, S., JENNINGS, J. C., TAYLOR, A. K., JEPSEN, S. & BAYLINK, D. J. 1990. Quantitation of growth factors IGF-I, SGF/IGF-II, and TGF-beta in human dentin. *J Bone Miner Res,* 5**,** 717-23.

FISCHER, E. J., ARENS, D. E. & MILLER, C. H. 1998. Bacterial leakage of mineral trioxide aggregate as compared with zinc-free amalgam, intermediate restorative material, and Super-EBA as a root-end filling material. *J Endod,* 24**,** 176-9.

FISHER, L. W. & FEDARKO, N. S. 2003. Six genes expressed in bones and teeth encode the current members of the SIBLING family of proteins. *Connect Tissue Res,* 44 Suppl 1**,** 33-40.

FISHER, L. W., TORCHIA, D. A., FOHR, B., YOUNG, M. F. & FEDARKO, N. S. 2001. Flexible structures of SIBLING proteins, bone sialoprotein, and osteopontin. *Biochem Biophys Res Commun,* 280**,** 460-5.

FITZGERALD, M. 1979. Cellular mechanics of dentinal bridge repair using 3H-thymidine. *J Dent Res,* 58**,** 2198-206.

FITZGERALD, M., CHIEGO, D. J., JR. & HEYS, D. R. 1990. Autoradiographic analysis of odontoblast replacement following pulp exposure in primate teeth. *Arch Oral Biol,* 35**,** 707-15.

FLEMING, W. H., ALPERN, E. J., UCHIDA, N., IKUTA, K. & WEISSMAN, I. L. 1993. Steel factor influences the distribution and activity of murine hematopoietic stem cells in vivo. *Proc Natl Acad Sci U S A,* 90**,** 3760-4.

FORD, T. R., TORABINEJAD, M., ABEDI, H. R., BAKLAND, L. K. & KARIYAWASAM, S. P. 1996. Using mineral trioxide aggregate as a pulp-capping material. *J Am Dent Assoc,* 127**,** 1491-4.

FOUAD, A. F. 2012. Molecular mediators of pulpal inflammation. *In:* HARGREAVES, K. M., GOODIS, H. E. & TAY, F. R. (eds.) *Seltzer and Bender's Dental Pulp*. 2nd ed.: Quintessence Books.

FRANK, R. M. 1979. Electron microscope autoradiography of calcified tissues. *Int Rev Cytol,* 56**,** 183-253.

FRANK, R. M. & STEUER, P. 1988. Transmission electron microscopy of the human odontoblast process in peripheral root dentine. *Arch Oral Biol,* 33**,** 91-8.

FRIDLAND, M. & ROSADO, R. 2003. Mineral trioxide aggregate (MTA) solubility and porosity with different water-to-powder ratios. *J Endod,* 29**,** 814-7.

FRIDLAND, M. & ROSADO, R. 2005. MTA solubility: a long term study. *J Endod,* 31**,** 376-9.

FROZONI, M., ZAIA, A. A., LINE, S. R. & MINA, M. 2012. Analysis of the contribution of nonresident progenitor cells and hematopoietic cells to reparative dentinogenesis using parabiosis model in mice. *J Endod,* 38**,** 1214-9.

FUJIMURA, K., BESSHO, K., KUSUMOTO, K., OGAWA, Y. & IIZUKA, T. 1995. Experimental studies on bone inducing activity of composites of atelopeptide type I collagen as a carrier for ectopic osteoinduction by rhBMP-2. *Biochem Biophys Res Commun,* 208**,** 316-22.

GALE, Z., COOPER, P. R. & SCHEVEN, B. A. 2011. Effects of glial cell line-derived neurotrophic factor on dental pulp cells. *J Dent Res,* 90**,** 1240-5.

GARAYOA, M., BODEGAS, E., CUTTITTA, F. & MONTUENGA, L. M. 2002. Adrenomedullin in mammalian embryogenesis. *Microsc Res Tech,* 57**,** 40-54.

GARBEROGLIO, R. & BRANNSTROM, M. 1976. Scanning electron microscopic investigation of human dentinal tubules. *Arch Oral Biol,* 21**,** 355-62.

GARCIA, J. M., MARTINS, M. D., JAEGER, R. G. & MARQUES, M. M. 2003. Immunolocalization of bone extracellular matrix proteins (type I collagen, osteonectin and bone sialoprotein) in human dental pulp and cultured pulp cells. *Int Endod J,* 36**,** 404-10.

GEORGE, A., SABSAY, B., SIMONIAN, P. A. & VEIS, A. 1993. Characterization of a novel dentin matrix acidic phosphoprotein. Implications for induction of biomineralization. *J Biol Chem,* 268**,** 12624-30.

GLASS, R. L. & ZANDER, H. A. 1949. Pulp healing. *J Dent Res,* 28**,** 97-107.

GOFF, S. P. & BERG, P. 1976. Construction of hybrid viruses containing SV40 and lambda phage DNA segments and their propagation in cultured monkey cells. *Cell,* 9**,** 695-705.

GOLDBERG, H. A., WARNER, K. J., STILLMAN, M. J. & HUNTER, G. K. 1996. Determination of the hydroxyapatite-nucleating region of bone sialoprotein. *Connect Tissue Res,* 35**,** 385-92.

GOLDBERG, M., FARGES, J. C., LACERDA-PINHEIRO, S., SIX, N., JEGAT, N., DECUP, F., SEPTIER, D., CARROUEL, F., DURAND, S., CHAUSSAIN-MILLER, C., DENBESTEN, P., VEIS, A. & POLIARD, A. 2008. Inflammatory and immunological aspects of dental pulp repair. *Pharmacol Res,* 58**,** 137-47.

GOLDBERG, M., KULKARNI, A. B., YOUNG, M. & BOSKEY, A. 2011. Dentin: structure, composition and mineralization. *Front Biosci (Elite Ed),* 3**,** 711-35.

GOLDBERG, M., RAPOPORT, O., SEPTIER, D., PALMIER, K., HALL, R., EMBERY, G., YOUNG, M. & AMEYE, L. 2003a. Proteoglycans in predentin: the last 15 micrometers before mineralization. *Connect Tissue Res,* 44 Suppl 1**,** 184-8.

GOLDBERG, M., SIX, N., DECUP, F., LASFARGUES, J. J., SALIH, E., TOMPKINS, K. & VEIS, A. 2003b. Bioactive molecules and the future of pulp therapy. *Am J Dent,* 16**,** 66-76.

GOLDBERG, M. & SMITH, A. J. 2004. CELLS AND EXTRACELLULAR MATRICES OF DENTIN AND PULP: A BIOLOGICAL BASIS FOR REPAIR AND TISSUE ENGINEERING. *Crit Rev Oral Biol Med,* 15**,** 13-27.

GOTZ, W., HEINEN, M., LOSSDORFER, S. & JAGER, A. 2006. Immunohistochemical localization of components of the insulin-like growth factor system in human permanent teeth. *Arch Oral Biol,* 51**,** 387-95.

GOWEN, L. C., PETERSEN, D. N., MANSOLF, A. L., QI, H., STOCK, J. L., TKALCEVIC, G. T., SIMMONS, H. A., CRAWFORD, D. T., CHIDSEY-FRINK, K. L., KE, H. Z., MCNEISH, J. D. & BROWN, T. A. 2003. Targeted disruption of the osteoblast/osteocyte factor 45 gene (OF45) results in increased bone formation and bone mass. *J Biol Chem,* 278**,** 1998-2007.

GRAHAM, L., COOPER, P. R., CASSIDY, N., NOR, J. E., SLOAN, A. J. & SMITH, A. J. 2006. The effect of calcium hydroxide on solubilisation of bio-active dentine matrix components. *Biomaterials,* 27**,** 2865-73.

GRAHAM, L., SMITH, A. J. & COOPER, P. R. 2007. Cytokine release from human dentine. *J Dent Res,* 86.

GREGORY, C. A., GUNN, W. G., PEISTER, A. & PROCKOP, D. J. 2004. An Alizarin red-based assay of mineralization by adherent cells in culture: comparison with cetylpyridinium chloride extraction. *Anal Biochem,* 329**,** 77-84.

GRONTHOS, S., GRAVES, S. E., OHTA, S. & SIMMONS, P. J. 1994. The STRO-1+ fraction of adult human bone marrow contains the osteogenic precursors. *Blood,* 84**,** 4164-73.

GRONTHOS, S., MANKANI, M., BRAHIM, J., ROBEY, P. G. & SHI, S. 2000. Postnatal human dental pulp stem cells (DPSCs) in vitro and in vivo. *Proc Natl Acad Sci U S A,* 97**,** 13625-30.

GROSE, R. & WERNER, S. 2004. Wound-healing studies in transgenic and knockout mice. *Mol Biotechnol,* 28**,** 147-66.

GU, K., SMOKE, R. H. & RUTHERFORD, R. B. 1996. Expression of genes for bone morphogenetic proteins and receptors in human dental pulp. *Arch Oral Biol,* 41**,** 919-23.

GURTNER, G. C., WERNER, S., BARRANDON, Y. & LONGAKER, M. T. 2008. Wound repair and regeneration. *Nature,* 453**,** 314-21.

HADDAD, M., LEFRANC, G. & AFTIMOS, G. 2003. Local application of IGF1 on dental pulp mechanically exposed; in vivo study on rabbit. *Bull Group Int Rech Sci Stomatol Odontol,* 45**,** 12-7.

HAKKI, S. S., BOZKURT, S. B., HAKKI, E. E. & BELLI, S. 2009. Effects of mineral trioxide aggregate on cell survival, gene expression associated with mineralized tissues, and biomineralization of cementoblasts. *J Endod,* 35**,** 513-9.

HAMILTON, J. A. 2008. Colony-stimulating factors in inflammation and autoimmunity. *Nat Rev Immunol,* 8**,** 533-44.

HANKS, C. T., FANG, D., SUN, Z., EDWARDS, C. A. & BUTLER, W. T. 1998a. Dentin-specific proteins in MDPC-23 cell line. *Eur J Oral Sci,* 106 Suppl 1**,** 260-6.

HANKS, C. T., SUN, Z. L., FANG, D. N., EDWARDS, C. A., WATAHA, J. C., RITCHIE, H. H. & BUTLER, W. T. 1998b. Cloned 3T6 cell line from CD-1 mouse fetal molar dental papillae. *Connect Tissue Res,* 37**,** 233-49.

HANNAS, A. R., PEREIRA, J. C., GRANJEIRO, J. M. & TJADERHANE, L. 2007. The role of matrix metalloproteinases in the oral environment. *Acta Odontol Scand,* 65**,** 1-13.

HAUG, S. R. & HEYERAAS, K. J. 2006. Modulation of dental inflammation by the sympathetic nervous system. *J Dent Res,* 85**,** 488-95.

HE, G., DAHL, T., VEIS, A. & GEORGE, A. 2003. Nucleation of apatite crystals in vitro by self-assembled dentin matrix protein 1. *Nat Mater,* 2**,** 552-8.

HE, W. X., NIU, Z. Y., ZHAO, S. L., JIN, W. L., GAO, J. & SMITH, A. J. 2004. TGF-beta activated Smad signalling leads to a Smad3-mediated down-regulation of DSPP in an odontoblast cell line. *Arch Oral Biol,* 49**,** 911-8.

HEIJL, L., HEDEN, G., SVARDSTROM, G. & OSTGREN, A. 1997. Enamel matrix derivative (EMDOGAIN) in the treatment of intrabony periodontal defects. *J Clin Periodontol,* 24**,** 705-14.

HELFFERICH, F. 1995. *Ion Exchange,* N.Y. USA, Dover Publications.

HERBERT, K. E., MORGAN, S., PRINCE, H. M., WESTERMAN, D. A., WOLF, M. M., CARNEY, D. A., YUEN, K., DI IULIO, J. & SEYMOUR, J. F. 2009. Stem cell factor and high-dose twice daily filgrastim is an effective strategy for peripheral blood stem cell mobilization in patients with indolent lymphoproliferative disorders previously treated with fludarabine: results of a Phase II study with an historical comparator. *Leukemia,* 23**,** 305-12.

HERBERT, K. E., PRINCE, H. M., RITCHIE, D. S. & SEYMOUR, J. F. 2010. The role of ancestim (recombinant human stem-cell factor, rhSCF) in hematopoietic stem cell mobilization and hematopoietic reconstitution. *Expert Opin Biol Ther,* 10**,** 113-25.

HERMANN, B. 1920. Calcium hydroxyd als mitten zum behandeln und fullen von Wurzelkanallen (dissertation) Wursburg. (printed in: Malo PRT, Kessler Nieto F, Vadillo MVM (1987) Hidroxido de calcio y apicoformacion. Revista *Espanola de Endodoncia* 5, 41-61)

HERNANDEZ, E. P., BOTERO, T. M., MANTELLINI, M. G., MCDONALD, N. J. & NOR, J. E. 2005. Effect of ProRoot MTA mixed with chlorhexidine on apoptosis and cell cycle of fibroblasts and macrophages in vitro. *Int Endod J,* 38**,** 137-43.

HEYS, D. R., COX, C. F., HEYS, R. J. & AVERY, J. K. 1981. Histological considerations of direct pulp capping agents. *J Dent Res,* 60**,** 1371-9.

HOLLAND, G. R. 1985. The odontoblast process: form and function. *J Dent Res,* 64 Spec No**,** 499-514.

HOLLAND, R., FILHO, J. A., DE SOUZA, V., NERY, M. J., BERNABE, P. F. & JUNIOR, E. D. 2001. Mineral trioxide aggregate repair of lateral root perforations. *J Endod,* 27**,** 281-4.

HOLT, D. M., WATTS, J. D., BEESON, T. J., KIRKPATRICK, T. C. & RUTLEDGE, R. E. 2007. The anti-microbial effect against enterococcus faecalis and the compressive strength of two types of mineral trioxide aggregate mixed with sterile water or 2% chlorhexidine liquid. *J Endod,* 33**,** 844-7.

HOPPE, A., GULDAL, N. S. & BOCCACCINI, A. R. 2011. A review of the biological response to ionic dissolution products from bioactive glasses and glass-ceramics. *Biomaterials,* 32**,** 2757-74.

HORSTED-BINDSLEV, P., VILKINIS, V. & SIDLAUSKAS, A. 2003. Direct capping of human pulps with a dentin bonding system or with calcium hydroxide cement. *Oral Surg Oral Med Oral Pathol Oral Radiol Endod,* 96**,** 591-600.

HOSOYA, S., MATSUSHIMA, K., OHBAYASHI, E., YAMAZAKI, M., SHIBATA, Y. & ABIKO, Y. 1996. Stimulation of interleukin-1beta-independent interleukin-6 production in human dental pulp cells by lipopolysaccharide. *Biochem Mol Med,* 59**,** 138-43.

HOWARD, C., MURRAY, P. E. & NAMEROW, K. N. 2010. Dental pulp stem cell migration. *J Endod,* 36**,** 1963-6.

HU, C. C., ZHANG, C., QIAN, Q. & TATUM, N. B. 1998. Reparative dentin formation in rat molars after direct pulp capping with growth factors. *J Endod,* 24**,** 744-51.

HUNTER, G. K. & GOLDBERG, H. A. 1993. Nucleation of hydroxyapatite by bone sialoprotein. *Proc Natl Acad Sci U S A,* 90**,** 8562-5.

HWAS, M. & SANDRIK, J. L. 1984. Acid and water solubility and strength of calcium hydroxide bases. *J Am Dent Assoc,* 108**,** 46-8.

IOANNIDIS, K., MISTAKIDIS, I., BELTES, P. & KARAGIANNIS, V. 2013. Spectrophotometric analysis of coronal discolouration induced by grey and white MTA. *Int Endod J,* 46**,** 137-44.

ISHIMATSU, H., KITAMURA, C., MOROTOMI, T., TABATA, Y., NISHIHARA, T., CHEN, K. K. & TERASHITA, M. 2009. Formation of dentinal bridge on surface of regenerated dental pulp in dentin defects by controlled release of fibroblast growth factor-2 from gelatin hydrogels. *J Endod,* 35**,** 858-65.

ISLAM, I., CHNG, H. K. & YAP, A. U. 2006. Comparison of the physical and mechanical properties of MTA and portland cement. *J Endod,* 32**,** 193-7.

IWAMOTO, C. E., ADACHI, E., PAMEIJER, C. H., BARNES, D., ROMBERG, E. E. & JEFFERIES, S. 2006. Clinical and histological evaluation of white ProRoot MTA in direct pulp capping. *Am J Dent,* 19**,** 85-90.

IWASAKI, Y., OTSUKA, H., YANAGISAWA, N., HISAMITSU, H., MANABE, A., NONAKA, N. & NAKAMURA, M. 2011. In situ proliferation and differentiation of macrophages in dental pulp. *Cell Tissue Res,* 346**,** 99-109.

IZUMI, T., INOUE, H., MATSUURA, H., MUKAE, F., OSOEGAWA, H., HIRANO, H. & TAMURA, N. 2001. Changes in the pattern of horseradish peroxidase diffusion into predentin and dentin after cavity preparation in rat molars. *Oral Surg Oral Med Oral Pathol Oral Radiol Endod,* 92**,** 675-81.

JOHNSON, H. H. 1908. Silicate cements and their uses. *Dental Cosmos***,** 827-829.

JONES, J. I. & CLEMMONS, D. R. 1995. Insulin-like growth factors and their binding proteins: biological actions. *Endocr Rev,* 16**,** 3-34.

JONTELL, M., BERGENHOLTZ, G., SCHEYNIUS, A. & AMBROSE, W. 1988. Dendritic cells and macrophages expressing class II antigens in the normal rat incisor pulp. *J Dent Res,* 67**,** 1263-6.

JONTELL, M., OKIJI, T., DAHLGREN, U. & BERGENHOLTZ, G. 1998. Immune defense mechanisms of the dental pulp. *Crit Rev Oral Biol Med,* 9**,** 179-200.

JOSEPH, B. K., SAVAGE, N. W., DALEY, T. J. & YOUNG, W. G. 1996. In situ hybridization evidence for a paracrine/autocrine role for insulin-like growth factor-I in tooth development. *Growth Factors,* 13**,** 11-7.

KAJIHARA, T., OHNISHI, T., ARAKAKI, N., SEMBA, I. & DAIKUHARA, Y. 1999. Expression of hepatocyte growth factor/scatter factor and c-Met in human dental papilla and fibroblasts from dental papilla. *Arch Oral Biol,* 44**,** 135-47.

KAKEHASHI, S., STANLEY, H. R. & FITZGERALD, R. 1969. The exposed germ-free pulp: effects of topical corticosteroid medication and restoration. *Oral Surg Oral Med Oral Pathol,* 27**,** 60-7.

KAKEHASHI, S., STANLEY, H. R. & FITZGERALD, R. J. 1965. THE EFFECTS OF SURGICAL EXPOSURES OF DENTAL PULPS IN GERM-FREE AND CONVENTIONAL LABORATORY RATS. *Oral Surg Oral Med Oral Pathol,* 20**,** 340-9.

KANATO, Y., ONO, S., KITAJIMA, K. & SATO, C. 2009. Complex formation of a brain-derived neurotrophic factor and glycosaminoglycans. *Biosci Biotechnol Biochem,* 73**,** 2735-41.

KANG, S. K., SHIN, I. S., KO, M. S., JO, J. Y. & RA, J. C. 2012. Journey of mesenchymal stem cells for homing: strategies to enhance efficacy and safety of stem cell therapy. *Stem Cells Int,* 2012**,** 342968.

KARDOS, T. B., HUNTER, A. R., HANLIN, S. M. & KIRK, E. E. 1998. Odontoblast differentiation: a response to environmental calcium? *Endod Dent Traumatol,* 14**,** 105-11.

KARLOVIC, Z., PEZELJ-RIBARIC, S., MILETIC, I., JUKIC, S., GRGUREVIC, J. & ANIC, I. 2005. Erbium:YAG laser versus ultrasonic in preparation of root-end cavities. *J Endod,* 31**,** 821-3.

KARSENTY, G. 2000. Bone formation and factors affecting this process. *Matrix Biol,* 19**,** 85-9.

KEISER, K., JOHNSON, C. C. & TIPTON, D. A. 2000. Cytotoxicity of mineral trioxide aggregate using human periodontal ligament fibroblasts. *J Endod,* 26**,** 288-91.

KIKUCHI, N., KITAMURA, C., MOROTOMI, T., INUYAMA, Y., ISHIMATSU, H., TABATA, Y., NISHIHARA, T. & TERASHITA, M. 2007. Formation of dentin-like particles in dentin defects above exposed pulp by controlled release of fibroblast growth factor 2 from gelatin hydrogels. *J Endod,* 33**,** 1198-202.

KILLOUGH, S. A., LUNDY, F. T. & IRWIN, C. R. 2010. Dental pulp fibroblasts express neuropeptide Y Y1 receptor but not neuropeptide Y. *Int Endod J,* 43**,** 835-42.

KIM, J. Y., XIN, X., MOIOLI, E. K., CHUNG, J., LEE, C. H., CHEN, M., FU, S. Y., KOCH, P. D. & MAO, J. J. 2010. Regeneration of dental-pulp-like tissue by chemotaxis-induced cell homing. *Tissue Eng Part A,* 16**,** 3023-31.

KITAMURA, C., NISHIHARA, T., TERASHITA, M., TABATA, Y. & WASHIO, A. 2012. Local regeneration of dentin-pulp complex using controlled release of fgf-2 and naturally derived sponge-like scaffolds. *Int J Dent,* 2012**,** 190561.

KOCAOEMER, A., KERN, S., KLUTER, H. & BIEBACK, K. 2007. Human AB serum and thrombin-activated platelet-rich plasma are suitable alternatives to fetal calf serum for the expansion of mesenchymal stem cells from adipose tissue. *Stem Cells,* 25**,** 1270-8.

KUANG, Z., YAO, S., KEIZER, D. W., WANG, C. C., BACH, L. A., FORBES, B. E., WALLACE, J. C. & NORTON, R. S. 2006. Structure, dynamics and heparin binding of the C-terminal domain of insulin-like growth factor-binding protein-2 (IGFBP-2). *J Mol Biol,* 364**,** 690-704.

KURATATE, M., YOSHIBA, K., SHIGETANI, Y., YOSHIBA, N., OHSHIMA, H. & OKIJI, T. 2008. Immunohistochemical analysis of nestin, osteopontin, and proliferating cells in the reparative process of exposed dental pulp capped with mineral trioxide aggregate. *J Endod,* 34**,** 970-4.

KUTTLER, Y. 1959. Classification of dentine into primary, secondary, and tertiary. *Oral Surg Oral Med Oral Pathol,* 12**,** 996-9.

KWON, S. M., KIM, S. A., YOON, J. H. & AHN, S. G. 2010. Transforming growth factor beta1-induced heat shock protein 27 activation promotes migration of mouse dental papilla-derived MDPC-23 cells. *J Endod,* 36**,** 1332-5.

LAIRD, D. J., VON ANDRIAN, U. H. & WAGERS, A. J. 2008. Stem cell trafficking in tissue development, growth, and disease. *Cell,* 132**,** 612-30.

LARRAIN, J., BACHILLER, D., LU, B., AGIUS, E., PICCOLO, S. & DE ROBERTIS, E. M. 2000. BMP-binding modules in chordin: a model for signalling regulation in the extracellular space. *Development,* 127**,** 821-30.

LAURENS, N., KOOLWIJK, P. & DE MAAT, M. P. 2006. Fibrin structure and wound healing. *J Thromb Haemost,* 4**,** 932-9.

LAZAR-MOLNAR, E., HEGYESI, H., TOTH, S. & FALUS, A. 2000. Autocrine and paracrine regulation by cytokines and growth factors in melanoma. *Cytokine,* 12**,** 547-54.

LEE, S. J., MONSEF, M. & TORABINEJAD, M. 1993. Sealing ability of a mineral trioxide aggregate for repair of lateral root perforations. *J Endod,* 19**,** 541-4.

LENHERR, P., ALLGAYER, N., WEIGER, R., FILIPPI, A., ATTIN, T. & KRASTL, G. 2012. Tooth discoloration induced by endodontic materials: a laboratory study. *Int Endod J,* 45**,** 942-9.

LESOT, H., LISI, S., PETERKOVA, R., PETERKA, M., MITOLO, V. & RUCH, J. V. 2001. Epigenetic signals during odontoblast differentiation. *Adv Dent Res,* 15**,** 8-13.

LESOT, H., SMITH, A. J., MATTHEWS, J. B. & RUCH, J. V. 1988. An extracellular matrix protein of dentine, enamel, and bone shares common antigenic determinants with keratins. *Calcif Tissue Int,* 42**,** 53-7.

LESOT H., BÈGUE-KIRN C., KUBLER M.D., MEYER J.M., SMITH A.J., CASSADY N. & J.V., R. 1993. Experimental induction of odontoblast differentiation and stimulation during reparative processes. *Cells and Materials,* 3**,** 201-217.

LI, R., PENG, L., REN, L., TAN, H. & YE, L. 2009. Hepatocyte growth factor exerts promoting functions on murine dental papilla cells. *J Endod,* 35**,** 382-8.

LIESCHKE, G. J., GRAIL, D., HODGSON, G., METCALF, D., STANLEY, E., CHEERS, C., FOWLER, K. J., BASU, S., ZHAN, Y. F. & DUNN, A. R. 1994. Mice lacking granulocyte colony-stimulating factor have chronic neutropenia, granulocyte and macrophage progenitor cell deficiency, and impaired neutrophil mobilization. *Blood,* 84**,** 1737-46.

LINDE, A. 1984. Non-collagenous proteins and proteoglycans in dentinogenesis. *In:* LINDE, A. (ed.) *Dentin and dentinogenesis.* FL: CRC Press.

LINDE, A. 1985. The extracellular matrix of the dental pulp and dentin. *J Dent Res,* 64 Spec No**,** 523-9.

LINDE, A. 1989. Dentin matrix proteins: composition and possible functions in calcification. *Anat Rec,* 224**,** 154-66.

LINDE, A. & GOLDBERG, M. 1993. Dentinogenesis. *Crit Rev Oral Biol Med,* 4**,** 679-728.

LINDE, A. & LUNDGREN, T. 1995. From serum to the mineral phase. The role of the odontoblast in calcium transport and mineral formation. *Int J Dev Biol,* 39**,** 213-22.

LIU, Y., WILKINSON, F. L., KIRTON, J. P., JEZIORSKA, M., IIZASA, H., SAI, Y., NAKASHIMA, E., HEAGERTY, A. M., CANFIELD, A. E. & ALEXANDER, M. Y. 2007. Hepatocyte growth factor and c-Met expression in pericytes: implications for atherosclerotic plaque development. *J Pathol,* 212**,** 12-9.

LLANO, E., PENDAS, A. M., KNAUPER, V., SORSA, T., SALO, T., SALIDO, E., MURPHY, G., SIMMER, J. P., BARTLETT, J. D. & LOPEZ-OTIN, C. 1997. Identification and structural and functional characterization of human enamelysin (MMP-20). *Biochemistry,* 36**,** 15101-8.

LOVSCHALL, H., FEJERSKOV, O. & FLYVBJERG, A. 2001. Pulp-capping with recombinant human insulin-like growth factor I (rhIGF-I) in rat molars. *Adv Dent Res,* 15**,** 108-12.

LU, Y., LIU, T., LI, H. & PI, G. 2008. Histological evaluation of direct pulp capping with a self-etching adhesive and calcium hydroxide on human pulp tissue. *Int Endod J,* 41**,** 643-50.

LUNDQUIST, P. 2002. Odontoblast phosphate and calcium transport in dentinogenesis. *Swed Dent J Suppl***,** 1-52.

MACDONALD, K. K., CHEUNG, C. Y. & ANSETH, K. S. 2007. Cellular delivery of TGFbeta1 promotes osteoinductive signalling for bone regeneration. *J Tissue Eng Regen Med,* 1**,** 314-7.

MACDOUGALL, M., GU, T. T., LUAN, X., SIMMONS, D. & CHEN, J. 1998. Identification of a novel isoform of mouse dentin matrix protein 1: spatial expression in mineralized tissues. *J Bone Miner Res,* 13**,** 422-31.

MAGLOIRE, H., ROMEAS, A., MELIN, M., COUBLE, M. L., BLEICHER, F. & FARGES, J. C. 2001. Molecular regulation of odontoblast activity under dentin injury. *Adv Dent Res,* 15**,** 46-50.

MANIATOPOULOS, C. & SMITH, D. C. 1983. A scanning electron microscopic study of the odontoblast process in human coronal dentine. *Arch Oral Biol,* 28**,** 701-10.

MANIATOPOULOS, C., SODEK, J. & MELCHER, A. H. 1988. Bone formation in vitro by stromal cells obtained from bone marrow of young adult rats. *Cell Tissue Res,* 254**,** 317-30.

MAO, J. J., STOSICH, M. S., MOIOLI, E. K., LEE, C. H., FU, S. Y., BASTIAN, B., EISIG, S. B., ZEMNICK, C., ASCHERMAN, J., WU, J., ROHDE, C. & AHN, J. 2010. Facial reconstruction by biosurgery: cell transplantation versus cell homing. *Tissue Eng Part B Rev,* 16**,** 257-62.

MARTELL, B. & CHANDLER, N. P. 2002. Electrical and dye leakage comparison of three root-end restorative materials. *Quintessence Int,* 33**,** 30-4.

MARTINEZ, A., OH, H. R., UNSWORTH, E. J., BREGONZIO, C., SAAVEDRA, J. M., STETLER-STEVENSON, W. G. & CUTTITTA, F. 2004. Matrix metalloproteinase-2

cleavage of adrenomedullin produces a vasoconstrictor out of a vasodilator. *Biochem J,* 383**,** 413-8.

MARTINEZ, E. F. & ARAUJO, V. C. 2004. In vitro immunoexpression of extracellular matrix proteins in dental pulpal and gingival human fibroblasts. *Int Endod J,* 37**,** 749-55.

MASTERTON, J. B. 1966. Inherent healing potential of the dental pulp. *Br Dent J,* 120**,** 430-6.

MASUDA-MURAKAMI, Y., KOBAYASHI, M., WANG, X., YAMADA, Y., KIMURA, Y., HOSSAIN, M. & MATSUMOTO, K. 2010. Effects of mineral trioxide aggregate on the differentiation of rat dental pulp cells. *Acta Histochem,* 112**,** 452-8.

MATSUO, T., EBISU, S., NAKANISHI, T., YONEMURA, K., HARADA, Y. & OKADA, H. 1994. Interleukin-1 alpha and interleukin-1 beta periapical exudates of infected root canals: correlations with the clinical findings of the involved teeth. *J Endod,* 20**,** 432-5.

MATSUO, T., NAKANISHI, T., SHIMIZU, H. & EBISU, S. 1996. A clinical study of direct pulp capping applied to carious-exposed pulps. *J Endod,* 22**,** 551-6.

MAZZONI, A., MANNELLO, F., TAY, F. R., TONTI, G. A., PAPA, S., MAZZOTTI, G., DI LENARDA, R., PASHLEY, D. H. & BRESCHI, L. 2007. Zymographic analysis and characterization of MMP-2 and -9 forms in human sound dentin. *J Dent Res,* 86**,** 436-40.

MCKINNEY, M. & ROBBINS, M. 1992. Chronic atropine administration up-regulates rat cortical muscarinic m1 receptor mRNA molecules: assessment with the RT/PCR. *Brain Res Mol Brain Res,* 12**,** 39-45.

MCKINNON, H., GHERARDI, E., REIDY, M. & BOWYER, D. 2006. Hepatocyte growth factor/scatter factor and MET are involved in arterial repair and atherogenesis. *Am J Pathol,* 168**,** 340-8.

MCLACHLAN, J. L., SLOAN, A. J., SMITH, A. J., LANDINI, G. & COOPER, P. R. 2004. S100 and cytokine expression in caries. *Infect Immun,* 72**,** 4102-8.

MCLACHLAN, J. L., SMITH, A. J., BUJALSKA, I. J. & COOPER, P. R. 2005. Gene expression profiling of pulpal tissue reveals the molecular complexity of dental caries. *Biochim Biophys Acta,* 1741**,** 271-81.

MCLACHLAN, J. L., SMITH, A. J., SLOAN, A. J. & COOPER, P. R. 2003. Gene expression analysis in cells of the dentine-pulp complex in healthy and carious teeth. *Arch Oral Biol,* 48**,** 273-83.

MELIN, M., JOFFRE-ROMEAS, A., FARGES, J. C., COUBLE, M. L., MAGLOIRE, H. & BLEICHER, F. 2000. Effects of TGFbeta1 on dental pulp cells in cultured human tooth slices. *J Dent Res,* 79**,** 1689-96.

MILLER, W. D. 1894. An Introduction to the Study of the Bacterio-Pathology of the Dental Pulp. *Dental Cosmos,* 36**,** 505-528.

MIN, K. S., PARK, H. J., LEE, S. K., PARK, S. H., HONG, C. U., KIM, H. W., LEE, H. H. & KIM, E. C. 2008. Effect of mineral trioxide aggregate on dentin bridge formation and expression of dentin sialoprotein and heme oxygenase-1 in human dental pulp. *J Endod,* 34**,** 666-70.

MIURA, M., GRONTHOS, S., ZHAO, M., LU, B., FISHER, L. W., ROBEY, P. G. & SHI, S. 2003. SHED: stem cells from human exfoliated deciduous teeth. *Proc Natl Acad Sci U S A,* 100**,** 5807-12.

MIYAMOTO, S., YANO, K., SUGIMOTO, S., ISHII, G., HASEBE, T., ENDOH, Y., KODAMA, K., GOYA, M., CHIBA, T. & OCHIAI, A. 2004. Matrix metalloproteinase-7 facilitates insulin-like growth factor bioavailability through its proteinase activity on insulin-like growth factor binding protein 3. *Cancer Res,* 64**,** 665-71.

MIYASHITA, H., WORTHINGTON, H. V., QUALTROUGH, A. & PLASSCHAERT, A. 2007. Pulp management for caries in adults: maintaining pulp vitality. *Cochrane Database Syst Rev***,** CD004484.

MOGHADDAME-JAFARI, S., MANTELLINI, M. G., BOTERO, T. M., MCDONALD, N. J. & NOR, J. E. 2005. Effect of ProRoot MTA on pulp cell apoptosis and proliferation in vitro. *J Endod,* 31**,** 387-91.

MOSMANN, T. 1983. Rapid colorimetric assay for cellular growth and survival: application to proliferation and cytotoxicity assays. *J Immunol Methods,* 65**,** 55-63.

MULDER, G. D. & VANDE BERG, J. S. 2002. Cellular senescence and matrix metallo proteinase activity in chronic wounds. Relevance to debridement and new technologies. *J Am Podiatr Med Assoc,* 92**,** 34-7.

MURRAY, P. E., ABOUT, I., LUMLEY, P. J., FRANQUIN, J. C., REMUSAT, M. & SMITH, A. J. 2002. Cavity remaining dentin thickness and pulpal activity. *Am J Dent,* 15**,** 41-6.

MURRAY, P. E., ABOUT, I., LUMLEY, P. J., SMITH, G., FRANQUIN, J. C. & SMITH, A. J. 2000. Postoperative pulpal and repair responses. *J Am Dent Assoc,* 131**,** 321-9.

MUSSON, D. S., MCLACHLAN, J. L., SLOAN, A. J., SMITH, A. J. & COOPER, P. R. 2010. Adrenomedullin is expressed during rodent dental tissue development and promotes cell growth and mineralization. *Biol Cell,* 102**,** 145-57.

NAGAI, N. & FRANK, R. M. 1974. Electron microscopic autoradiography of Ca-45 during dentinogenesis. *Cell Tissue Res,* 155**,** 513-23.

NAIR, P. N., DUNCAN, H. F., PITT FORD, T. R. & LUDER, H. U. 2008. Histological, ultrastructural and quantitative investigations on the response of healthy human pulps to experimental capping with mineral trioxide aggregate: a randomized controlled trial. *Int Endod J,* 41**,** 128-50.

NAKASHIMA, M., NAGASAWA, H., YAMADA, Y. & REDDI, A. H. 1994. Regulatory role of transforming growth factor-beta, bone morphogenetic protein-2, and protein-4 on gene expression of extracellular matrix proteins and differentiation of dental pulp cells. *Dev Biol,* 162**,** 18-28.

NANCI, A. 2013. *Ten Cate's Oral Histology,* USA, Elsevier.

NAOT, D., CALLON, K. E., GREY, A., COOPER, G. J., REID, I. R. & CORNISH, J. 2001. A potential role for adrenomedullin as a local regulator of bone growth. *Endocrinology,* 142**,** 1849-57.

NING, W., SONG, R., LI, C., PARK, E., MOHSENIN, A., CHOI, A. M. & CHOI, M. E. 2002. TGF-beta1 stimulates HO-1 via the p38 mitogen-activated protein kinase in A549 pulmonary epithelial cells. *Am J Physiol Lung Cell Mol Physiol,* 283**,** L1094-102.

NOMIYAMA, K., KITAMURA, C., TSUJISAWA, T., NAGAYOSHI, M., MOROTOMI, T., TERASHITA, M. & NISHIHARA, T. 2007. Effects of lipopolysaccharide on newly established rat dental pulp-derived cell line with odontoblastic properties. *J Endod,* 33**,** 1187-91.

NOSRAT, C. A., FRIED, K., EBENDAL, T. & OLSON, L. 1998. NGF, BDNF, NT3, NT4 and GDNF in tooth development. *Eur J Oral Sci,* 106 Suppl 1**,** 94-9.

NOVICKAS, D., FIOCCA, V. L. & GRAJOWER, R. 1989. Linings and caries in retrieved permanent teeth with amalgam restorations. *Oper Dent,* 14**,** 33-9.

ODLER, I. 1993. Hydration, setting and hardening of portland cement. *In:* HEWLETT, P. C. (ed.) *Lea's chemistry of cement on concrete.* Elsevier Butterworth Heinemann.

OGATA, Y., NIISATO, N., MORIWAKI, K., YOKOTA, Y., FURUYAMA, S. & SUGIYA, H. 1997. Cementum, root dentin and bone extracts stimulate chemotactic behavior in cells from periodontal tissue. *Comp Biochem Physiol B Biochem Mol Biol,* 116**,** 359-65.

OHSHIMA, H., SATO, O., KAWAHARA, I., MAEDA, T. & TAKANO, Y. 1995. Responses of immunocompetent cells to cavity preparation in rat molars: an immunohistochemical study using OX6-monoclonal antibody. *Connect Tissue Res,* 32**,** 303-11.

OKAMOTO, R., MATSUMOTO, T. & WATANABE, M. 2006. Regeneration of the intestinal epithelia: regulation of bone marrow-derived epithelial cell differentiation towards secretory lineage cells. *Hum Cell,* 19**,** 71-5.

OKAMURA, K., MAEDA, M., NISHIKAWA, T. & TSUTSUI, M. 1980. Dentinal response against carious invasion: localization of antibodies in odontoblastic body and process. *J Dent Res,* 59**,** 1368-73.

OKAMURA, K., TSUBAKIMOTO, K., UOBE, K., NISHIDA, K. & TSUTSUI, M. 1979. Serum proteins and secretory component in human carious dentin. *J Dent Res,* 58**,** 1127-23.

OKIJI, T. 2012. Pulp as a connective tissue. *In:* HARGREAVES, K. M., GOODIS, H. E. & TAY, F. R. (eds.) *Seltzer and Bender's Dental Pulp.* Second ed.: Quintessence Publishing.

OKIJI, T., KAWASHIMA, N., KOSAKA, T., MATSUMOTO, A., KOBAYASHI, C. & SUDA, H. 1992. An immunohistochemical study of the distribution of immunocompetent cells, especially macrophages and Ia antigen-expressing cells of heterogeneous populations, in normal rat molar pulp. *J Dent Res,* 71**,** 1196-202.

OLIVEIRA, M. G., XAVIER, C. B., DEMARCO, F. F., PINHEIRO, A. L., COSTA, A. T. & POZZA, D. H. 2007. Comparative chemical study of MTA and Portland cements. *Braz Dent J,* 18**,** 3-7.

OLSSON, H., PETERSSON, K. & ROHLIN, M. 2006. Formation of a hard tissue barrier after pulp cappings in humans. A systematic review. *Int Endod J,* 39**,** 429-42.

PAPAGERAKIS, P., BERDAL, A., MESBAH, M., PEUCHMAUR, M., MALAVAL, L., NYDEGGER, J., SIMMER, J. & MACDOUGALL, M. 2002. Investigation of osteocalcin, osteonectin, and dentin sialophosphoprotein in developing human teeth. *Bone,* 30**,** 377-85.

PARALKAR, V. M., NANDEDKAR, A. K., POINTER, R. H., KLEINMAN, H. K. & REDDI, A. H. 1990. Interaction of osteogenin, a heparin binding bone morphogenetic protein, with type IV collagen. *J Biol Chem,* 265**,** 17281-4.

PARALKAR, V. M., VUKICEVIC, S. & REDDI, A. H. 1991. Transforming growth factor beta type 1 binds to collagen IV of basement membrane matrix: implications for development. *Dev Biol,* 143**,** 303-8.

PARIROKH, M. & TORABINEJAD, M. 2010. Mineral trioxide aggregate: a comprehensive literature review--Part I: chemical, physical, and antibacterial properties. *J Endod,* 36**,** 16-27.

PARK, J. W., HONG, S. H., KIM, J. H., LEE, S. J. & SHIN, S. J. 2010. X-Ray diffraction analysis of white ProRoot MTA and Diadent BioAggregate. *Oral Surg Oral Med Oral Pathol Oral Radiol Endod,* 109**,** 155-8.

PASHLEY, D. H. 1996. Dynamics of the pulpo-dentin complex. *Crit Rev Oral Biol Med,* 7**,** 104-33.

PASHLEY, D. H. & TAY, F. R. 2012. Pulpodentin Complex. *In:* HARGREAVES, K. M., GOODIS, H. E. & TAY, F. R. (eds.) *Seltzer and Bender's Dental Pulp*. 2nd ed.: Quintessence Publishing.

PASHLEY, D. H., TAY, F. R., YIU, C., HASHIMOTO, M., BRESCHI, L., CARVALHO, R. M. & ITO, S. 2004. Collagen degradation by host-derived enzymes during aging. *J Dent Res,* 83**,** 216-21.

PATEL, M., SMITH, A. J., SLOAN, A. J., SMITH, G. & COOPER, P. R. 2009. Phenotype and behaviour of dental pulp cells during expansion culture. *Arch Oral Biol,* 54**,** 898-908.

PEREIRA, J. C., MANFIO, A. P., FRANCO, E. B. & LOPES, E. S. 1990. Clinical evaluation of Dycal under amalgam restorations. *Am J Dent,* 3**,** 67-70.

PEZELJ-RIBARIC, S., ANIC, I., BREKALO, I., MILETIC, I., HASAN, M. & SIMUNOVIC-SOSKIC, M. 2002. Detection of tumor necrosis factor alpha in normal and inflamed human dental pulps. *Arch Med Res,* 33**,** 482-4.

PFAF, P. 1756. *Abhandlung von den Zähnen des menschlichen Körpers und deren Krankheiten,* Berlin, Haude und Spener.

PIERCE, G. F., TARPLEY, J. E., YANAGIHARA, D., MUSTOE, T. A., FOX, G. M. & THOMASON, A. 1992. Platelet-derived growth factor (BB homodimer), transforming growth factor-beta 1, and basic fibroblast growth factor in dermal wound healing. Neovessel and matrix formation and cessation of repair. *Am J Pathol,* 140**,** 1375-88.

PISANTI, S. & SCIAKY, I. 1964. Origin of calcium in the repair wall after pulp exposure in the dog. *J Dent Res,* 43**,** 641-4.

PISTORIUS, A., WILLERSHAUSEN, B. & BRISENO MARROQUIN, B. 2003. Effect of apical root-end filling materials on gingival fibroblasts. *Int Endod J,* 36**,** 610-5.

PITT FORD, T. R. 1979. Pulpal response to Procal for capping exposures in dog's teeth. *J Br Endod Soc,* 12**,** 67-72.

PITT FORD, T. R. 1985. Pulpal response to a calcium hydroxide material for capping exposures. *Oral Surg Oral Med Oral Pathol,* 59**,** 194-7.

PITT FORD, T. R. & ROBERTS, G. J. 1991. Immediate and delayed direct pulp capping with the use of a new visible light-cured calcium hydroxide preparation. *Oral Surg Oral Med Oral Pathol,* 71**,** 338-42.

POGGIO, C., LOMBARDINI, M., ALESSANDRO, C. & SIMONETTA, R. 2007. Solubility of root-end-filling materials: a comparative study. *J Endod,* 33**,** 1094-7.

POOL, J. G. 1977. Normal hemostatic mechanisms: a review. *Am J Med Technol,* 43**,** 776-80.

QIN, C., BABA, O. & BUTLER, W. T. 2004. Post-translational modifications of sibling proteins and their roles in osteogenesis and dentinogenesis. *Crit Rev Oral Biol Med,* 15**,** 126-36.

QIN, C., D'SOUZA, R. & FENG, J. Q. 2007. Dentin matrix protein 1 (DMP1): new and important roles for biomineralization and phosphate homeostasis. *J Dent Res,* 86**,** 1134-41.

RAHMAN, S., PATEL, Y., MURRAY, J., PATEL, K. V., SUMATHIPALA, R., SOBEL, M. & WIJELATH, E. S. 2005. Novel hepatocyte growth factor (HGF) binding domains on fibronectin and vitronectin coordinate a distinct and amplified Met-integrin induced signalling pathway in endothelial cells. *BMC Cell Biol,* 6**,** 8.

RAVN, J. J. 1982. Follow-up study of permanent incisors with complicated crown fractures after acute trauma. *Scand J Dent Res,* 90**,** 363-72.

REBEL, H. 1922. Über die Ausheilung der freigelegten Pulpa. *Deutsche Zahnheilkunde,* 55**,** 3-83.

RECHENBERG, D. K., DE-DEUS, G. & ZEHNDER, M. 2011. Potential systematic error in laboratory experiments on microbial leakage through filled root canals: review of published articles. *Int Endod J,* 44**,** 183-94.

REYES-CARMONA, J. F., FELIPPE, M. S. & FELIPPE, W. T. 2009. Biomineralization ability and interaction of mineral trioxide aggregate and white portland cement with dentin in a phosphate-containing fluid. *J Endod,* 35**,** 731-6.

RIBATTI, D., CONCONI, M. T. & NUSSDORFER, G. G. 2007. Nonclassic endogenous novel [corrected] regulators of angiogenesis. *Pharmacol Rev,* 59**,** 185-205.

RICHARD, G. 2010. *RE: Biodentine, a new standard in endodontics and restorative dentistry: from scientific concept to the clinical use - Personal Communication.*

ROBBINS, M. & MCKINNEY, M. 1992. Transcriptional regulation of neuromodulin (GAP-43) in mouse neuroblastoma clone N1E-115 as evaluated by the RT/PCR method. *Brain Res Mol Brain Res,* 13**,** 83-92.

ROBERTS-CLARK, D. J. & SMITH, A. J. 2000. Angiogenic growth factors in human dentine matrix. *Arch Oral Biol,* 45**,** 1013-6.

RUCH, J. V., LESOT, H. & BEGUE-KIRN, C. 1995. Odontoblast differentiation. *Int J Dev Biol,* 39**,** 51-68.

SAADA, A., REICHERT, F. & ROTSHENKER, S. 1996. Granulocyte macrophage colony stimulating factor produced in lesioned peripheral nerves induces the up-regulation of cell surface expression of MAC-2 by macrophages and Schwann cells. *J Cell Biol,* 133**,** 159-67.

SAITO, K., NAKATOMI, M., IDA-YONEMOCHI, H., KENMOTSU, S. & OHSHIMA, H. 2011. The expression of GM-CSF and osteopontin in immunocompetent cells precedes the odontoblast differentiation following allogenic tooth transplantation in mice. *J Histochem Cytochem,* 59**,** 518-29.

SANTOS, A. D., ARAUJO, E. B., YUKIMITU, K., BARBOSA, J. C. & MORAES, J. C. 2008. Setting time and thermal expansion of two endodontic cements. *Oral Surg Oral Med Oral Pathol Oral Radiol Endod,* 106**,** e77-9.

SANTOS, J., CARRILHO, M., TERVAHARTIALA, T., SORSA, T., BRESCHI, L., MAZZONI, A., PASHLEY, D., TAY, F., FERRAZ, C. & TJADERHANE, L. 2009. Determination of matrix metalloproteinases in human radicular dentin. *J Endod,* 35**,** 686-9.

SARKAR, N. K., CAICEDO, R., RITWIK, P., MOISEYEVA, R. & KAWASHIMA, I. 2005. Physicochemical basis of the biologic properties of mineral trioxide aggregate. *J Endod,* 31**,** 97-100.

SASAKI, M., ABE, R., FUJITA, Y., ANDO, S., INOKUMA, D. & SHIMIZU, H. 2008. Mesenchymal stem cells are recruited into wounded skin and contribute to wound repair by transdifferentiation into multiple skin cell type. *J Immunol,* 180**,** 2581-7.

SASAKI, T., NAKAGAWA, K. & HIGASHI, S. 1982. Ultrastructure of odontoblasts in kitten tooth germs as revealed by freeze-fracture. *Arch Oral Biol,* 27**,** 897-904.
SAUNDERS, W. P. 2008. A prospective clinical study of periradicular surgery using mineral trioxide aggregate as a root-end filling. *J Endod,* 34**,** 660-5.
SAWA, Y., HORIE, Y., YAMAOKA, Y., EBATA, N., KIM, T. & YOSHIDA, S. 2003. Production of colony-stimulating factor in human dental pulp fibroblasts. *J Dent Res,* 82**,** 96-100.
SCHEMBRI, M., PEPLOW, G. & CAMILLERI, J. 2010. Analyses of heavy metals in mineral trioxide aggregate and Portland cement. *J Endod,* 36**,** 1210-5.
SCHOUR, I. & HOFFMAN, M. M. 1939. Studies in tooth development: II. The rate of apposition of enamel and dentine in man and other mammals. *J Dent Res* 18**,** 161-175.
SCHRODER, U. 1972. Evaluation of healing following experimental pulpotomy of intact human teeth and capping with calcium hydroxide. *Odontol Revy,* 23**,** 329-40.
SCHRODER, U. 1973. Effect of an extra-pulpal blood clot on healing following experimental pulpotomy and capping with calcium hydroxide. *Odontol Revy,* 24**,** 257-68.
SCHRODER, U. 1985. Effects of calcium hydroxide-containing pulp-capping agents on pulp cell migration, proliferation, and differentiation. *J Dent Res,* 64 Spec No**,** 541-8.
SCHRODER, U. & GRANATH, L. E. 1971. Early reaction of intact human teeth to calcium hydroxide following experimental pulpotomy and its significance to the development of hard tissue barrier. *Odontol Revy,* 22**,** 379-95.
SCHRODER, U. & SUNDSTROM, B. 1974. Transmission electron microscopy of tissue changes following experimental pulpotomy of intact human teeth and capping with calcium hydroxide. *Odontol Revy,* 25**,** 57-68.
SCIAKY, I. & PISANTI, S. 1960. Localization of calcium placed over amputated pulps in dogs' teeth. *J Dent Res,* 39**,** 1128-32.
SELTZER, S. & BENDER, I. B. 1990. Retrogressive and age changes of the dental pulp. . *In:* SELTZER, S. & BENDER, I. B. (eds.) *The dental pulp: biologic considerations in dental procedures.*: St.Louis: Ishiyaku EuroAmerica,.
SHANNON, D. B., MCKEOWN, S. T., LUNDY, F. T. & IRWIN, C. R. 2006. Phenotypic differences between oral and skin fibroblasts in wound contraction and growth factor expression. *Wound Repair Regen,* 14**,** 172-8.
SHIE, M. Y., HUANG, T. H., KAO, C. T., HUANG, C. H. & DING, S. J. 2009. The effect of a physiologic solution pH on properties of white mineral trioxide aggregate. *J Endod,* 35**,** 98-101.
SHOVELTON, D. S., FRIEND, L. A., KIRK, E. E. & ROWE, A. H. 1971. The efficacy of pulp capping materials. A comparative trial. *Br Dent J,* 130**,** 385-91.
SIGAL, M. J., AUBIN, J. E. & TEN CATE, A. R. 1985. An immunocytochemical study of the human odontoblast process using antibodies against tubulin, actin, and vimentin. *J Dent Res,* 64**,** 1348-55.
SIGAL, M. J., AUBIN, J. E., TEN CATE, A. R. & PITARU, S. 1984. The odontoblast process extends to the dentinoenamel junction: an immunocytochemical study of rat dentine. *J Histochem Cytochem,* 32**,** 872-7.
SIMON, S., COOPER, P., SMITH, A., PICARD, B., IFI, C. N. & BERDAL, A. 2008. Evaluation of a new laboratory model for pulp healing: preliminary study. *Int Endod J,* 41**,** 781-90.
SIMON, S., PERARD, M., ZANINI, M., SMITH, A. J., CHARPENTIER, E., DJOLE, S. X. & LUMLEY, P. J. 2013. Should pulp chamber pulpotomy be seen as a permanent treatment? Some preliminary thoughts. *Int Endod J,* 46**,** 79-87.
SIMON, S., SMITH, A. J., BERDAL, A., LUMLEY, P. J. & COOPER, P. R. 2010. The MAP kinase pathway is involved in odontoblast stimulation via p38 phosphorylation. *J Endod,* 36**,** 256-9.
SIMON, S., SMITH, A. J., LUMLEY, P. J., BERDAL, A., SMITH, G., FINNEY, S. & COOPER, P. R. 2009. Molecular characterization of young and mature odontoblasts. *Bone,* 45**,** 693-703.

SLOAN, A. J., MOSELEY, R., DOBIE, K., WADDINGTON, R. J. & SMITH, A. J. 2002. TGF-beta latency-associated peptides (LAPs) in human dentin matrix and pulp. *Connect Tissue Res,* 43**,** 381-6.

SLOAN, A. J., PERRY, H., MATTHEWS, J. B. & SMITH, A. J. 2000. Transforming growth factor-beta isoform expression in mature human healthy and carious molar teeth. *Histochem J,* 32**,** 247-52.

SLOAN, A. J. & SMITH, A. J. 1999. Stimulation of the dentine-pulp complex of rat incisor teeth by transforming growth factor-beta isoforms 1-3 in vitro. *Arch Oral Biol,* 44**,** 149-56.

SLOAN, A. J. & SMITH, A. J. 2007. Stem cells and the dental pulp: potential roles in dentine regeneration and repair. *Oral Dis,* 13**,** 151-7.

SLOAN, A. J. & WADDINGTON, R. J. 2009. Dental pulp stem cells: what, where, how? *Int J Paediatr Dent,* 19**,** 61-70.

SMITH, A. J. 2002. Pulpal responses to caries and dental repair. *Caries Res,* 36**,** 223-32.

SMITH, A. J. 2003. Vitality of the dentin-pulp complex in health and disease: growth factors as key mediators. *J Dent Educ,* 67**,** 678-89.

SMITH, A. J. 2008. Dentin-pulp complex. *In:* NANCI, A. (ed.) *Ten Cate's Oral HIstology: development, structure and function.* 7th ed. China: Mosby Elsevier.

SMITH, A. J. 2012. Formation and repair of dentine in the adult. *In:* HARGREAVES, K. M., GOODIS, H. E. & TAY, F. R. (eds.) *Seltzer and Bender's Dental Pulp.* 2nd ed.: Quintessence Publishing.

SMITH, A. J., CASSIDY, N., PERRY, H., BEGUE-KIRN, C., RUCH, J. V. & LESOT, H. 1995. Reactionary dentinogenesis. *Int J Dev Biol,* 39**,** 273-80.

SMITH, A. J. & LEAVER, A. G. 1979. Non-collagenous components of the organic matrix of rabbit incisor dentine. *Arch Oral Biol,* 24**,** 449-54.

SMITH, A. J. & LESOT, H. 2001. Induction and regulation of crown dentinogenesis: embryonic events as a template for dental tissue repair? *Crit Rev Oral Biol Med,* 12**,** 425-37.

SMITH, A. J., MATTHEWS, J. B. & HALL, R. C. 1998. Transforming growth factor-beta1 (TGF-beta1) in dentine matrix. Ligand activation and receptor expression. *Eur J Oral Sci,* 106 Suppl 1**,** 179-84.

SMITH, A. J., MURRAY, P. E., SLOAN, A. J., MATTHEWS, J. B. & ZHAO, S. 2001. Trans-dentinal stimulation of tertiary dentinogenesis. *Adv Dent Res,* 15**,** 51-4.

SMITH, A. J., SCHEVEN, B. A., TAKAHASHI, Y., FERRACANE, J. L., SHELTON, R. M. & COOPER, P. R. 2012a. Dentine as a bioactive extracellular matrix. *Arch Oral Biol,* 57**,** 109-21.

SMITH, A. J. & SMITH, G. 1998. Solubilisation of TGF-b1 by dentine conditioning agents. *J Dent Res,* 77**,** 1034.

SMITH, A. J., SMITH, J. G., SHELTON, R. M. & COOPER, P. R. 2012b. Harnessing the natural regenerative potential of the dental pulp. *Dent Clin North Am,* 56**,** 589-601.

SMITH, A. J., TOBIAS, R. S., PLANT, C. G., BROWNE, R. M., LESOT, H. & RUCH, J. V. 1990. In vivo morphogenetic activity of dentine matrix proteins. *J Biol Buccale,* 18**,** 123-9.

SMITH, J. G., SMITH, A. J., SHELTON, R. M. & COOPER, P. R. 2012c. Recruitment of dental pulp cells by dentine and pulp extracellular matrix components. *Exp Cell Res,* 318**,** 2397-406.

SMITH, P. K., KROHN, R. I., HERMANSON, G. T., MALLIA, A. K., GARTNER, F. H., PROVENZANO, M. D., FUJIMOTO, E. K., GOEKE, N. M., OLSON, B. J. & KLENK, D. C. 1985. Measurement of protein using bicinchoninic acid. *Anal Biochem,* 150**,** 76-85.

SOMASUNDARAM, R., RUEHL, M., TILING, N., ACKERMANN, R., SCHMID, M., RIECKEN, E. O. & SCHUPPAN, D. 2000. Collagens serve as an extracellular store of bioactive interleukin 2. *J Biol Chem,* 275**,** 38170-5.

SONG, J. S., MANTE, F. K., ROMANOW, W. J. & KIM, S. 2006. Chemical analysis of powder and set forms of Portland cement, gray ProRoot MTA, white ProRoot MTA, and gray MTA-Angelus. *Oral Surg Oral Med Oral Pathol Oral Radiol Endod,* 102**,** 809-15.

SONNENBERG, E., MEYER, D., WEIDNER, K. M. & BIRCHMEIER, C. 1993. Scatter factor/hepatocyte growth factor and its receptor, the c-met tyrosine kinase, can mediate a signal exchange between mesenchyme and epithelia during mouse development. *J Cell Biol,* 123**,** 223-35.

SONOYAMA, W., LIU, Y., FANG, D., YAMAZA, T., SEO, B. M., ZHANG, C., LIU, H., GRONTHOS, S., WANG, C. Y., WANG, S. & SHI, S. 2006. Mesenchymal stem cell-mediated functional tooth regeneration in swine. *PLoS One,* 1**,** e79.

SREENATH, T., THYAGARAJAN, T., HALL, B., LONGENECKER, G., D'SOUZA, R., HONG, S., WRIGHT, J. T., MACDOUGALL, M., SAUK, J. & KULKARNI, A. B. 2003. Dentin sialophosphoprotein knockout mouse teeth display widened predentin zone and develop defective dentin mineralization similar to human dentinogenesis imperfecta type III. *J Biol Chem,* 278**,** 24874-80.

SRISAWASDI, S. & PAVASANT, P. 2007. Different roles of dexamethasone on transforming growth factor-beta1-induced fibronectin and nerve growth factor expression in dental pulp cells. *J Endod,* 33**,** 1057-60.

STANLEY, H. R. 1989. Pulp capping: conserving the dental pulp--can it be done? Is it worth it? *Oral Surg Oral Med Oral Pathol,* 68**,** 628-39.

STANLEY, H. R. & LUNDY, T. 1972. Dycal therapy for pulp exposures. *Oral Surg Oral Med Oral Pathol,* 34**,** 818-27.

STAQUET, M. J., DURAND, S. H., COLOMB, E., ROMEAS, A., VINCENT, C., BLEICHER, F., LEBECQUE, S. & FARGES, J. C. 2008. Different roles of odontoblasts and fibroblasts in immunity. *J Dent Res,* 87**,** 256-61.

STEELE, J. G., TREASURE, E. T., O'SULLIVAN, I., MORRIS, J. & MURRAY, J. J. 2012. Adult Dental Health Survey 2009: transformations in British oral health 1968-2009. *Br Dent J,* 213**,** 523-7.

STOWE, T. J., SEDGLEY, C. M., STOWE, B. & FENNO, J. C. 2004. The effects of chlorhexidine gluconate (0.12%) on the antimicrobial properties of tooth-colored ProRoot mineral trioxide aggregate. *J Endod,* 30**,** 429-31.

TABATA, M. J., KIM, K., LIU, J. G., YAMASHITA, K., MATSUMURA, T., KATO, J., IWAMOTO, M., WAKISAKA, S., MATSUMOTO, K., NAKAMURA, T., KUMEGAWA, M. & KURISU, K. 1996. Hepatocyte growth factor is involved in the morphogenesis of tooth germ in murine molars. *Development,* 122**,** 1243-51.

TAKESHITA, S., ZHENG, L. P., BROGI, E., KEARNEY, M., PU, L. Q., BUNTING, S., FERRARA, N., SYMES, J. F. & ISNER, J. M. 1994. Therapeutic angiogenesis. A single intraarterial bolus of vascular endothelial growth factor augments revascularization in a rabbit ischemic hind limb model. *J Clin Invest,* 93**,** 662-70.

TANG, H. M., TORABINEJAD, M. & KETTERING, J. D. 2002. Leakage evaluation of root end filling materials using endotoxin. *J Endod,* 28**,** 5-7.

TARTAIX, P. H., DOULAVERAKIS, M., GEORGE, A., FISHER, L. W., BUTLER, W. T., QIN, C., SALIH, E., TAN, M., FUJIMOTO, Y., SPEVAK, L. & BOSKEY, A. L. 2004. In vitro effects of dentin matrix protein-1 on hydroxyapatite formation provide insights into in vivo functions. *J Biol Chem,* 279**,** 18115-20.

TAY, F. R., PASHLEY, D. H., LOUSHINE, R. J., WELLER, R. N., MONTICELLI, F. & OSORIO, R. 2006. Self-etching adhesives increase collagenolytic activity in radicular dentin. *J Endod,* 32**,** 862-8.

TAY, F. R., PASHLEY, D. H., RUEGGEBERG, F. A., LOUSHINE, R. J. & WELLER, R. N. 2007. Calcium phosphate phase transformation produced by the interaction of the portland cement component of white mineral trioxide aggregate with a phosphate-containing fluid. *J Endod,* 33**,** 1347-51.

TECLES, O., LAURENT, P., ZYGOURITSAS, S., BURGER, A. S., CAMPS, J., DEJOU, J. & ABOUT, I. 2005. Activation of human dental pulp progenitor/stem cells in response to odontoblast injury. *Arch Oral Biol,* 50**,** 103-8.

TEN CATE, J. M. 2012. Novel anticaries and remineralizing agents: prospects for the future. *J Dent Res,* 91**,** 813-5.

THOMAS, H. F. & CARELLA, P. 1983. A scanning electron microscope study of dentinal tubules from un-erupted human teeth. *Arch Oral Biol,* 28**,** 1125-30.

THOMAS, H. F. & CARELLA, P. 1984. Correlation of scanning and transmission electron microscopy of human dentinal tubules. *Arch Oral Biol,* 29**,** 641-6.

THYAGARAJAN, T., SREENATH, T., CHO, A., WRIGHT, J. T. & KULKARNI, A. B. 2001. Reduced expression of dentin sialophosphoprotein is associated with dysplastic dentin in mice overexpressing transforming growth factor-beta 1 in teeth. *J Biol Chem,* 276**,** 11016-20.

TINGEY, M. C., BUSH, P. & LEVINE, M. S. 2008. Analysis of mineral trioxide aggregate surface when set in the presence of fetal bovine serum. *J Endod,* 34**,** 45-9.

TJADERHANE, L., SALO, T., LARJAVA, H., LARMAS, M. & OVERALL, C. M. 1998. A novel organ culture method to study the function of human odontoblasts in vitro: gelatinase expression by odontoblasts is differentially regulated by TGF-beta1. *J Dent Res,* 77**,** 1486-96.

TORABINEJAD, M., HIGA, R. K., MCKENDRY, D. J. & PITT FORD, T. R. 1994. Dye leakage of four root end filling materials: effects of blood contamination. *J Endod,* 20**,** 159-63.

TORABINEJAD, M., HONG, C. U., LEE, S. J., MONSEF, M. & PITT FORD, T. R. 1995a. Investigation of mineral trioxide aggregate for root-end filling in dogs. *J Endod,* 21**,** 603-8.

TORABINEJAD, M., HONG, C. U., MCDONALD, F. & PITT FORD, T. R. 1995b. Physical and chemical properties of a new root-end filling material. *J Endod,* 21**,** 349-53.

TORABINEJAD, M., HONG, C. U., PITT FORD, T. R. & KETTERING, J. D. 1995c. Antibacterial effects of some root end filling materials. *J Endod,* 21**,** 403-6.

TORABINEJAD, M. & PARIROKH, M. 2010. Mineral trioxide aggregate: a comprehensive literature review--part II: leakage and biocompatibility investigations. *J Endod,* 36**,** 190-202.

TORABINEJAD, M., RASTEGAR, A. F., KETTERING, J. D. & PITT FORD, T. R. 1995d. Bacterial leakage of mineral trioxide aggregate as a root-end filling material. *J Endod,* 21**,** 109-12.

TORABINEJAD, M. & WHITE, D. J. 1995. U. S. Patent. 5,415,547.

TORNECK, C. D., MOE, H. & HOWLEY, T. P. 1983. The effect of calcium hydroxide on porcine pulp fibroblasts in vitro. *J Endod,* 9**,** 131-6.

TOY, L. W. 2005. Matrix metalloproteinases: their function in tissue repair. *J Wound Care,* 14**,** 20-2.

TOYOSAWA, S., OKABAYASHI, K., KOMORI, T. & IJUHIN, N. 2004. mRNA expression and protein localization of dentin matrix protein 1 during dental root formation. *Bone,* 34**,** 124-33.

TRAN-HUNG, L., MATHIEU, S. & ABOUT, I. 2006. Role of human pulp fibroblasts in angiogenesis. *J Dent Res,* 85**,** 819-23.

TRONSTAD, L. 1974. Reaction of the exposed pulp to Dycal treatment. *Oral Surg Oral Med Oral Pathol,* 38**,** 945-53.

TRUSOLINO, L., BERTOTTI, A. & COMOGLIO, P. M. 2010. MET signalling: principles and functions in development, organ regeneration and cancer. *Nat Rev Mol Cell Biol,* 11**,** 834-48.

TURNER, D. F., MARFURT, C. F. & SATTELBERG, C. 1989. Demonstration of physiological barrier between pulpal odontoblasts and its perturbation following routine restorative procedures: a horseradish peroxidase tracing study in the rat. *J Dent Res,* 68**,** 1262-8.

TZIAFAS, D., ALVANOU, A., PANAGIOTAKOPOULOS, N., SMITH, A. J., LESOT, H., KOMNENOU, A. & RUCH, J. V. 1995. Induction of odontoblast-like cell differentiation in dog dental pulps after in vivo implantation of dentine matrix components. *Arch Oral Biol,* 40**,** 883-93.

TZIAFAS, D., SMITH, A. J. & LESOT, H. 2000. Designing new treatment strategies in vital pulp therapy. *J Dent,* 28**,** 77-92.

UZAN, B., VILLEMIN, A., GAREL, J. M. & CRESSENT, M. 2008. Adrenomedullin is anti-apoptotic in osteoblasts through CGRP1 receptors and MEK-ERK pathway. *J Cell Physiol,* 215**,** 122-8.

VAN AMERONGEN, J. P., LEMMENS, I. G. & TONINO, G. J. 1983. The concentration, extractability and characterization of collagen in human dental pulp. *Arch Oral Biol,* 28**,** 339-45.

VAN AMERONGEN, J. P., LEMMENS, I. G. & TONINO, G. J. 1984. Immunofluorescent localization and extractability of fibronectin in human dental pulp. *Arch Oral Biol,* 29**,** 93-9.

VAN WEEMEN, B. K. & SCHUURS, A. H. 1971. Immunoassay using antigen-enzyme conjugates. *FEBS Lett,* 15**,** 232-236.

VEERAYUTTHWILAI, O., BYERS, M. R., PHAM, T. T., DARVEAU, R. P. & DALE, B. A. 2007. Differential regulation of immune responses by odontoblasts. *Oral Microbiol Immunol,* 22**,** 5-13.

VEIS, A. 1993. Mineral-matrix interactions in bone and dentin. *J Bone Miner Res,* 8 Suppl 2**,** S493-7.

VELNAR, T., BAILEY, T. & SMRKOLJ, V. 2009. The wound healing process: an overview of the cellular and molecular mechanisms. *J Int Med Res,* 37**,** 1528-42.

VOELKER, C. C. 1916. Dental silicate cements in theory and practice. *Dental Cosmos***,** 1098-.

WAKEFIELD, L. M., WINOKUR, T. S., HOLLANDS, R. S., CHRISTOPHERSON, K., LEVINSON, A. D. & SPORN, M. B. 1990. Recombinant latent transforming growth factor beta 1 has a longer plasma half-life in rats than active transforming growth factor beta 1, and a different tissue distribution. *J Clin Invest,* 86**,** 1976-84.

WEINSTOCK, A., WEINSTOCK, M. & LEBLOND, C. P. 1972. Autoradiographic detection of 3 H-fucose incorporation into glycoprotein by odontoblasts and its deposition at the site of the calcification front in dentin. *Calcif Tissue Res,* 8**,** 181-9.

WEINSTOCK, M. & LEBLOND, C. P. 1973. Radioautographic visualization of the deposition of a phosphoprotein at the mineralization front in the dentin of the rat incisor. *J Cell Biol,* 56**,** 838-45.

WEINSTOCK, M. & LEBLOND, C. P. 1974. Synthesis, migration, and release of precursor collagen by odontoblasts as visualized by radioautography after (3H)proline administration. *J Cell Biol,* 60**,** 92-127.

WERNER, S. & GROSE, R. 2003. Regulation of wound healing by growth factors and cytokines. *Physiol Rev,* 83**,** 835-70.

WILLINGHAM, S. B., ALLEN, I. C., BERGSTRALH, D. T., BRICKEY, W. J., HUANG, M. T., TAXMAN, D. J., DUNCAN, J. A. & TING, J. P. 2009. NLRP3 (NALP3, Cryopyrin) facilitates in vivo caspase-1 activation, necrosis, and HMGB1 release via inflammasome-dependent and -independent pathways. *J Immunol,* 183**,** 2008-15.

WONG, A. P., KEATING, A., LU, W. Y., DUCHESNEAU, P., WANG, X., SACHER, A., HU, J. & WADDELL, T. K. 2009. Identification of a bone marrow-derived epithelial-like population capable of repopulating injured mouse airway epithelium. *J Clin Invest,* 119**,** 336-48.

WONG, L. Y., CHEUNG, B. M., LI, Y. Y. & TANG, F. 2005. Adrenomedullin is both proinflammatory and antiinflammatory: its effects on gene expression and secretion of cytokines and macrophage migration inhibitory factor in NR8383 macrophage cell line. *Endocrinology,* 146**,** 1321-7.

WU, M. K., KONTAKIOTIS, E. G. & WESSELINK, P. R. 1998. Long-term seal provided by some root-end filling materials. *J Endod,* 24**,** 557-60.

WU, M. K. & WESSELINK, P. R. 1993. Endodontic leakage studies reconsidered. Part I. Methodology, application and relevance. *Int Endod J,* 26**,** 37-43.

YAMAKOSHI, Y., HU, J. C., IWATA, T., KOBAYASHI, K., FUKAE, M. & SIMMER, J. P. 2006. Dentin sialophosphoprotein is processed by MMP-2 and MMP-20 in vitro and in vivo. *J Biol Chem,* 281**,** 38235-43.

YAMASAKI, M., NAKAMURA, K., AMANO, K., MATSUI, H. & NAKAMURA, H. 2008. Granulocyte colony-stimulating factor induced reduction in pulpal necrosis. *Int Endod J,* 41**,** 593-601.

YAN, X. Q., BRIDDELL, R., HARTLEY, C., STONEY, G., SAMAL, B. & MCNIECE, I. 1994. Mobilization of long-term hematopoietic reconstituting cells in mice by the combination of stem cell factor plus granulocyte colony-stimulating factor. *Blood,* 84**,** 795-9.

YASUDA, Y., OGAWA, M., ARAKAWA, T., KADOWAKI, T. & SAITO, T. 2008. The effect of mineral trioxide aggregate on the mineralization ability of rat dental pulp cells: an in vitro study. *J Endod,* 34**,** 1057-60.

YE, L., MACDOUGALL, M., ZHANG, S., XIE, Y., ZHANG, J., LI, Z., LU, Y., MISHINA, Y. & FENG, J. Q. 2004. Deletion of dentin matrix protein-1 leads to a partial failure of maturation of predentin into dentin, hypomineralization, and expanded cavities of pulp and root canal during postnatal tooth development. *J Biol Chem,* 279**,** 19141-8.

YE, L., PENG, L., TAN, H. & ZHOU, X. 2006. HGF enhanced proliferation and differentiation of dental pulp cells. *J Endod,* 32**,** 736-41.

YE, Z., LICH, J. D., MOORE, C. B., DUNCAN, J. A., WILLIAMS, K. L. & TING, J. P. 2008. ATP binding by monarch-1/NLRP12 is critical for its inhibitory function. *Mol Cell Biol,* 28**,** 1841-50.

YOKOTA, M., NAGATA, T., ISHIDA, H. & WAKANO, Y. 1992. Clonal dental pulp cells (RDP4-1, RPC-C2A) synthesize and secrete osteopontin (SPP1, 2ar). *Biochem Biophys Res Commun,* 189**,** 892-8.

YONGCHAITRAKUL, T. & PAVASANT, P. 2007. Transforming growth factor-beta1 up-regulates the expression of nerve growth factor through mitogen-activated protein kinase signaling pathways in dental pulp cells. *Eur J Oral Sci,* 115**,** 57-63.

YOSHIBA, K., YOSHIBA, N., EJIRI, S., IWAKU, M. & OZAWA, H. 2002. Odontoblast processes in human dentin revealed by fluorescence labeling and transmission electron microscopy. *Histochem Cell Biol,* 118**,** 205-12.

YOSHIBA, N., YOSHIBA, K., IWAKU, M., NAKAMURA, H. & OZAWA, H. 1994. A confocal laser scanning microscopic study of the immunofluorescent localization of fibronectin in the odontoblast layer of human teeth. *Arch Oral Biol,* 39**,** 395-400.

YOSHIBA, N., YOSHIBA, K., NAKAMURA, H., IWAKU, M. & OZAWA, H. 1996. Immunohistochemical localization of HLA-DR-positive cells in unerupted and erupted normal and carious human teeth. *J Dent Res,* 75**,** 1585-9.

ZHANG, R., COOPER, P. R., SMITH, G., NOR, J. E. & SMITH, A. J. 2011. Angiogenic activity of dentin matrix components. *J Endod,* 37**,** 26-30.

ZHAO, Q., CHEN, N., WANG, W. M., LU, J. & DAI, B. B. 2004. Effect of transforming growth factor-beta on activity of connective tissue growth factor gene promoter in mouse NIH/3T3 fibroblasts. *Acta Pharmacol Sin,* 25**,** 485-9.

ZHAO, S., SLOAN, A. J., MURRAY, P. E., LUMLEY, P. J. & SMITH, A. J. 2000. Ultrastructural localisation of TGF-beta exposure in dentine by chemical treatment. *Histochem J,* 32**,** 489-94.

ZHU, Y., OGANESIAN, A., KEENE, D. R. & SANDELL, L. J. 1999. Type IIA procollagen containing the cysteine-rich amino propeptide is deposited in the extracellular matrix of prechondrogenic tissue and binds to TGF-beta1 and BMP-2. *J Cell Biol,* 144**,** 1069-80.

APPENDIX I

Sensitivity thresholds for multiplex ELISA

	Limits of Detection (pg/mL)			Limits of Detection (pg/mL)	
	Lower	Upper		Lower	Upper
HGF	4.9	8 000	IGF1	9 244.9	400 000
TGF-β1	1 648	200 000	IGF1-BP1	4.1	8 000
G-CSF	50.8	40 000	IGF1-SR	564.6	200 000
GM-CSF	9.5	4 000	IGF2	378.1	200 000
M-CSF	19.5	8 000	PDGF-AA	5.3	8 000
SCF	25.6	20 000	VEGF	6.7	40 000
GDNF	11.6	4 000	FGF	1 166.2	40 000
NGF	1.3	8 000	BMP4	41.0	200 000
NT-3	17.8	40 000	BMP7	566 2	400 000
NT-4	12.1	40 000	EGF	2.2	800

APPENDIX II

Research papers published in peer review journals

Tomson PL, Lumley PJ, Alexander MY, Smith AJ, Cooper PR. Hepatocyte growth factor is sequestered in dentine matrix and promotes regeneration-associated events in dental pulp cells. Cytokine. 2013 Feb;61(2):622-9.

Tomson PL, Grover LM, Lumley PJ, Sloan AJ, Smith AJ, Cooper PR. Dissolution of bio-active dentine matrix components by mineral trioxide aggregate. J Dent. 2007 Aug;35(8):636-42.

Published abstracts

Hepatocyte Growth Factor Promotes Mineralisation in Dental Pulp Cells. **Tomson PL**, Lumley PJ, Alexander MY, Smith AJ, Cooper PR. J Dent Res 89 (Spec Iss B):2849, 2010. (http://iadr.confex.com/iadr/2010barce/webprogramschedule/Paper132983.html)

Tomson PL, Grover LM, Smith AJ, Lumley PJ, Sloan AJ, Cooper PR. Comparison of dentine matrix components extracted by the soluble products of white and grey MTA. Int End J 2007 Dec 40 (12): 981.

Dentine Matrix Components Released by Calcium Hydroxide and MTA Solutions. **Tomson PL***, Grover LM, Smith AJ, Lumley PJ, Sloan AJ, Cooper PR. J Dent Res 86 (Spec Iss B):0143 (British Society for Dental Research), 2007. (http://iadr.confex.com/iadr/bsdr07/techprogram/abstract_95086.htm)

Tomson PL, Graham L, Smith AJ, Lumley PJ, Sloan AJ, Cooper PR: In vitro characterization of the dentinogenic potential of Mineral Trioxide Aggregate. Int End J 2005 Dec 38 (12): 916.

APPENDIX III

Conference presentations (without published abstracts)

Tomson PL*, Lumley PJ, Yan J, Alexander MY, Smith AJ, Cooper PR. Hepatocyte growth factor is sequestered in dentine matrix and promotes regenerative events in dental pulp cells Academy of Medical Sciences Research Conference, University of Birmingham, 25th September 2012.

Tomson PL*, Lumley PJ, Yan J, Alexander MY, Smith AJ, Cooper PR. Dental materials liberate growth factors from mineralised tissue to induce pulpal healing. College of Medical and Dental Sciences Research Gala, University of Birmingham, April 2011.

Tomson PL*, Lumley PJ, Smith AJ, Cooper PR. Growth factor release by pulp capping agents promotes cell proliferation. IADR - Pulp Biology and Regeneration Group, Tissue Injury and Regeneration, Geneva, July 18 - 20th, 2010.

Tomson PL*, Lumley PJ, Yan J, Alexander MY, Smith AJ, Cooper PR. Pulp capping agents release hepatocyte growth factor from dentine which may contribute to mineralised tissue repair in the dentine-pulp complex. Tissue and Cell Engineering Society. Manchester, July 2010.

Tomson PL*, Lumley PJ, Yan J, Alexander MY, Smith AJ, Cooper PR Hepatocyte Growth Factor Promotes Mineralisation in Dental Pulp Cells. College of Medical and Dental Sciences Research Gala, University of Birmingham, April 2010.

Tomson PL*, Graham L, Smith AJ, Lumley PJ, Sloan AJ, Cooper PR. Signalling Molecule Induction by Mineral Trioxide Aggregate during Tooth Tissue Repair – Set for Britain, House of Commons, London, March 2006.

APPENDIX IV

Prizes and awards

Wladimir Adlivankine European Society of Endodontology Research Prize ESE Biennial Meeting (Dublin) September 2005.

The Royal College of Surgeons of England Faculty of Dental Surgery **Research Fellowship** 2008/9.

Highly commended poster prize. College of Medical and Dental Sciences, Research Gala. University of Birmingham. April 2010.

JOURNAL OF DENTISTRY 35 (2007) 636–642

available at www.sciencedirect.com

ScienceDirect

journal homepage: www.intl.elsevierhealth.com/journals/jden

Dissolution of bio-active dentine matrix components by mineral trioxide aggregate

Phillip L. Tomson [a,*], *Liam M. Grover* [b], *Philip J. Lumley* [a], *Alastair J. Sloan* [c], *Anthony J. Smith* [a], *Paul R. Cooper* [a]

[a] *Oral Biology, School of Dentistry, The University of Birmingham, St Chad's Queensway, Birmingham B4 6NN, UK*
[b] *School of Chemical Engineering, The University of Birmingham, Edgbaston, Birmingham B15 2TT, UK*
[c] *Department of Oral Surgery, Medicine & Pathology, Cardiff University, Wales College of Medicine, School of Dentistry, Heath Park, Cardiff CF14 4XY, UK*

ARTICLE INFO

Article history:
Received 20 February 2007
Received in revised form
19 April 2007
Accepted 20 April 2007

Keywords:
Mineral trioxide aggregate (MTA)
Dentine
Pulp
Regeneration
Growth factors
TGF
ADM

ABSTRACT

Objectives: To analyze the soluble components of setting and set mineral trioxide aggregate (MTA), assess the abilities of two varieties of MTA and $Ca(OH)_2$ solutions to solubilise dentine matrix proteins (DMPs) and determine if these extracts contain signalling molecules important to pulpal repair and regeneration.

Methods: The metallic ion composition of solutions of white and grey MTA (pH 11.7), 0.02 M $Ca(OH)_2$ (pH 11.9) and 10% EDTA (pH 7.2) was determined using atomic absorption spectroscopy. Extracellular dentine matrix components from powdered human dentine were extracted using all solutions over 14 days. Extracts were analysed for concentrations of non-collagenous proteins (NCPs) and glycosaminoglycans (GAGs), and protein profiles were examined using 1D-polyacrylamide gel electrophoresis (1D-PAGE). ELISAs for TGF-β1 and adrenomedullin (ADM) were also performed.

Results: Aluminium, calcium, potassium, and sodium ions were detected in both white and grey MTA solutions. MTA and $Ca(OH)_2$ solutions liberated similar amounts of GAGs and NCPs although yields were considerably lower than those obtained using the EDTA solution. 1D-PAGE analysis demonstrated differences in protein profiles solubilised from dentine for all solutions. All extracts contained TGF-β1 and ADM, EDTA solution liberated significantly greater amounts of TGF-β1, and $Ca(OH)_2$ and grey MTA solutions released more ADM.

Conclusions: These data imply that when placed clinically soluble components of set and setting MTA may release dentine matrix components that potentially influence cellular events for dentine repair and regeneration.

1. Introduction

Mineral trioxide aggregate (MTA) was developed in the 1990s initially for use as a root-end filling material due to its ability to set in the presence of moisture.[1] Whilst its chemistry was based on that of ordinary Portland cement, significant differences preclude use of the latter as a clinical substitute.[2] MTA has been shown capable of inducing mineralised tissue formation at a variety of oral and dental tissue sites and subsequently its potential applications within dentistry have expanded.[3] The chemical composition of MTA is a mixture of oxides with approximately 65% being calcium

* *Corresponding author*. Tel.: +44 121 237 2877; fax: +44 121 625 8815.
E-mail address: p.l.tomson@bham.ac.uk (P.L. Tomson).
0300-5712/$ – see front matter
doi:10.1016/j.jdent.2007.04.008

Cytokine 61 (2013) 622–629

Contents lists available at SciVerse ScienceDirect

Cytokine

journal homepage: www.journals.elsevier.com/cytokine

Hepatocyte growth factor is sequestered in dentine matrix and promotes regeneration-associated events in dental pulp cells

Phillip L. Tomson [a,*], Philip J. Lumley [a], M. Yvonne Alexander [b], Anthony J. Smith [a], Paul R. Cooper [a]

[a] Oral Biology, The University of Birmingham College of Medical and Dental Sciences, School of Dentistry, St. Chad's Queensway, Birmingham B4 6NN, UK
[b] Cardiovascular Research Group, Division of Cardiovascular and Endocrine Science, University of Manchester, Core Technology Facility, 46 Grafton St., Manchester M13 9NT, UK

ARTICLE INFO

Article history:
Received 13 September 2012
Received in revised form 9 November 2012
Accepted 16 November 2012
Available online 28 December 2012

Keywords:
Hepatocyte growth factor (HGF)
Mineral trioxide aggregate (MTA)
Dentine
Pulp
Regeneration

ABSTRACT

Extracellular matrix of dentine contains a rich cocktail of soluble cytokines and growth factors which mediate wound repair of the dentine–pulp complex. Hepatocyte growth factor (HGF) is a mesenchyme derived growth factor regulating a broad range of physiological processes including tissue development and regeneration. In this study, we have investigated the sequestration of HGF in the dentine matrix and analysed its action as a chemokine in the induction of differentiation and mineral deposition in pulp derived cells in vitro. Using ELISA, the presence of HGF was demonstrated in solubilised fractions of dentine matrix released by the therapeutic pulp repair materials of white and grey mineral trioxide aggregate. HGF was shown to be a chemo-attractant for primary rat dental pulp cells (RDPCs) in transwell assays highlighting its potential in progenitor cell recruitment during dentine–pulp tissue repair. Transcription factors Osterix and Runx2, and genes encoding for Osteopontin and Osteocalcin, were up-regulated in HGF-exposed RDPC cultures compared with controls. Adenoviral-mediated expression of HGF in RDPCs or exposure to recombinant HGF induced mineral secretion in RDPCs which was significantly greater than controls. The receptor of HGF, c-Met was also detected within human dental pulp indicating the potential for HGF released from dentine matrix to contribute to cellular signalling events following tissue injury. Combined, these data suggest that HGF is important in the repair of the dentine–pulp complex potentially participating in several aspects of wound healing.

1. Introduction

Wound healing begins immediately following injury to a tissue initiating a cascade of events involving resident and migratory cell populations, extracellular matrix (ECM) and the action of soluble mediators [1]. Several soluble signalling molecules have been implicated in the molecular interactions of the dentine–pulp complex during pulp repair [2], although the underlying mechanisms are only beginning to be elucidated. Repair of the pulp is a complex process of cellular events requiring progenitor/stem cell recruitment, involving chemoattraction to the injured pulp site, signalling of odontoblast-like cell differentiation and subsequent up-regulation of dentine matrix secretion and mineralisation [3]. While these cellular events are likely to be regulated by a multitude of cytokines and other signalling factors, studies are now starting to uncover the key molecules involved. Transforming growth factor-β1 (TGF-β1) has previously been shown to play a pivotal role in pulp tissue repair, acting as a chemotactic agent [4] and signaller of cellular differentiation [5]. It may also regulate activity of terminally differentiated odontoblasts switching between primary, secondary and tertiary dentinogensis via its action on the p38-mitogen-protein activated kinase pathway [6]. TGF-β1 is sequestered within dentine matrix together with other cytokines and growth factors including fibroblast growth factor-2, insulin-like growth factor-1 and 2, adrenomedullin, vascular endothelial growth factor and platelet derived growth factor [7–10]. Unlike bone, dentine demonstrates minimal physiological remodelling during its lifetime, however, its dissolution can occur pathologically during caries and much more locally following therapeutic application of dental materials, such as calcium hydroxide and mineral trioxide aggregate (MTA) [11,12]. The dissolution process releases matrix bound growth factors and cytokines, which can subsequently trigger cellular and tissue repair associated responses, including tertiary dentinogenesis [2]. The dentine matrix is complex and harbours a rich cocktail of growth factors many of which are not yet well characterised and which regulate dentine–pulp complex homeostasis and repair.

Hepatocyte growth factor (HGF) has previously been demonstrated to regulate liver regeneration [13,14], but it also exhibits bioactivity in platelets [15] and plasma [16,17]. HGF is considered a multifunctional growth factor and cytokine that can act as a

* Corresponding author. Tel.: +44 121 466 5173; fax: +44 121 466 5491.
E-mail addresses: p.l.tomson@bham.ac.uk (P.L. Tomson), p.j.lumley@bham.ac.uk (P.J. Lumley), yvonne.alexander@manchester.ac.uk (M.Y. Alexander), a.j.smith@bham.ac.uk (A.J. Smith), p.r.cooper@bham.ac.uk (P.R. Cooper).

1043-4666/$ - see front matter © 2012 Elsevier Ltd. All rights reserved.
http://dx.doi.org/10.1016/j.cyto.2012.11.009